8-20-2020 2:15 PM

The Effect of Nitric Oxide on Microglia Function and Activity: Implications on Transient Receptor Potential Channels

Matthew J-E. Maksoud, *The University of Western Ontario*

Supervisor: Lu, Wei-Yang, *The University of Western Ontario*

A thesis submitted in partial fulfillment of the requirements for the Doctor of Philosophy degree in Neuroscience

Abstract

Microglia proliferation and phagocytosis is critical for proper development and maintenance of the central nervous system (CNS), whereas dysregulated proliferation and phagocytosis contributes to various CNS pathologies. Specifically, in response to pathology or tissue injury, microglia transform to an activated state characterized by elevated inducible nitric oxide synthase (iNOS) expression, increased nitric oxide (NO) production, active phagocytosis, and decreased proliferation. Importantly, microglial phagocytosis and proliferation are tightly regulated by intracellular calcium levels. As non-excitable cells, microglia rely on calcium entry through transient receptor potential (TRP) channels to carry out phagocytosis and proliferation. However, the role of iNOS/NO signaling in regulating TRP channel mediated calcium dynamics in microglia is not entirely understood. We hypothesized that NO signaling regulates the activity of TRP channels in microglia to influence phagocytosis and proliferation. Using pharmacology, immuno-blots, cellular patch-clamp electrophysiology, calcium-imaging, polymerase chain reaction, and assays for phagocytosis and proliferation, this work determined that NO critically regulates microglial calcium homeostasis. We demonstrated that NO regulates the calcium dynamics of TRP vanilloid type 2 (TRPV2) and TRP canonical 1 and 3 (TRPC1/3) channels to enhance microglial phagocytosis and inhibit proliferation. Specifically, iNOS/NO signaling in microglia restricted calcium influx through TRPC1/3 channels independent of protein kinase G (PKG) signaling, while a simultaneous enhancement in the plasma membrane expression and calcium influx through TRPV2 channels occurred in a PKG-dependent mechanism. The plasma membrane expression of TRPV2 was negatively associated with cell-cycle progression in microglia cultures. Specifically, increased production of NO, plasma membrane expression of TRPV2, and calcium influx was observed in non-dividing microglia. The calcium influx through TRPV2 channels caused nuclear translocation of the transcription factor nuclear factor of activating T-cells cytoplasmic 2 and increased mRNA expression of the cyclin dependent kinase inhibitor p21 in murine microglia. The work from this thesis identified NO as a crucial regulator of TRP channel activity and calcium homeostasis within microglia. Future studies can apply these findings to better understand CNS pathologies that display altered microglial proliferation or phagocytosis such as Alzheimer's disease, Parkinson's disease, stroke recovery, or cancer progression.

Keywords

Transient Receptor Potential Channel

Store Operated Calcium Channel

Calcium

Phagocytosis

Proliferation

Microglia

Inflammation

Nitric Oxide

Protein Kinase G

S-nitrosylation

Lay Abstract

Microglia are the only immune cells residing in the brain. Their main roles are to ensure that neurons develop properly and remain healthy throughout life. When microglia fail to perform these roles, degenerative disorders such as Alzheimer's disease or Parkinson's disease may develop. Microglia carry out two specialized tasks that include removing cellular waste and/or pathogens through a process called phagocytosis and multiplying to increase their cellular numbers through a process called proliferation. In order to perform these specialized tasks, microglia take cues from changing calcium concentrations in their environments. However, the surrounding calcium can only enter microglia through specific channels on their cell surface that are formed from transient receptor potential (TRP) proteins. There are a variety of different TRP proteins, however they all act as a path for calcium to enter and activate microglia. When microglia become active, they produce a gas called nitric oxide. From previous studies, we know that nitric oxide influences microglia to carry out their specialized tasks such as phagocytosis and proliferation. However, it remains unknown whether nitric oxide is produced in microglia to directly regulate TRP channels and calcium entry, influencing their ability to perform these specialized tasks. In the following experiments, we demonstrated that nitric oxide does in fact regulate specific TRP channels on microglia to influence their ability to perform tasks. Specifically, in the presence of nitric oxide, the TRP vanilloid type 2 (TRPV2) channel, normally present within microglia, is transferred to the surface of microglia to cause calcium entry into microglia. We also demonstrated that nitric oxide restricted calcium influx through TRP canonical type 1 and 3 (TRPC1/3) channels on the surface of microglia. Importantly, we further demonstrated that the calcium influx from TRPV2 channels caused microglia to engulf more objects through phagocytosis, while simultaneously restricting their ability to multiply and proliferate. In many neurodegenerative disorders such as Alzheimer's and Parkinson's disease, microglia present with abnormal phagocytosis and proliferation. Therefore, studies such as the ones presented in this dissertation may be the first step to uncovering therapeutic targets for the neurodegenerative diseases that arise due to abnormal microglial activities.

Co-Authorship Statement

The following people contributed to the publication of work undertaken as part of this thesis and their contributions are listed under each manuscript:

Candidate: Matthew Joseph-Elias Maksoud, The University of Western Ontario
Author 2: Vasiliki Tellios, The University of Western Ontario
Author 3: Dong An, The University of Western Ontario
Author 4: Yun-Yan Xiang, Robarts Research Institute
Author 5: Wei-Yang Lu, The University of Western Ontario, Robarts Research Institute

Contribution of work by co-authors for each paper and manuscript.

PAPER 1: Located in Chapter 2
Matthew J.E. Maksoud, Vasiliki Tellios, Dong An, Yun-Yan Xiang, and Wei-Yang Lu, Nitric Oxide upregulates microglia phagocytosis and increases transient receptor potential vanilloid type 2 channel expression on the plasma membrane, Glia. 67 (2019) 2294–2311. https://doi.org/10.1002/glia.23685

Author Contributions:
Conceived and designed experiments: Candidate, Author 5
Performed Experiments: Candidate
Performed Experiments for Figure 2.4g: Author 2
Performed Experiments for Figure 2.6a: Author 3
Contributed technical troubleshooting: Author 4
Analyzed the data: Candidate, Author 2
Wrote the manuscript: Candidate
Revised the manuscript: Author 2, Author 5

PAPER 2: Located in Chapter 3

Matthew J.E. Maksoud, Vasiliki Tellios, Yun-Yan Xiang, and Wei-Yang Lu, Nitric oxide displays a biphasic effect on calcium dynamics within microglia, Submitted.

Author Contributions

Conceived and designed experiments: Candidate, Author 5

Performed the Experiments: Candidate

Contributed technical troubleshooting: Candidate, Author 2, Author 4

Analyzed the data: Candidate

Contributed to organizing data: Candidate, Author 2, Author 5

Wrote the manuscript: Candidate

Revised the manuscript: Author 2, Author 5

PAPER 3: Located in Chapter 4

Matthew J.E. Maksoud, Vasiliki Tellios, Yun-Yan Xiang, and Wei-Yang Lu, Nitric oxide signaling inhibits microglia proliferation by activation of protein kinase-G, Nitric Oxide. 94 (2019) 125–134. https://doi.org/10.1016/j.niox.2019.11.005

Author Contributions

Conceived and designed experiments: Candidate, Author 5

Performed the Experiments: Candidate

Contributed technical troubleshooting: Candidate, Author 2, Author 4

Analyzed the data: Candidate

Contributed to organizing data: Candidate, Author 2, Author 5

Wrote the manuscript: Candidate

Revised the manuscript: Author 2, Author 5

PAPER 4: Located in Chapter 5

Matthew J.E. Maksoud, Vasiliki Tellios, and Wei-Yang Lu, Nitric oxide attenuates murine microglia proliferation by sequential activation of TRPV2-mediated calcium influx, NFATC2 nuclear translocation, and p21 expression., Submitted.

Author Contributions

Conceived and designed experiments: Candidate, Author 5

Performed the experiments: Candidate

Contributed technical troubleshooting: Candidate, Author 2

Analyzed the data: Candidate

Contributed to organizing data: Candidate, Author 2, Author 5

Wrote the manuscript: Candidate

Revised the manuscript: Author 2, Author 5

Acknowledgments

I could not have successfully progressed through this dissertation without a strong support group. First of all, my parents, who continuously supported my aspirations while constantly making every holiday away from the lab a fantastic feast. Secondly, my fellow lab members that have come and gone throughout the years. Particularly, Amy Lin and Vasiliki Tellios, for helping make the lab a fun and inviting atmosphere, where we could carry out research, but more importantly enjoy each other's stories. Additionally, I would like to thank Ravneet Nagra, Dong An, Yimo Wang, Jason Kim, and John Lee, who showed exceptional interest in research, which made my teaching experience that much more enjoyable during their undergraduate theses. Furthermore, I must extend a special thank you to Dr. Yun-Yan Xiang for her constant guidance and helpfulness in the early years of my graduate school career. Dr. Xiang taught me many techniques that I will continue to use in the future, while also contributing extensively to my productivity early on in my degree. Thirdly, I would like to thank my committee consisting of Drs. Peter Stathopulos, Marco Prado, Vania Prado, and Wataru Inoue, for their constant guidance, support, and critical input throughout my ever-changing projects. Finally, I would like to thank Dr. Wei-Yang Lu for his supervision and support throughout the entirety of my dissertation. Dr. Lu had a mentorship style that has greatly supported my critical thinking while instructing me to always trust my instincts. As a result of all the support I received during my dissertation, my highs felt exceptionally high, while my lows seemed not so low.

Table of Contents

List of Figures

List of Abbreviations

1400W	N-(3-(Aminomethyl)Benzyl)Acetamidine
2-AG	2-Arachidonoylglycerol
2APB	2-Aminoethoxydiphenyl Borate
8Br-cGMP	8-Bromo-Cyclic-Guanosine Monophosphate
Akt	Protein kinase B
ANP	Atrial Natriuretic Peptide
AP1	Activator Protein-1
ASL	Argininosuccinate Lyase
Ass1	Argininosuccinate Synthase-1
ATP	Adenosine Triphosphate
AUC	Area Under the Curve
AUI	Arbitrary Unit of Intensity
BAPTA	(1,2-Bis(O-Aminophenoxy)Ethane-N,N,N',N'-Tetraacetic Acid
BDNF	Brain Derived Neurotrophic Factor
BL	Baseline
BNP	B Type Natriuretic Peptide
BRCA1	Breast Cancer Susceptibility Gene 1
BrdU	Bromodeoxyuridine
BSA	Bovine Serum Albumen
Ca^{2+}	Calcium Ion
cAMP	Cyclic Adenosine Monophosphate
CB1R	Cannabinoid Receptor 1
CB2R	Cannabinoid Receptor 2
CD11b	Cluster of Differentiation Molecule 11B
CD18	Integrin Beta Chain 2
CD32A	Cluster of Differentiation 32 Activating Subtype
CD32B	Cluster of Differentiation 32 Inhibitory Subtype
CDK	Cyclin Dependent Kinase
CDK2	Cyclin Dependent Kinase 2
CDK4	Cyclin Dependent Kinase 4
cGMP	Cyclic Guanosine Monophosphate

Cl^-	Chlorine ion
CNP	C-Type Natriuretic Peptide
CNS	Central Nervous System
CR3	Complement Receptor 3 or Macrophage-1 Antigen or CD11b/CD18
CRAC	Calcium Release Activated Calcium Channel
CREB	cAMP Response Element Binding Protein
CSF1	Colony Stimulating Factor 1
CX3CL1	Fractalkine
CX3CR1	Fractalkine Receptor
Cys	Cysteine
DAG	Diacylglycerol
DAPI	4',6-Diamidino-2-Phenylindole
DIC	Differential Interface Contrast
DMEM	Dulbecco's Modified Eagles Medium
eNOS	Endothelial Nitric Oxide Synthase
ER	Endoplasmic Reticulum
ERK	Extracellular Signal-Regulated Kinase
EsR	Estrogen Receptor
ET	Endothelin
FBS	Fetal Bovine Serum
FcγR	Fc- Gamma Receptor
FcγRI	Fc- Gamma Receptor Type 1
FcγRIIa	Fc- Gamma Receptor Type 2 (Activating) Or CD32A
FcγRIIb	Fc- Gamma Receptor Type 2 (Inhibitory) Or CD32B
FcγRIII	Fc- Gamma Receptor Type 3
FcγRIV	Fc- Gamma Receptor Type 4
G0	G0 Phase (Cell Cycle Stage)
G_1	Growth Stage 1 (Cell Cycle Stage)
G_2	Growth Stage 2 (Cell Cycle Stage)
GADPH	Glyceraldehyde 3-Phosphate Dehydrogenase
GiPCR	Gi Protein Coupled Receptor

GPCR	G Protein Coupled Receptor
GqPCR	Gq Protein Coupled Receptor
GTP	Guanosine-5'-Triphosphate
H_2O	Water
HEPES	4-(2-Hydroxyethyl)-1-Piperazineethanesulfonic Acid
HO-1	Heme Oxygenase-1
HRP	Horseradish Peroxidase
Iba1	Ionized Calcium Binding Adapter Molecule 1
IFNγ	Interferon Gamma
Ig	Immunoglobulin
IgA	Immunoglobulin A
IgD	Immunoglobulin D
IgE	Immunoglobulin E
IGF	Insulin Like Growth Factor
IGFR	Insulin-Like Growth Factor Receptor
IgG	Immunoglobulin G
IgM	Immunoglobulin M
IKK	Inhibitor of Nuclear Factor Kb Kinase
IL-10	Interleukin-10
IL-1β	Interleukin-1 Beta
IL-34	Interleukin-34
IL-6	Interleukin-6
iNOS	Inducible Nitric Oxide Synthase
$iNOS^{-/-}$	Inducible Nitric Oxide Synthase Knockout
IP_3	Inositol Triphosphate
IP_3R	Inositol Triphosphate Receptor
ITAM	Immunoreceptor Tyrosine Based Activation Motifs
ITIM	Immunoreceptor Tyrosine Based Inhibitory Motifs
IκB	Inhibitor of Nuclear Factor κB
JNK	C-Jun N-Terminal Kinases
K^+	Potassium Ion
Ki67	Antigen KI-67

L-NAME	G-Nitro-L-Arginine-Methyl Ester
L-NMMA	NG-monomethyl-L-arginine
LPS	Lipopolysaccharide
M	Mitosis (Cell Cycle Stage)
MAPK	Mitogen Activated Protein Kinase
mCSF1	Macrophage Colony Stimulating Factor 1 or CSF1
MEK	Mitogen Activated Protein Kinase Kinase
Mg	Magnesium
mRNA	Messenger Ribonucleic Acid
Na^+	Sodium Ion
NADPH	Nicotinamide Adenine Dinucleotide Phosphate
NDS	Normal Donkey Serum
NFAT	Nuclear Factor of Activated T-Cells
NFATC1	Nuclear Factor of Activated T-Cells Cytoplasmic 1, Or NFAT2
NFATC2	Nuclear Factor of Activated T-Cells Cytoplasmic 2, Or NFAT1
NFκB	Nuclear Factor kappa-light-chain-enhancer of Activated B Cells
nNOS	Neuronal Nitric Oxide Synthase
NO	Nitric Oxide
NOC18	Diethylenetriamine NONOate
NOS	Nitric Oxide Synthase
NOS2	Inducible Nitric Oxide Synthase 2 Gene
O_2	Oxygen
OTC	Ornithine Transcarbamylase
P/S	Penicillin and Streptomycin
P0	Postnatal Day 0
p10	Postnatal Day 10
P21	Cyclin Dependent Kinase Inhibitor 1
P_2Y_xR	P2 Metabotropic Purinergic Receptor Subclass Y_x
p53	Tumor Suppressor p53 or The Guardian of the Genome
pA	Picoamp
PBS	Phosphate Buffered Saline
PCR	Polymerase Chain Reaction

PDL	Poly-D-Lysine
pF	Picofarad
PFA	Paraformaldehyde
pGC	Particulate Guanylyl Cyclase
pH3	Phosphorylated Histone-3
PI3K	Phosphoinositide-3-Kinase
PIP_2	Phosphatidylinositol 4,5-Biphosphate
PKG	Protein Kinase G
PLC	Phospholipase C
PM	Plasma Membrane
qPCR	Quantitative Polymerase Chain Reaction
RIPA	Radioimmunoprecipitation Assay
RNS	Reactive Nitrogen Species
ROI	Region of Interest
ROS	Reactive Oxygen Species
RR	Ruthenium Red
RT	Room Temperature
RT-qPCR	Reverse Transcription Quantitative Polymerase Chain Reaction
S	Synthesis (Cell Cycle Stage)
SAM	Sterile Alpha Motif
SEM	Standard Error around the Mean
SERCA	Sarco/Endoplasmic Reticulum Calcium ATPase
sGC	Soluble Guanylyl Cyclase
SHIP1	SH-2 Containing Inositol 5’ Polyphosphatase 1
SHP-1	Src Homology Region 2 Domain-Containing Phosphatase-1
SMAD	Mothers Against Decapentaplegic
SMAD1	Mothers Against Decapentaplegic Homolog 1
SMAD3	Mothers Against Decapentaplegic Homolog 3
SNAP	S-Nitroso-N-Acetyl-DL-Penicillamine
SNP	Sodium Nitroprusside
SOCC	Store Operated Calcium Channel
SOCE	Store Operated Calcium Entry

STAT1α	Signal Transducer and Activator of Transcription 1α
STIM1	Stromal Interaction Molecule
Syk	Tyrosine Protein Kinase Syk
TG	Thapsigargin
TGFβ	Transforming Growth Factor Beta
THC	Tetrahydrocannabinol
TLR	Toll-Like Receptor
TLR4	Toll-Like Receptor 4
TLR7	Toll-Like Receptor 7
TLR9	Toll-Like Receptor 9
TNFα	Tumor Necrosis Factor Alpha
TRP	Transient Receptor Potential
TRPC	Transient Receptor Potential Canonical
TRPC1	Transient Receptor Potential Canonical Type 1
TRPC3	Transient Receptor Potential Canonical Type 3
TRPC4	Transient Receptor Potential Canonical Type 4
TRPC5	Transient Receptor Potential Canonical Type 5
TRPC6	Transient Receptor Potential Canonical Type 6
TRPM	Transient Receptor Potential Melastatin
TRPV	Transient Receptor Potential Vanilloid
TRPV1	Transient Receptor Potential Vanilloid Type 1
TRPV2	Transient Receptor Potential Vanilloid Type 2
TRPV3	Transient Receptor Potential Vanilloid Type 3
UV	Ultraviolet
V–I	Voltage-Current
WT	Wild-Type
ΔCt	Difference in Cycle Threshold

Preface

I set out on a journey to do my Master's in 2015 with one important request that – in my head – took priority over everything else. This request was that I wanted to work with microglia. My attention was originally drawn to the highly ramified nature that microglia display within the brain, and my curiosity surrounding the functions of these cells resulted in me pursuing a PhD. These small but mighty cells have been constantly overlooked in the past, are actively involved in many neurological functions, and implicated in many neurological diseases. Although more research now than ever focuses on microglia, there remains a large deficit in the literature surrounding how microglia cells regulate their function and activity. Within my studies, I have used many different cellular techniques, some intricate and time-consuming while others were simple and concise to learn as much about microglia as I possibly could within the span of ~5 years. I would again like to thank my entire support group one last time for making this academic experience that much more enjoyable.

Chapter 1

1 Introduction

1.1 Microglia: important immune cells

Microglia are the immune cells within the central nervous system (CNS) that were first characterized by Pío del Río Hortega in the early 1900's. Present throughout the entire brain and spinal cord, microglia account for over 10% of the glia population within the CNS and quickly became known for their rapid immune response. Over the years, microglia have emerged in the spotlight as having key physiological functions in CNS development, surveillance, maintenance, synaptic pruning, and defense. Through their ability to migrate, proliferate, secrete cytokines, and phagocytose, microglia are critical players in regulating neuronal activity while being heavily implicated in many neurological disorders such as Alzheimer's, Parkinson's, multiple sclerosis, ischemic stroke, and even autism spectrum disorders. Although intensely studied to date, interest in microglia has only recently grown over the past 20 years, with countless features and characteristics of these cells yet to be discovered.

1.2 Microglia cell lineage, origin and infiltration

Since recognized as important immune cells within the CNS, the origin of microglia has been widely disputed over the years. Microglia share many similarities and functions with macrophages – peripheral immune monocytes found in tissues and circulation – and therefore have been thought to originate from the same myeloid precursor during development (Ginhoux et al., 2013). Although microglia have been commonly compared to macrophages in terms of having similar functions, receptor expression, and activities, microglia originate from different precursors during development (Schulz et al., 2012). Once believed to be of monocyte origin, microglia are now known to originate directly from fetal yolk sac progenitors. (Alliot et al., 1999; Alliot et al., 1991). During embryogenesis, the formation of the blood brain barrier restricts fetal liver and bone

marrow monocyte/macrophage progenitors from infiltrating the neuroepithelium (Ginhoux et al., 2013). Conversely, microglia may also infiltrate the CNS through alternative pathways, independent of vasculature, such as through ventricles and meninges (Cuadros & Navascués, 1998; Hurley & Streit, 1995). For example, Kaur and colleagues injected crotoxin-coated beads into the ventricles of 5-day-old rats and demonstrated that ventricular macrophages bind to the beads and developed a ramified microglia-like appearance 30 days after initial bead injection (Kaur et al., 1990). Similarly, another study examined microglia development in quail cerebellum and observed round microglia-like cells traversing the ventricular layers from the pial surface (Cuadros et al., 1997). These studies demonstrate the possibility that microglia-like cells may also infiltrate the CNS through the ventricles in addition to the vasculature.

Once microglia progenitors infiltrate the neuroepithelium, they rapidly proliferate postnatally up until day 14 and become a self-maintained cell population throughout adulthood, independent of hematopoietic progenitors (Alliot et al., 1999). After infiltration, a distinct change in microglia morphology from ameboid to ramified phenotype (Schwarz et al., 2013) is accompanied by a decrease in proliferative capacity (Nikodemova et al., 2015). Importantly, as microglia become more ramified, each cell occupies a defined territory in the CNS, and these cells only proliferate when the contact between neighboring cells is lost, which usually occurs in response to insult or injury (Fukushima et al., 2015). However, speculations about why and how the morphology of microglia changes are not fully understood and are usually attributed to occur in response to neuronal and other glial cell maturation in the CNS.

1.3 Microglia surveillance and morphology *in vivo*

Within the adult murine CNS, microglia morphology is tightly associated with their activity level (Davalos et al., 2005; Fontainhas et al., 2011; Nimmerjahn et al., 2005). Under physiological conditions, microglia in the adult murine brain occupy their defined territory and display small cell somas with long ramified processes that constantly contact neighboring neuronal synapses and dendrites (Nimmerjahn et al., 2005). Although classified as a “resting” state, microglial processes are highly mobile under physiological

conditions and actively interact with surrounding cells within the occupied territory (Tremblay et al., 2010; Wake et al., 2009).

One strategy by which microglia interact with surrounding neurons is through the expression of fractalkine receptor-1 (CX3CR1) (Kettenmann et al., 2011; Wolf et al., 2013). CX3CR1 is the receptor for fractalkine (CX3CL1), a membrane-bound chemokine. CX3CR1 is present on some peripheral immune leukocytes including but not limited to T-cells, natural killer cells, and macrophages, and is primarily involved in adhesion and migration (Imai & Yasuda, 2016). As a $G\alpha_i$-coupled seven-transmembrane receptor, CX3CR1 is present on microglia and recognizes its heavily glycosylated ligand (CX3CL1) that is present on the surface of neurons throughout the entire brain (Wolf et al., 2013). The CX3CR1/L1 interaction between microglia and neurons crucially influences microglial synaptic pruning and homeostasis, which is reflected in the morphology of microglia (Biber et al., 2007). Specifically, CX3CR1 directly recognizes CX3CL1 on the surface of neurons or CX3CL1 shed from neurons to suppress microglial activities and maintain the microglia in a surveying state (Bachstetter et al., 2011; Cipriani et al., 2011; Pabon et al., 2011). However, in response to an insult inducing inflammation, microglia morphology rapidly changes to an amoeboid phenotype characterized by thickened processes and an enlarged soma (Kozlowski & Weimer, 2012). This change in morphology allows microglia to migrate to the affected area and carry out phagocytic activities.

It is important to note that deficiencies in CX3CR1/L1 signaling results in activated microglia, which can be detrimental or beneficial, depending on the environment and disease setting in which it occurs (Wolf et al., 2013). For example, in a murine model of lipopolysaccharide (LPS) induced neuroinflammation, CX3CR1 deficient microglia displayed neurotoxic activity (Cardona et al., 2006), while in models of ischemic damage (Dénes et al., 2008) or spinal cord injury (Donnelly et al., 2011), CX3CR1 deficient microglia are not neurotoxic. Microglia morphology and activity *in vivo* depend on a variety of factors. Although morphology can be a sign of whether microglia are responding to their environment, one should not strictly equate microglial activity or morphology to a beneficial or detrimental outcome (Town et al., 2005).

Throughout the entire brain, microglia morphology differs between brain regions in their degree of ramification, the size of their occupied territory, as well as their cell density per area (Lawson et al., 1990). For example, Lawson and colleagues demonstrated that the cell density of F4/80$^+$ stained microglia throughout the cerebrum of adult BALB/c female mice were generally similar in quantity (Lawson et al., 1990). However, throughout deep grey matter regions of the same mice – including the thalamic nuclei, substantia nigra, and basal ganglia – a higher density of microglia were observed than in the cerebrum (Lawson et al., 1990).

Lawson and colleagues also classified the morphology of the F4/80$^+$ microglia into three categories: compact cells that are highly ameboid in nature with intense F4/80$^+$ staining and most common around the ventricular regions; longitudinally branched cells that encompassed a larger territory than compact cells and most common in white matter fiber tracts; and radially branched cells that contain many branches radially extending out of a cell body and were the most common morphology throughout grey matter (Lawson et al., 1990). Furthermore, another study examining microglia morphology in the prefrontal rat cortex demonstrated a homogeneous morphology throughout the five layers of the rat cortex (Kongsui et al., 2014). Specifically, microglia in the rat cortex displayed four to five primary processes that each branch out an average two times (Kongsui et al., 2014), further supporting previous studies that demonstrate microglia morphology within grey matter appears highly ramified (Lawson et al., 1990).

There has also been reports of sex differences in microglia morphology between regions of the rat brain. Specifically, more ramified microglia were present within the parietal cortex, hippocampus, and amygdala within female rats when compared to male rats (Schwarz et al., 2013). These differences were accompanied by increased cytokine mRNA such as IL10, IL1β, IL16, and IL36 within the adult rat brain (Schwarz et al., 2013). Further research must be conducted to examine the potential effects of the estrogen hormone on microglia morphology and potentially, microglia function.

1.4 Microglia morphology *in vitro*

It is very rare for cultured primary microglia to display the highly ramified morphology that is commonly seen *in vivo*. In fact, microglia *in vitro* display a diverse morphology ranging from amoeboid to long bipolar shapes (Tam & Ma, 2015). Although microglia morphology may appear variable *in vivo*, it is still possible to polarize the morphological appearance of microglia through the addition of various agents. For example, LPS treatment polarizes microglia to an ameboid morphology to appear flat along the bottom of the culture vessel (Tam & Ma, 2015). This amoeboid morphology is accompanied by an increase in inflammatory cytokine secretion, increased motility, and increased phagocytosis (Szabo & Gulya, 2013; Tam & Ma, 2015). On the other hand, culturing microglia on fibronectin-coated plates induces bipolar rod-shaped microglia that have been reported to be associated with increased proliferation, and decreased cytokine production (Chamak & Mallat, 1991; Tam & Ma, 2015). It is important to note that microglia morphology *in vitro* does not fully dictate the specific function or activity, which must be examined in depth using more direct methods.

1.5 Microglia polarization markers and phenotype

It is traditionally believed that like macrophages, microglia exist in inflammatory or anti-inflammatory phenotypes that are influenced by microenvironmental cues. In response to inflammatory signals such as bacterial infection or tissue damage, microglia produce inflammatory cytokines such as IL-1β, TNFα, and/or IL-6 (Norden & Godbout, 2013). Additionally, reactive oxygen species (ROS) as well as nitric oxide (NO) are produced through NADPH oxidase and inducible nitric oxide synthase (iNOS) respectively (Orihuela et al., 2016). These classically activated microglia are termed M1 phenotype and propagate inflammation within the CNS. Notable, iNOS mediated NO production critically contributes to microglia function and activity during inflammation, which will be discussed in depth in the next section.

On the other hand, microglia also participate in inflammation resolution to restore homeostasis. For instance, in the presence of cytokines such as IL-4 and IL-13, microglia

produce the anti-inflammatory cytokine IL-10 that reduces TNFα expression and resolves inflammation (Orihuela et al., 2016). These alternatively activated microglia are termed M2-phenotype and are characterized with anti-inflammatory features and increased expression of arginase (Orihuela et al., 2016). Although this traditional M1/M2 classification of monocytes was once thought to be mutually exclusive, *in vitro* and *in vivo* studies have demonstrated that microglia and macrophages can simultaneously express both M1 and M2 markers (Crain et al., 2013). Therefore, this dichotomy of M1/M2 is largely disputed and instead replaced with a spectrum of possible activation states between the two extremes of M1 and M2 phenotypes.

New studies have demonstrated that endocannabinoid signaling regulates microglial phenotypes (Nakagawa & Chiba, 2014). Specifically, microglia express cannabinoid receptor 2 (CB2R), a G_i protein coupled receptor (G_iPCR) that recognizes and binds the endocannabinoid 2-arachidonoylglycerol (2-AG). Activation of microglial CB2Rs by 2-AG enhances the alternative activation of M2-phenotype and resolves inflammation through the activation of 5' AMP activated protein kinase (Nakagawa & Chiba, 2014). On the other hand, cannabinoid receptor 1 (CB1R) is expressed on neurons and possibly microglia (Carlisle et al., 2002). Stimulation of CB1Rs enhances inflammatory cytokine secretion from neurons, which can directly affect the inflammatory state of microglia. However, CB1R is internalized as it is stimulated, thus allowing CB2 activity to dominate. Cannabinoids and their receptors may strongly contribute to microglia polarization states, which warrants further investigation.

The next section will examine iNOS, an important enzymatic marker expressed in the M1-phenotype that contributes to NO production and microglia functions during inflammation.

1.6 Nitric oxide synthase isoforms and nitric oxide production

NO is a gaseous signaling molecule that is produced in various mammalian cells through the catabolism of L-arginine. There are 3 enzymes that produce NO: neuronal nitric oxide synthase (nNOS), endothelial nitric oxide synthase (eNOS), and inducible

nitric oxide synthase (iNOS). Both nNOS and eNOS are constitutively present within neurons and endothelial cells, respectively, and the catalytic activity of both nNOS and eNOS are calcium dependent. On the other hand, iNOS is not highly expressed within cells under basal conditions, but its expression is upregulated in response to certain inflammatory stimuli such as cytokines, chemokines, adenosine triphosphate (ATP), certain hormones, and pathogens. Once present, iNOS is constitutively active and produces substantial amounts of NO, independent of calcium availability within the cell. Given that iNOS expression is regulated by various microenvironmental changes, the regulation of iNOS in different tissues has become an important area of research. In particular, iNOS/NO signaling in the CNS is becoming more evident in pathology, including ischemic stroke (Pérez-Asensio et al., 2005) and Alzheimer's disease (Nathan et al., 2005), which will be discussed in detail later.

1.6.1 Molecular regulation of iNOS expression

The regulation of iNOS expression in microglia is highly dependent on microenvironmental factors, ligand binding to receptors, kinase activity, as well as the induction of transcription factors. Below I will discuss key factors that regulate the expression of iNOS within microglia.

The expression of iNOS in microglia occurs in response to various proinflammatory factors including bacterial products, which are recognized by toll-like receptors (TLRs) present on the surface of microglia. Both lipopolysaccharide (LPS), a membrane component from gram-negative bacteria, and bacterial DNA have been shown to induce iNOS expression in microglia through binding to TLR4 and TLR9, respectively (Bowman et al., 2003; Dalpke et al., 2002). Additionally, proinflammatory cytokines such as IFNγ, IL-6, TNFα, and IL-1β, have been associated with inducing iNOS expression in microglia. Notably, previous studies have demonstrated that either IFNγ or IL-1β treatment alone is enough to induce iNOS expression, while IL-6 or TNFα can only induce iNOS expression when present in combination with LPS, IFNγ, or IL-1β (Jana et al., 2001). Similarly, microglia have been known to induce iNOS expression in response to Aβ-peptides, prion-proteins, and ischemic stroke (Barger & Harmon, 1997; Combs et al., 2001; Park et al.,

2002). The expression of iNOS in microglia has been shown to influence microglia function and the progression of these neurological disorders.

The iNOS gene – *NOS2* – has promotor binding sites for the transcription factors, AP1, CREB, NFκB, STAT1α, HIF-1α, and HO-1, which all regulate iNOS expression (Bhat et al., 2002; Jana et al., 2005). Of this vast array of transcription factors, NFκB activity – which occurs in response to LPS, IFNγ, and IL1β signaling – seems to be the fundamental transcription factor for iNOS expression due to the multiple promotor binding regions for NFκB within *NOS2* (Taylor et al., 1998).

NFκB is a conserved transcription factor and expressed within many different cell types. Important for regulating genes associated with inflammation, cell death, and cell proliferation, NFκB activity may also be associated with a stress response. However, NFκB activity promotes the production of pro-inflammatory cytokines in microglia to fend off infections and produce inflammation (Zusso et al., 2019). The activation of NFκB and induction of iNOS is illustrated in **Figure 1.1**. Specifically, under normal conditions NFκB is always present within the cytoplasm and its activity is sequestered through inhibitor of κB (IκB) binding (Baeuerle & Baltimore, 1988; Grimm & Baeuerle, 1993). In response to bacterial, cytokine, or chemokine receptor activation, IκB-kinase (IKK) activity phosphorylates IκB, which results in ubiquitination of IκB, proteolysis, and removal from NFκB (Brown et al., 1995; DiDonato et al., 1996). Once no longer restrained by IκB binding, NFκB is free to enter the nucleus to promote the transcription of genes including *NOS2*. This mechanism of NFκB activation and translocation occurs quickly, allowing microglia to rapidly respond to dangerous stimuli in their microenvironment.

Alternatively, stimulation of estrogen receptors (EsRs) results in inhibition of NFκB activity and anti-inflammatory effects (Chadwick et al., 2005; Valentine et al., 2000). When estrogen binds to EsRs present within the cytosol, dimerization of the EsRs allows for nuclear translocation and DNA transcription. To this extent, estrogen receptor-β (EsRβ) is expressed within microglia and when stimulated, reduces NFκB activity and iNOS expression (W. Wu et al., 2013). This anti-inflammatory response to the sex hormone estrogen in microglia may account for sex-dependent differences seen within neurological

conditions such as ischemic stroke and should be examined with respect to pathology in future studies.

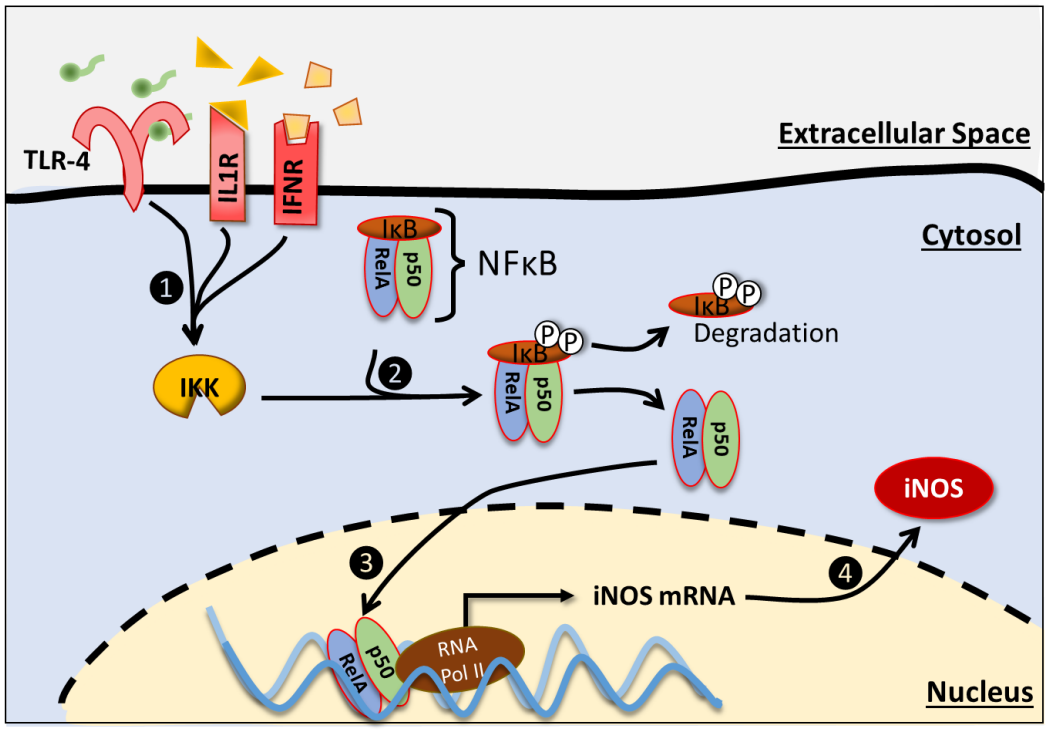

Figure 1.1 Activation of NFκB and transcription of iNOS.

1) Lipopolysaccharide binding to TLR-4, IL-1β binding to IL1R, or IFNγ binding to IFNRs on the plasma membrane of microglia induce IκB-kinase (IKK) activity. **2)** IκB-kinase phosphorylates the NFκB inhibitor IκB, which leads to the proteasomal degradation of IκB and release of active NFκB – comprised of p50 and RelA subunits. **3)** NFκB enters into the nucleus and binds the promoter region of NFκB to induce transcription of iNOS mRNA. **4)** Translation of iNOS mRNA results in iNOS protein expression within the cytosol.

1.6.2 Function and regulation of the iNOS protein

Once expressed within microglia, the constitutive activity of iNOS can catalyze large amounts of NO independent of calcium availability, which is the key difference between iNOS and the other two NOS isoforms, eNOS and nNOS. Below, I will introduce iNOS protein structure and activity, while discussing some alternative mechanisms that regulate iNOS function.

The iNOS protein is made up of an N-terminal oxygenase domain that binds heme and O_2, a calmodulin binding sight, and a C-terminal reductase domain that contains binding sights for various redox-active coenzymes. There are key differences between iNOS and the other two NOS isoforms, nNOS and eNOS. For example, calmodulin binding is required for proper iNOS protein folding, whereas nNOS and eNOS do not require calmodulin for proper protein folding (Wu et al., 1996). Importantly, the binding of calmodulin to iNOS does not dissociate and leads to constitutive activity of iNOS, while on the other hand, calmodulin binding to nNOS and eNOS depends on calcium availability within the cell (Wu et al., 1996).

As shown in **Figure 1.2**, iNOS forms a homodimer in response to heme binding of the oxygenase sight (Ghosh et al., 1997). The cofactor tetrahydrobiopterin (BH_4) as well as the substrate L-arginine are required for iNOS activity and NO-production (Lefèvre-Groboillot et al., 2005). Briefly, within the iNOS dimer, L-arginine and oxygen bind the oxygenase domain while available NADPH binds to the reductase domain (Ghosh et al., 1997; Lefèvre-Groboillot et al., 2005). Electron transfer from the reducing agent, NADPH, is shuttled to the oxygenase domain where oxygen and L-arginine are catalyzed into citrulline, NO, and H_2O (Stuehr et al., 2009). Importantly, the presence of NO may compete with oxygen for heme binding within the iNOS protein (Abu-Soud et al., 1995; Hurshman & Marletta, 1995). The competitive inhibition of NO binding to the heme may reduce iNOS activity when oxygen abundance is low (Abu-Soud et al., 1995; Hurshman & Marletta, 1995). Therefore, NO production may inhibit iNOS activity in a reversible manner depending on heme and O_2 availability within the cell.

As depicted in **Figure 1.3,** the activity of iNOS is highly dependent on the availability of L-arginine within microglia. L-arginine availability is regulated by two distinct enzymatic pathways that will be discussed next. First, the enzyme arginase actively competes with iNOS for the substrate L-arginine, and in doing so catalyzes L-arginine into urea and ornithine (Michel, 2013; Morris, 2009). The expression and activity of arginase can actively deplete the L-arginine availability within the cell and can therefore decrease iNOS activity and NO production. Second, microglia express the enzymes argininosuccinate synthase-1 (Ass1) and argininosuccinate lyase (ASL) which together catalyze the production of L-arginine from L-citrulline (Michel, 2013; Zhang et al., 2016). Therefore, the intracellular L-arginine pool can be restored from available L-citrulline allowing iNOS activity to continue to produce NO within the cell in the presence of Ass1 and ASL. In conclusion, iNOS expression and activity are regulated by many factors from the transcription level to the protein level within microglia.

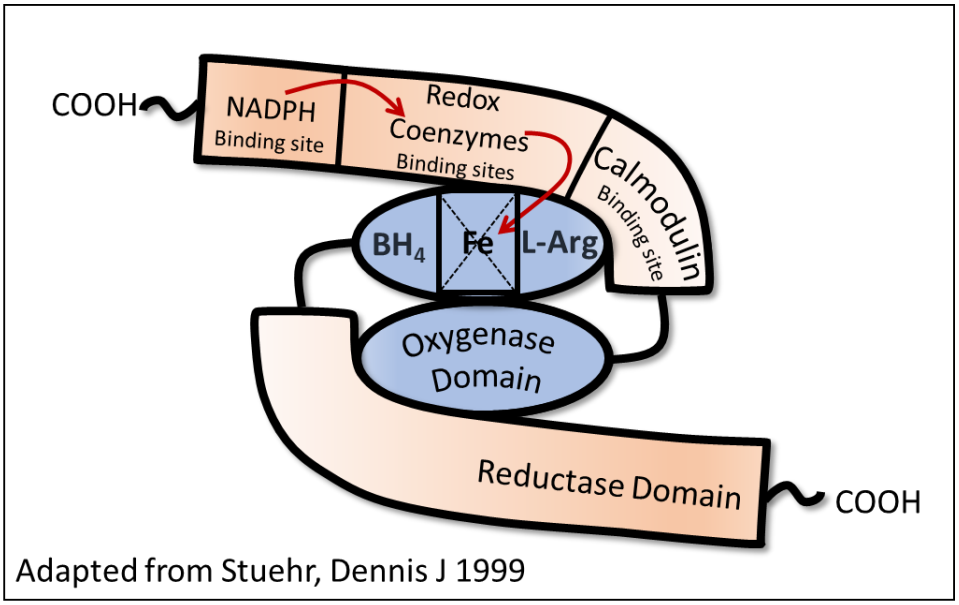

Figure 1.2 Representative iNOS protein structure.

The functional iNOS protein is comprised of a homodimer consisting of a C-terminal reductase domain (orange) and an N-terminal oxygenase domain (blue). L-arginine and oxygen bind the oxygenase domain. Electron transfer (red arrows) from NADPH binding to the reductase domain through the redox sensitive coenzymes, such as flavin adenine dinucleotide and flavin mononucleotide, to the oxygenase domain where oxygen and L-arginine is catalyzed into NO, citrulline and H_2O.

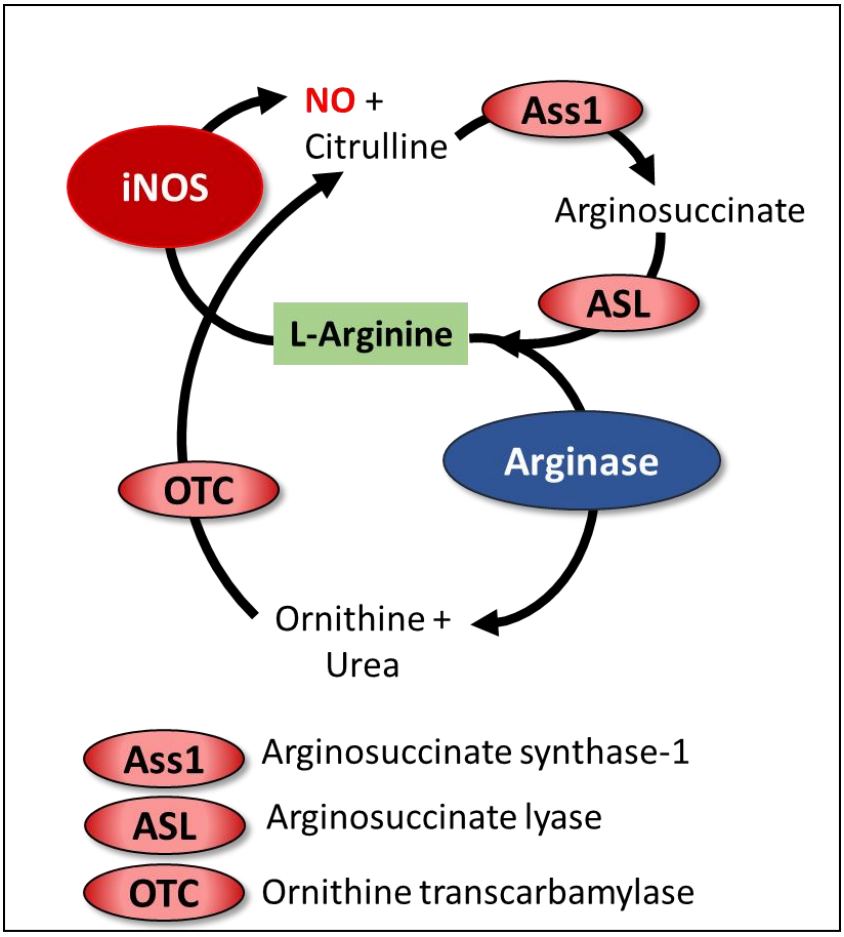

Figure 1.3 Regulation of L-arginine from the urea cycle and iNOS activity.

Catabolism of L-arginine by iNOS results in the production of NO and citrulline. The enzyme arginosuccinate synthase-1 converts citrulline into arginosuccinate, which is further catabolized into L-arginine by arginosuccinate lyase. L-arginine is also catabolized by arginase into ornithine and urea. Ornithine is converted into citrulline by ornithine transcarboxylase activity. Together, these enzymes regulate L-arginine bioavailability within cells.

1.6.3 Nitric oxide signaling pathways

As a gaseous bioactive molecule produced by many mammalian cells, NO signaling regulates a wide range of physiological functions. Originally discovered as an endothelium-derived molecule influencing vasodilation (Furchgott & Zawadzki, 1980), NO is now known to play key roles in many physiological functions such as cell proliferation, synaptic transmission, and immune functions. To carry out these functions, NO acts through two main signaling mechanisms at physiological concentrations that are most pertinent to this area of study: 1) activation of soluble guanylyl cyclase (sGC) signaling and induction of protein kinase-G (PKG), or 2) *S*-nitrosylation of protein cysteine residues. In the following sections, I will discuss these two mechanisms and how NO influences microglia activity.

1.6.3.1 Classical protein kinase-G signaling

PKG is a serine/threonine kinase that is activated by cyclic guanosine monophosphate (cGMP). As depicted in **Figure 1.4**, the production of cGMP occurs from either particulate or soluble guanylyl cyclase (pGC or sGC, respectively) activity (Baltrons et al., 2008; Prado et al., 2010). The membrane bound pGC binds to natriuretic peptides – of which there are 3 main types; atrial (ANP), B-type (BNP), and C-type (CNP) – to hydrolyze guanosine-5'-triphosphate (GTP) into cGMP. Therefore, the activity of pGC occurs independent of NO production. Boran and colleagues demonstrated how ANP-pGC-cGMP-PKG signaling induced a phagocytic phenotype of isolated rat microglia *in vitro* (Borán et al., 2008). Importantly, the phagocytic phenotype that rat microglia displayed in response to ANP-PKG signaling was associated with decreased iNOS activity, NO production, and TNFα expression (Borán et al., 2008). Therefore, ANP-PKG signaling may regulate multiple pathways and activities within microglia (Baltrons et al., 2008; Borán et al., 2008).

On the other hand, sGC is the only known endogenous receptor for NO. NO binding to the heme in sGC enhances GTP affinity for the cyclase domain and results in a higher rate of GTP hydrolysis into cGMP (Montfort et al., 2017). As introduced before,

inflammatory states of microglia are associated with increased cytokine production, iNOS expression, and NO production. Additionally, NO directly activates sGC-cGMP-PKG pathway (Coletta et al., 2012). Through this “classical” signaling pathway, iNOS/NO signaling significantly modulates microglia functions during inflammation.

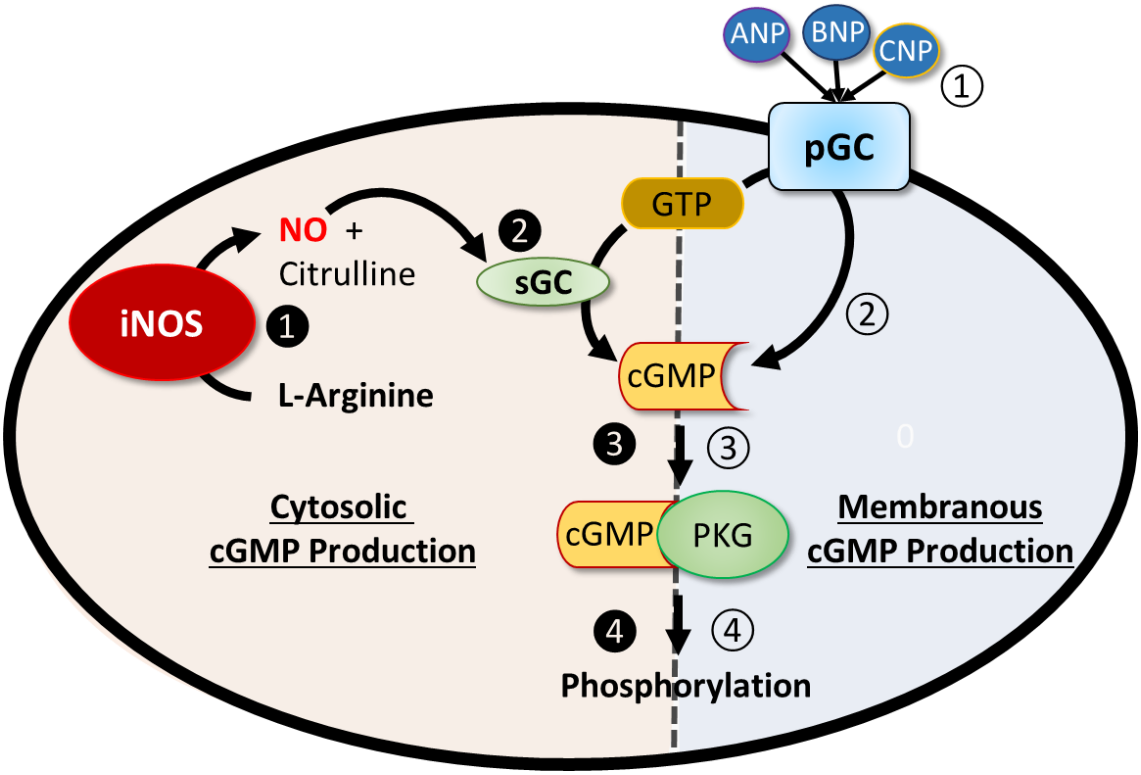

Figure 1.4 Production of cGMP from cytosolic soluble guanylyl cyclase or membranous particulate guanylyl cyclase.

Left side: **1)** L-arginine is catabolized by iNOS into NO and citrulline. **2)** NO binds soluble guanylyl cyclase (sGC) that will convert GTP into cGMP. *Right side:* **1)** Natriuretic peptides – ANP, BNP, CNP – bind to the membrane bound particulate guanylyl cyclase. **2)** particulate guanylyl cyclase converts GTP into cGMP. **3)** cGMP binds and activates PKG. **4)** PKG is a kinase that leads to the phosphorylation of proteins.

1.6.3.2 *S*-Nitrosylation of cysteine thiols

The sGC-cGMP-PKG pathway represents the classical signaling pathway for NO to regulate cellular functions. However, NO can directly interact with and modify cysteine residues in a reversible manner; this type of modification is termed *S*-nitrosylation (Hess et al., 2005; Stamler et al., 1992, 2001). S-nitrosylation of proteins is a very quick and reversible process that occurs in the presence of abundant NO in the cellular environment. *S*-Nitrosylation does not require the presence or activity of enzyme catalysts to occur but instead depends on the redox state within the cell (Stamler et al., 2001). Importantly, in a highly oxidative environment, *S*-nitrosylation of cysteine residues occurs when a protein cysteine-thiol becomes a thiol radical that can easily react with NO (Gaston, 1999). Additionally, the redox state within each cell during oxidative stress can also lead to *S*-glutathionylation. Glutathione is a low molecular mass tripeptide present within many cells including microglia (Hirrlinger et al., 2000). Glutathione acts as an antioxidant that interacts with ROS as well as reactive nitrogen species, including NO, to prevent oxidative damage within microglia (Hirrlinger et al., 2000). In a highly oxidative environment, glutathione may form thiol radicals that result in *S*-glutathione modifications on protein cysteine residues (Martínez-Ruiz & Lamas, 2007). As a result, glutathione levels reflect the redox state within macrophages and microglia, and are elevated after oxidative burst (Dobashi et al., 2001; Hirrlinger et al., 2000).

1.6.4 Regulation of iNOS expression in pathology and disease conditions

The expression of iNOS is tightly regulated and crucial for microglial functions. However, dysregulation of iNOS expression in microglia is associated with a variety of neurological illnesses such as Alzheimer's disease (Vodovotz et al., 1996) and stroke (Forster et al., 1999).

Both Alzheimer's disease and stroke are inflammatory brain disorders characterized by prolonged and elevated levels of inflammation. Widespread expression of iNOS in both Alzheimer's (Vodovotz et al., 1996) and stroke (Forster et al., 1999)

pathologies have been observed and reported. The high throughput activity of iNOS is capable of quickly inflicting both nitrosative and oxidative injury to neurons and supporting tissue. For example, iNOS/NO signaling can induce cytotoxicity from mitochondrial electron transport chain inhibition, release of free radicals, and through the promotion of secondary inflammation. Therefore, mice with genetic ablation of the iNOS protein are shown to have smaller infarcts after middle cerebral artery occlusion (Nagayama et al., 1999; Pérez-Asensio et al., 2005), and better behavioral and motor outcomes when compared to wildtype (WT) mice (Iadecola et al., 1997). Similarly, using a double transgenic mouse model that expresses human β-amyloid precursor protein and human presenilin-1, Nathan and colleagues demonstrated that ablation of iNOS protected the hAPP+hPS1 double transgenic mice from Alzheimer's-like pathology (Nathan et al., 2005). Specifically, removal of iNOS expression within the transgenic mouse model revealed significantly increased survival as well as decreased plaque load within the cortex and hippocampus, when compared to the transgenic mouse model that over-expressed iNOS (Nathan et al., 2005). Additionally, decreased microgliosis was observed in the cortex and hippocampus in the transgenic mouse model lacking iNOS compared to WT mice (Nathan et al., 2005). Evidently, chronic iNOS expression may be associated with microglia contribution to stroke and Alzheimer's pathology. However, examining how iNOS/NO signaling influences specific microglia functions will be critical in revealing potential therapeutic targets for these pathologies. The expression of iNOS and production of NO fundamentally regulates specific microglia functions such as calcium signaling and ion channels. In the following paragraphs I will discuss calcium signaling and ion channel expression in microglia.

1.7 Calcium Signaling and ion channels

Calcium is a very important second messenger that is required for many microglia functions. In response to environmental stimuli, receptors and ligand gated ion channels on the microglia cell surface are activated, resulting in intracellular calcium increase that consequently causes cytokine and chemokine secretion, migration, proliferation, and phagocytosis. Although calcium influx is important for microglia activity, it is important to note that microglial activities can be classified as either neuroprotective or neurotoxic

depending on the environmental stimuli and presence of pathology (Hanisch & Kettenmann, 2007; Hoffmann et al., 2003; Streit, 2002).

Calcium homeostasis within microglia is controlled by a wide variety of calcium channels and transporters that mediate calcium influx and efflux from the cell. Contrary to neurons that express voltage-gated calcium channels, the expression of voltage-gated calcium channels in microglia remains controversial despite evidence demonstrating the presence of mRNA transcripts for these channels (Espinosa-Parrilla et al., 2015). However, it is confirmed that microglia rely primarily on ligand gated calcium channels as well as intracellular calcium stores for excitability. Of these groups, transient receptor potential (TRP) channels as well as store operated calcium channels make up a large proportion of the calcium permeable channels expressed within microglia and will be discussed in depth.

1.7.1 TRP channels

TRP channels encompass a family of nonselective cation channels that are highly permeable to calcium as well as sodium and potassium. The TRP family contains three main subfamilies deemed vanilloid (TRPV), canonical (TRPC), and melastatin (TRPM). These three subfamilies of TRP channels share a similar structure consisting of 6 transmembrane domains that form tetramers (Gaudet, 2008). However, channel gating between these three subfamilies of TRP channels differ. TRPV channels are generally known as thermosensors, which can be activated by increased temperature and certain vanilloid compounds (Hu et al., 2004; Yao et al., 2011), while TRPC channels are known to be gated by the interaction with the calcium sensor proteins present in the endoplasmic reticulum (ER) membrane following calcium store depletion (Yuan et al., 2007).

1.7.1.1 TRPV1 ion channel

TRPV1 was the first member of the vanilloid subfamily to be discovered, with a role in temperature sensing above 42^{o}C resulting in the perception of heat and pain (Caterina et al., 1997; Marrone et al., 2017; Tominaga et al., 1998). Additionally, TRPV1 opening and subsequent calcium influx is gated by vanilloid-like compounds such as capsaicin – the active compound in chili peppers – as well as heat and low pH (Ferrer-

Montiel et al., 2012; Reilly et al., 2012). TRPV1 is localized within many cellular compartments such as the plasma membrane (PM), mitochondria, as well as the ER. Localization of TRPV1 in murine microglia is reported on the mitochondria membrane and activity of TRPV1 is important for microglia migration (Miyake et al., 2015). Moreover, application of capsaicin to cultured rat microglia leads to mitochondrial release of cytochrome c and cell death (Miyake et al., 2015), suggesting TRPV1 may regulate cell death in microglia (Kim et al., 2006). Finally, Maronne and colleagues demonstrated that TRPV1 stimulation promoted extracellular vesicle release from microglia, which interacted with neurons to increase glutamatergic neurotransmission and contribute to chronic pain (Marrone et al., 2017).

Microglia are active phagocytes that produce copious amounts of ROS through the activity of NADPH-oxidase. Using the ROS-sensitive probe 2'-7'-Dichlorodihydrofluorescein diacetate (DCFHDA) and pharmacological inhibitors of TRPV1, Schilling and Eder suggested that TRPV1 activity is correlated to NADPH-oxidase activity and ROS generation (Schilling & Eder, 2009). Conversely, a previous report demonstrated the lack of TRPV1 expression and activity in LPS-treated murine microglia (Bhatia et al., 2017). Therefore, it is important to consider alternative vanilloid channels, such as TRPV2, that may also contribute to regulating microglial functions. For example, microglia express both TRPV1 and TRPV2 ion channels, and common activators for TRPV1, such as cannabidiol, and 2APB also activate TRPV2 channels (Hassan et al., 2014).

1.7.1.2 TRPV2 ion channel

TRPV2 expression is highly abundant throughout the nervous system as well as the immune system. Within the nervous system, TRPV2 expression is reported within the paraventricular nucleus of the hypothalamus, which is a hub for osmoregulation, as well as within certain sensory and motor neurons (Wainwright et al., 2004). Additionally, throughout the immune system TRPV2 is abundantly expressed within cells including but not limited to macrophages and T-cells, and expression of TRPV2 within these cells

influences migration, phagocytosis and antigen presentation (Hassan et al., 2014; Link et al., 2010; Nagasawa et al., 2007)

TRPV2 shares over 50% sequence identity with TRPV1 while being permeable to a variety of cations including potassium, sodium, magnesium and calcium (Caterina et al., 1999). TRPV2 forms homotetramers that display greater permeability to divalent cations such as calcium over monovalent cations such as potassium and sodium (Caterina et al., 1999). The TRPV2 protein structure contains an N-terminal cytoplasmic domain consisting of ankyrin repeats, 6 transmembrane domains that orient a pore-forming loop, and lastly a C-terminal cytoplasmic domain (Gaudet, 2008). Unlike TRPV1 that is regulated by ATP and calmodulin through binding sites within its N- and C-terminal domains, TRPV2 contains a phosphatidylinositol 4,5-bisphosphate (PIP_2) binding site within its C-terminal that acts as the main regulatory process for channel gating and activity (Lishko et al., 2007; Mercado et al., 2010). Mercado and colleagues demonstrated that PIP_2 hydrolysis – by phospholipase C (PLC) – contributes to TRPV2 desensitization; therefore, TRPV2 activity is directly regulated by PIP_2 abundance (Mercado et al., 2010). Along these lines, TRPV2 has been shown to display osmolarity, mechanosensory, and thermosensitive channel regulation; however, thermosensitive regulation occurs only at temperatures of $>50^oC$, which is well outside physiological range (Katanosaka et al., 2018; Muraki et al., 2003).

The signaling of TRPV2 is highly dependent on its translocation from the membrane of intracellular organelles to the plasma membrane as illustrated in **Figure 1.5**. TRPV2 translocation from subcellular compartments occurs within minutes upon insulin like-growth factor-1 stimulation, and this process is highly dependent on phosphoinositide-3-kinase (PI3K) signaling (Kanzaki et al., 1999), and glycosylation (Jahnel et al., 2003). Although microglia express TRPV2, not much is known about how TRPV2 activity influences microglia functions. Hassan and colleagues previously demonstrated that cannabidiol treatment on cultured microglia induces TRPV2 translocation, calcium influx, modulating microglia functions and activities (Hassan et al., 2014). Interestingly, knockdown of TRPV2 induces degradation of inhibitor of nuclear factor-κB-α (IκBα) and attenuates LPS-induced expression of TNFα and IL-6 mRNA (Yamashiro et al. 2010), indicating that TRPV2 is also involved in toll-like receptor 4 signaling.

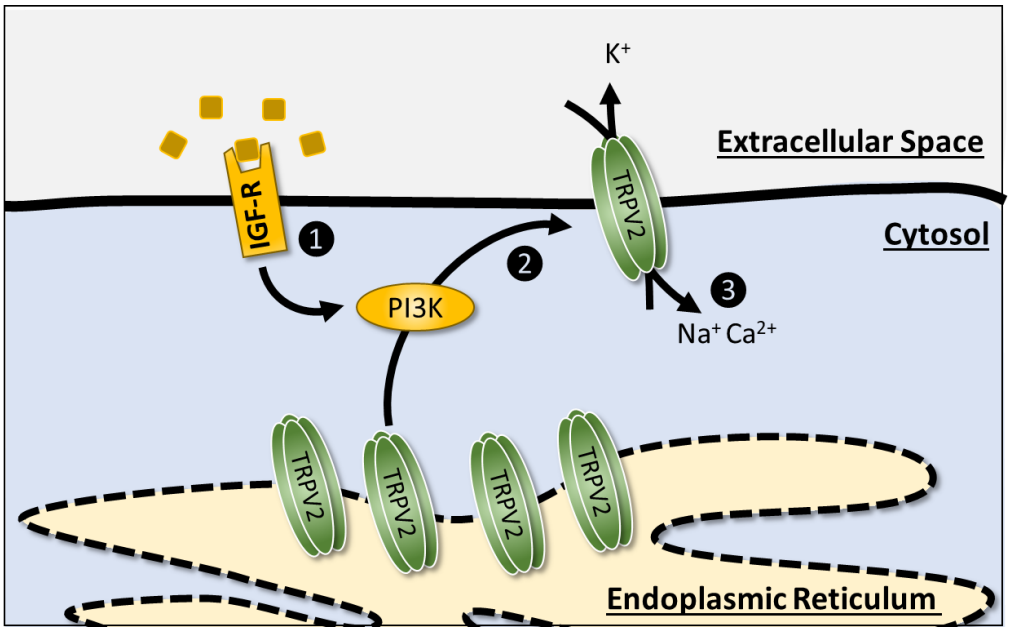

Figure 1.5 TRPV2 translocation the plasma membrane.

1) Cytokines such as insulin like growth factor 1 binds and activates IGFR on the plasma membrane surface of microglia. 2) IGFR activation induces PI3K activity that results in TRPV2 translocation from the endoplasmic reticulum membrane to the plasma membrane. 3) plasma membrane expression of TRPV2 allows for potassium, sodium, and calcium ion shuttling.

1.7.1.3 Store operated calcium entry and stromal interaction molecule

Calcium homeostasis within microglia also relies on endogenous calcium stores in the ER (Ohana et al., 2009). The induction of store operated calcium entry is depicted in **Figure 1.6.** For instance, the binding of extracellular ATP to purinergic P_2Y_x receptors (P_2Y_xR) – a group of G_qPCRs – on the microglia plasma membrane activates PLC to catabolize PIP_2 into diacylglycerol (DAG) and inositol trisphosphate (IP_3) (Ferreira & Schlichter, 2013). Binding of IP_3 to the IP_3 receptors on the ER induces calcium release from the ER lumen into the cytosol of the cell (Ferreira & Schlichter, 2013; Marques et al., 2009; Michaelis et al., 2015; Parekh, 2010). The calcium depleted ER lumen is sensed by the protein stromal interaction molecule 1 (STIM1) (Parekh, 2010; Roos et al., 2005; Srikanth & Gwack, 2012).

STIM1 is a transmembrane protein that spans the ER membrane (Parekh, 2010). Under "resting conditions", the luminal end of STIM1 contains an EF hand region that binds to endogenous calcium present in the ER lumen (Stathopulos et al., 2006). Upon significant calcium depletion in the ER lumen, calcium dissociates from the EF hand region, which leads to unfolding and exposure of the sterile-α-motif (SAM) domain in STIM1. This SAM domain is required for STIM1 oligomerization (Liou et al., 2007; Stathopulos et al., 2006). The cytoplasmic domain of STIM1 contains multiple regions that will physically or electrostatically interact with the intracellular domains of store operated calcium channel proteins on the plasma membrane surface of microglia to induce calcium influx from the extracellular space. For instance, oligomerized STIM1 can bind and gate the opening of TRPC channels as well as Orai-formed calcium release activated calcium (CRAC) channels (Moccia et al., 2015; Parekh, 2010; Srikanth & Gwack, 2012) on the microglia PM (Kettenmann et al., 2011; Worley et al., 2007).

The rapid and transient increase of intracellular calcium from ER calcium release and store operated calcium entry (SOCE) is a strong indication that microglia are responding to microenvironmental cues. Ultimately, the calcium influx through store operated calcium channels (SOCCs) facilitates ER-calcium refilling (Liou et al., 2007).

Specifically, the sarcoplasmic-endoplasmic reticulum calcium ATPase (SERCA) on the ER membrane actively pumps calcium from the cytosol into the ER lumen to replenish the intracellular calcium reservoir (Periasamy & Kalyanasundaram, 2007).

It was previously shown that knockout of STIM significantly attenuates SOCE, demonstrating its importance in gating SOCC activity (Baba et al., 2008; Oh-hora et al., 2008; Stiber et al., 2008; Varga-Szabo et al., 2008). Additionally, NO has been shown to regulate Orai-mediated calcium influx through *S*-nitrosylation of STIM1 in cardiomyocytes (Gui et al., 2018). Although this *S*-nitrosylation event has been shown to inhibit calcium influx in cardiomyocytes, the effect on microglia remains unknown, with further research required to uncover any interaction between STIM and iNOS-mediated NO production.

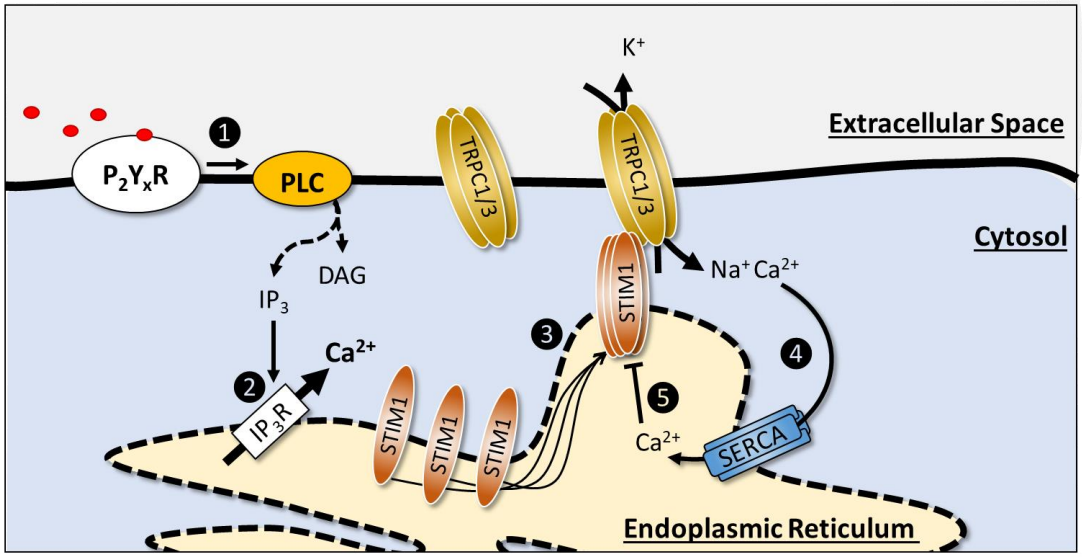

Figure 1.6 Store operated calcium entry in microglia.

1) ATP or ADP binding to P_2Y_xR induce PLC-mediated cleavage of PIP_2 into IP_3 and DAG. **2)** IP_3 binding to IP_3Rs on the endoplasmic reticulum membrane cause calcium efflux from the ER into the cytosol of the cell. **3)** Decreased calcium within the ER lumen results in STIM1 oligomerization and clustering to gate store operated TRPC channels on the plasma membrane of microglia. **4)** elevated levels of calcium within the cytosol is pumped into the ER lumen through SERCA. **5)** Increased calcium levels within the ER lumen inhibits STIM1 clustering to restrain store operated calcium channel activity.

1.7.1.4 TRPC ion channels

A variety of TRPC channels are present on microglia (Ohana et al., 2009) and form nonselective cation channels that are permeable to calcium (Echeverry et al., 2016; Worley et al., 2007). Previous research has shown that TRPC1 and TRPC3 function as SOCCs, however TRPC3 displays larger permeability to calcium over monovalent ions than TRPC1. Importantly, TRPC1 directly interacts with STIM1 while TRPC3 may interact with STIM1 by forming heteromultimers with TRPC1 (Yuan et al., 2007). By examining the mRNA expression of various TRPC channels within cultured neonatal rat microglia, Ohana and colleagues demonstrated that TRPC6 expression > TRPC1 > TRPC3 ≥ TRPC4 > TRPC5 (Ohana et al., 2009). However, by examining mRNA expression of TRPC channels within cultured microglia from postnatal rodent retinas, Papanikolaou and colleagues showed that TRPC1 expression > TRPC3 > TRPC6 mRNA expression (Papanikolaou et al., 2017). Interestingly, these differences could stem from microglia performing tissue specific activities in the cortex versus the retina. For instance, TRPC3 was shown to be important for brain-derived neurotrophic factor (BDNF)-mediated suppression of NO production in microglia (Mizoguchi & Monji, 2017). TRPC1 has also been suggested to inhibit microglia inflammatory pathways (Sun et al., 2014).

Although a variety of TRPC channels are present and active in microglia, the function and regulation of these channels are not entirely known. For instance, NO can directly regulate TRPC channel activity and function through *S*-nitrosylation of cysteine residues Cys^{553} and Cys^{558} conserved within TRPC1, TRPC4, and TRPC5 (Wong et al., 2010; Xu et al., 2008; Yoshida et al., 2006). Although this nitrosylation event on TRPC channels remains controversial in endothelial cells, with some studies suggesting it mediates calcium influx (Yoshida et al., 2006) while others suggesting it attenuates calcium influx (Wong et al., 2010), the effect within microglia has not been fully examined.

1.8 Microglia Phagocytosis

Phagocytosis is a process where cellular debris and pathogens are removed by specialized cells called phagocytes. Within the CNS, microglia are considered the

professional phagocytes engulfing cellular debris from apoptotic cells, removing pathogens, and eliminating redundant neurons and synapses within the central nervous system. Microglia possess a wide array of receptors that allows them to recognize and remove variety of structures and objects through phagocytosis.

1.8.1 TLRs and TLR4 mediated phagocytosis

Traditionally, microglial phagocytosis is often associated with the recognition and removal of foreign substances such as viruses and bacteria through their toll-like receptors (TLRs) that recognize foreign substances. For example, TLR4 recognizes bacterial endotoxins such as LPS (Olson & Miller, 2004), TLR7 detects single stranded RNA (Lehmann et al., 2012), and TLR9 recognizes viral and bacterial DNA (Dalpke et al., 2002). Additionally, TLR4 has been implicated in phagocytosis of α-synuclein (Stefanova et al., 2011) and Aβ-plaques (Balducci et al., 2017) commonly seen in Parkinson's disease and Alzheimer's disease, respectively. By examining Parkinson's pathology in TLR4 knockout mice, Stefanova and colleagues demonstrated that uptake of α-synuclein was reduced when compared to mice expressing functional TLR4 (Stefanova et al., 2011). Moreover, TLR4 activity has been shown to have both beneficial and detrimental influences on AD pathology. For example, TLR4 signaling has been associated with increasing microglial phagocytosis and the removal of Aβ-plaques (Balducci et al., 2017). However, TLR4 has also been shown to reduce microglial phagocytosis of Aβ-plaques (Li et al., 2015). Although TLR4 seems necessary for microglial activation in various disease conditions, its beneficial or detrimental activity with respect to AD may be correlated to the progression and stage of the disease.

1.8.2 Complement receptor 3 mediated phagocytosis

Complement receptor 3 (CR3) – also known as macrophage-1 antigen, or CD11b/CD18 integrin – is a surface receptor expressed on monocytes with a crucial role in phagocytosis. Microglia also possess CR3s that recognize and remove redundant neuronal precursor cells, synapses, dendritic spines, and boutons during development and throughout life. Specifically, CR3 in microglia can recognize and phagocytose complement

proteins that tag weak synapses, dendrites, or redundant neuronal precursor cells to remove the abnormal or redundant neuronal structures (Cunningham et al., 2013; Marín-Teva et al., 2004; Paolicelli et al., 2011; Wakselman et al., 2008; Zhan et al., 2014). For example, Marín-Teva and colleagues have demonstrated that microglia phagocytose and promote Purkinje neuron death through CR3 receptors during cerebellar development (Marín-Teva et al., 2004). Along those lines, knockout of CR3 receptors in microglia resulted in an increase in the number of viable neurons in the hippocampus (Wakselman et al., 2008). Finally, mice lacking certain complement components also displayed decreased microglia phagocytosis and increased number of synapses within the postnatal murine brain (Schafer et al., 2012). These studies further demonstrate the importance of CR3 signaling in regulating the number of progenitor cells and synapses within the brain.

1.8.3 Fc-receptors and Fc$_\gamma$-receptor mediated phagocytosis

Another family of phagocytic receptors present on the surface of microglia are Fc receptors (Nakahara & Aiso, 2006; Song et al., 2002). These receptors recognize and mediate phagocytosis of cellular structures that are opsonized by antibodies.

Antibodies, also known as immunoglobulins, are produced and released by B-lymphocytes and comprised of four polypeptide chains; two identical light chains and two identical heavy chains (Katzmann et al., 2002). The heavy chain consists of a variable domain – specific for the antigen of interest – as well as a constant domain that contains the Fc-region. The variable regions of both a light and heavy chain comes together to form the unique binding site that will recognize the antigen of interest. The Fc region of the antibody is formed from the linking of both heavy chain constant regions.

When the variable region of the antibody binds the antigen of interest, the Fc-region remains exposed allowing receptors on the surface of professional phagocytes to recognize and remove the opsonized target (Young et al., 1985). Each antibody subtype has a specific Fc-receptor associated with recognizing its Fc-region. The most prominent Fc-receptor in microglia is the Fcγ-receptor (FcγR) that recognizes the Fc-region of IgG antibodies (Peress et al., 1993; Ulvestad et al., 1994; Vedeler et al., 1994). Microglia express 4 different subtypes of FcγRs: FcγRI, FcγRIIa/b, FcγRIII, FcγRIV (Vedeler et al., 1994).

Although stimulation of most FcγRs result in microglia activation, FcγRIIb stimulation attenuates cell activity. The next section will discuss FcγR endogenous signaling within microglia.

1.8.3.1 FcγR endogenous signaling cascade in phagocytes

Although FcγRs have similar structure, there exists a specific amino acid sequence motif in the cytosolic portion of the FcγR that activates or inhibits the cell. For example, stimulation of FcγRI/IIa/III/IV in phagocytes leads to phagocytosis and release of inflammatory mediators, whereas stimulation of FcγIIb dampens these responses. These activating or inhibitory sequence motifs are termed immunoreceptor tyrosine-based activation motifs (ITAMs) or immunoreceptor tyrosine based inhibitory motifs (ITIMS), respectively. Generally, ITAMs activation causes the recruitment of kinases (Underhill & Goodridge, 2007) while ITIM activation leads to the recruitment of phosphatases (Verbrugge & Meyaard, 2005), which will be discussed in greater detail next.

The majority of FcγRs fall into the category of promoting cell activation and include FcγRI/IIa/III/IV. When one of these FcγRs bind to the Fc-region of an IgG antibody, there is clustering of the FcγR ITAM region. A member of the Src kinase family recognizes and phosphorylates two conserved tyrosine residues in the ITAM region (Underhill & Goodridge, 2007). Upon ITAM phosphorylation, the tyrosine kinase Syk binds to the ITAM region and activates downstream proteins such as PI3K or PLC (Underhill & Goodridge, 2007). Importantly, inhibiting Src or Syc kinases reduced phagocytosis in human microglia (Song et al., 2002). Downstream signaling cascades from activation of FcγRs are depicted in **(Figure 1.7)**. Activation of PLC and hydrolysis of PIP_2 into DAG and IP_3 result in SOCE (Getahun & Cambier, 2015). The mobilized calcium influx further influences cell activity. For instance, phagocytosis, oxidative burst, and cytotoxicity occur in response to stimulation of FcγRs in microglia. Specifically, FcγR stimulation in microglia activates the transcription factor NFκB (Jin et al., 2006) and phagocytosis (Le et al., 2001; Sánchez-Mejorada & Rosales, 1998; Song et al., 2004). Additionally, in the presence of inflammatory mediators such as IFNγ, TNFα, or LPS, microglia increase FcγR expression (Loughlin et al., 1992, 1993; Woodroofe et al., 1989)

and superoxide production from NADPH oxidase activity (Haslund-Vinding et al., 2017; Lanone et al., 2005). Microglia produce superoxide to kill engulphed pathogens within the lysosome of the microglia. These results all demonstrate the importance of FcγR on microglia phagocytosis of opsonized targets.

On the other hand, FcγRIIb activity has distinct differences that result in inhibitory signaling within cells (Verbrugge & Meyaard, 2005). For example, stimulation of FcγRIIb by IgG antibodies results in a member of the Src kinase family phosphorylating two conserved tyrosine residues, similar to ITAM signaling. Upon ITIM phosphorylation, the phosphatases SHP-1 and SHIP1 are recruited (Verbrugge & Meyaard, 2005) and dephosphorylate downstream signaling molecules that inhibit PI3K signaling **(Figure 1.7)**. Although inhibitory in nature, FcγRIIb has a lower affinity for IgG than FcγRI. Importantly, out of all the FcγR subtypes, FcγRI has the highest affinity for IgG. Nevertheless, both ITAM and ITIM amino acid motifs are crucial for endogenous signaling of FcγRs. Expression of FcγRs on microglia respond to both development and pathological conditions, which will be discussed next.

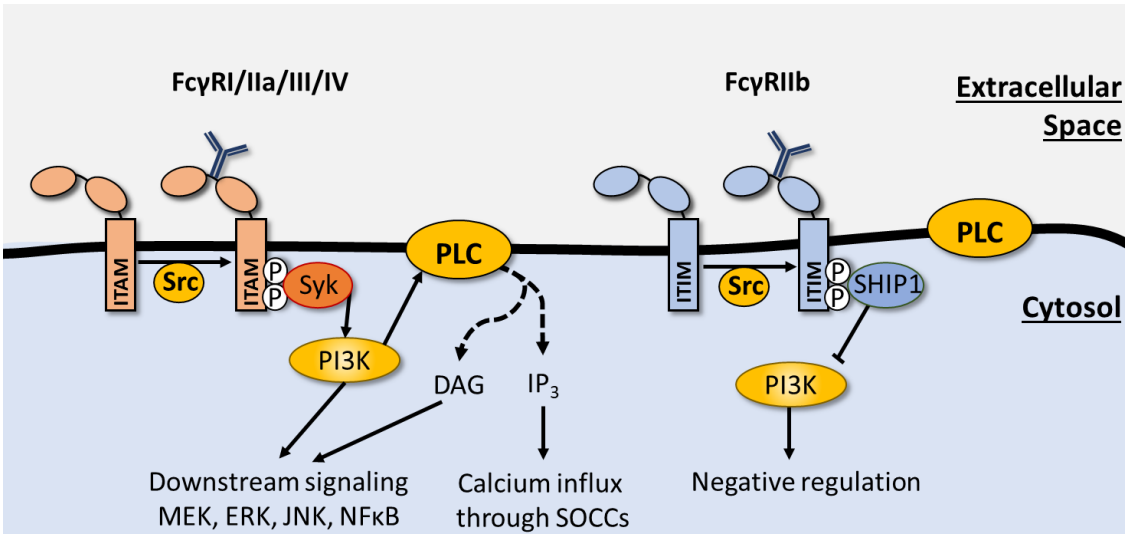

Figure 1.7 Activating and inhibitory signaling of Fcγ Receptors.

Left side: Activating FcγRI/IIa/III/IV signaling. Upon antibody binding, a Src kinase will phosphorylate the ITAM region of the FcγRI/IIa/III/IV. The Tyrosine kinase Syk will recognize and bind the phosphorylated ITAM region and activate PI3K. Activation of PI3K induces PLC-mediated cleavage of PIP_2 into DAG and IP_3 resulting in downstream signaling through MEK, ERK, JNK, NFκB, or SOCCs respectively. *Right side:* Inhibitory FcγRIIb signaling. Upon antibody binding, a Src kinase will phosphorylate the ITIM region of the FcγRIIb. The tyrosine kinase SHIP1 will recognize and bind the phosphorylated ITIM region and inhibit PI3K activity. Decreased PI3K activity has negative effects on PLC activity and downstream signaling through MEK, ERK, JNK, NFκB, as well as SOCCs.

1.8.3.2 FcγR expression in pathology and disease conditions.

A vast number of studies show FcγR expression and activity in microglia during pathology and disease (Lunnon et al., 2011; Peress et al., 1993). Many degenerative diseases such as Alzheimer's and Parkinson's disease contain misfolded proteins and protein aggregates such as Aβ-plaques, α-synuclein, and hyper-phosphorylated tau that exist in neurons or extracellular locations. Additionally, increased FcyR expression and neuroinflammation has been observed in these CNS pathologies (Cao et al., 2010; Cribbs et al., 2012; Lira et al., 2011; Lunnon et al., 2011). For example, in Alzheimer's disease, FcγRI-III was observed in microglia and surrounding plaques throughout the white matter and cortex of humans (Peress et al., 1993; Ulvestad et al., 1994). Interestingly, intraperitoneal injection of antibodies against Aβ plaques were able to pass the blood brain barrier and reduce the presence of Aβ plaques in the frontal cortex of a mouse model of AD (Bard et al., 2000). Using an *ex vivo* model, Bard and colleagues further demonstrated that the antibodies against Aβ-plaques triggered Fcγ-receptors on microglia and removal of the Aβ-plaques (Bard et al., 2000). Similarly in multiple sclerosis patients, microglia displayed ameboid phenotype and FcγRI,II,III immunostaining around white matter lesions while in healthy controls microglia displayed a ramified phenotype and faint FcγRI, II, III white matter staining (Nyland et al., 1980; Ulvestad et al., 1994; Vedeler et al., 1994). These reports support a strong correlation between increased FcγR expression and progression of neurodegenerative diseases.

As previously mentioned, FcγR expression is widely associated with inflammation from increased NFκB activity. For example, FcγR levels increase in microglia exposed to IFNγ, TNFα, or LPS, or in the presence of superoxide (Haslund-Vinding et al., 2017; Lanone et al., 2005; Loughlin et al., 1992, 1993; Woodroofe et al., 1989). However, it remains unclear if FcγR expression is solely beneficial or detrimental. For instance, to examine the effect of microglial FcγRs on dopaminergic neuron degeneration, Cao and colleagues virally transfected human α-synuclein into WT or FcγR knockout ($Fc\gamma R^{-/-}$) mice as a model of Parkinson's disease (Cao et al., 2010). The authors demonstrated that virally transfecting human α-synuclein in $Fc\gamma R^{-/-}$ mice displayed less NFκB expression and less inflammation than WT mice expressing FcγRs (Cao et al., 2010). Furthermore, following

α-synuclein transfection, the FcγR$^{-/-}$ mice displayed less NADPH oxidase activity and more viable dopaminergic neurons compared to WT mice expressing FcγRs (Cao et al., 2010). The results from this study suggest that proinflammatory signaling through FcγRs may contribute to the progression of pathology in some neurodegenerative diseases.

1.8.4 The role of NO in phagocytosis

Microglial phagocytosis is finely regulated by environmental factors and endogenous metabolites such as ROS and reactive nitrogen species (RNS). During phagocytosis, large quantities of RNS and ROS are produced by professional phagocytes through a process termed oxidative burst (Kettenmann et al., 2011). High concentrations of RNS and ROS act as antimicrobials to degrade and neutralize engulfed pathogens and cell debris (Khanna et al., 2001). The presence of NO is correlated with increased microglial phagocytosis (Kakita et al., 2013; Kraus et al., 2010; Scheiblich & Bicker, 2016). For example, Kraus and colleagues demonstrated that attenuated NFκB activity reduces BV2 microglia phagocytosis of zymosan-labelled fluorescent particles as well as iNOS expression and NO production (Kraus et al., 2010). Additionally, Kakita and colleagues demonstrated that exogenous application of the NO donor sodium nitroprusside enhanced the number of latex beads phagocytosed in a rodent microglia culture (Kakita et al., 2013). Furthermore, using an *in vitro* microglia-neuron coculture paradigm, Scheiblich and Bicker demonstrated that both LPS or NO activated BV2 microglia and increase phagocytosis of cultured neurons (Scheiblich & Bicker, 2016). In contrast, the addition of an NO scavenging compound or the iNOS inhibitor L-NAME significantly attenuated the ability for BV2 microglia to phagocytose neurons in this same paradigm (Scheiblich & Bicker, 2016). The correlation between increased iNOS activity/NO production and increased phagocytosis is substantiated in another study where inhibition of iNOS activity in microglia cultures – using the inhibitor L-NMMA – caused significantly decreased phagocytosis of latex beads (Kakita et al., 2013). All of these studies strongly demonstrate a correlation between NO production and phagocytic activity; however, the underlying mechanism in which NO regulates phagocytosis is still unknown.

1.8.5 The role of TRPV2 in phagocytosis

The TRPV2 ion channel is critical for professional phagocytes such as macrophages and microglia to carry out phagocytosis (Hassan et al., 2014; Link et al., 2010). Specifically, peritoneal macrophages isolated from TRPV2 deficient mice display decreased binding and phagocytosis of complement, IgG, and zymosan particles when compared to WT peritoneal macrophages (Lévêque et al., 2018; Link et al., 2010). Importantly, Link and colleagues demonstrated that macrophages lacking TRPV2 displayed a significantly decreased calcium influx in response to 50 μM tetrahydrocannabinol (THC) stimulation *in vitro* (Link et al., 2010). Additionally, WT macrophages displayed decreased membrane depolarization and phagocytic binding of beads in the absence of extracellular sodium, further suggesting that a membrane depolarization through the nonselective cation channel TRPV2 is important for FcγR mediated phagocytosis (Link et al., 2010).

A more recent study in 2018 demonstrated that calcium influx through TRPV2 channels is critical for TRPV2-mediated bacterial phagocytosis in macrophages (Lévêque et al., 2018). Specifically, using peripheral blood monocytes collected from healthy human patients, Lévêque and colleagues demonstrated that TRPV2 is highly localized to lipid rafts in macrophages exposed to *P. aeruginosa* (Lévêque et al., 2018). Lipid rafts are specialized membrane domains with highly organized and specific expressions of glycolipids, cholesterol, and proteins that signal membrane ruffling, protein trafficking, and phagocytosis. In response to *P. aeruginosa* infection, TRPV2 on intracytoplasmic lipid rafts are translocated to the plasma membrane within 60 min to further facilitate calcium influx and phagocytosis (Lévêque et al., 2018). Taken together, these results demonstrate the importance of TRPV2 activity for facilitating phagocytosis in professional phagocytes such as macrophages. Future research examining if TRPV2 activity is important for phagocytosis in specifically microglia remains to be explored.

1.9 Microglia Proliferation

Microglia constitute 10% of the glial population within the adult brain. Studies have shown that the vast majority of microglia proliferation occurs early during CNS development, as previously described. Briefly, upon infiltration of the neuroepithelium, microglia progenitors rapidly proliferate to encompass the entire CNS. After this rapid stage of proliferation, microglia remain within the CNS parenchyma and only proliferate to maintain a stable cell number within the healthy brain (Nikodemova et al., 2015). It is of particular importance for the population of microglia to remain stable because behavioral and learning deficits may arise otherwise (Parkhurst et al., 2013).

During postnatal development in mice, microglia proliferation has been shown to occur up until the first two postnatal weeks before a rapid decline thereafter (Nikodemova et al., 2015). This decline in proliferative microglia is likely due to both increased microglia apoptosis as well as decreased microglia proliferation (Nikodemova et al., 2015). Although the rate of microglia proliferation is strongly linked to CNS development, the underlying factors that contribute to microglia proliferation *in vivo* remains controversial and requires more consideration.

Previous studies have shown that cytokines influence microglia proliferation. For example, colony-stimulating-factor-1 receptor (CSF-1R), present on the surface of microglia, induces microglia proliferation when stimulated by macrophage colony-stimulating-factor-1 (m-CSF1) or IL-34 (Greter et al., 2012; Nandi et al., 2012; Ohsawa et al., 2000; Wang et al., 2012). Additionally, IL34 or m-CSF1 deficient mice display decreased microglia numbers within the CNS (Wang et al., 2012; Węgiel et al., 1998). More importantly, intracellular calcium signaling is known to regulate cell-cycle progression and proliferation (Lu & Means, 1993). For example, lysophosphatidic acid or BDNF induction of store operated calcium channels resulted in increased murine microglia proliferation *in vitro* (Mizoguchi et al., 2009; Möller et al., 2001). Therefore, examining intracellular calcium signaling as well as calcium binding proteins that regulate proliferation may prove beneficial when attempting to understand the regulation of microglia proliferation (Lu & Means, 1993).

In addition to the normal developmental pathways that regulate microglia proliferation, certain molecular characteristics and signaling pathways have been shown to contribute to microglia proliferation. Specifically, NO (Kawahara et al., 2001) and elevated cAMP levels (Fujita et al., 1998) have been associated with decreased microglia proliferation *in vitro*. However, the mechanisms by which NO regulates microglia proliferation remains elusive.

1.9.1 Calcium-dependent regulation of NFAT in proliferation

Calcium critically regulates cell activity by interacting with calcium regulatory proteins such as calmodulin. Calmodulin is essential for regulating the activity of many kinases and phosphatases that affect cell-cycle progression and proliferation (Berchtold & Villalobo, 2014; Casal et al., 2001). Of particular importance is the phosphatase calcineurin, which is known to activate various isoforms of nuclear factor of activated T-cells (NFAT) that are present within microglia (Furman & Norris, 2014). **Figure 1.8** illustrates how calcium regulates NFAT activation. Specifically, when intracellular calcium levels increase, calmodulin binding to calcineurin activates phosphatase activity resulting in the dephosphorylation of NFAT (Furman & Norris, 2014; Rao et al., 1997). Once dephosphorylated, NFAT translocates into the nucleus to regulate the transcription of targeted genes (Rao et al., 1997).

The isoforms NFATC1 and NFATC2 – also known as NFAT2 and NFAT1 respectively – have been shown to be abundantly expressed within microglia as well as influence microglia activation (Manocha et al., 2017; Nagamoto-Combs & Combs, 2010). For example, both calcineurin and NFAT activity have been implicated in chronic inflammatory responses within glia. Specifically, stimulation with the bacterial-endotoxin LPS increased the expression and activity of NFAT within microglia, which was also accompanied by increases in proinflammatory cytokine secretions (Nagamoto-Combs & Combs, 2010). Additionally, deletion of NFATC2 within microglia cultures attenuated proinflammatory cytokine production and secretion in a mouse model of Alzheimer's disease (Manocha et al., 2017).

The importance of NFATC2 activity on cell-cycle progression and proliferation is becoming clearer (Carvalho et al., 2007). NFATC2 inhibits cell-cycle progression from G_1/S or G_2/M by interacting with the promoter regions of cyclin-dependent kinase-4 as well as cyclin A2 respectively, to downregulate their expression (Baksh et al., 2000; Carvalho et al., 2007) **(Figure 1.9)**. Finally, NFATC2 also stimulates the expression of p21 (Santini et al., 2001), which is a potent cyclin dependent kinase inhibitor that will be discussed in greater detail next.

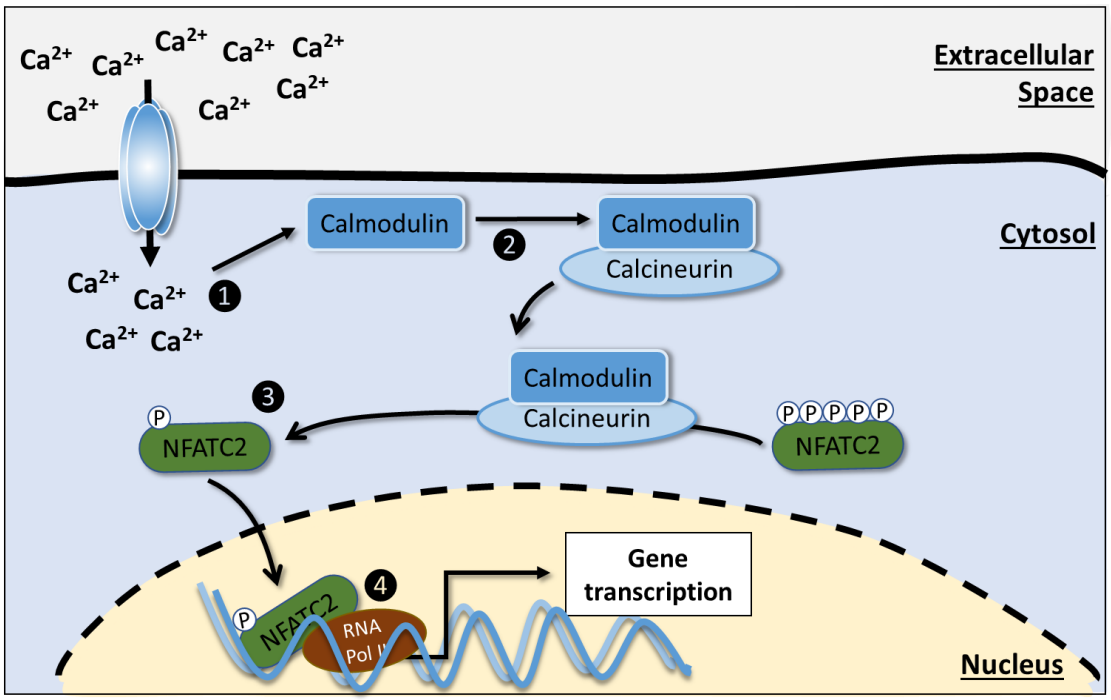

Figure 1.8 Regulation of NFATC2 activity and nuclear translocation.

1) Increased cytoplasmic calcium binds calmodulin. 2) Calmodulin binding to the phosphatase calcineurin to dephosphorylate NFATC2. 3) Dephosphorylated NFATC2 can enter into the nucleus to transcribe genes. 4) NFATC2 transcription of genes such as p21 occurs.

1.9.2 p21 in cell proliferation and cell-cycle progression.

The cell cycle is divided into four phases that include G_1, S-phase, G_2, and mitosis. Many environmental factors such as nutrients, temperature, pH, and oxygen availability contribute to regulating cell proliferation. These factors influence cell proliferation by regulating the activity of cyclin-dependent kinases (CDKs), which are a group of kinases that regulate cell-cycle progression. Generally, CDKs require binding to a cyclin before their kinase ability becomes active. A variety of CDKs exist, however CDK2 is a cyclin dependent kinase that binds a variety of different cyclins to regulate the cell-cycle transition from G_1 to S phase as well as G_2 to mitosis. Importantly, cyclin-dependent kinase inhibitor 1 – also known as p21 – acts potently on CDK2 to inhibit cell-cycle progression from G_1 to S and G_2 to mitosis **(Figure 1.9)**. In fact, cells with high levels of p21 eventually enter G0, a phase where DNA replication stops, and the cell exists in a quiescent state outside of the cell-cycle. Although proliferation stops in G0, other cellular functions and activities are still maintained.

As a key regulator of the cell-cycle, the expression of p21 occurs from either p53 -dependent or -independent mechanisms (Karimian et al., 2016; Macleod et al., 1995). The transcription factor p53 is known as a tumor suppressor that restricts cell proliferation/division in response to DNA damage from UV radiation or oxidative stress. The ability for p53 to inhibit cell proliferation occurs mainly through upregulating the expression of p21 (He et al., 2005). It is known that within the promoter region of the p21 gene there exists five binding sites for p53 (Saramaki, 2006). In response to phosphorylation, p53 becomes more stable and the transcriptional activity increases, ultimately increasing p21 expression.

On the other hand, there exists other transcription factors that have been linked to p21 expression as well. For example, breast cancer susceptibility gene 1 (BRCA1) has been shown to induce p21 gene expression independent of p53 activity. Additionally, the cytokine TGFβ signals to increase p21 expression. Specifically, TGFβ signaling results in the phosphorylation of SMAD1/3 proteins and leads to the activation of mitogen activated protein kinases (MAPKs) that increase p21 expression. Furthermore, inflammatory

mediators that upregulate NFκB have been shown to induce the expression of p21 in a cell line for myeloid leukemia.

Along those lines, LPS treatment on BV2 microglia cultures induced p21 expression and arrested microglia in G1 (Kaneko et al., 2015). Additionally, IL-1β produced from LPS stimulated microglia cultures mediated cell-cycle arrest through p53-p21 signaling in neuronal progenitor cells (Guadagno et al., 2015). These results further demonstrate an association between inflammation induction and the inhibition of cell-cycle progression. Considering NO is produced during inflammation, the effect of NO on proliferation will be discussed next.

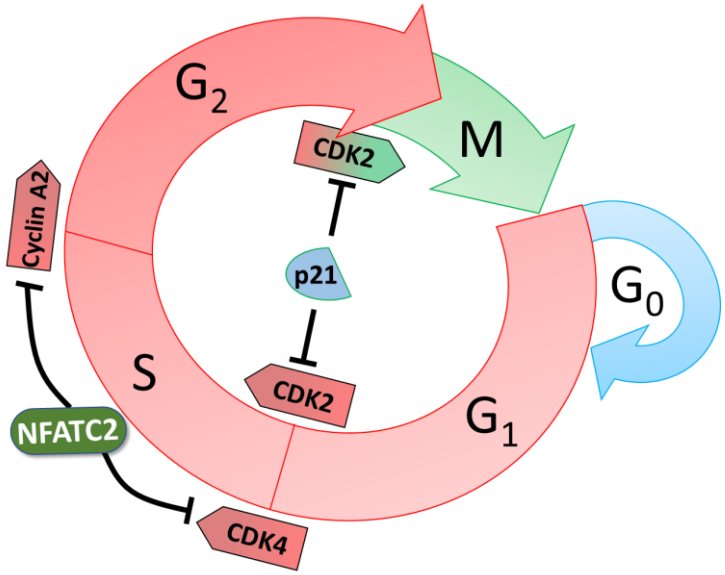

Figure 1.9 Cell-cycle regulation by NFATC2 and p21.

The cell-cycle contains three main stages: 1) Interphase (red) is comprised of an initial growth stage (G_1), DNA synthesis stage (S), and a second growth stage (G_2). 2) Mitosis (green, M) is comprised stages that result in equal division of DNA material into the two daughter cells. 3) G0 is the quiescent state of the cell-cycle where no proliferation occurs. Cyclins and CDKs are proteins that regulate cell-cycle progression through the different stages. NFATC2 can inhibit CDK4 and cyclin A2 expression to inhibit interphase progression at the G_1/S phase and S/G_2 phase respectively. The expression of p21 inhibits CDK2 activity and cell-cycle progression at the G_1/S phase and G_2/M phase.

1.9.3 Microglia proliferation in pathology and disease conditions

Microglia are the most prominent immune cells that infiltrate and proliferate within gliomas (Simmons et al., 2011), however, the extent of the proliferative role microglia play within gliomas remains disputed. Importantly, microglia present within the glioma mass express increased anti-inflammatory cytokines such as IL-10 and TGFβ1 (Komohara et al., 2008; Qiu et al., 2011; Zhang et al., 2007) that promote tumor progression, while also expressing reduced iNOS (He et al., 2006; Kim et al., 2006). Further examination into how microglia proliferation contributes to glioma progression could be beneficial for future studies.

Microglia may proliferate to combat a variety of challenges within the brain (Denes et al., 2007; Solomon et al., 2006). In stroke for instance, microglia proliferate to produce enough phagocytes to efficiently remove damaged cells and debris from infarcted regions, helping with tissue repair. Importantly, in a mouse model of stroke whereby a middle cerebral artery occlusion was employed to induce an infarct, microglia proliferation in the peri-infarct region occurred during the first three days (Denes et al., 2007). However, under a more severe stroke condition, such as induced by 60 min treatment with middle cerebral artery occlusion, microglia proliferation significantly declined in the peri-infarct region (Denes et al., 2007). Importantly, negligible microglia proliferation was seen within the infarct core (Denes et al., 2007). Notably, increased nNOS activity in neurons during acute stroke phase, along with increased iNOS induction within astrocytes and microglia during chronic stroke phase, results in a pathological production of NO within ischemic tissue throughout stroke recovery. This pathological production of NO results in cell stress, DNA damage, and may contribute to the restrained proliferative properties of microglia within the ischemic core (Li et al., 2013). Examining how iNOS/NO signaling regulates proliferation in microglia may uncover potential therapeutic targets for pathological conditions that exhibit altered microglia proliferation.

1.9.4 The role of NO in cell proliferation

NO is widely known as a modulator of proliferation in many cells including microglia. Generally, NO attenuates cell-cycle progression through influencing a variety of cellular signaling mechanisms. The expression of iNOS in breast cancer cells is correlated with a reduced proliferation rate (Reveneau et al., 1999). Additionally, macrophage-like cells treated with IL6 displayed increased iNOS expression and cell-cycle arrest in G_1/S and G_2/M (Takagi et al., 1994). Importantly, NO is widely associated with inhibiting cell-cycle progression in the G_1/S or G_2/M stage. To inhibit proliferation, NO mainly targets p21 (Gansauge et al., 1998; Gu et al., 2000; Huang et al., 2005; Oliveira et al., 2003). For example, in MG5 microglia, NO increases the expression of p21 and inhibits cell-cycle progression (Kawahara et al., 2001). The inhibitory effect of NO on MG5 microglia proliferation occurs independent of cGMP signaling (Kawahara et al., 2001) while NO signaling through sGC-cGMP-PKG pathway is important for p21 enhancement (Gu et al., 2000; Gu & Brecher, 2000). These results indicate that the underlying mechanism by which NO signaling increases p21 expression is unclear and should be examined in primary microglia to fully understand the competing effects of NO on microglial proliferation.

1.9.5 The role of TRPV2 in differentiation and proliferation

The expression and activity of TRPV2 has been associated with cell differentiation (Morelli et al., 2012) and proliferation (Nabissi et al., 2010). For example, in astrocytes, inhibition of TRPV2 expression has been shown to enhance proliferation (Zhang et al., 2016). Using oxygen-glucose deprivation and reoxygenation as a stroke model *in vitro*, Zhang and colleagues demonstrated an increase in TRPV2 expression in cultured rat astrocytes when compared to controls (Zhang et al., 2016). Furthermore, blocking TRPV2 activity increased astrocyte proliferation in their stroke paradigm (Zhang et al., 2016). Along those lines, the expression and activity of TRPV2 inhibits glioma cell proliferation (Nabissi et al., 2010). Glioblastoma multiform is a very fast growing and aggressive cancer consisting of glia cells such as astrocytes and oligodendrocytes. Using human glioma tissues, Nabissi and colleagues demonstrated a progressive decline in TRPV2 mRNA

expression with glioma severity (Nabissi et al., 2010). Furthermore, using the U87MG glioblastoma cell line, Morelli and colleagues demonstrated that inhibiting TRPV2 expression increased the percentage of cells incorporating BrdU and hence proliferation (Morelli et al., 2012). In contrast, overexpression of TRPV2 in a glioblastoma cell line increased apoptosis and reduced the viability of the cells (Morelli et al., 2012; Nabissi et al., 2010). These results demonstrate TRPV2 channel activity negatively regulates cell proliferation.

1.9.6 The role of store operated calcium channels in proliferation

SOCCs are known to facilitate proliferation in many types of cells. For instance, Chen and colleagues demonstrated in multiple cell lines that SOCCs mediate the transition of G_1/S phase while a decrease in SOCE is necessary for G_2/M transition (Chen et al., 2016). Specifically, calcium influx through Orai channels directly induce CDK2 phosphorylation and activity (Chen et al., 2016). Importantly, knockdown or inhibition of Orai channels in a cervical cancer cell line using siRNA or SKF96365, respectively, results in decreased levels of pCDK2 (Chen et al., 2016). Additionally, mouse embryonic fibroblasts lacking STIM1 expression display decreased nuclear expression of pCDK2, whereas STIM1 over-expression further rescues pCDK2 nuclear expression in the mouse embryonic fibroblasts (Chen et al., 2016).

Along those lines, STIM1 positively regulates proliferation in smooth muscle cells (Guo et al., 2009; Takahashi et al., 2007). Specifically, using a model of carotid artery damage in rats, Guo and colleagues demonstrated that vascular smooth muscle cells that lack STIM1 show cell arrest in G_1/S and decreased proliferation in damaged tissue when compared to controls (Guo et al., 2009). Furthermore, Takahashi and colleagues demonstrated that knockdown of STIM1 suppress cell proliferation and protein synthesis in primary human coronary artery smooth muscle cells (Takahashi et al., 2007). Specifically, Takahashi and colleagues demonstrated that knockdown of STIM1 caused decreased thymidine incorporation into DNA as well as decreased radio labelled leucine incorporation into proteins (Takahashi et al., 2007). Furthermore, the authors proposed that STIM1 mediated calcium influx may progress cell growth through CREB phosphorylation

and activation (Takahashi et al., 2007), which occurs in response to STIM1-mediated calcium entry (Pulver-Kaste et al., 2006; Pulver et al., 2004). Evidently, this data demonstrates a positive influence of SOCC activity on cell-cycle progression and proliferation.

1.10 Rationale, hypothesis, aims

1.10.1 Rationale

In response to inflammatory signals, activated microglia display elevated iNOS expression and NO production, increased phagocytic activity, and reduced proliferation. It is known that the production of NO is linked to the phagocytic and proliferative activity of microglia, however, the underlying mechanism(s) by which NO regulates microglia phagocytosis and proliferation remains elusive.

Previous studies have demonstrated that microglia phagocytosis and proliferation is tightly regulated by intracellular calcium levels. As non-excitable cells, microglia rely on calcium entry primarily through TRP channels. Indeed, the expression of iNOS and production of NO are correlated with phagocytosis and proliferation of other phagocytes such as macrophages, however, the effect of NO on TRP-mediated calcium dynamics in microglia remains largely elusive. For example, Yoshida and colleagues demonstrated that NO activates a variety of TRP channels through *S*-nitrosylation of two conserved cysteine residues, C^{553} and C^{558} (Yoshida et al., 2006), whereas Gui and colleagues showed that NO induces *S*-nitrosylation of two cysteine residues in the intraluminal region of STIM1, which reduces STIM1 oligomerization and the calcium influx through SOCCs (Gui et al., 2018). However, very little information about the effects of NO on TRP channel activity in microglia exist in the literature. Therefore, I set out to examine the interaction of NO on calcium permeable TRP channels that regulates microglial phagocytosis and proliferation.

1.10.2 Hypothesis

It was hypothesized that iNOS/NO signaling critically regulates TRP ion channel activity and microglia functions such as phagocytosis and proliferation. Specifically, we hypothesize that NO signaling will increase TRPV2 channel activity while decreasing SOCC activity, and in doing so increase microglial phagocytosis and attenuate microglia proliferation respectively.

1.10.3 Aims

To test this hypothesis, I carried out *in vivo* experiments in WT and iNOS knockout ($iNOS^{-/-}$) mice, and *in vitro* experiments in primary microglia isolated from these mice with the following aims.

Aim 1:

To examine if a signaling mechanism between NO and TRPV2 channel activity exists and if this interaction influences microglia phagocytosis *in vitro*.

Aim 2:

To examine if NO signaling influences SOCCs within murine microglia *in vitro*.

Aim 3:

To examine if NO regulates microglia proliferation at p10 and if NO regulates microglia proliferation through a PKG-mediated mechanism *in vitro*.

Aim 4:

To examine if the NO-TRPV2 interaction regulates microglia cell-cycle progression *in vitro*.

1.11 References

Abu-Soud, H. M., Wang, J., Rousseau, D. L., Fukuto, J. M., Ignarro, L. J., & Stuehr, D. J. (1995). Neuronal Nitric Oxide Synthase Self-inactivates by Forming a Ferrous-Nitrosyl Complex during Aerobic Catalysis. Journal of Biological Chemistry, 270(39), 22997–23006. https://doi.org/10.1074/jbc.270.39.22997

Alliot, Francoise, Godin, I., & Pessac, B. (1999). Microglia derive from progenitors , originating from the yolk sac , and which proliferate in the brain. Developmental Brain Research, 117, 145–152.

Alliot, Françoise, Lecain, E., Grima, B., & Pessac, B. (1991). Microglial progenitors with a high proliferative potential in the embryonic and adult mouse brain. Proceedings of the National Academy of Sciences, 88(4), 1541–1545. https://doi.org/10.1073/pnas.88.4.1541

Baba, Y., Nishida, K., Fujii, Y., Hirano, T., Hikida, M., & Kurosaki, T. (2008). Essential function for the calcium sensor STIM1 in mast cell activation and anaphylactic responses. Nature Immunology, 9(1), 81–88. https://doi.org/10.1038/ni1546

Bachstetter, A. D., Morganti, J. M., Jernberg, J., Schlunk, A., Mitchell, S. H., Brewster, K. W., Hudson, C. E., Cole, M. J., Harrison, J. K., Bickford, P. C., & Gemma, C. (2011). Fractalkine and CX3CR1 regulate hippocampal neurogenesis in adult and aged rats. Neurobiology of Aging, 32(11), 2030–2044. https://doi.org/10.1016/j.neurobiolaging.2009.11.022

Baeuerle, P. A., & Baltimore, D. (1988). I kappa B: a specific inhibitor of the NF-kappa B transcription factor. Science (New York, N.Y.), 242(4878), 540–546. https://doi.org/10.1126/science.3140380

Baksh, S., DeCaprio, J. A., & Burakoff, S. J. (2000). Calcineurin regulation of the mammalian G0/G1 checkpoint element, cyclin dependent kinase 4. Oncogene, 19(24), 2820–2827. https://doi.org/10.1038/sj.onc.1203585

Balducci, C., Frasca, A., Zotti, M., La Vitola, P., Mhillaj, E., Grigoli, E., Iacobellis, M., Grandi, F., Messa, M., Colombo, L., Molteni, M., Trabace, L., Rossetti, C., Salmona, M., & Forloni, G. (2017). Toll-like receptor 4-dependent glial cell activation mediates the impairment in memory establishment induced by β-amyloid

oligomers in an acute mouse model of Alzheimer's disease. Brain, Behavior, and Immunity, 60, 188–197. https://doi.org/10.1016/j.bbi.2016.10.012

Baltrons, M. A., Borán, M. S., Pifarré, P., & García, A. (2008). Regulation and Function of Cyclic GMP-Mediated Pathways in Glial Cells. Neurochemical Research, 33(12), 2427–2435. https://doi.org/10.1007/s11064-008-9681-1

Bard, F., Cannon, C., Barbour, R., Burke, R.-L., Games, D., Grajeda, H., Guido, T., Hu, K., Huang, J., Johnson-Wood, K., Khan, K., Kholodenko, D., Lee, M., Lieberburg, I., Motter, R., Nguyen, M., Soriano, F., Vasquez, N., Weiss, K., … Yednock, T. (2000). Peripherally administered antibodies against amyloid β-peptide enter the central nervous system and reduce pathology in a mouse model of Alzheimer disease. Nature Medicine, 6(8), 916–919. https://doi.org/10.1038/78682

Barger, S. W., & Harmon, A. D. (1997). Microglial activation by Alzheimer amyloid precursor protein and modulation by apolipoprotein E. Nature, 388(6645), 878–881. https://doi.org/10.1038/42257

Berchtold, M. W., & Villalobo, A. (2014). The many faces of calmodulin in cell proliferation, programmed cell death, autophagy, and cancer. Biochimica et Biophysica Acta (BBA) - Molecular Cell Research, 1843(2), 398–435. https://doi.org/10.1016/j.bbamcr.2013.10.021

Bhat, N. R., Feinstein, D. L., Shen, Q., & Bhat, A. N. (2002). p38 MAPK-mediated Transcriptional Activation of Inducible Nitric-oxide Synthase in Glial Cells. Journal of Biological Chemistry, 277(33), 29584–29592. https://doi.org/10.1074/jbc.M204994200

Bhatia, H. S., Roelofs, N., Muñoz, E., & Fiebich, B. L. (2017). Alleviation of Microglial Activation Induced by p38 MAPK/MK2/PGE2 Axis by Capsaicin: Potential Involvement of other than TRPV1 Mechanism/s. Scientific Reports, 7(1), 116. https://doi.org/10.1038/s41598-017-00225-5

Biber, K., Neumann, H., Inoue, K., & Boddeke, H. W. G. M. (2007). Neuronal 'On' and 'Off' signals control microglia. Trends in Neurosciences, 30(11), 596–602. https://doi.org/10.1016/j.tins.2007.08.007

Borán, M. S., Baltrons, M. A., & García, A. (2008). The ANP-cGMP-protein kinase G pathway induces a phagocytic phenotype but decreases inflammatory gene

expression in microglial cells. Glia, 56(4), 394–411. https://doi.org/10.1002/glia.20618

Bowman, C. C., Rasley, A., Tranguch, S. L., & Marriott, I. (2003). Cultured astrocytes express toll-like receptors for bacterial products. Glia, 43(3), 281–291. https://doi.org/10.1002/glia.10256

Brown, K., Gerstberger, S., Carlson, L., Franzoso, G., & Siebenlist, U. (1995). Control of I kappa B-alpha proteolysis by site-specific, signal-induced phosphorylation. Science, 267(5203), 1485–1488. https://doi.org/10.1126/science.7878466

Cao, S., Theodore, S., & Standaert, D. G. (2010). Fcγ receptors are required for NF-κB signaling, microglial activation and dopaminergic neurodegeneration in an AAV-synuclein mouse model of Parkinson's disease. Molecular Neurodegeneration, 5(1), 42. https://doi.org/10.1186/1750-1326-5-42

Cardona, A. E., Pioro, E. P., Sasse, M. E., Kostenko, V., Cardona, S. M., Dijkstra, I. M., Huang, D., Kidd, G., Dombrowski, S., Dutta, R., Lee, J.-C., Cook, D. N., Jung, S., Lira, S. A., Littman, D. R., & Ransohoff, R. M. (2006). Control of microglial neurotoxicity by the fractalkine receptor. Nature Neuroscience, 9(7), 917–924. https://doi.org/10.1038/nn1715

Carlisle, S. ., Marciano-Cabral, F., Staab, A., Ludwick, C., & Cabral, G. . (2002). Differential expression of the CB2 cannabinoid receptor by rodent macrophages and macrophage-like cells in relation to cell activation. International Immunopharmacology, 2(1), 69–82. https://doi.org/10.1016/S1567-5769(01)00147-3

Carvalho, L. D. S., Teixeira, L. K., Carrossini, N., Caldeira, A. T. N., Ansel, K. M., Rao, A., & Viola, J. P. B. (2007). The NFAT1 Transcription Factor is a Repressor of Cyclin A2 Gene Expression. Cell Cycle, 6(14), 1789–1795. https://doi.org/10.4161/cc.6.14.4473

Casal, C., Tusell, J. M., & Serratosa, J. (2001). Role of calmodulin in the differentiation/activation of microglial cells. Brain Research, 902(1), 101–107. https://doi.org/10.1016/S0006-8993(01)02380-0

Caterina, M. J., Rosen, T. A., Tominaga, M., Brake, A. J., & Julius, D. (1999). A capsaicin-receptor homologue with a high threshold for noxious heat. Nature, 398(6726), 436–441. https://doi.org/10.1038/18906

Caterina, M. J., Schumacher, M. A., Tominaga, M., Rosen, T. A., Levine, J. D., & Julius, D. (1997). The capsaicin receptor: a heat-activated ion channel in the pain pathway. Nature, 389(6653), 816–824. https://doi.org/10.1038/39807

Chadwick, C. C., Chippari, S., Matelan, E., Borges-Marcucci, L., Eckert, A. M., Keith, J. C., Albert, L. M., Leathurby, Y., Harris, H. A., Bhat, R. A., Ashwell, M., Trybulski, E., Winneker, R. C., Adelman, S. J., Steffan, R. J., & Harnish, D. C. (2005). Identification of pathway-selective estrogen receptor ligands that inhibit NFkB transcriptional activity. Proceedings of the National Academy of Sciences, 102(7), 2543–2548. https://doi.org/10.1073/pnas.0405841102

Chamak, B., & Mallat, M. (1991). Fibronectin and laminin regulate thein vitro differentiation of microglial cells. Neuroscience, 45(3), 513–527. https://doi.org/10.1016/0306-4522(91)90267-R

Chen, Y., Chen, Y., Chen, Y., Chiu, W., & Shen, M. (2016). The STIM1-Orai1 pathway of store-operated Ca 2 + entry controls the checkpoint in cell cycle G1 / S transition. Nature Publishing Group, February, 1–13. https://doi.org/10.1038/srep22142

Cipriani, R., Villa, P., Chece, G., Lauro, C., Paladini, A., Micotti, E., Perego, C., De Simoni, M.-G., Fredholm, B. B., Eusebi, F., & Limatola, C. (2011). CX3CL1 Is Neuroprotective in Permanent Focal Cerebral Ischemia in Rodents. Journal of Neuroscience, 31(45), 16327–16335. https://doi.org/10.1523/JNEUROSCI.3611-11.2011

Coletta, C., Papapetropoulos, A., Erdelyi, K., Olah, G., Modis, K., Panopoulos, P., Asimakopoulou, A., Gero, D., Sharina, I., Martin, E., & Szabo, C. (2012). Hydrogen sulfide and nitric oxide are mutually dependent in the regulation of angiogenesis and endothelium-dependent vasorelaxation. Proceedings of the National Academy of Sciences, 109(23), 9161–9166. https://doi.org/10.1073/pnas.1202916109

Combs, C. K., Karlo, J. C., Kao, S.-C., & Landreth, G. E. (2001). β-Amyloid Stimulation of Microglia and Monocytes Results in TNFα-Dependent Expression of Inducible

Nitric Oxide Synthase and Neuronal Apoptosis. The Journal of Neuroscience, 21(4), 1179–1188. https://doi.org/10.1523/JNEUROSCI.21-04-01179.2001

Crain, J. M., Nikodemova, M., & Watters, J. J. (2013). Microglia express distinct M1 and M2 phenotypic markers in the postnatal and adult central nervous system in male and female mice. Journal of Neuroscience Research, 91(9), 1143–1151. https://doi.org/10.1002/jnr.23242

Cribbs, D. H., Berchtold, N. C., Perreau, V., Coleman, P. D., Rogers, J., Tenner, A. J., & Cotman, C. W. (2012). Extensive innate immune gene activation accompanies brain aging, increasing vulnerability to cognitive decline and neurodegeneration: a microarray study. Journal of Neuroinflammation, 9(1), 643. https://doi.org/10.1186/1742-2094-9-179

Cuadros, M. A., & Navascués, J. (1998). The origin and differentiation of microglial cells during development. Progress in Neurobiology, 56(2), 173–189. https://doi.org/10.1016/S0301-0082(98)00035-5

Cuadros, M. A., Rodríguez-Ruiz, J., Calvente, R., Almendros, A., Marín-Teva, J. L., & Navascués, J. (1997). Microglia development in the quail cerebellum. The Journal of Comparative Neurology, 389(3), 390–401. https://doi.org/10.1002/(SICI)1096-9861(19971222)389:3<390::AID-CNE3>3.0.CO;2-W

Cunningham, C. L., Martinez-Cerdeno, V., & Noctor, S. C. (2013). Microglia Regulate the Number of Neural Precursor Cells in the Developing Cerebral Cortex. Journal of Neuroscience, 33(10), 4216–4233. https://doi.org/10.1523/JNEUROSCI.3441-12.2013

Dalpke, A. H., Schäfer, M. K.-H., Frey, M., Zimmermann, S., Tebbe, J., Weihe, E., & Heeg, K. (2002). Immunostimulatory CpG-DNA Activates Murine Microglia. The Journal of Immunology, 168(10), 4854–4863. https://doi.org/10.4049/jimmunol.168.10.4854

Davalos, D., Grutzendler, J., Yang, G., Kim, J. V., Zuo, Y., Jung, S., Littman, D. R., Dustin, M. L., & Gan, W. (2005). ATP mediates rapid microglial response to local brain injury in vivo. Nature Neuroscience, 8(6), 752–758. https://doi.org/10.1038/nn1472

Dénes, Á., Ferenczi, S., Halász, J., Környei, Z., & Kovács, K. J. (2008). Role of CX3CR1 (Fractalkine Receptor) in Brain Damage and Inflammation Induced by Focal

Cerebral Ischemia in Mouse. Journal of Cerebral Blood Flow & Metabolism, 28(10), 1707–1721. https://doi.org/10.1038/jcbfm.2008.64

Denes, A., Vidyasagar, R., Feng, J., Narvainen, J., McColl, B. W., Kauppinen, R. A., & Allan, S. M. (2007). Proliferating Resident Microglia after Focal Cerebral Ischaemia in Mice. Journal of Cerebral Blood Flow & Metabolism, 27(12), 1941–1953. https://doi.org/10.1038/sj.jcbfm.9600495

DiDonato, J., Mercurio, F., Rosette, C., Wu-Li, J., Suyang, H., Ghosh, S., & Karin, M. (1996). Mapping of the inducible IkappaB phosphorylation sites that signal its ubiquitination and degradation. Molecular and Cellular Biology, 16(4), 1295–1304. https://doi.org/10.1128/MCB.16.4.1295

Dobashi, K., Aihara, M., Araki, T., Shimizu, Y., Utsugi, M., Iizuka, K., Murata, Y., Hamuro, J., Nakazawa, T., & Mori, M. (2001). Regulation of LPS induced IL-12 production by IFN-gamma and IL-4 through intracellular glutathione status in human alveolar macrophages. Clinical and Experimental Immunology, 124(2), 290–296. https://doi.org/10.1046/j.1365-2249.2001.01535.x

Donnelly, D. J., Longbrake, E. E., Shawler, T. M., Kigerl, K. A., Lai, W., Tovar, C. A., Ransohoff, R. M., & Popovich, P. G. (2011). Deficient CX3CR1 Signaling Promotes Recovery after Mouse Spinal Cord Injury by Limiting the Recruitment and Activation of Ly6Clo/iNOS+ Macrophages. Journal of Neuroscience, 31(27), 9910–9922. https://doi.org/10.1523/JNEUROSCI.2114-11.2011

Echeverry, S., Rodriguez, M. J., & Torres, Y. P. (2016). Transient Receptor Potential Channels in Microglia: Roles in Physiology and Disease. Neurotoxicity Research, 30(3), 467–478. https://doi.org/10.1007/s12640-016-9632-6

Espinosa-Parrilla, J. F., Martínez-Moreno, M., Gasull, X., Mahy, N., & Rodríguez, M. J. (2015). The L-type voltage-gated calcium channel modulates microglial pro-inflammatory activity. Molecular and Cellular Neuroscience, 64, 104–115. https://doi.org/10.1016/j.mcn.2014.12.004

Ferreira, R., & Schlichter, L. C. (2013). Selective Activation of KCa3.1 and CRAC Channels by P2Y2 Receptors Promotes Ca2+ Signaling, Store Refilling and Migration of Rat Microglial Cells. PLoS ONE, 8(4), e62345. https://doi.org/10.1371/journal.pone.0062345

Ferrer-Montiel, A., Fernández-Carvajal, A., Planells-Cases, R., Fernández-Ballester, G., González-Ros, J. M., Messeguer, À., & González-Muñiz, R. (2012). Advances in modulating thermosensory TRP channels. Expert Opinion on Therapeutic Patents, 22(9), 999–1017. https://doi.org/10.1517/13543776.2012.711320

Fontainhas, A. M., Wang, M., Liang, K. J., Chen, S., Mettu, P., Damani, M., Fariss, R. N., Li, W., & Wong, W. T. (2011). Microglial morphology and dynamic behavior is regulated by ionotropic glutamatergic and GABAergic neurotransmission. PLoS ONE, 6(1), e15973. https://doi.org/10.1371/journal.pone.0015973

Forster, C., Clark, H. B., Ross, M. E., & Iadecola, C. (1999). Inducible nitric oxide synthase expression in human cerebral infarcts. Acta Neuropathologica, 97(3), 215–220. https://doi.org/10.1007/s004010050977

Fujita, H., Tanaka, J., Maeda, N., & Sakanaka, M. (1998). Adrenergic agonists suppress the proliferation of microglia through β2-adrenergic receptor. Neuroscience Letters, 242(1), 37–40. https://doi.org/10.1016/S0304-3940(98)00003-2

Fukushima, S., Furube, E., Itoh, M., Nakashima, T., & Miyata, S. (2015). Robust increase of microglia proliferation in the fornix of hippocampal axonal pathway after a single LPS stimulation. Journal of Neuroimmunology, 285, 31–40. https://doi.org/10.1016/j.jneuroim.2015.05.014

Furchgott, R. F., & Zawadzki, J. V. (1980). The obligatory role of endothelial cells in the relaxation of arterial smooth muscle by acetylcholine. Nature, 288(5789), 373–376. https://doi.org/10.1038/288373a0

Furman, J. L., & Norris, C. M. (2014). Calcineurin and glial signaling: neuroinflammation and beyond. Journal of Neuroinflammation, 11(1), 158. https://doi.org/10.1186/s12974-014-0158-7

Gansauge, S., Nussler, A. K., Beger, H. G., & Gansauge, F. (1998). Nitric oxide-induced apoptosis in human pancreatic carcinoma cell lines is associated with a G1-arrest and an increase of the cyclin-dependent kinase inhibitor p21WAF1/CIP1. Cell Growth & Differentiation : The Molecular Biology Journal of the American Association for Cancer Research, 9(8), 611–617. http://www.ncbi.nlm.nih.gov/pubmed/9716178

Gaston, B. (1999). Nitric oxide and thiol groups. Biochimica et Biophysica Acta (BBA) - Bioenergetics, 1411(2–3), 323–333. https://doi.org/10.1016/S0005-2728(99)00023-7

Gaudet, R. (2008). TRP channels entering the structural era. The Journal of Physiology, 586(15), 3565–3575. https://doi.org/10.1113/jphysiol.2008.155812

Getahun, A., & Cambier, J. C. (2015). Of ITIMs, ITAMs, and ITAMis: revisiting immunoglobulin Fc receptor signaling. Immunological Reviews, 268(1), 66–73. https://doi.org/10.1111/imr.12336

Ghosh, D. K., Wu, C., Pitters, E., Moloney, M., Werner, E. R., Mayer, B., & Stuehr, D. J. (1997). Characterization of the Inducible Nitric Oxide Synthase Oxygenase Domain Identifies a 49 Amino Acid Segment Required for Subunit Dimerization and Tetrahydrobiopterin Interaction †. Biochemistry, 36(35), 10609–10619. https://doi.org/10.1021/bi9702290

Ginhoux, F., Lim, S., Hoeffel, G., Low, D., & Huber, T. (2013). Origin and differentiation of microglia. Frontiers in Cellular Neuroscience, 7(April), 1–14. https://doi.org/10.3389/fncel.2013.00045

Greter, M., Lelios, I., Pelczar, P., Hoeffel, G., Price, J., Leboeuf, M., Kündig, T. M., Frei, K., Ginhoux, F., Merad, M., & Becher, B. (2012). Stroma-Derived Interleukin-34 Controls the Development and Maintenance of Langerhans Cells and the Maintenance of Microglia. Immunity, 37(6), 1050–1060. https://doi.org/10.1016/j.immuni.2012.11.001

Grimm, S., & Baeuerle, P. A. (1993). The inducible transcription factor NF-κB: structure-function relationship of its protein subunits. Biochemical Journal, 290(2), 297–308. https://doi.org/10.1042/bj2900297

Gu, M., & Brecher, P. (2000). Nitric Oxide-Induced Increase in p21 Expression During the Cell Cycle in Aortic Adventitial Fibroblasts. Arterioscler Thromb Vasc Biol., 20, 27–34.

Gu, M., Lynch, J., & Brecher, P. (2000). Nitric Oxide Increases p21 Waf1 / Cip1 Expression by a cGMP-dependent Pathway That Includes Activation of Extracellular Signal-regulated Kinase and p70 S6k *. 275(15), 11389–11396.

Guadagno, J., Swan, P., Shaikh, R., & Cregan, S. P. (2015). Microglia-derived IL-1β triggers p53-mediated cell cycle arrest and apoptosis in neural precursor cells. Cell Death & Disease, 6(6), e1779–e1779. https://doi.org/10.1038/cddis.2015.151

Gui, L., Zhu, J., Lu, X., Sims, S. M., Lu, W.-Y., Stathopulos, P. B., & Feng, Q. (2018). S -Nitrosylation of STIM1 by Neuronal Nitric Oxide Synthase Inhibits Store-Operated Ca 2+ Entry. Journal of Molecular Biology, 430(12), 1773–1785. https://doi.org/10.1016/j.jmb.2018.04.028

Guo, R.-W., Wang, H., Gao, P., Li, M.-Q., Zeng, C.-Y., Yu, Y., Chen, J.-F., Song, M.-B., Shi, Y.-K., & Huang, L. (2009). An essential role for stromal interaction molecule 1 in neointima formation following arterial injury. Cardiovascular Research, 81(4), 660–668. https://doi.org/10.1093/cvr/cvn338

Hanisch, U.-K., & Kettenmann, H. (2007). Microglia: active sensor and versatile effector cells in the normal and pathologic brain. Nature Neuroscience, 10(11), 1387–1394. https://doi.org/10.1038/nn1997

Haslund-Vinding, J., McBean, G., Jaquet, V., & Vilhardt, F. (2017). NADPH oxidases in oxidant production by microglia: activating receptors, pharmacology and association with disease. British Journal of Pharmacology, 174(12), 1733–1749. https://doi.org/10.1111/bph.13425

Hassan, S., Eldeeb, K., Millns, P. J., Bennett, A. J., Alexander, S. P. H., & Kendall, D. A. (2014). Cannabidiol enhances microglial phagocytosis via transient receptor potential (TRP) channel activation. British Journal of Pharmacology, 171(9), 2426–2439. https://doi.org/10.1111/bph.12615

He, B. P., Wang, J. J., Zhang, X., Wu, Y., Wang, M., Bay, B.-H., & Chang, A. Y.-C. (2006). Differential Reactions of Microglia to Brain Metastasis of Lung Cancer. Molecular Medicine, 12(7–8), 161–170. https://doi.org/10.2119/2006-00033.He

He, G., Siddik, Z. H., Huang, Z., Wang, R., Koomen, J., Kobayashi, R., Khokhar, A. R., & Kuang, J. (2005). Induction of p21 by p53 following DNA damage inhibits both Cdk4 and Cdk2 activities. Oncogene, 24(18), 2929–2943. https://doi.org/10.1038/sj.onc.1208474

Hess, D. T., Matsumoto, A., Kim, S.-O., Marshall, H. E., & Stamler, J. S. (2005). Protein S-nitrosylation: purview and parameters. Nature Reviews. Molecular Cell Biology, 6(2), 150–166. https://doi.org/10.1038/nrm1569

Hirrlinger, J., Gutterer, J. M., Kussmaul, L., Hamprecht, B., & Dringen, R. (2000). Microglial Cells in Culture Express a Prominent Glutathione System for the Defense against Reactive Oxygen Species. Developmental Neuroscience, 22(5–6), 384–392. https://doi.org/10.1159/000017464

Hoffmann, A., Kann, O., Ohlemeyer, C., Hanisch, U.-K., & Kettenmann, H. (2003). Elevation of Basal Intracellular Calcium as a Central Element in the Activation of Brain Macrophages (Microglia): Suppression of Receptor-Evoked Calcium Signaling and Control of Release Function. The Journal of Neuroscience, 23(11), 4410–4419. https://doi.org/10.1523/JNEUROSCI.23-11-04410.2003

Hu, H. Z., Gu, Q., Wang, C., Colton, C. K., Tang, J., Kinoshita-Kawada, M., Lee, L. Y., Wood, J. D., & Zhu, M. X. (2004). 2-Aminoethoxydiphenyl borate is a common activator of TRPV1, TRPV2, and TRPV3. Journal of Biological Chemistry, 279(34), 35741–35748. https://doi.org/10.1074/jbc.M404164200

Huang, J. S., Chuang, L. Y., Guh, J. Y., Chen, C. J., Yang, Y. L., Chiang, T. A., Hung, M. Y., & Liao, T. N. (2005). Effect of nitric oxide-cGMP-dependent protein kinase activation on advanced glycation end-product-induced proliferation in renal fibroblasts. Journal of the American Society of Nephrology, 16(8), 2318–2329. https://doi.org/10.1681/ASN.2005010030

Hurley, S. D., & Streit, W. J. (1995). Griffonia simplicifolia II Lectin Labels a Population of Radial Glial Cells in the Embryonic Rat Brain. Developmental Neuroscience, 17(5–6), 324–334. https://doi.org/10.1159/000111302

Hurshman, A. R., & Marletta, M. A. (1995). Spectral Characterization and Effect on Catalytic Activity of Nitric Oxide Complexes of Inducible Nitric Oxide Synthase. Biochemistry, 34(16), 5627–5634. https://doi.org/10.1021/bi00016a038

Iadecola, C., Zhang, F., Casey, R., Nagayama, M., & Ross, M. E. (1997). Delayed Reduction of Ischemic Brain Injury and Neurological Deficits in Mice Lacking the Inducible Nitric Oxide Synthase Gene. The Journal of Neuroscience, 17(23), 9157–9164. https://doi.org/10.1523/JNEUROSCI.17-23-09157.1997

Imai, T., & Yasuda, N. (2016). Therapeutic intervention of inflammatory / immune diseases by inhibition of the fractalkine (CX3CL1) -CX3CR1 pathway. Inflammation and Regeneration, 36(9), 16–20. https://doi.org/10.1186/s41232-016-0017-2

Jahnel, R., Bender, O., Münter, L. M., Dreger, M., Gillen, C., & Hucho, F. (2003). Dual expression of mouse and rat VRL-1 in the dorsal root ganglion derived cell line F-11 and biochemical analysis of VRL-1 after heterologous expression. European Journal of Biochemistry, 270(21), 4264–4271. https://doi.org/10.1046/j.1432-1033.2003.03811.x

Jana, M., Anderson, J. A., Saha, R. N., Liu, X., & Pahan, K. (2005). Regulation of inducible nitric oxide synthase in proinflammatory cytokine-stimulated human primary astrocytes. Free Radical Biology and Medicine, 38(5), 655–664. https://doi.org/10.1016/j.freeradbiomed.2004.11.021

Jana, M., Liu, X., Koka, S., Ghosh, S., Petro, T. M., & Pahan, K. (2001). Ligation of CD40 Stimulates the Induction of Nitric-oxide Synthase in Microglial Cells. Journal of Biological Chemistry, 276(48), 44527–44533. https://doi.org/10.1074/jbc.M106771200

JIN, C., MOON, D., LEE, K., KIM, M., LEE, J., CHOI, Y., PARK, Y., & KIM, G. (2006). Piceatannol attenuates lipopolysaccharide-induced NF-κB activation and NF-κB-related proinflammatory mediators in BV2 microglia. Pharmacological Research, 54(6), 461–467. https://doi.org/10.1016/j.phrs.2006.09.005

Kakita, H., Aoyama, M., Nagaya, Y., Asai, H., Hussein, M. H., Suzuki, M., Kato, S., Saitoh, S., & Asai, K. (2013). Diclofenac enhances proinflammatory cytokine-induced phagocytosis of cultured microglia via nitric oxide production. Toxicology and Applied Pharmacology, 268(2), 99–105. https://doi.org/10.1016/j.taap.2013.01.024

Kaneko, Y. S., Ota, A., Nakashima, A., Nagasaki, H., Kodani, Y., Mori, K., & Nagatsu, T. (2015). Lipopolysaccharide treatment arrests the cell cycle of BV-2 microglial cells in G1 phase and protects them from UV light-induced apoptosis. Journal of Neural Transmission, 122(2), 187–199. https://doi.org/10.1007/s00702-014-1256-5

Kanzaki, M., Zhang*, Y.-Q., Mashima*, H., Li*, L., Shibata*, H., & Kojima, I. (1999). Translocation of a calcium-permeable cation channel induced by insulin-like growth factor-I. Nature Cell Biology, 1(3), 165–170. https://doi.org/10.1038/11086

Karimian, A., Ahmadi, Y., & Yousefi, B. (2016). Multiple functions of p21 in cell cycle, apoptosis and transcriptional regulation after DNA damage. DNA Repair, 42, 63–71. https://doi.org/10.1016/j.dnarep.2016.04.008

Katanosaka, K., Takatsu, S., Mizumura, K., Naruse, K., & Katanosaka, Y. (2018). TRPV2 is required for mechanical nociception and the stretch-evoked response of primary sensory neurons. Scientific Reports, 8(1), 16782. https://doi.org/10.1038/s41598-018-35049-4

Katzmann, J. A., Clark, R. J., Abraham, R. S., Bryant, S., Lymp, J. F., Bradwell, A. R., & Kyle, R. A. (2002). Serum reference intervals and diagnostic ranges for free κ and free λ immunoglobulin light chains: Relative sensitivity for detection of monoclonal light chains. Clinical Chemistry, 48(9), 1437–1444. https://doi.org/10.1093/clinchem/48.9.1437

Kaur, C., Ling, E. A., Gopalakrishnakone, P., & Wong, W. C. (1990). Response of intraventricular macrophages to crotoxin-coated microcarrier beads injected into the lateral ventricle of postnatal rats. Journal of Anatomy, 168, 63–72.

Kawahara, K., Gotoh, T., Oyadomari, S., Kuniyasu, A., Kohsaka, S., Mori, M., & Nakayama, H. (2001). Nitric oxide inhibits the proliferation of murine microglial MG5 cells by a mechanism involving p21 but independent of p53 and cyclic guanosine monophosphate. Neuroscience Letters, 310(2–3), 89–92. https://doi.org/10.1016/S0304-3940(01)02079-1

Kettenmann, H., Hanisch, U.-K., Noda, M., & Verkhratsky, A. (2011). Physiology of microglia. Physiological Reviews, 91(2), 461–553. https://doi.org/10.1152/physrev.00011.2010

Khanna, R., Roy, L., Zhu, X., & Schlichter, L. C. (2001). K + channels and the microglial respiratory burst. American Journal of Physiology-Cell Physiology, 280(4), C796–C806. https://doi.org/10.1152/ajpcell.2001.280.4.C796

Kim, S. R., Kim, S. U., Oh, U., & Jin, B. K. (2006). Transient Receptor Potential Vanilloid Subtype 1 Mediates Microglial Cell Death In Vivo and In Vitro via Ca 2+ -

Mediated Mitochondrial Damage and Cytochrome c Release. The Journal of Immunology, 177(7), 4322–4329. https://doi.org/10.4049/jimmunol.177.7.4322

Kim, Y. J., Hwang, S. Y., & Han, I. O. (2006). Insoluble matrix components of glioma cells suppress LPS-mediated iNOS/NO induction in microglia. Biochemical and Biophysical Research Communications, 347(3), 731–738. https://doi.org/10.1016/j.bbrc.2006.06.149

Komohara, Y., Ohnishi, K., Kuratsu, J., & Takeya, M. (2008). Possible involvement of the M2 anti-inflammatory macrophage phenotype in growth of human gliomas. The Journal of Pathology, 216(1), 15–24. https://doi.org/10.1002/path.2370

Kongsui, R., Beynon, S. B., Johnson, S. J., & Walker, F. (2014). Quantitative assessment of microglial morphology and density reveals remarkable consistency in the distribution and morphology of cells within the healthy prefrontal cortex of the rat. Journal of Neuroinflammation, 11(1), 182. https://doi.org/10.1186/s12974-014-0182-7

Kozlowski, C., & Weimer, R. M. (2012). An Automated Method to Quantify Microglia Morphology and Application to Monitor Activation State Longitudinally In Vivo. PLoS ONE, 7(2), e31814. https://doi.org/10.1371/journal.pone.0031814

Kraus, B., Wolff, H., Elstner, E. F., & Heilmann, J. (2010). Hyperforin is a modulator of inducible nitric oxide synthase and phagocytosis in microglia and macrophages. Naunyn-Schmiedeberg's Archives of Pharmacology, 381(6), 541–553. https://doi.org/10.1007/s00210-010-0512-y

Lanone, S., Bloc, S., Foresti, R., Almolki, A., Taillé, C., Callebert, J., Conti, M., Goven, D., Aubier, M., Dureuil, B., El-Benna, J., Mottierlini, R., & Boczkowski, J. (2005). Bilirubin decreases NOS2 expression via inhibition of NAD(P)H oxidase: implications for protection against endotoxic shock in rats. The FASEB Journal, 19(13), 1890–1892. https://doi.org/10.1096/fj.04-2368fje

Lawson, L. J., Perry, V. H., Dri, P., & Gordon, S. (1990). Heterogeneity in the distribution and morphology of microglia in the normal adult mouse brain. Neuroscience, 39(1), 151–170. https://doi.org/10.1016/0306-4522(90)90229-W

Le, W., Rowe, D., Xie, W., Ortiz, I., He, Y., & Appel, S. H. (2001). Microglial Activation and Dopaminergic Cell Injury: An In Vitro Model Relevant to Parkinson's Disease. J. Neurosci., 21(21), 8447–8455. https://doi.org/21/21/8447 [pii]

Lefèvre-Groboillot, D., Boucher, J.-L., Stuehr, D. J., & Mansuy, D. (2005). Relationship between the structure of guanidines and N-hydroxyguanidines, their binding to inducible nitric oxide synthase (iNOS) and their iNOS-catalysed oxidation to NO. FEBS Journal, 272(12), 3172–3183. https://doi.org/10.1111/j.1742-4658.2005.04736.x

Lehmann, S. M., Rosenberger, K., Krüger, C., Habbel, P., Derkow, K., Kaul, D., Rybak, A., Brandt, C., Schott, E., Wulczyn, F. G., & Lehnardt, S. (2012). Extracellularly Delivered Single-Stranded Viral RNA Causes Neurodegeneration Dependent on TLR7. The Journal of Immunology, 189(3), 1448–1458. https://doi.org/10.4049/jimmunol.1201078

Lévêque, M., Penna, A., Le Trionnaire, S., Belleguic, C., Desrues, B., Brinchault, G., Jouneau, S., Lagadic-Gossmann, D., & Martin-Chouly, C. (2018). Phagocytosis depends on TRPV2-mediated calcium influx and requires TRPV2 in lipids rafts: Alteration in macrophages from patients with cystic fibrosis. Scientific Reports, 8(1), 1–13. https://doi.org/10.1038/s41598-018-22558-5

Li, T., Pang, S., Yu, Y., Wu, X., Guo, J., & Zhang, S. (2013). Proliferation of parenchymal microglia is the main source of microgliosis after ischaemic stroke. Brain, 136(12), 3578–3588. https://doi.org/10.1093/brain/awt287

Li, X., Melief, E., Postupna, N., Montine, K. S., Keene, C. D., & Montine, T. J. (2015). Prostaglandin E2 Receptor Subtype 2 Regulation of Scavenger Receptor CD36 Modulates Microglial Aβ42 Phagocytosis. The American Journal of Pathology, 185(1), 230–239. https://doi.org/10.1016/j.ajpath.2014.09.016

Link, T. M., Park, U., Vonakis, B. M., Raben, D. M., Soloski, M. J., & Caterina, M. J. (2010). TRPV2 has a pivotal role in macrophage particle binding and phagocytosis. Nature Immunology, 11(3), 232–239. https://doi.org/10.1038/ni.1842

Liou, J., Fivaz, M., Inoue, T., & Meyer, T. (2007). Live-cell imaging reveals sequential oligomerization and local plasma membrane targeting of stromal interaction

molecule 1 after Ca2+ store depletion. Proceedings of the National Academy of Sciences, 104(22), 9301–9306. https://doi.org/10.1073/pnas.0702866104

Lira, A., Kulczycki, J., Slack, R., Anisman, H., & Park, D. S. (2011). Involvement of the Fcγ receptor in a chronic N-methyl-4-phenyl-1,,2, 3,6-tetrahydropyridine mouse model of dopaminergic loss. Journal of Biological Chemistry, 286(33), 28783–28793. https://doi.org/10.1074/jbc.M111.244830

Lishko, P. V., Procko, E., Jin, X., Phelps, C. B., & Gaudet, R. (2007). The Ankyrin Repeats of TRPV1 Bind Multiple Ligands and Modulate Channel Sensitivity. Neuron, 54(6), 905–918. https://doi.org/10.1016/j.neuron.2007.05.027

Loughlin, A. J., Woodroofe, M. N., & Cuzner, M. L. (1992). Regulation of Fc receptor and major histocompatibility complex antigen expression on isolated rat microglia by tumour necrosis factor, interleukin-1 and lipopolysaccharide: Effects on interferon-gamma induced activation. Immunology, 75(1), 170–175.

Loughlin, A. J., Woodroofe, M. N., & Cuzner, M. L. (1993). Modulation of interferon-γ-induced major histocompatibility complex class II and Fc receptor expression on isolated microglia by transforming growth factor-β1, interleukin-4, noradrenaline and glucocorticoids. Immunology, 79(1), 125–130.

Lu, K. P., & Means, A. R. (1993). Regulation of the Cell Cycle by Calcium and Calmodulin. Endocrine Reviews, 14(1), 40–58. https://doi.org/10.1210/edrv-14-1-40

Lunnon, K., Teeling, J. L., Tutt, A. L., Cragg, M. S., Glennie, M. J., & Perry, V. H. (2011). Systemic Inflammation Modulates Fc Receptor Expression on Microglia during Chronic Neurodegeneration. The Journal of Immunology, 186(12), 7215–7224. https://doi.org/10.4049/jimmunol.0903833

Macleod, K. F., Sherry, N., Hannon, G., Beach, D., Tokino, T., Kinzler, K., Vogelstein, B., & Jacks, T. (1995). p53-dependent and independent expression of p21 during cell growth, differentiation, and DNA damage. Genes & Development, 9(8), 935–944. https://doi.org/10.1101/gad.9.8.935

Manocha, G. D., Ghatak, A., Puig, K. L., Kraner, S. D., Norris, C. M., & Combs, C. K. (2017). NFATc2 Modulates Microglial Activation in the AβPP/PS1 Mouse Model

of Alzheimer's Disease. Journal of Alzheimer's Disease, 58(3), 775–787. https://doi.org/10.3233/JAD-151203

Marín-Teva, J. L., Dusart, I., Colin, C., Gervais, A., van Rooijen, N., & Mallat, M. (2004). Microglia Promote the Death of Developing Purkinje Cells. Neuron, 41(4), 535–547. https://doi.org/10.1016/S0896-6273(04)00069-8

Marques, C. P., Cheeran, M. C., Palmquist, J. M., Hu, S., & James, R. (2009). Experimental Herpes Encephalitis. 14(3), 229–238. https://doi.org/10.1080/13550280802093927.Microglia

Marrone, M. C., Morabito, A., Giustizieri, M., Chiurchiù, V., Leuti, A., Mattioli, M., Marinelli, S., Riganti, L., Lombardi, M., Murana, E., Totaro, A., Piomelli, D., Ragozzino, D., Oddi, S., Maccarrone, M., Verderio, C., & Marinelli, S. (2017). TRPV1 channels are critical brain inflammation detectors and neuropathic pain biomarkers in mice. Nature Communications, 8(1), 15292. https://doi.org/10.1038/ncomms15292

Martínez-Ruiz, A., & Lamas, S. (2007). Signalling by NO-induced protein S-nitrosylation and S-glutathionylation: Convergences and divergences. Cardiovascular Research, 75(2), 220–228. https://doi.org/10.1016/j.cardiores.2007.03.016

Mercado, J., Gordon-Shaag, A., Zagotta, W. N., & Gordon, S. E. (2010). Ca2+-Dependent Desensitization of TRPV2 Channels Is Mediated by Hydrolysis of Phosphatidylinositol 4,5-Bisphosphate. Journal of Neuroscience, 30(40), 13338–13347. https://doi.org/10.1523/JNEUROSCI.2108-10.2010

Michaelis, M., Nieswandt, B., Stegner, D., Eilers, J., & Kraft, R. (2015). STIM1, STIM2, and orai1 regulate store-operated calcium entry and purinergic activation of microglia. Glia, 63(4), 652–663. https://doi.org/10.1002/glia.22775

Michel, T. (2013). R Is for Arginine: Metabolism of Arginine Takes off again, in New Directions. Circulation, 128(13), 1400–1404. https://doi.org/10.1161/CIRCULATIONAHA.113.005924

Miyake, T., Shirakawa, H., Nakagawa, T., & Kaneko, S. (2015). Activation of mitochondrial transient receptor potential vanilloid 1 channel contributes to microglial migration. Glia, 63(10), 1870–1882. https://doi.org/10.1002/glia.22854

Mizoguchi, Y., & Monji, A. (2017). Microglial Intracellular Ca2+ Signaling in Synaptic Development and its Alterations in Neurodevelopmental Disorders. Frontiers in Cellular Neuroscience, 11(March), 1–9. https://doi.org/10.3389/fncel.2017.00069

Mizoguchi, Y., Monji, A., Kato, T., Seki, Y., Gotoh, L., Horikawa, H., Suzuki, S. O., Iwaki, T., Yonaha, M., Hashioka, S., & Kanba, S. (2009). Brain-Derived Neurotrophic Factor Induces Sustained Elevation of Intracellular Ca 2+ in Rodent Microglia. The Journal of Immunology, 183(12), 7778–7786. https://doi.org/10.4049/jimmunol.0901326

Moccia, F., Zuccolo, E., Soda, T., Tanzi, F., Guerra, G., Mapelli, L., Lodola, F., & D'Angelo, E. (2015). Stim and Orai proteins in neuronal Ca2+ signaling and excitability. Frontiers in Cellular Neuroscience, 9(April), 1–14. https://doi.org/10.3389/fncel.2015.00153

Möller, T., Contos, J. J., Musante, D. B., Chun, J., & Ransom, B. R. (2001). Expression and Function of Lysophosphatidic Acid Receptors in Cultured Rodent Microglial Cells. Journal of Biological Chemistry, 276(28), 25946–25952. https://doi.org/10.1074/jbc.M102691200

Montfort, W. R., Wales, J. A., & Weichsel, A. (2017). Structure and Activation of Soluble Guanylyl Cyclase, the Nitric Oxide Sensor. Antioxidants & Redox Signaling, 26(3), 107–121. https://doi.org/10.1089/ars.2016.6693

Morelli, M. B., Nabissi, M., Amantini, C., Farfariello, V., Ricci-Vitiani, L., di Martino, S., Pallini, R., Larocca, L. M., Caprodossi, S., Santoni, M., De Maria, R., & Santoni, G. (2012). The transient receptor potential vanilloid-2 cation channel impairs glioblastoma stem-like cell proliferation and promotes differentiation. International Journal of Cancer, 131(7), E1067–E1077. https://doi.org/10.1002/ijc.27588

Morris Jr, S. M. (2009). Recent advances in arginine metabolism: roles and regulation of the arginases. British Journal of Pharmacology, 157(6), 922–930. https://doi.org/10.1111/j.1476-5381.2009.00278.x

Muraki, K., Iwata, Y., Katanosaka, Y., Ito, T., Ohya, S., Shigekawa, M., & Imaizumi, Y. (2003). TRPV2 Is a Component of Osmotically Sensitive Cation Channels in Murine Aortic Myocytes. Circulation Research, 93(9), 829–838. https://doi.org/10.1161/01.RES.0000097263.10220.0C

Nabissi, M., Morelli, M. B., Amantini, C., Farfariello, V., Ricci-Vitiani, L., Caprodossi, S., Arcella, A., Santoni, M., Giangaspero, F., De Maria, R., & Santoni, G. (2010). TRPV2 channel negatively controls glioma cell proliferation and resistance to Fas-induced apoptosis in ERK-dependent manner. Carcinogenesis, 31(5), 794–803. https://doi.org/10.1093/carcin/bgq019

Nagamoto-Combs, K., & Combs, C. K. (2010). Microglial Phenotype Is Regulated by Activity of the Transcription Factor, NFAT (Nuclear Factor of Activated T Cells). Journal of Neuroscience, 30(28), 9641–9646. https://doi.org/10.1523/JNEUROSCI.0828-10.2010

Nagasawa, M., Nakagawa, Y., Tanaka, S., & Kojima, I. (2007). Chemotactic peptide fMetLeuPhe induces translocation of the TRPV2 channel in macrophages. Journal of Cellular Physiology, 210(3), 692–702. https://doi.org/10.1002/jcp.20883

Nagayama, M., Aber, T., Nagayama, T., Ross, M. E., & Iadecola, C. (1999). Age-Dependent Increase in Ischemic Brain Injury in Wild-Type Mice and in Mice Lacking the Inducible Nitric Oxide Synthase Gene. Journal of Cerebral Blood Flow & Metabolism, 19(6), 661–666. https://doi.org/10.1097/00004647-199906000-00009

Nakagawa, Y., & Chiba, K. (2014). Role of microglial M1/M2 polarization in relapse and remission of psychiatric disorders and diseases. Pharmaceuticals, 7(12), 1028–1048. https://doi.org/10.3390/ph7121028

Nakahara, J., & Aiso, S. (2006). Fc Receptor-Positive Cells in Remyelinating Multiple Sclerosis Lesions. Journal of Neuropathology & Experimental Neurology, 65(6), 582–591. https://doi.org/10.1097/00005072-200606000-00006

Nandi, S., Gokhan, S., Dai, X.-M., Wei, S., Enikolopov, G., Lin, H., Mehler, M. F., & Stanley, E. R. (2012). The CSF-1 receptor ligands IL-34 and CSF-1 exhibit distinct developmental brain expression patterns and regulate neural progenitor cell maintenance and maturation. Developmental Biology, 367(2), 100–113. https://doi.org/10.1016/j.ydbio.2012.03.026

Nathan, C., Calingasan, N., Nezezon, J., Ding, A., Lucia, M. S., La Perle, K., Fuortes, M., Lin, M., Ehrt, S., Kwon, N. S., Chen, J., Vodovotz, Y., Kipiani, K., & Beal, M. F. (2005). Protection from Alzheimer's-like disease in the mouse by genetic ablation

of inducible nitric oxide synthase. Journal of Experimental Medicine, 202(9), 1163–1169. https://doi.org/10.1084/jem.20051529

Nikodemova, M., Kimyon, R. S., De, I., Small, A. L., Collier, L. S., & Watters, J. J. (2015). Microglial numbers attain adult levels after undergoing a rapid decrease in cell number in the third postnatal week ☆. Journal of Neuroimmunology, 278, 280–288. https://doi.org/10.1016/j.jneuroim.2014.11.018

Nimmerjahn, A., Kirchhoff, F., & Helmchen, F. (2005). Resting Microglial Cells Are Highly Dynamic Surveillants of Brain Parenchyma in Vivo. Science, 308(May), 1314–1319.

Norden, D. M., & Godbout, J. P. (2013). Microglia of the aged brain: primed to be activated and resistant to regulation. Neuropathology and Applied Neurobiology, 39(1), 19–34. https://doi.org/10.1111/j.1365-2990.2012.01306.x

Nyland, H., Matre, R., & Mork, S. (1980). Fc Receptors on Microglial Lipophages in Multiple Sclerosis. New England Journal of Medicine, 302(2), 120–121. https://doi.org/10.1056/NEJM198001103020218

Oh-hora, M., Yamashita, M., Hogan, P. G., Sharma, S., Lamperti, E., Chung, W., Prakriya, M., Feske, S., & Rao, A. (2008). Dual functions for the endoplasmic reticulum calcium sensors STIM1 and STIM2 in T cell activation and tolerance. Nature Immunology, 9(4), 432–443. https://doi.org/10.1038/ni1574

Ohana, L., Newell, E. W., Stanley, E. F., & Schlichter, L. C. (2009). The Ca 2+ release-activated Ca 2+ current (I CRAC) mediates store-operated Ca 2+ entry in rat microglia. Channels, 3(2), 129–139. https://doi.org/10.4161/chan.3.2.8609

Ohsawa, K., Imai, Y., Kanazawa, H., Sasaki, Y., & Kohsaka, S. (2000). Involvement of Iba1 in membrane ruffling and phagocytosis of macrophages/microglia. Journal of Cell Science, 113 (Pt 1, 3073–3084.

Oliveira, C. J. ., Schindler, F., Ventura, A. M., Morais, M. S., Arai, R. J., Debbas, V., Stern, A., & Monteiro, H. P. (2003). Nitric oxide and cGMP activate the Ras-MAP kinase pathway-stimulating protein tyrosine phosphorylation in rabbit aortic endothelial cells. Free Radical Biology and Medicine, 35(4), 381–396. https://doi.org/10.1016/S0891-5849(03)00311-3

Olson, J. K., & Miller, S. D. (2004). Microglia Initiate Central Nervous System Innate and Adaptive Immune Responses through Multiple TLRs. The Journal of Immunology, 173(6), 3916–3924. https://doi.org/10.4049/jimmunol.173.6.3916

Orihuela, R., McPherson, C. A., & Harry, G. J. (2016). Microglial M1/M2 polarization and metabolic states. British Journal of Pharmacology, 173(4), 649–665. https://doi.org/10.1111/bph.13139

Pabon, M. M., Bachstetter, A. D., Hudson, C. E., Gemma, C., & Bickford, P. C. (2011). CX3CL1 reduces neurotoxicity and microglial activation in a rat model of Parkinson's disease. Journal of Neuroinflammation, 8(1), 9. https://doi.org/10.1186/1742-2094-8-9

Paolicelli, R. C., Bolasco, G., Pagani, F., Maggi, L., Scianni, M., Panzanelli, P., Giustetto, M., Ferreira, T. A., Guiducci, E., Dumas, L., Ragozzino, D., & Gross, C. T. (2011). Synaptic Pruning by Microglia Is Necessary for Normal Brain Development. Science, 333(September), 1456–1459. https://doi.org/10.1126/science.1202529

Papanikolaou, M., Lewis, A., & Butt, A. M. (2017). Store-operated calcium entry is essential for glial calcium signalling in CNS white matter. Brain Structure and Function, 222(7), 2993–3005. https://doi.org/10.1007/s00429-017-1380-8

Parekh, A. B. (2010). Store-operated CRAC channels: function in health and disease. Nature Reviews. Drug Discovery, 9(5), 399–410. https://doi.org/10.1038/nrd3136

Park, S. Y., Lee, H., Hur, J., Kim, S. Y., Kim, H., Park, J.-H., Cha, S., Kang, S. S., Cho, G. J., Choi, W. S., & Suk, K. (2002). Hypoxia induces nitric oxide production in mouse microglia via p38 mitogen-activated protein kinase pathway. Molecular Brain Research, 107(1), 9–16. https://doi.org/10.1016/S0169-328X(02)00421-7

Parkhurst, C. N., Yang, G., Ninan, I., Savas, J. N., Iii, J. R. Y., Lafaille, J. J., Hempstead, B. L., Littman, D. R., Gan, W., Yates, J. R., Lafaille, J. J., Hempstead, B. L., Littman, D. R., & Gan, W. (2013). Microglia Promote Learning-Dependent Synapse Formation through Brain-Derived Neurotrophic Factor. Cell, 155(7), 1596–1609. https://doi.org/10.1016/j.cell.2013.11.030

Peress, N. S., Fleit, H. B., Perillo, E., Kuljis, R., & Pezzullo, C. (1993). Identification of FcγRI, II and III on normal human brain ramified microglia and on microglia in

senile plaques in Alzheimer's disease. Journal of Neuroimmunology, 48(1), 71–79. https://doi.org/10.1016/0165-5728(93)90060-C

Pérez-Asensio, F. J., Hurtado, O., Burguete, M. C., Moro, M. A., Salom, J. B., Lizasoain, I., Torregrosa, G., Leza, J. C., Alborch, E., Castillo, J., Knowles, R. G., & Lorenzo, P. (2005). Inhibition of iNOS activity by 1400W decreases glutamate release and ameliorates stroke outcome after experimental ischemia. Neurobiology of Disease, 18(2), 375–384. https://doi.org/10.1016/j.nbd.2004.10.018

Periasamy, M., & Kalyanasundaram, A. (2007). SERCA pump isoforms: Their role in calcium transport and disease. Muscle & Nerve, 35(4), 430–442. https://doi.org/10.1002/mus.20745

Prado, J., Baltrons, M. A., Pifarré, P., & García, A. (2010). Glial cells as sources and targets of natriuretic peptides. Neurochemistry International, 57(4), 367–374. https://doi.org/10.1016/j.neuint.2010.03.004

Pulver-Kaste, R. A., Barlow, C. A., Bond, J., Watson, A., Penar, P. L., Tranmer, B., & Lounsbury, K. M. (2006). Ca 2+ source-dependent transcription of CRE-containing genes in vascular smooth muscle. American Journal of Physiology-Heart and Circulatory Physiology, 291(1), H97–H105. https://doi.org/10.1152/ajpheart.00753.2005

Pulver, R. A., Rose-Curtis, P., Roe, M. W., Wellman, G. C., & Lounsbury, K. M. (2004). Store-Operated Ca 2+ Entry Activates the CREB Transcription Factor in Vascular Smooth Muscle. Circulation Research, 94(10), 1351–1358. https://doi.org/10.1161/01.RES.0000127618.34500.FD

Qiu, B., Zhang, D., Wang, C., Tao, J., Tie, X., Qiao, Y., Xu, K., Wang, Y., & Wu, A. (2011). IL-10 and TGF-β2 are overexpressed in tumor spheres cultured from human gliomas. Molecular Biology Reports, 38(5), 3585–3591. https://doi.org/10.1007/s11033-010-0469-4

Rao, A., Luo, C., & Hogan, P. G. (1997). TRANSCRIPTION FACTORS OF THE NFAT FAMILY:Regulation and Function. Annual Review of Immunology, 15(1), 707–747. https://doi.org/10.1146/annurev.immunol.15.1.707

Reilly, R. M., McDonald, H. A., Puttfarcken, P. S., Joshi, S. K., Lewis, L., Pai, M., Franklin, P. H., Segreti, J. A., Neelands, T. R., Han, P., Chen, J., Mantyh, P. W.,

Ghilardi, J. R., Turner, T. M., Voight, E. A., Daanen, J. F., Schmidt, R. G., Gomtsyan, A., Kort, M. E., … Kym, P. R. (2012). Pharmacology of Modality-Specific Transient Receptor Potential Vanilloid-1 Antagonists That Do Not Alter Body Temperature. Journal of Pharmacology and Experimental Therapeutics, 342(2), 416–428. https://doi.org/10.1124/jpet.111.190314

Reveneau, S., Arnould, L., Jolimoy, G., Hilpert, S., Lejeune, P., Saint-Giorgio, V., Belichard, C., & Jeannin, J. F. (1999). Nitric oxide synthase in human breast cancer is associated with tumor grade, proliferation rate, and expression of progesterone receptors. Laboratory Investigation, 79(10), 1215–1225. https://doi.org/10532585

Roos, J., DiGregorio, P. J., Yeromin, A. V., Ohlsen, K., Lioudyno, M., Zhang, S., Safrina, O., Kozak, J. A., Wagner, S. L., Cahalan, M. D., Veliçelebi, G., & Stauderman, K. A. (2005). STIM1, an essential and conserved component of store-operated Ca2+ channel function. Journal of Cell Biology, 169(3), 435–445. https://doi.org/10.1083/jcb.200502019

Sánchez-Mejorada, G., & Rosales, C. (1998). Fcγ receptor-mediated mitogen-activated protein kinase activation in monocytes is independent of Ras. Journal of Biological Chemistry, 273(42), 27610–27619. https://doi.org/10.1074/jbc.273.42.27610

Santini, M. P., Talora, C., Seki, T., Bolgan, L., & Dotto, G. P. (2001). Cross talk among calcineurin, Sp1/Sp3, and NFAT in control of p21WAF1/CIP1 expression in keratinocyte differentiation. Proceedings of the National Academy of Sciences, 98(17), 9575–9580. https://doi.org/10.1073/pnas.161299698

Saramaki, A. (2006). Regulation of the human p21(waf1/cip1) gene promoter via multiple binding sites for p53 and the vitamin D3 receptor. Nucleic Acids Research, 34(2), 543–554. https://doi.org/10.1093/nar/gkj460

Schafer, D. P., Lehrman, E. K., Kautzman, A. G., Koyama, R., Mardinly, A. R., Yamasaki, R., Ransohoff, R. M., Greenberg, M. E., Barres, B. A., & Stevens, B. (2012). Microglia Sculpt Postnatal Neural Circuits in an Activity and Complement-Dependent Manner. Neuron, 74(4), 691–705. https://doi.org/10.1016/j.neuron.2012.03.026

Scheiblich, H., & Bicker, G. (2016). Nitric oxide regulates antagonistically phagocytic and neurite outgrowth inhibiting capacities of microglia. Developmental Neurobiology, 76(5), 566–584. https://doi.org/10.1002/dneu.22333

Schilling, T., & Eder, C. (2009). Importance of the non-selective cation channel TRPV1 for microglial reactive oxygen species generation. Journal of Neuroimmunology, 216(1–2), 118–121. https://doi.org/10.1016/j.jneuroim.2009.07.008

Schulz, C., Perdiguero, E. G., Chorro, L., Szabo-Rogers, H., Cagnard, N., Kierdorf, K., Prinz, M., Wu, B., Jacobsen, S. E. W., Pollard, J. W., Frampton, J., Liu, K. J., & Geissmann, F. (2012). A lineage of myeloid cells independent of myb and hematopoietic stem cells. Science, 335(6077), 86–90. https://doi.org/10.1126/science.1219179

Schwarz, J.M., Sholar, P.W., Bilbo, S. D. (2013). Sex differences in microglial colonization of the developing rat brain. National Institute of Health, 120(6), 948–963. https://doi.org/10.1111/j.1471-4159.2011.07630.x.Sex

Simmons, G. W., Pong, W. W., Emnett, R. J., White, C. R., Gianino, S. M., Rodriguez, F. J., & Gutmann, D. H. (2011). Neurofibromatosis-1 Heterozygosity Increases Microglia in a Spatially and Temporally Restricted Pattern Relevant to Mouse Optic Glioma Formation and Growth. Journal of Neuropathology & Experimental Neurology, 70(1), 51–62. https://doi.org/10.1097/NEN.0b013e3182032d37

Solomon, J. N., Lewis, C.-A. B., Ajami, B., Corbel, S. Y., Rossi, F. M. V., & Krieger, C. (2006). Origin and distribution of bone marrow-derived cells in the central nervous system in a mouse model of amyotrophic lateral sclerosis. Glia, 53(7), 744–753. https://doi.org/10.1002/glia.20331

Song, X., Shapiro, S., Goldman, D. L., Casadevall, A., Scharff, M., & Lee, S. C. (2002). Fcγ Receptor I- and III-Mediated Macrophage Inflammatory Protein 1α Induction in Primary Human and Murine Microglia. Infection and Immunity, 70(9), 5177–5184. https://doi.org/10.1128/IAI.70.9.5177-5184.2002

Song, X., Tanaka, S., Cox, D., & Lee, S. C. (2004). Fcγ receptor signaling in primary human microglia: differential roles of PI-3K and Ras/ERK MAPK pathways in phagocytosis and chemokine induction. Journal of Leukocyte Biology, 75(6), 1147–1155. https://doi.org/10.1189/jlb.0403128

Srikanth, S., & Gwack, Y. (2012). Orai1, STIM1, and their associating partners. The Journal of Physiology, 590(Pt 17), 4169–4177. https://doi.org/10.1113/jphysiol.2012.231522

Stamler, J. S., Lamas, S., & Fang, F. C. (2001). Nitrosylation: The Prototypic Redox-Based Signaling Mechanism. Cell, 106(6), 675–683. https://doi.org/10.1016/S0092-8674(01)00495-0

Stamler, J. S., Simon, D. I., Osborne, J. A., Mullins, M. E., Jaraki, O., Michel, T., Singel, D. J., & Loscalzo, J. (1992). S-nitrosylation of proteins with nitric oxide: synthesis and characterization of biologically active compounds. Proceedings of the National Academy of Sciences, 89(1), 444–448. https://doi.org/10.1073/pnas.89.1.444

Stathopulos, P. B., Li, G.-Y., Plevin, M. J., Ames, J. B., & Ikura, M. (2006). Stored Ca 2+ Depletion-induced Oligomerization of Stromal Interaction Molecule 1 (STIM1) via the EF-SAM Region. Journal of Biological Chemistry, 281(47), 35855–35862. https://doi.org/10.1074/jbc.M608247200

Stefanova, N., Fellner, L., Reindl, M., Masliah, E., Poewe, W., & Wenning, G. K. (2011). Toll-Like Receptor 4 Promotes α-Synuclein Clearance and Survival of Nigral Dopaminergic Neurons. The American Journal of Pathology, 179(2), 954–963. https://doi.org/10.1016/j.ajpath.2011.04.013

Stiber, J., Hawkins, A., Zhang, Z.-S., Wang, S., Burch, J., Graham, V., Ward, C. C., Seth, M., Finch, E., Malouf, N., Williams, R. S., Eu, J. P., & Rosenberg, P. (2008). STIM1 signalling controls store-operated calcium entry required for development and contractile function in skeletal muscle. Nature Cell Biology, 10(6), 688–697. https://doi.org/10.1038/ncb1731

Streit, W. J. (2002). Microglia as neuroprotective, immunocompetent cells of the CNS. Glia, 40(2), 133–139. https://doi.org/10.1002/glia.10154

Stuehr, D. J., Tejero, J., & Haque, M. M. (2009). Structural and mechanistic aspects of flavoproteins: electron transfer through the nitric oxide synthase flavoprotein domain. FEBS Journal, 276(15), 3959–3974. https://doi.org/10.1111/j.1742-4658.2009.07120.x

Sun, Y., Chauhan, A., Sukumaran, P., Sharma, J., Singh, B. B., & Mishra, B. B. (2014). Inhibition of store-operated calcium entry in microglia by helminth factors:

implications for immune suppression in neurocysticercosis. Journal of Neuroinflammation, 11(1), 210. https://doi.org/10.1186/s12974-014-0210-7

Szabo, M., & Gulya, K. (2013). Development of the microglial phenotype in culture. Neuroscience, 241, 280–295. https://doi.org/10.1016/j.neuroscience.2013.03.033

Takagi, K., Isobe, Y., Yasukawa, K., Okouchi, E., Suketa, Y., Takagf, K., Isobe, Y., Yasukawa, K., Okouchi, E., Suketac, Y., Takagi, K., Isobe, Y., Yasukawa, K., Okouchi, E., & Suketac, Y. (1994). Nitric oxide blocks the cell cycle of mouse macrophage-like cells in the early G2+M phase. FEBS Letters, 340(3), 159–162. https://doi.org/10.1016/0014-5793(94)80128-2

Takahashi, Y., Watanabe, H., Murakami, M., Ono, K., Munehisa, Y., Koyama, T., Nobori, K., Iijima, T., & Ito, H. (2007). Functional role of stromal interaction molecule 1 (STIM1) in vascular smooth muscle cells. Biochemical and Biophysical Research Communications, 361(4), 934–940. https://doi.org/10.1016/j.bbrc.2007.07.096

Tam, W. Y., & Ma, C. H. E. (2015). Bipolar/rod-shaped microglia are proliferating microglia with distinct M1/M2 phenotypes. Scientific Reports, 4(1), 7279. https://doi.org/10.1038/srep07279

Taylor, B. S., de Vera, M. E., Ganster, R. W., Wang, Q., Shapiro, R. A., Morris, S. M., Billiar, T. R., & Geller, D. A. (1998). Multiple NF-κB Enhancer Elements Regulate Cytokine Induction of the Human Inducible Nitric Oxide Synthase Gene. Journal of Biological Chemistry, 273(24), 15148–15156. https://doi.org/10.1074/jbc.273.24.15148

Tominaga, M., Caterina, M. J., Malmberg, A. B., Rosen, T. A., Gilbert, H., Skinner, K., Raumann, B. E., Basbaum, A. I., & Julius, D. (1998). The Cloned Capsaicin Receptor Integrates Multiple Pain-Producing Stimuli. Neuron, 21(3), 531–543. https://doi.org/10.1016/S0896-6273(00)80564-4

Town, T., Nikolic, V., & Tan, J. (2005). The microglial “activation” continuum: from innate to adaptive responses. Journal of Neuroinflammation, 2, 24. https://doi.org/10.1186/1742-2094-2-24

Tremblay, M.-È., Lowery, R. L., & Majewska, A. K. (2010). Microglial Interactions with Synapses Are Modulated by Visual Experience. PLoS Biology, 8(11), e1000527. https://doi.org/10.1371/journal.pbio.1000527

Ulvestad, E., Williams, K., Matre, R., Nyland, H., Olivier, A., & Antel, J. (1994). Fc Receptors for IgG on Cultured Human Microglia Mediate Cytotoxicity and Phagocytosis of Antibody-coated Targets. Journal of Neuropathology and Experimental Neurology, 53(1), 27–36. https://doi.org/10.1097/00005072-199401000-00004

Underhill, D. M., & Goodridge, H. S. (2007). The many faces of ITAMs. Trends in Immunology, 28(2), 66–73. https://doi.org/10.1016/j.it.2006.12.004

Valentine, J. E., Kalkhoven, E., White, R., Hoare, S., & Parker, M. G. (2000). Mutations in the Estrogen Receptor Ligand Binding Domain Discriminate between Hormone-dependent Transactivation and Transrepression. Journal of Biological Chemistry, 275(33), 25322–25329. https://doi.org/10.1074/jbc.M002497200

Varga-Szabo, D., Braun, A., Kleinschnitz, C., Bender, M., Pleines, I., Pham, M., Renné, T., Stoll, G., & Nieswandt, B. (2008). The calcium sensor STIM1 is an essential mediator of arterial thrombosis and ischemic brain infarction. Journal of Experimental Medicine, 205(7), 1583–1591. https://doi.org/10.1084/jem.20080302

Vedeler, C., Ulvestad, E., Grundt, I., Conti, G., Nyland, H., Matre, R., & Pleasure, D. (1994). Fc receptor for IgG (FcR) on rat microglia. Journal of Neuroimmunology, 49(1–2), 19–24. https://doi.org/10.1016/0165-5728(94)90176-7

Verbrugge, A., & Meyaard, L. (2005). Signaling by ITIM-Bearing Receptors. Current Immunology Reviews, 1(2), 201–212. https://doi.org/10.2174/1573395054065160

Vodovotz, Y., Lucia, M. S., Flanders, K. C., Chesler, L., Xie, Q. W., Smith, T. W., Weidner, J., Mumford, R., Webber, R., Nathan, C., Roberts, A. B., Lippa, C. F., & Sporn, M. B. (1996). Inducible nitric oxide synthase in tangle-bearing neurons of patients with Alzheimer's disease. The Journal of Experimental Medicine, 184(4), 1425–1433. https://doi.org/10.1084/jem.184.4.1425

Wainwright, A., Rutter, A. R., Seabrook, G. R., Reilly, K., & Oliver, K. R. (2004). Discrete expression of TRPV2 within the hypothalamo-neurohypophysial system: Implications for regulatory activity within the hypothalamic-pituitary-adrenal axis. The Journal of Comparative Neurology, 474(1), 24–42. https://doi.org/10.1002/cne.20100

Wake, H., Moorhouse, A. J., Jinno, S., Kohsaka, S., & Nabekura, J. (2009). Resting Microglia Directly Monitor the Functional State of Synapses In Vivo and Determine the Fate of Ischemic Terminals. Journal of Neuroscience, 29(13), 3974–3980. https://doi.org/10.1523/JNEUROSCI.4363-08.2009

Wakselman, S., Bechade, C., Roumier, A., Bernard, D., Triller, A., & Bessis, A. (2008). Developmental Neuronal Death in Hippocampus Requires the Microglial CD11b Integrin and DAP12 Immunoreceptor. Journal of Neuroscience, 28(32), 8138–8143. https://doi.org/10.1523/JNEUROSCI.1006-08.2008

Wang, Y., Szretter, K. J., Vermi, W., Gilfillan, S., Rossini, C., Cella, M., Barrow, A. D., Diamond, M. S., & Colonna, M. (2012). IL-34 is a tissue-restricted ligand of CSF1R required for the development of Langerhans cells and microglia. Nature Immunology, 13(8), 753–760. https://doi.org/10.1038/ni.2360

Węgiel, J., Wiśniewski, H. M., Dziewiątkowski, J., Tarnawski, M., Kozielski, R., Trenkner, E., & Wiktor-Jędrzejczak, W. (1998). Reduced number and altered morphology of microglial cells in colony stimulating factor-1-deficient osteopetrotic op/op mice. Brain Research, 804(1), 135–139. https://doi.org/10.1016/S0006-8993(98)00618-0

Wolf, Y., Yona, S., Kim, K.-W., & Jung, S. (2013). Microglia, seen from the CX3CR1 angle. Frontiers in Cellular Neuroscience, 7(March), 1–9. https://doi.org/10.3389/fncel.2013.00026

Wong, C.-O., Sukumar, P., Beech, D. J., & Yao, X. (2010). Nitric oxide lacks direct effect on TRPC5 channels but suppresses endogenous TRPC5-containing channels in endothelial cells. Pflügers Archiv - European Journal of Physiology, 460(1), 121–130. https://doi.org/10.1007/s00424-010-0823-3

Woodroofe, M. N., Hayes, G. M., & Cuzner, M. L. (1989). Fc receptor density, MHC antigen expression and superoxide production are increased in interferon-gamma-treated microglia isolated from adult rat brain. Immunology, 68(3), 421–426.

Worley, P. F., Zeng, W., Huang, G. N., Yuan, J. P., Kim, J. Y., Lee, M. G., & Muallem, S. (2007). TRPC channels as STIM1-regulated store-operated channels. Cell Calcium, 42(2), 205–211. https://doi.org/10.1016/j.ceca.2007.03.004

Wu, C., Zhang, J., Abu-Soud, H., Ghosh, D. K., & Stuehr, D. J. (1996). High-Level Expression of Mouse Inducible Nitric Oxide Synthase inEscherichia coliRequires Coexpression with Calmodulin. Biochemical and Biophysical Research Communications, 222(2), 439–444. https://doi.org/10.1006/bbrc.1996.0763

Wu, W., Tan, X., Dai, Y., Krishnan, V., Warner, M., & Gustafsson, J.-Å. (2013). Targeting estrogen receptor β in microglia and T cells to treat experimental autoimmune encephalomyelitis. Proceedings of the National Academy of Sciences, 110(9), 3543–3548. https://doi.org/10.1073/pnas.1300313110

Xu, S.-Z., Sukumar, P., Zeng, F., Li, J., Jairaman, A., English, A., Naylor, J., Ciurtin, C., Majeed, Y., Milligan, C. J., Bahnasi, Y. M., Al-Shawaf, E., Porter, K. E., Jiang, L.-H., Emery, P., Sivaprasadarao, A., & Beech, D. J. (2008). TRPC channel activation by extracellular thioredoxin. Nature, 451(7174), 69–72. https://doi.org/10.1038/nature06414

Yao, J., Liu, B., & Qin, F. (2011). Modular thermal sensors in temperature-gated transient receptor potential (TRP) channels. Proceedings of the National Academy of Sciences, 108(27), 11109–11114. https://doi.org/10.1073/pnas.1105196108

Yoshida, T., Inoue, R., Morii, T., Takahashi, N., Yamamoto, S., Hara, Y., Tominaga, M., Shimizu, S., Sato, Y., & Mori, Y. (2006). Nitric oxide activates TRP channels by cysteine S-nitrosylation. Nature Chemical Biology, 2(11), 596–607. https://doi.org/10.1038/nchembio821

Young, J. D., Unkeless, J. C., & Cohn, Z. A. (1985). Functional ion channel formation by mouse macrophage IgG Fc receptor triggered by specific ligands. Journal of Cellular Biochemistry, 29(4), 289–297. https://doi.org/10.1002/jcb.240290403

Yuan, J. P., Zeng, W., Huang, G. N., Worley, P. F., & Muallem, S. (2007). STIM1 heteromultimerizes TRPC channels to determine their function as store-operated channels. Nature Cell Biology, 9(6), 636–645. https://doi.org/10.1038/ncb1590

Zhan, Y., Paolicelli, R. C., Sforazzini, F., Weinhard, L., Bolasco, G., Pagani, F., Vyssotski, A. L., Bifone, A., Gozzi, A., Ragozzino, D., & Gross, C. T. (2014). Deficient neuron-microglia signaling results in impaired functional brain connectivity and social behavior. Nature Neuroscience, 17(3), 400–406. https://doi.org/10.1038/nn.3641

Zhang, H., Xiao, J., Hu, Z., Xie, M., Wang, W., & He, D. (2016). Blocking transient receptor potential vanilloid 2 channel in astrocytes enhances astrocyte-mediated neuroprotection after oxygen–glucose deprivation and reoxygenation. European Journal of Neuroscience, 44(7), 2493–2503. https://doi.org/10.1111/ejn.13352

Zhang, I., Alizadeh, D., Liang, J., Zhang, L., Gao, H., Song, Y., Ren, H., Ouyang, M., Wu, X., D'Apuzzo, M., & Badie, B. (2016). Characterization of Arginase Expression in Glioma-Associated Microglia and Macrophages. PLOS ONE, 11(12), e0165118. https://doi.org/10.1371/journal.pone.0165118

Zhang, L., Handel, M., Schartner, J., Hagar, A., Allen, G., Curet, M., & Badie, B. (2007). Regulation of IL-10 expression by upstream stimulating factor (USF-1) in glioma-associated microglia. Journal of Neuroimmunology, 184(1–2), 188–197. https://doi.org/10.1016/j.jneuroim.2006.12.006

Zusso, M., Lunardi, V., Franceschini, D., Pagetta, A., Lo, R., Stifani, S., Frigo, A. C., Giusti, P., & Moro, S. (2019). Ciprofloxacin and levofloxacin attenuate microglia inflammatory response via TLR4/NF-kB pathway. Journal of Neuroinflammation, 16(1), 148. https://doi.org/10.1186/s12974-019-1538-9

Chapter 2

This chapter was published in the journal *Glia*, volume 67, issue 12, pages 2294 – 2311. It has been reproduced with permission from Wiley.

2 Nitric oxide Upregulates Microglia Phagocytosis and Increases Transient Receptor Potential Vanilloid Type 2 Channel Expression on the Plasma Membrane.

2.1 Abstract

Microglia phagocytosis is critical for central nervous system development, and dysregulation of phagocytosis may contribute to a variety of neurological disorders. During initial stages of phagocytosis, microglia display increased nitric oxide (NO) production via iNOS activity and amplified calcium entry through transient receptor potential vanilloid type 2 (TRPV2) channels. The present study investigated the regulatory role of iNOS/NO signaling in microglial phagocytosis and TRPV2 channel activation using phagocytosis assay, calcium imaging, patch clamp electrophysiology, immunocytochemistry, and immunoblot assays. Results showed that primary microglia from iNOS-knockout ($iNOS^{-/-}$) mice exhibited substantial deficits in phagocytic capacity and TRPV2 channel activity relative to wild-type (WT) controls. Specifically, $iNOS^{-/-}$ microglia displayed a lower level of TRPV2 protein localized on the plasma membrane (PM) without any significant change in the mRNA levels of Fc-gamma receptors and TRPV2. In addition, $iNOS^{-/-}$ microglia, unlike their WT controls, failed to elicit a calcium influx in response to application of the TRPV2-agonist 2-aminoethoxydiphenyl borate (2APB). Importantly, the phagocytic capacity and the PM expression and activity of TRPV2 in $iNOS^{-/-}$ microglia were largely corrected by pretreatment with NO-donors. Accordingly, the 2APB-evoked calcium influx and the PM expression of TRPV2 in WT microglia were significantly decreased by selective inhibition of iNOS, protein kinase-G (PKG), or phosphoinositide-3-kinase (PI3K), respectively. Together, results from this study indicated that iNOS/NO signaling

upregulates microglial phagocytosis and increases TRPV2 trafficking to the PM via PKG/PI3K dependent pathway(s).

2.2 Introduction

As the primary immune cells within the central nervous system (CNS), microglia actively engage in phagocytosis under physiological as well as pathological conditions (Shemer et al., 2015). During CNS development, microglia phagocytosis influences neurogenesis as well as synaptogenesis (Aarum et al., 2003; Harry & Kraft, 2012; Sierra et al., 2010). For example, microglia display phagocytic activity engulfing neuronal precursor cells to regulate the number of neurons within the CNS (Marín-Teva et al., 2004; Sierra et al., 2010). Likewise, in the adult CNS, the elaborate processes of microglia are intimately associated with dendritic spines and neuronal synapses, such that phagocytosis of these neuronal structures can occur in response to aberrant synaptic transmission (Casano & Peri, 2015; Schafer et al., 2013). Under pathological conditions within the CNS such as pathogen infiltration or traumatic brain injury, microglia increase phagocytosis to engulf pathogens or cellular debris from injured neurons (Fu et al., 2014). Conversely, decreased phagocytosis has been observed in the progression of neurological disorders such as Parkinson's disease (Park et al., 2008), Alzheimer's disease (Chung et al., 1999), prion disease (Ciesielski-Treska et al., 2004), and Rett syndrome (Derecki et al., 2012). Therefore, microglial phagocytosis is critical for shaping the neuronal networks during CNS development and adulthood, while also protecting against the progress of neurological disorders.

Microglia phagocytosis occurs in response to changes in their microenvironment. Recent studies have correlated nitric oxide (NO) production to the initial increase in microglial phagocytosis (Kakita et al., 2013; Kraus et al., 2010; Scheiblich & Bicker, 2016). For example, responding to an increase of TNFα and IL1β, microglia increase the expression of inducible nitric oxide synthase (iNOS) and catalyzes the production of NO (Kraus et al., 2010; Sheng et al., 2011). As a highly diffusible and transient signaling molecule (Bogdan, 2001; Pautz et al., 2010), NO regulates cellular functions primarily by activating soluble guanylyl cyclase (sGC) production of cyclic guanosine monophosphate (cGMP) and ultimately increasing protein kinase-G (PKG) activity(Bogdan, 2001; Bogdan, 2015; Forstermann & Sessa, 2012). However, the molecular pathways by which NO signals phagocytosis in microglia remains unclear.

Studies report that the transient receptor potential vanilloid type 2 (TRPV2) ion channel is critical for phagocytosis in macrophages (Lévêque et al., 2018; Link et al., 2010; Santoni et al., 2013), and more recently this has also been shown in microglia (Hassan et al., 2014). As a member of the TRP channel family, TRPV2 is largely localized on the endoplasmic reticulum (ER) of phagocytes under resting conditions (Nagasawa et al., 2007; Nagasawa & Kojima, 2012). In response to increased cytokines such as insulin-like growth factors, TRPV2 proteins on the ER membrane are translocated to the plasma membrane (PM) in a phosphoinoside-3-kinase (PI3K)-dependent manner (Nagasawa et al., 2007; Nagasawa & Kojima, 2012; Perálvarez-Marín et al., 2013). Tetrameric TRPV2 proteins on the PM of phagocytes form nonselective cation channels, mediating a large influx of calcium and facilitating phagocytosis (Hassan et al., 2014; Lévêque et al., 2018; Link et al., 2010; Santoni & Amantini, 2013).

Given the important roles of NO and TRPV2 in cell phagocytosis, the present study sought to determine whether NO signaling increases TRPV2 channel activity to enhance phagocytosis. Using primary wild type (WT) and iNOS-knockout iNOS$^{-/-}$ microglia as well as the mouse microglial cell line BV2, we characterized differences in phagocytic capacities between WT and iNOS$^{-/-}$ microglia and determined the molecular mechanism by which NO regulates TRPV2 channel activity.

2.3 Materials and Methods

2.3.1 Primary Microglia Cultures

WT (n = 189) and iNOS$^{-/-}$ (n = 204) postnatal days 0–4 pups from 23 WT and 25 iNOS$^{-/-}$ litters were used for acquiring primary microglia. Briefly, pups were decapitated, and their brains were removed quickly and placed in ice cold Leibowitz L-15 media containing 100 mg/mL bovine serum albumin (BSA) and 1× penicillin/streptomycin (P/S) antibiotics (ThermoFischer Scientific, Waltham MA). Mouse cortices were dissected and then homogenized by pipetting through a 10 mL pipet, 1 mL pipet, and a 200 µL pipet sequentially. Homogenized cortices were filtered through a 70 µm nylon filter. The filtrate was centrifuged at 900g for 4 min at room temperature. The supernatant was aspirated, and the cells were resuspended in Dulbecco's modified eagle's medium (DMEM) containing 1× P/S, and 10% fetal bovine serum (FBS) (ThermoFischer Scientific). The cortical cells were grown in T-75 flasks with approximately three cortices per flask, under normal conditions of 5% CO_2 at 36^{o}C. Culture media was completely replaced in the T-75 flasks 5 days after plating, and then every 3 days until a confluent astrocyte monolayer formed with prominent microglia colonies on the surface. T-75 flasks containing the astrocyte-microglia co-culture were placed on a shaker at 36^{o}C and 200 rpm for 2 hours. After shaking, the supernatant containing microglia cells was removed, centrifuged at 900g for 4 min, and resuspended in fresh culture media. Isolated microglia were plated at 5×10^4 cells/mL in different dishes for experiments.

2.3.2 Drug Treatments

To control for TRPV2 channel expression, culture media was replaced with serum-free DMEM containing 1× P/S 2 hr before running experiments (Hisanaga et al., 2009; Kanzaki et al., 1999; Nagasawa et al., 2007). Fast-release NO-donors were used for all experiments except for phagocytosis, where a slow-release NO-donor was used. The following fast-release NO-donor drugs were treated at the following concentrations: S-nitroso-N-acetyl-DL-penicillamine (SNAP) 250 µM, and sodium nitroprusside (SNP) 300 µM (Santa Cruz Biotechnology, Dallas TX); slow release NO-donor: diethylenetriamine

NONOate (NOC18) 100 μM (Santa Cruz Biotechnology); TRPV agonist: 2-aminoethoxydiphenyl borate (2APB) 250 μM (Santa Cruz Biotechnology); TRPV1 agonist: capsaicin 2 μM (Tocris Bioscience, Oakville ON); TRP inhibitor: ruthenium red (RR) 3 μM (Enzo Life Sciences, Burlington, ON); TRPV2 inhibitor: Tranilast 75 μM (Tocris Bioscience); nitric oxide synthase (NOS) inhibitor: G-nitro-L-arginine-methyl ester (L-NAME) 100 μM (Santa Cruz Biotechnology); iNOS inhibitor: 1400W 5 μM (Tocris Bioscience); kinase inhibitors: arginyl-lysyl-arginyl-alanyl-arginyl-lysyl-glutamic acid (PKG_i) 10μM, (Santa Cruz Biotechnology), and LY294002 ($PI3K_i$) 10μM (Cayman Chemical, Ann Arbor, MI). Concentrations of SNAP (Gu et al., 2000; Kawasaki et al., 2003; Kopec & Carroll, 2000), 2APB (Hu et al., 2004; Juvin et al., 2007), and tranilast (Aoyagi et al., 2010; Hisanaga et al., 2009; Mihara et al., 2010) were adapted from previous literature, and the optimal concentrations were determined by examining the dose–response on rhod-4 fluorescence in BV2 microglia (**Figure 2.S1**).

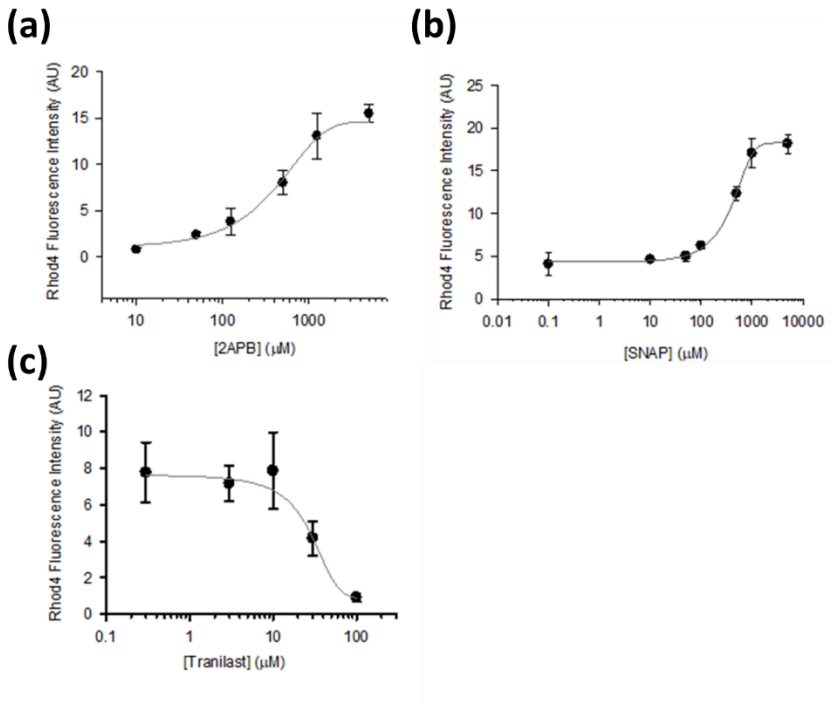

Figure 2.S1 Dose-response curves of 2APB and SNAP and tranilast.

Rhod-4 fluorescence in BV2 microglia were analyzed to determine the EC50 of 2APB and SNAP and IC50 of tranilast. **(a)** Dose-response curve of 2APB was produced by treating the cells at concentration of 10μM, 50μM, 125μM, 500μM, 1.25mM, and 5mM. The determined EC50 = 715μM. **(b)** Dose-response curve of SNAP effect on 2APB (250μM) induced rhod-4 fluorescence was obtained by treating the cells with SNAP at 0μM, 10μM, 50μM, 100μM, 500μM, 1mM, and 5mM. The determined EC50 = 299μM. **(c)** Dose-response curve of tranilast effect on 2APB (250μM) induced rhod-4 fluorescence was obtained by treating the cells with tranilast at 0μM, 3μM, 10μM, 30μM, 100μM. The determined IC50 = 37μM.

2.3.3 Phagocytosis Assay

WT and iNOS$^{-/-}$ primary microglia were treated with NOC18, a slow NO-donor more suitable for the longer assay period, 20 min before addition of latex-rabbit immunoglobulin-G (IgG) fluorescein isothiocyanate (FITC) beads (Cayman Chemical), at 1:500 for 2 hr to permit phagocytosis. After 2 hr incubation at normal condition, phagocytosis assay buffer was used to wash away debris, culture media and unbound beads. Two minutes incubation of trypan blue solution was used to quench IgG-FITC-bead surface fluorescence to help distinguish between phagocytosed beads and non-phagocytosed beads. 40,6-diamidino-2-phenylindole (DAPI) staining was then conducted. Microglia IgG-FITC-bead fluorescence as well as differential interference contrast (DIC) images were taken using the EVOS FL Auto 2 cell imaging system under 40x magnification. Cell surfaces from DIC images were used as a membrane marker to localize and count engulfed IgG-FITC-beads within microglia. Experimental N-values represent the number of individual wells analyzed per treatment. Cell images were analyzed using the FIJI open source software (Schindelin et al., 2012) and graphed using Excel.

2.3.4 NO Imaging

For NO-imaging, primary microglia were cultured on 24-well plates, and DMEM medium was washed out using the same extracellular solution for electrophysiology. Microglia were treated with 4 μM DAX-J2 (AAT Bioquest, Sunnyvale, CA) for 45 min at room temperature, and then excess DAX-J2 was washed out using the extracellular solution. Latex-rabbit IgG-FITC-beads were pretreated at 1:500 for 20 min before live cell imaging. NO imaging was performed using the EVOS FL Auto 2 system under 20× magnification. DAX-J2 fluorescence was recorded for 1.5 hr and the total fluorescence was quantified using the FIJI open source software (Schindelin et al., 2012) and graphed using Excel.

2.3.5 Reverse Transcription Polymerase Chain Reaction

Total RNAs were obtained from BV2 cells or primary WT and iNOS$^{-/-}$ microglia using RNeasy Mini Kit (Qiagen, Toronto, ON) following manufacturer's instructions. Total

RNAs isolated from the cortical tissues of three 7-week-old male WT or iNOS$^{-/-}$ mice were also used for examining endogenous Fc-gamma receptors (FcγRs) I and III expression. Reverse transcription of 1 μg extracted RNA to cDNA using qScript XLT cDNA SuperMix (Quantabio, Beverly, MA) was carried out as per manufacturer's instructions. Quantitative PCR was conducted using PerfeCTa SYBR Green FastMix for iQ (Quantabio, Beverly, MA), 25 ng of cDNA template, and 500 nM of forward and reverse primers specific to the gene of interest. Murine forward and reverse primers for the following genes of interest were used; TRPV1 forward 5'GAGGCTGTTCCCTGTTCCTT3', reverse 5'GATGATGTTGATCCCT GGGC3', TRPV2 forward 5'GGTATGGGTGAGCTGGCTTTT3', reverse 5'AGGACGTAGGTGAGGAGGAC3', TRPV3 forward 5'ATGAATGCCC ACTCCAAGGAGATGGTG3', reverse 5'AAACGCATAGAGGGTGGTTTT GCTATTGC3', Fc-γ receptor I (FcγRI) forward 5'TCTACTGGTGTGAGG TAGCC3', reverse 5'GGGGGTTGGGAGAACACTT3', FcγRIII forward 5'CCCCTCTACCCAAAAGGGAC3', reverse 5'CACCGATTTCCCACCT CAGT3'. RT-qPCR reactions were run in triplicate with a no-template control on a BioRad My iQ Single-colour real-time PCR detection system (Biorad, Mississauga, ON), in 25 μL reaction volumes with a 40-cycle protocol as per the manufacturer's instructions. The difference in cycle thresholds (ΔCt) between the reference gene β-actin forward 5'CTGTCCCTGTATGCCTCTG3', reverse 5'ATGTCACGCACGATTTCC3', and the genes of interest were graphed using Excel.

2.3.6 Calcium Imaging

For calcium imaging in microglial cultures, DMEM culture media was washed out with the same bath solution used in electrophysiology. Rhod-4AM (AAT Bioquest, Sunnyvale, CA) was equilibrated to room temperature for 1 hr before incubation of microglia cultures. Cells were bathed in 3 μM rhod-4AM under normal conditions and excess rhod-4 was washed out using bath solution 1 hr after incubation. Drug pretreatments were given 20 min before imaging. Calcium imaging of microglia grown on 35 mm glass bottom culture dishes was performed using Olympus FV1000 microscope under 20× magnification imaged every 3s, whereas calcium imaging of microglia grown in 24-well plates was performed using the EVOS FL Auto 2 system under 20× magnification every

10s. Baseline levels of calcium fluorescence were recorded before test drug application, and cellular calcium fluorescence responses were normalized to the average baseline level in every cell within the imaging field using the FIJI open source software (Schindelin et al., 2012). The averaged value of the normalized calcium fluorescence intensity of all test cells was plotted along with the time of imaging using Excel.

2.3.7 Whole-Cell Voltage-Clamp Recordings

Primary microglia plated on 35 mm dishes were kept in bath solution containing (in mM): 130 NaCl, 5 KCl, 3 $MgCl_2$, 2 $CaCl_2$, 5 glucose, and 10 4-(2-hydroxyethyl)-1-piperazineethanesulfonic acid (HEPES). Potassium free solution contained (in mM): 135 NaCl, 3 $MgCl_2$, 2 $CaCl_2$, 10 HEPES, and 5 glucose. The pH of all solutions was adjusted to 7.4 using NaOH and the osmolarity was adjusted to ~300 mOsm with glucose. The intracellular solution contained (in mM): 140 K-gluconate, 8 NaCl, 1 MgCl2, 10 cesium-BAPTA, and 10 HEPES, the pH of 7.4 was adjusted using cesium hydroxide. Cesium was used in the intracellular solution to block delayed rectified potassium channels, which can mask the TRP conductance when recording. Patch pipettes were pulled from thin-wall glass filaments from World Precision Instruments, Inc. (Sarasota, FL) using a two-stage glass microelectrode puller (Tritech Research, Los Angeles, CA), with final input resistance between 3 and 5 MΩ. Whole-cell recordings were performed at room temperature using MultiClamp 700B Amplifier and Digidata 1440A Low-noise Data Acquisition System (Molecular Devices, Sunnyvale, CA). Whole-cell voltage-ramps from -100 mV to +100 mV were applied over 150 ms from a holding potential of 0 mV, every 10 s. Recordings were performed on microglial cultures bathed in potassium-free solution, to remove inward rectified potassium channel conductance which may mask a TRP conductance. Drug solutions were perfused toward the recording cell using a gravity perfusion system delivering solution at 2 mL/min. The average of five ramps were taken for each cell after the drug response stabilized. Capacitance was recorded for each cell and ramps were reported in current density (pA/pF). Experimental n-values represent number of cells recorded over different days.

2.3.8 Immunocytochemistry

Microglia were grown on poly-D-lysine coated cover-glass placed in 24-well plates. Twenty minutes after specific treatments, cells were fixed with 4% paraformaldehyde (Sigma-Aldrich, Oakville, ON), and washed once with 0.1 M glycine, followed by two washes with phosphate-buffered saline (PBS) for 10 min each. Fixed cells were permeabilized by incubation with 0.1% triton in PBS for 5 min. Guinea pig TRPV2 antibody (Alomone Labs, Jerusalem Isreal, 1:100), and rat CD11b antibody (AbD Serotec, Hercules, CA, 1:200), were incubated overnight, followed by three washes with PBS for 10 min each. Alexa Fluor 488 anti-guinea pig and Cy3 anti-rat secondary antibodies (Jackson Immunoresearch, Burlington, ON), were incubated at 1:500 dilution for 45 min, respectively. After incubation with secondary antibodies, microglia were washed three times with PBS for 10 min each, and then incubated with DAPI (Sigma-Aldrich, Oakville, ON), for 15 min at room temperature.

Cells were washed twice with PBS for 10 min each wash. Finally, for cells plated on cover-glass, Fluoromount-G (Electron Microscopy Sciences, Hatfield, PA), was applied to each cover-glass before mounting cells on glass slides. For cells plated in 24-well plates, Fluoromount-G was applied to each well and covered with a coverslip. Microglia TRPV2, CD11b, and DAPI fluorescence images were taken using either the Olympus FV1000 or the EVOS FL Auto 2 cell imaging system under 20× and 40× magnification. Experimental N-values represent the number of cell samples analyzed per treatment. For examining the PM/cytosol ratio of TRPV2 fluorescence, image analyses were conducted using the FIJI open source software, and the image analysis procedure was described in **Figure 2.S2**.

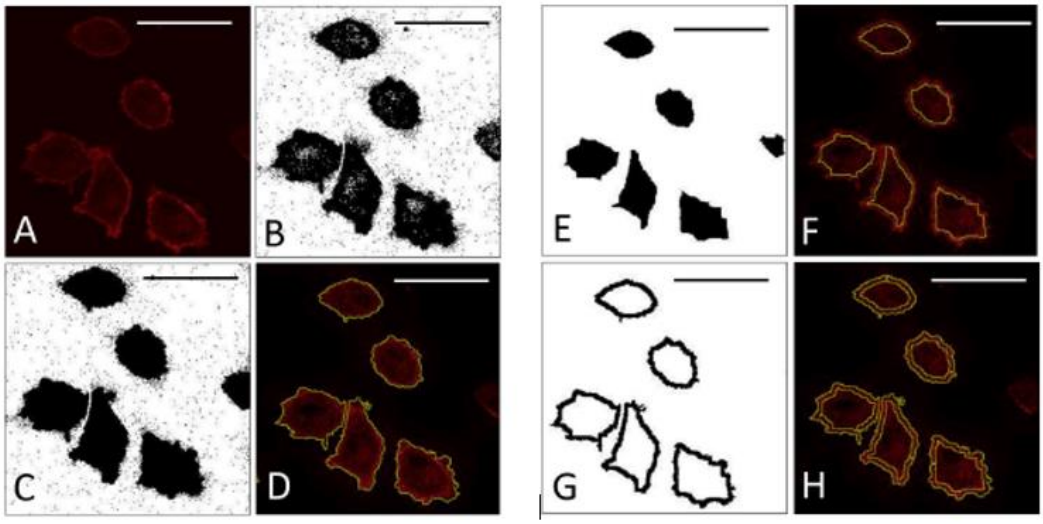

Figure 2.S2 Trafficking image analysis using FIJI open source software.

A) CD11b stain of microglia. **B)** Thresholded image of CD11b staining from (A). **C)** Mask of the thresholded CD11b staining which is used to obtain the region of interest (ROI) for the entire cell. **D)** Overlay of the entire cell ROI onto the CD11b stain from (A). **E)** The cell cytosol mask was obtained using the erode function in FIJI on the entire cell mask seen in (C). The erode metric remained unchanged when analyzing between images and treatments **F)** Overlay of the cytosolic ROI obtained from (E) on CD11b stain from (A). **G)** Using FIJI, the PM cell mask was obtained from subtracting the cytosolic mask (E) from entire cell mask (C). **H)** Overlay of the plasma membrane ROI obtained from (G) onto the CD11b stain from (A). The fraction of PM/cytosolic TRPV2 fluorescent intensity was reported to control for any intensity differences between cells and treatments. Images were taken at 20× magnification. Scale bars represent 25μm.

2.3.9 Biotinylation of Surface Proteins

After treatments, BV2 microglia were washed 3× with PBS before being homogenized into Eppendorf tubes using 1 mL of PBS. Microglia were centrifuged at 13,000g for 15 s and the supernatant was aspirated. Cells were incubated with EZ-Link™ Sulfo-NHS-SS-Biotin (ThermoFischer Scientific), at room temperature for 30 min with constant shaking. Biotin-bound microglia were washed with PBS and centrifuged at 13,000g to remove the supernatant. Microglia were incubated with NP-40 lysis buffer at 4 ^{o}C with constant shaking for 30 min, followed by the addition of streptavidin (Sigma-Aldrich, Oakville, ON), in 4 ^{o}C for 1 hr. Microglia were centrifuged at 13,000g for 5 min and the supernatant containing cytosolic proteins were removed and stored at -80^{o}C. Biotinylated proteins in the PM bound to streptavidin were washed 4× with PBS removing the supernatant each time before incubating sample in radioimmunoprecipitation assay buffer for 1 hr at room temperature with constant shaking. Samples were centrifuged at 13,000g for 5 min and the remaining super-natant containing PM proteins were collected and stored at –80 ^{o}C before running western blots.

2.3.10 Western Blot

BV2 and/or WT cortical tissue proteins were measured using Bradford assay (Bio-Rad, Hercules, CA). Proteins were run through SDS-PAGE using an 8% polyacrylamide gel at 100 V before being transferred to a polyvinylidene difluoride membrane. Membranes were blocked using 5% BSA solution for 1 hr before being incubated with TRPV1 antibody at 1:200 dilution, or TRPV2 antibody at 1:2,000 dilution (Alomone Labs, Jerusalem, Israel). Secondary anti-rabbit IgG horseradish peroxidase (HRP) conjugate (1:5,000) or Guinea-pig IgG HRP (1:5,000) (Jackson Immuno-research, Burlington, ON), was then incubated for 1.5 hr. Protein isolated from male, 7-week-old WT cortical tissue was used as a positive control for TRP channel expression. For biotinylated surface protein, the PM housekeeping protein Na+/K+ ATPase (1:10,000; Abcam Inc., Toronto, ON) was used to normalize PM TRPV2 expression. For total and cytosolic proteins, TRP channel expression was normalized to the housekeeping protein glyceraldehyde 3-phosphate

dehydrogenase (GAPDH; 1:10,000; Abcam Inc.). Experimental N-values represent the number of individual wells in which lysates were collected from per treatment.

2.3.11 Statistics

Statistical analyses were done using Graphpad Prism 6. All statistic results were shown as mean ± SEM. One-way or two-way ANOVAs were conducted using Tukey's or Bonferroni post hoc comparison, respectively. Unpaired two-tailed t test was used when only comparing two groups. All statistical significance was determined from at least N = 3 and a p value of less than .05 (*$p < .05$, **$p < .01$, ***$p < .001$, ****$p < .0001$).

2.4 Results

2.4.1 NO upregulates phagocytic activity of WT and iNOS$^{-/-}$ microglia.

To examine the importance of NO for microglial phagocytosis, we incubated WT and iNOS$^{-/-}$ microglia with FITC-IgG-latex beads in the absence (control) or presence of NOC18, a slow-release NO-donor **(Figure 2.1A)**. Fluorescence analyses indicated that under control conditions, iNOS$^{-/-}$ microglia displayed significantly less FITC-bead occupancy and fluorescence intensity compared to WT controls **(Figure 2.1B, C)**. NOC18 treatment significantly increased FITC-bead occupancy and fluorescence intensity in both WT and iNOS$^{-/-}$ microglia; however, iNOS$^{-/-}$ microglia displayed less FITC-bead occupancy and fluorescence intensity relative to WT cells **(Figure 2.1B, C)**. Nevertheless, NOC18 restored the phagocytic capacity of iNOS$^{-/-}$ microglia to the control level of WT microglia **(Figure 2.1B, C)**. These results indicate that NO signaling fundamentally regulates microglia phagocytosis.

To examine the impact of latex-IgG-beads on NO production in WT and iNOS$^{-/-}$ microglia, we measured NO levels by means of DAX-J2 fluorescence imaging 1.5 hr after IgG-beads incubation of the cells. Analyses revealed significantly higher NO production in WT microglia compared to iNOS$^{-/-}$ microglia **(Figure 2.1D)**. On the other hand, RT-qPCR analyses demonstrated similar mRNA levels of the phagocytic receptors FcγRI and FcγRIII within isolated WT and iNOS$^{-/-}$ microglia, as well as in 7-week-old male WT and iNOS$^{-/-}$ mouse cortices **(Figure 2.1E, F)**. Together, these data indicated that the defective phagocytosis of iNOS$^{-/-}$ microglia was not due to decreased expression of phagocytic receptors but because of insufficient NO production.

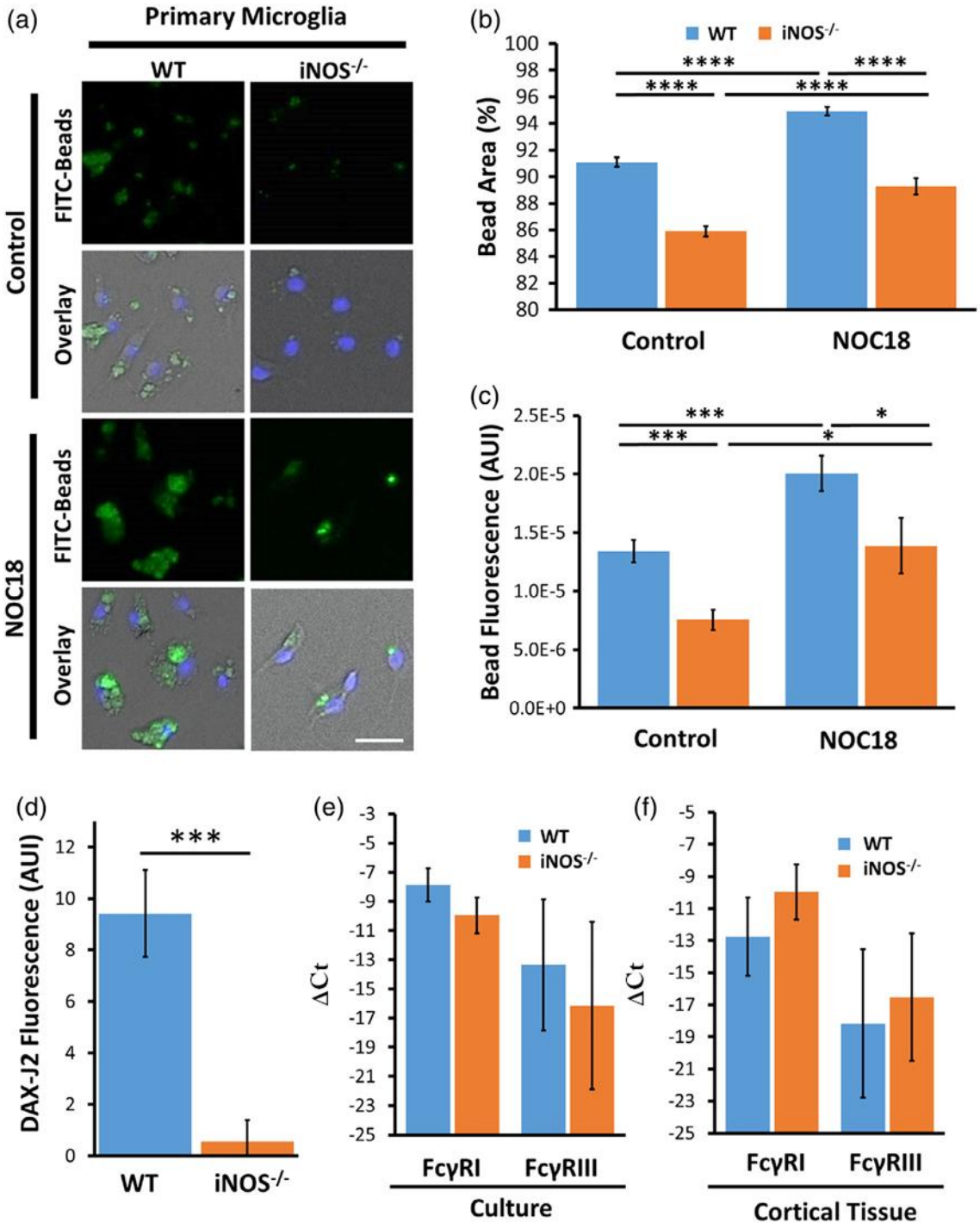

Figure legend on next page

Figure 2.1 Nitric oxide upregulates phagocytic capacity of WT and iNOS$^{-/-}$ microglia.

A) Representative images of microglia 2 hr after incubation of FITC-IgG beads (green). Primary microglia isolated from WT and iNOS$^{-/-}$ mice stained with DAPI (blue). The fluorescence of IgG beads and DAPI was overlaid onto DIC images of control WT or iNOS$^{-/-}$ microglia, and cells that were pretreated with NOC18 (100 μM). Scale bars represent 25 μm. **B)** Plotted graph shows the percentage of area of FITC-IgG-bead within control and NOC18-treated WT (blue) or iNOS$^{-/-}$ microglia (orange). **C)** Bar graph reports the fluorescent of FITC-IgG-beads (AUI, arbitrary units of intensity) in WT or iNOS$^{-/-}$ microglia under naive or NOC18-treated conditions. **D)** Graph reports the arbitrary units of DAX-J2 fluorescent intensity in control WT and iNOS$^{-/-}$ microglia 1.5 hr after FITC-IgG bead incubation. **E)** The mRNA levels of FcγRI and FcγRIII mRNA levels are presented as ΔCt in WT and iNOS$^{-/-}$ microglia cultures as well as in **F)** 7-week-old WT and iNOS$^{-/-}$ cortical tissue.

2.4.2 NO-donor restores a 2APB evoked calcium influx in iNOS$^{-/-}$ microglia.

It was reported that TRPV1 and TRPV2, but not TRPV3 channels, are expressed in mouse microglia (Cao & Ramsey, 2016). Considering that the TRPV2 channel-mediated calcium entry is essential for phagocytosis (Hassan et al., 2014; Lévêque et al., 2018; Link et al., 2010; Santoni & Amantini, 2013) we carried out calcium imaging to examine the effect of 2APB, a TRPV1-3 agonist, on intracellular calcium levels in WT and iNOS$^{-/-}$ microglia. Calcium imaging analyses showed that 2APB induced a large but transient calcium influx in WT microglia, but not in iNOS$^{-/-}$ microglia **(Figure 2.2A**). In the presence of 2APB, application of SNAP had no significant effect on calcium influx in WT microglia or iNOS$^{-/-}$ microglia (**Figure 2.2A**). Interestingly, 5-10 min after administration of the rapid-release NO-donor SNAP, application of 2APB to iNOS$^{-/-}$ microglia induced a large calcium influx with an amplitude comparable to that in WT microglia (**Figure 2.2B**). These results indicated that the 2APB-induced calcium influx in mouse microglia depends on the presence of NO signaling.

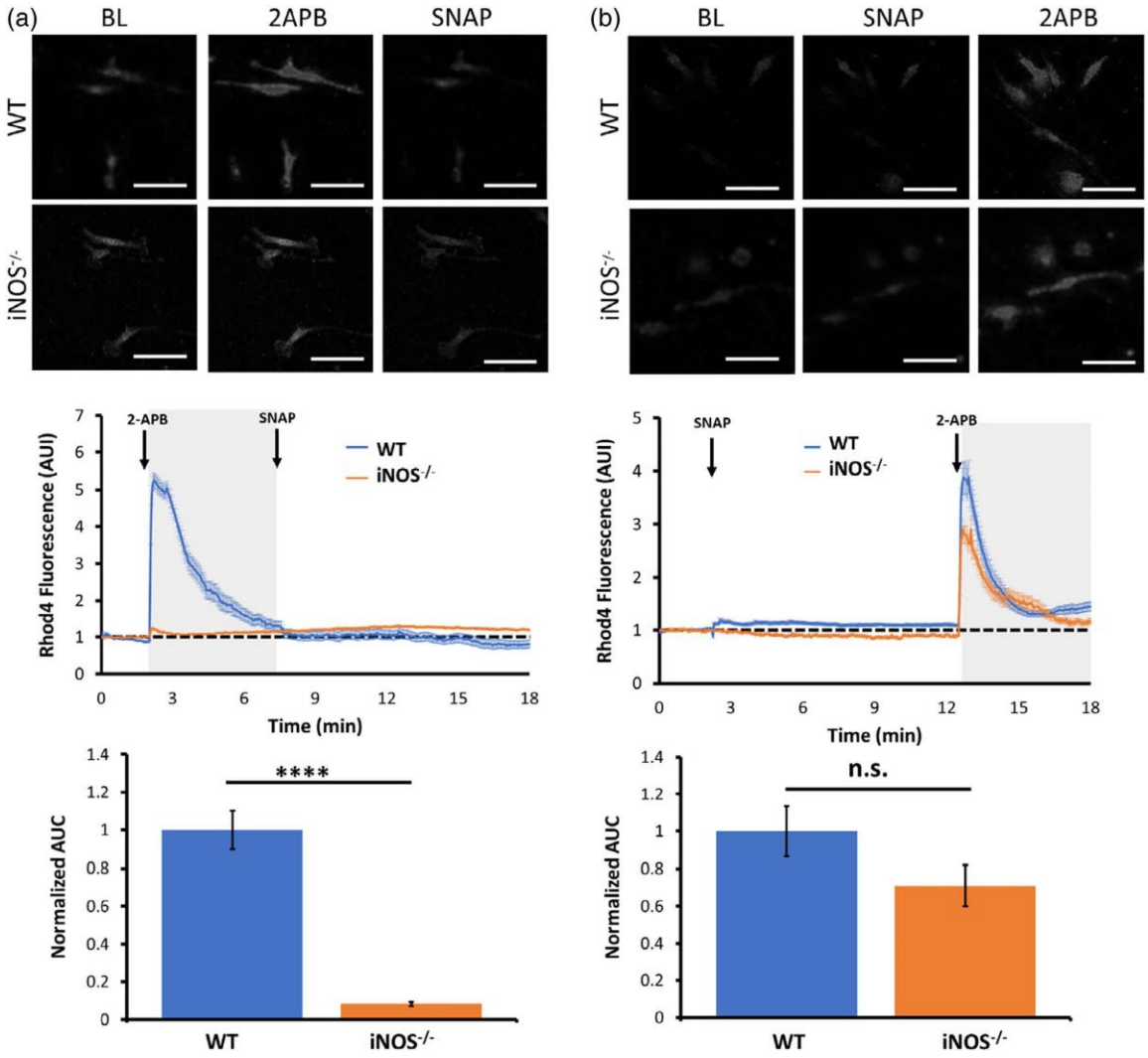

Figure legend on next page

Figure 2.2 NO is necessary for 2APB to induce calcium entry in iNOS$^{-/-}$ microglia.

A) *Top:* Representative images of rhod-4 fluorescence illustrate intracellular calcium levels within WT (upper row) and iNOS$^{-/-}$ microglia (lower row) before (BL) and after sequential application of 2APB (250 μM) and SNAP (250 μM). Scale bar represents 50 μm. *Mid:* Plotted curves show the temporal changes in rhod-4 fluorescence (AUI) in the group of WT microglia (shown above) and the group of iNOS$^{-/-}$ microglia (shown above), in response to application of 2APB and SNAP, respectively. *Bottom:* The area under the calcium curve (AUC) of iNOS$^{-/-}$ microglia was normalized to that of WT cells (N = 3), quantifying the 2APB induced response before SNAP treatment. **B)** *Top:* Representative images of rhod-4 fluorescence illustrate calcium response in WT and iNOS$^{-/-}$ microglia sequentially treated with SNAP then 2APB. *Mid:* Plotted curves depict the temporal changes in rhod-4 fluorescence in WT and iNOS$^{-/-}$ microglia in response to application of SNAP and 2APB, respectively. *Bottom:* Normalized AUC values quantify the 2APB induced response in WT and iNOS$^{-/-}$ microglia after SNAP treatment (N = 3).

2.4.3 NO-donor evokes a TRP channel conductance in WT and iNOS$^{-/-}$ microglia.

TRPV2 channels mediate a nonselective cation conductance with a high calcium permeability. To further examine if the 2APB-elicited calcium influx in mouse microglia is mediated by TRPV channels, we performed whole-cell voltage-clamp recordings in both WT and iNOS$^{-/-}$ microglia. Under our experimental conditions, applying a voltage-ramp to the naïve WT and iNOS$^{-/-}$ microglia revealed a low-amplitude basal transmembrane current **(Figure 2.3A, B,** blue and orange traces, respectively**)**. The amplitude of transmembrane current in WT microglia increased significantly 1–2 min after perfusion of SNAP, whereas in iNOS$^{-/-}$ microglia, the current amplitude started to increase 3–4 min after SNAP perfusion **(Figure 2.3A, B,** green traces**)**. This SNAP-induced current displayed a linear voltage–current relationship and reversed at 0 mV, signifying a nonselective cation conductance. Importantly, the SNAP-induced conductance in both WT and iNOS$^{-/-}$ microglia was significantly inhibited by ruthenium red (RR), a nonselective TRPV channel inhibitor **(Figure 2.3A, B,** red traces**)**. These results confirmed that NO signaling induces a TRPV channel mediated nonselective cation current in primary mouse microglia.

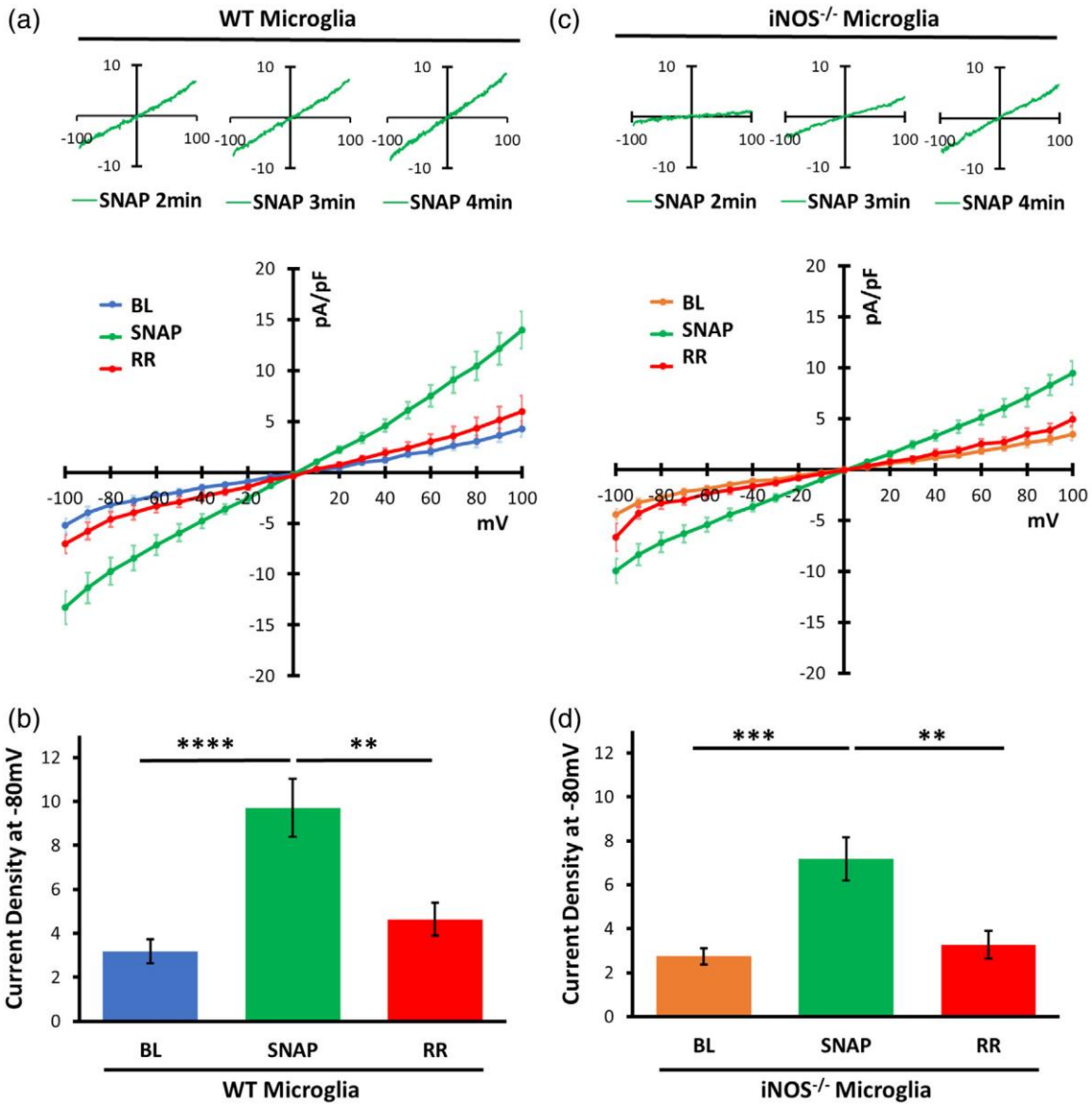

Figure legend on next page

Figure 2.3 NO induces a TRP conductance in microglia.

A) *Top panel:* Representative traces illustrate the temporal change in the current–voltage (V–I) relationship of transmembrane conductance evoked by a voltage-slope in a WT microglia 2–4 min after application of SNAP. *Lower panel:* V–I plots summarize the current density of the voltage-slope (−100 to 100 mV) induced conductance in WT microglia before treatment (BL = baseline), 4 min after 250 μM SNAP treatment and immediately after 3 μM RR treatment (n = 12 cells). **B)** Plot summarizes the current density of WT microglia when their membrane potential was held at –80 mV. **C)** *Top panel:* Representative traces illustrate the temporal change in the V–I relationship of transmembrane conductance evoked by a voltage-slope in $iNOS^{-/-}$ microglia 2–4min after application of SNAP. *Lower panel:* V–I plots summarize the current density of the voltage-slope (−100 to 100 mV) induced conductance in $iNOS^{-/-}$ microglia before treatment, 4 min after SNAP treatment and immediately after RR treatment (n = 12 cells). **D)** Plot summarizes the current density of $iNOS^{-/-}$ microglia when their membrane potential was held at –80 mV.

2.4.4 2APB induces calcium influx into microglia primarily through TRPV2 channels in an NO-signaling dependent manner.

A previous study reported that 2APB selectively activates TRPV2, but not TRPV1/3 channels, in mouse microglia (Cao & Ramsey, 2016). To verify whether 2APB-induced calcium entry is specifically through TRPV2 channels, we performed calcium imaging in mouse microglia in the presence or absence of the selective TRPV2 antagonist tranilast. Results showed that application of 2APB induced a rapid and large calcium influx, which was sustained for more than 10 min in BV2 microglia, but transient in WT primary microglia. Importantly, the 2APB-induced calcium influx in both BV2 and WT microglia was completely abolished by tranilast **(Figure 2.4A, B)**. Notably, application of the TRPV1 agonist capsaicin to WT microglia did not elicit a significant calcium influx either in the absence (control) or in the presence of SNAP **(Figure 2.4C)**. Unlike their WT controls, iNOS$^{-/-}$ microglia failed to generate a calcium influx following application of either capsaicin or 2APB **(Figure 2.4D)**. In the presence of 2APB, SNAP induced a small and delayed calcium influx in iNOS$^{-/-}$ microglia **(Figure 2.4D)**. In contrast, in the presence of SNAP, application of 2APB induced a large calcium influx in iNOS$^{-/-}$ cells with an amplitude comparable to that in WT microglia, although capsaicin still failed to induce detect-able calcium influx **(Figure 2.4E)**.

The expression levels of TRPV1-3 in microglia were further examined by gene transcription and expression analyses. Specifically, our RT-qPCR assays revealed a higher ΔCt value of TRPV2 mRNA than that of TRPV1 mRNA in BV2, WT and iNOS$^{-/-}$ microglia **(Figure 2.4F)**, whereas TRPV3 mRNA was not detected in these cells (not shown). Moreover, immunoblot assays detected relatively high levels of TRPV2 protein in BV2 cells as well as cortical tissue, while TRPV1 protein was found in cortical tissue but not in BV2 microglia **(Figure 2.4G)**. These results implied that 2APB induces calcium influx into microglia primarily through TRPV2 channels (and not TRPV1 or 3) in an NO signaling-dependent manner.

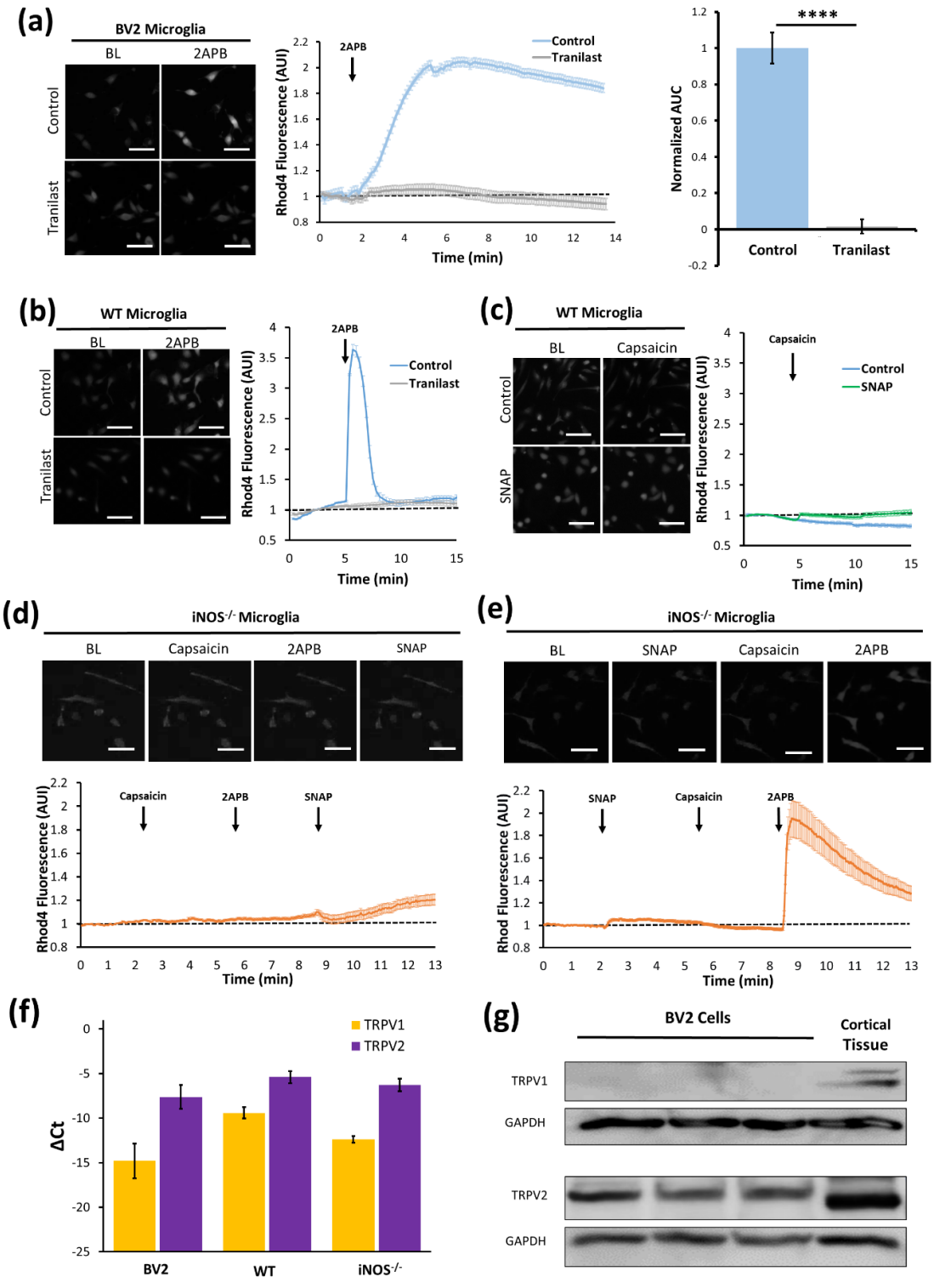

Figure legend on next page

Figure 2.4 2APB induces calcium entry primarily through TRPV2 channels in mouse microglia.

2APB induces calcium entry primarily through TRPV2 channels in mouse microglia. **A)** Left panel: Representative images of rhod-4 fluorescence in BV2 microglia before (BL) and after application of 2APB (250 μM) in the absence (control) and presence of tranilast (75 μM). Mid panel: Plotted curves of temporal changes in rhod-4 fluorescence within BV2 cells in the absence and presence of tranilast (N =3). Right Panel: Normalized AUC summarizes the 2APB-induced response in BV2 microglia before and after SNAP treatment (N = 3). **B)** Left panel: Representative images of rhod-4 fluorescence in WT microglia before and after application of 2APB in the absence and presence of tranilast. Right panel: Plotted traces of temporal changes in rhod-4 fluorescence within WT microglia in the absence and presence of tranilast (N = 3). **C)** Left panel: Representative images of rhod-4 fluorescence in WT microglia before and after application of capsaicin in the absence and presence of SNAP. Right panel: Plotted curves of temporal changes in rhod-4 fluorescence within WT microglia in the absence and presence of SNAP (N = 2). **D)** Upper row: Representative images of rhod-4 fluorescence in $iNOS^{-/-}$ microglia after sequential application of capsaicin (2 μM), 2APB (250 μM), and SNAP (250 μM), respectively. Lower panel: Plotted curves of temporal changes in rhod-4 fluorescence within multiple $iNOS^{-/-}$ microglia from N = 2. **E)** Upper row: Representative images of rhod-4 fluorescence in $iNOS^{-/-}$ microglia after sequential application of SNAP, capsaicin, and 2APB, respectively. Lower panel: Plotted curves of temporal changes in rhod-4 fluorescence within multiple $iNOS^{-/-}$ microglia from N = 2. Scale bars represent 50 μm. **F)** Plot reports the ΔCt values of TRPV1 and TRPV2 mRNAs, in relation to β-actin mRNA, within isolated WT and $iNOS^{-/-}$ microglia (N = 3). TRPV3 mRNA was not detected after 30 reaction cycles. **G)** Immunoblots of total proteins of TRPV1 and TRPV2, as well as GAPDH (loading control) in BV2 cells and WT male mouse cortical tissues (used as positive control for TRPV1 and TRPV2 expression).

2.4.5 TRPV2-mediated calcium influx in microglia is attenuated by inhibiting iNOS, PKG, or PI3K.

Next, we examined whether NO regulates the TRPV2-mediated calcium entry in BV2 microglia via PKG- and/or PI3K- dependent signaling. Application of 2APB to naïve BV2 cells induced a large calcium influx, and the 2APB effect was largely blocked by pretreating the naïve cells with PKG_i- or $PI3K_i$ **(Figure 2.5A)**. Notably, pretreating BV2 cells with the nonspecific NOS inhibitor L-NAME **(Figure 2.5B)** or with the selective iNOS inhibitor 1400W (Garvey et al., 1997) **(Figure 2.5C)** completely abolished the 2APB-induced calcium influx and occluded the effects of PKG_i and $PI3K_i$ **(Figure 2.5B, C)**. Interestingly, 2APB caused a slow-onset but long lasting and high-amplitude calcium influx in SNAP-pretreated BV2 microglia, which was also completely blocked with PKG_i or $PI3K_i$ **(Figure 2.5D)** treatment. These combined results strongly suggest that either iNOS-related endogenous NO or exogenous NO can effectively upregulate TRPV2 channel activity in mouse microglia through PKG- and PI3K-dependent signaling pathway(s).

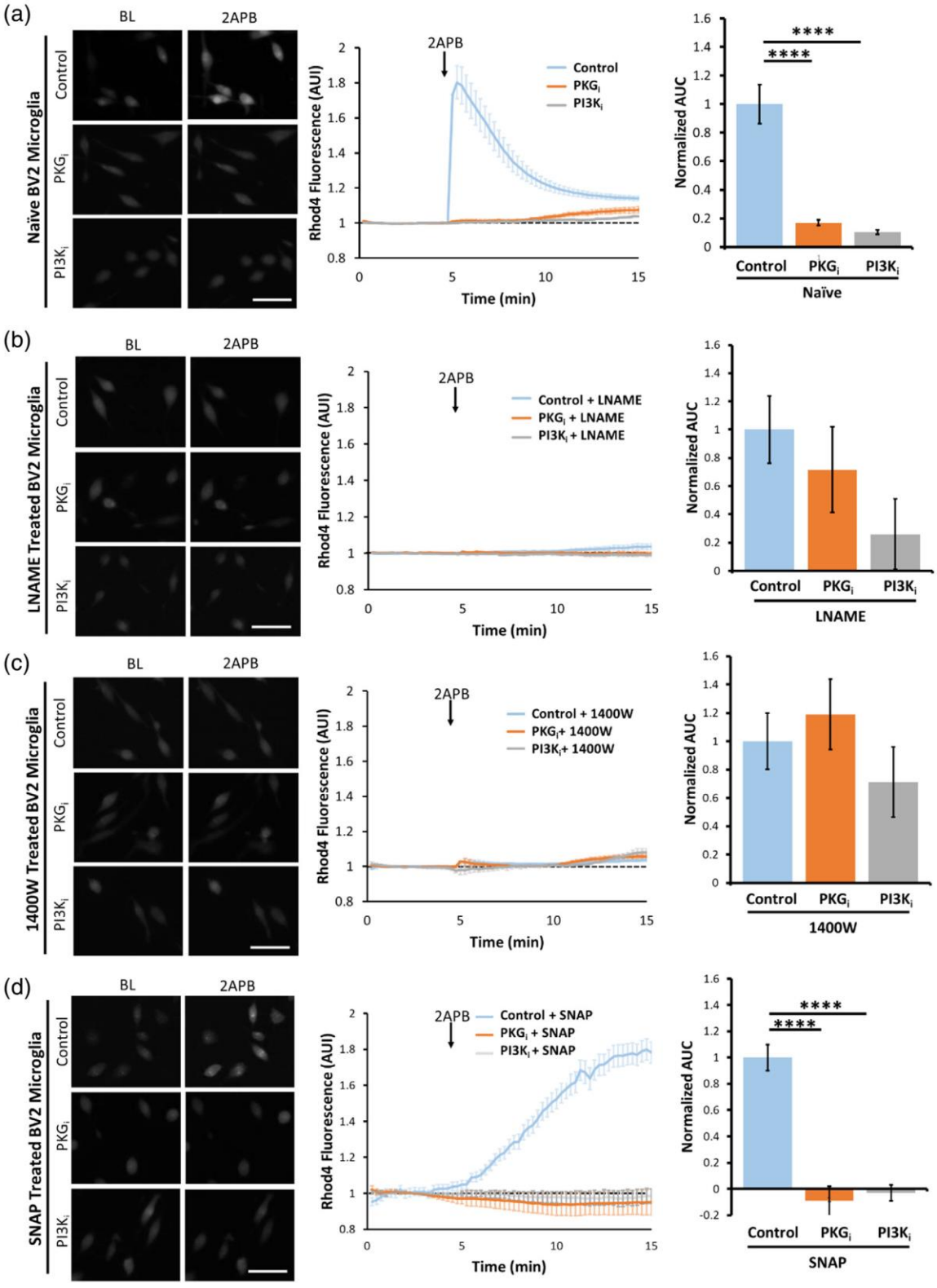

Figure legend on next page

Figure 2.5 2APB-induced calcium response in BV2 microglia is largely attenuated by inhibiting iNOS, PKG, or PI3K.

Shown are calcium responses in naive BV2 cells and BV2 cells pretreated with PKG_i or $PI3K_i$ **A)**; in BV2 cells pretreated with L-NAME (100 μM), L-NAME+PKG_i, or L-NAME+$PI3K_i$ **B)**; in BV2 cells pretreated with 1400W (5 μM), 1400W + PKG_i, or 1400W + $PI3K_i$ **C)**; and in BV2 cells pretreated with SNAP (250 μM), SNAP+PKG_i, or SNAP+$PI3K_i$ **D)**. Left panels in (A)-(D): Representative images of rhod-4 fluorescence in differently treated BV2 microglia before (BL) and after application of 2APB (250 μM). Scale bar represents 50 μm. Mid panels in (A)-(D): Plotted curves of temporal changes in Rhod-4 fluorescence within differently treated BV2 microglia before and after 2APB. Right panels in (A)-(D): Normalized AUC values quantify the 2APB-induced response in BV2 microglia under different treatment conditions.

2.4.6 NO signaling increases TRPV2 expression on the plasma membrane in BV2 microglia.

Tetrameric TRPV2 complexes on the ER membrane and Golgi apparatus can translocate to the PM where they act as nonselective cation channels (Nagasawa et al., 2007; Nagasawa & Kojima, 2012; Perálvarez-Marín et al., 2013). Immunocytochemistry and confocal image analyses revealed that under control conditions the immunofluorescence of TRPV2 was distributed on the PM and in the cytosol of BV2 cells displaying a higher ratio of PM versus cytosol intensity **(Figure 2.6A)**. Inhibiting endogenous NOS activity using L-NAME resulted in significantly higher intensity of TRPV2 fluorescence within the cytosol of cells **(Figure 2.6A, B**). In contrast, application of SNAP significantly increased the TRPV2 fluorescence intensity on the PM when compared to control conditions (**Figure 2.6A, B**). An alternative fast-release NO-donor, SNP, also increased TRPV2 fluorescence on the PM (**Figure 2.6A, B**). Moreover, immunoblotting assays of the biotin-labeled surface TRPV2 and the cytosolic TRPV2 demonstrated a significant increase in the PM/cytosol ratio of TRPV2 proteins in SNAP-treated BV2 microglia (**Figure 2.6C**). Moreover, treating the cells with PKG_i or with PKG_i + SNAP significantly decreased the PM localization of TRPV2 proteins to the same degree relative to control (**Figure 2.6A-C**). These results further imply that NO signaling increases TRPV2 channel expression on the PM of BV2 microglia in a PKG-dependent manner.

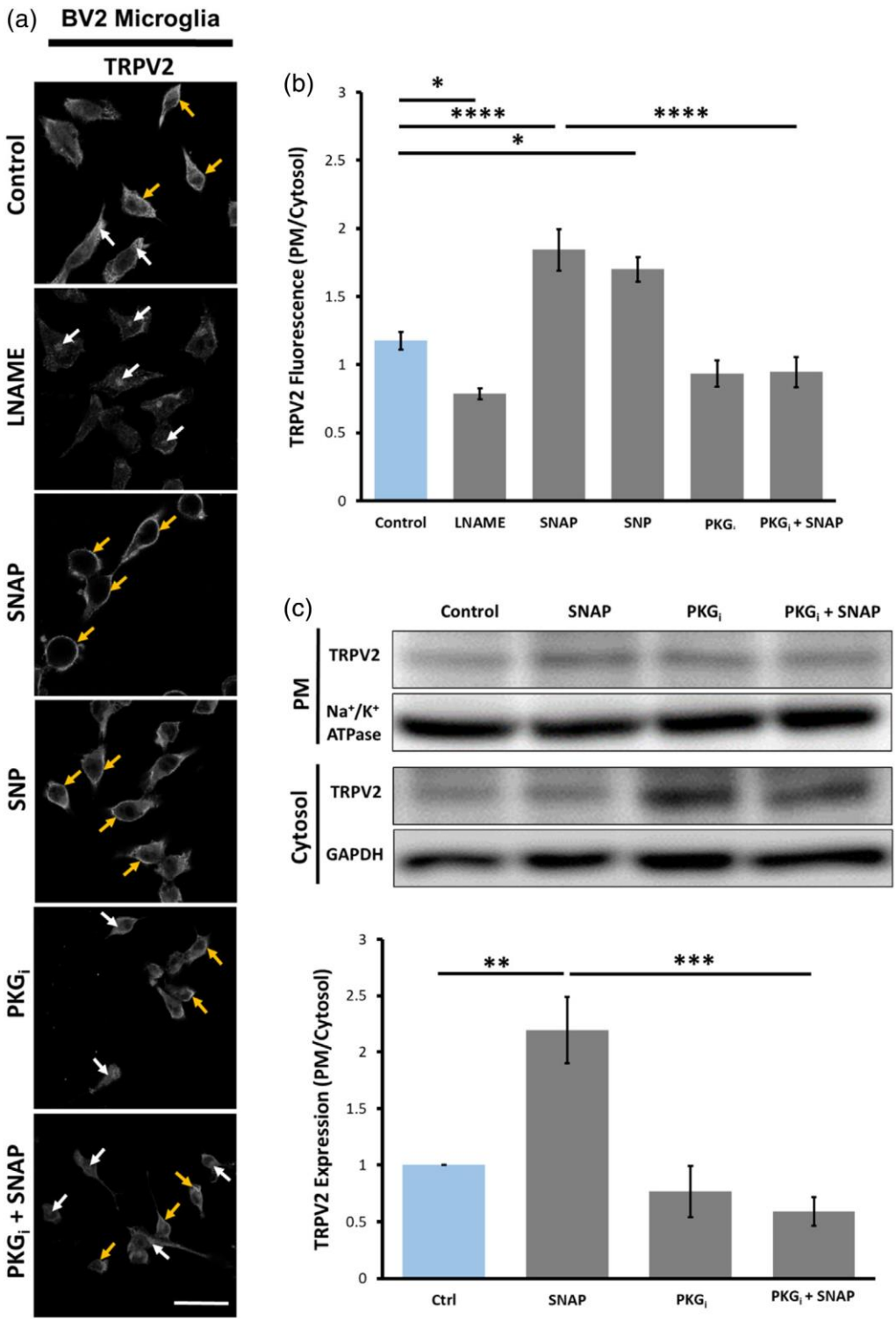

Figure legend on next page

Figure 2.6 NO increases the PM localization of TRPV2 in BV2 microglia in a PKG dependent manner. BV2 microglia.

NO signaling increases the PM localization of TRPV2 in BV2 microglia in a PKG dependent manner. **A)** Representative images of immunostained TRPV2 (grey) in control BV2 cells (control and BV2 cell pretreated with L-NAME (100 μM), SNAP (250 μM), SNP (300 μM), PKG_i (10 μM), or PKG_i + SNAP, respectively). Yellow arrows indicate abundant immunofluorescence of TRPV2 on the plasma membrane, and white arrows point to cytosolic immunofluorescence of TRPV2. Scale bars depict 25 μm. **B)** Bar graph reports the PM/cytosol ratio of TRPV2 fluorescence intensity within BV2 microglia pretreated with the test compounds (N = 3). **C)** Upper panel: Representative blots of biotinylated PM TRPV2 proteins and cytosolic TRPV2 proteins of BV2 microglia treated with the test compounds. Na+/K+-ATPase was used as a loading control for PM protein whereas GAPDH was used as a loading control for cytosolic protein. Lower panel: Bar graph reports the normalized PM/cytosol ratio of TRPV2 protein (normalized to their respective loading controls; N = 4).

2.4.7 NO regulates TRPV2 subcellular localization in WT and iNOS$^{-/-}$ microglia through PKG and PI3K.

Next, we investigated whether NO influences subcellular localization of TRPV2 in primary microglia through a PKG- or PI3K-dependent manner. To this end, we performed immunocytochemistry to examine the ratio of TRPV2 immunofluorescence on the PM and in the cytosol of primary microglia. Analyses revealed notable TRPV2 fluorescence in the PM and cytosol of control WT microglia. Treating WT microglia with 1400W significantly decreased the PM/cytosol ratio of TRPV2 fluorescence, although SNAP could not increase the TRPV2 fluorescence on the PM of WT microglia (**Figure 2.7A, B**). Remarkably, treating WT microglia with PKG_i or $PI3K_i$ significantly increased cytosolic TRPV2 fluorescence in comparison to control WT cells (**Figure 2.7C)**. In the presence of 1400W, however, PKG_i or $PI3K_i$ did not change the cytosolic TRPV2 fluorescence further (**Figure 2.7D)**. In contrast, in SNAP-treated WT microglia, PKG_i or $PI3K_i$ largely reduced the PM/cytosol ratio of TRPV2 (**Figure 2.7E**).

As expected, control iNOS$^{-/-}$ microglia displayed significantly less TRPV2 fluorescence on their PM when compared to control WT microglia (data not shown). While 1400W treatment had no effect on subcellular localization of TRPV2 fluorescence, SNAP treatment displayed significantly higher TRPV2 fluorescence on the PM when compared to control iNOS$^{-/-}$ microglia or 1400W-treated iNOS$^{-/-}$ microglia (**Figure 2.8A, B**). Unexpectedly, in control iNOS$^{-/-}$ microglia (**Figure 2.8C**), and in iNOS$^{-/-}$ microglia pretreated with 1400W (**Figure 2.8D**) or with SNAP (**Figure 2.8E**), application of PKG_i or $PI3K_i$ caused a relatively small but significant decrease in the PM localization of TRPV2 fluorescence. Altogether, these results demonstrated the importance of iNOS/NO signaling as well as PKG and PI3K in regulating subcellular localization of TRPV2 in primary mouse microglia.

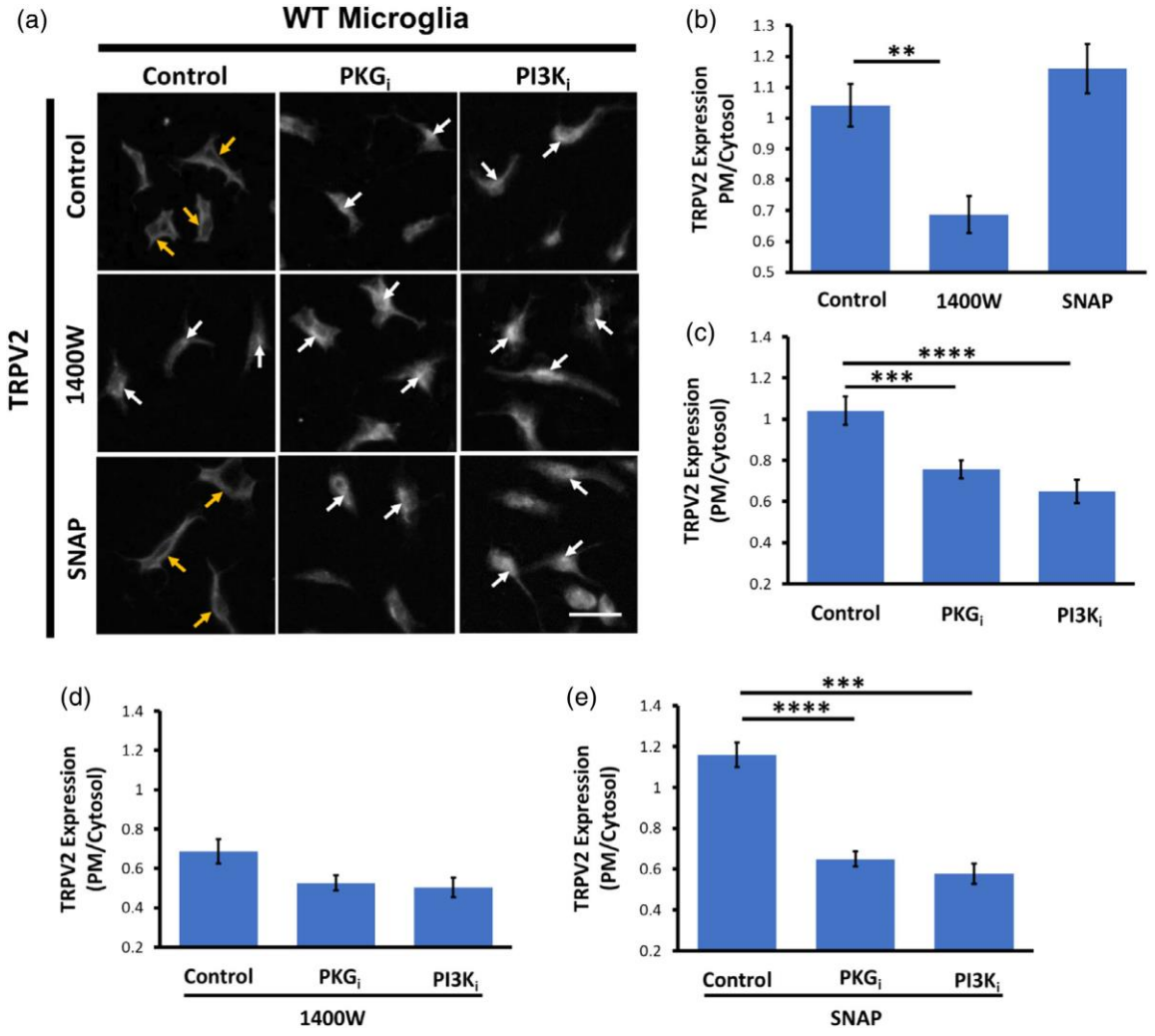

Figure 2.7 NO increases the PM localization of TRPV2 in WT microglia in a PKG dependent manner.

A) Representative images of immunostaining of TRPV2 (grey) in control WT microglia and WT microglia pretreated with 1400W (5 μM) or SNAP (250 μM) and/or crossly treated with PKG$_i$ (10 μM) or PI3K$_i$ (10 μM). The scale bar depicts 25 μm. Plotted graphs in **B), C)** and **D)** report the PM/cytosol ratio of TRPV2 fluorescence intensity within WT microglia under different test conditions

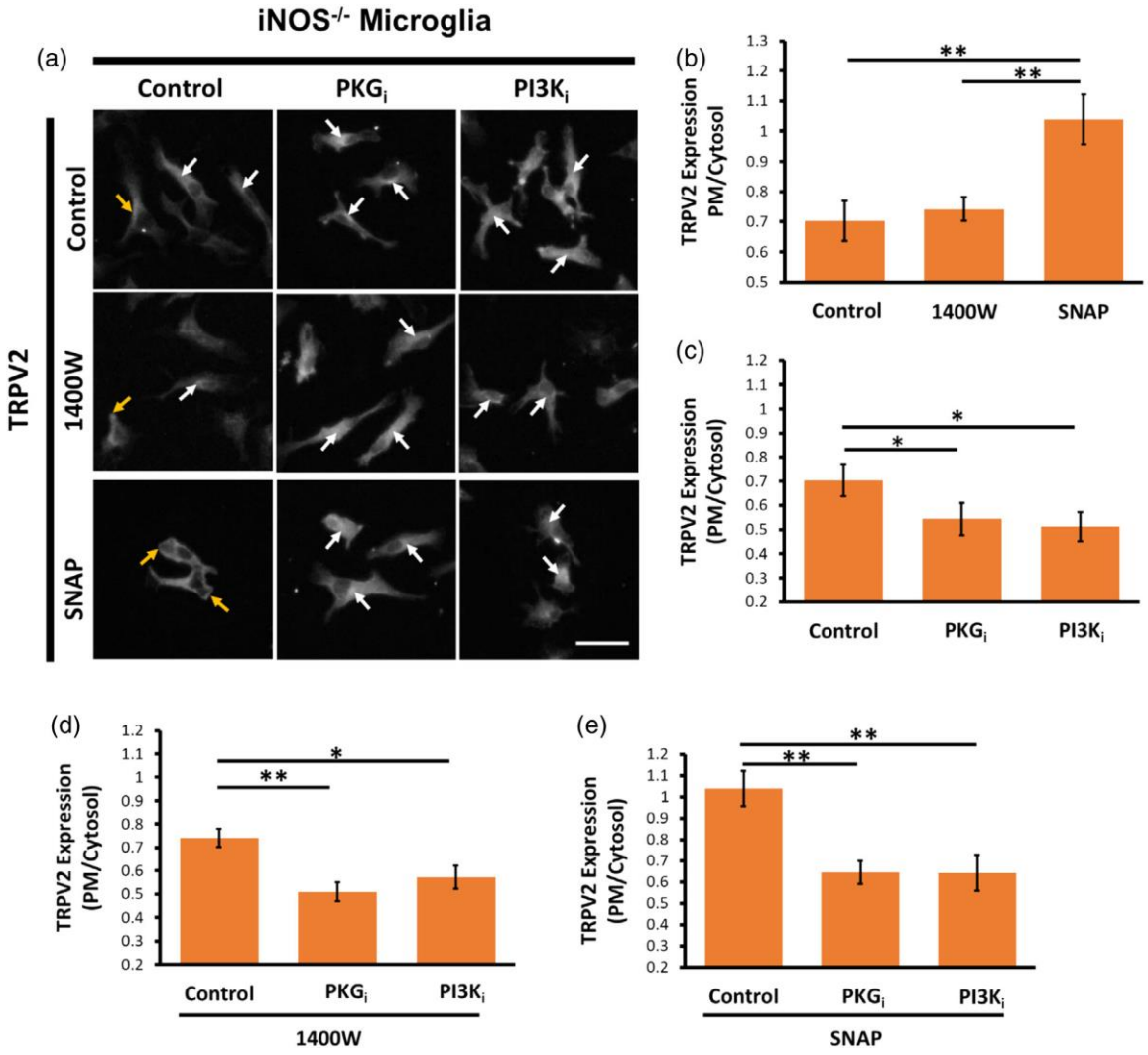

Figure 2.8 NO increases the PM localization of TRPV2 in iNOS$^{-/-}$ microglia in a PKG dependent manner.

A) Representative images of immunostaining of TRPV2 (grey) in control iNOS$^{-/-}$ microglia and iNOS$^{-/-}$ microglia pretreated with 1400W (5 μM) or SNAP (250 μM) and/or crossly-treated with PKG_i (10 μM) or $PI3K_i$ (10 μM). The scale bar depicts 25 μm. Plotted graphs in **B), C)** and **D)** report the PM/cytosol ratio of TRPV2 fluorescence intensity within iNOS$^{-/-}$ microglia under different test conditions.

2.5 Discussion

2.5.1 NO signaling upregulates phagocytic activity of mouse microglia

Numerous early studies show that an initial increase in NO production (Kakita et al., 2013; Scheiblich & Bicker, 2016) leads to enhanced microglial phagocytosis. Microglia possess a wide range of phagocytic receptors allowing them to recognize various substrates under different microenvironments. For example, microglia express receptors that recognize externalized phosphatidylserine on the surface of apoptotic neurons (Brown & Neher, 2014). Microglia also express various types of FcγRs that recognize and bind IgG. Activation of FcγR induces NAPDH oxidase activity to produce reactive oxygen species (ROS) (Haslund-Vinding et al., 2017; Lanone et al., 2005), and activates the transcription factor nuclear factor kappa-light-chain-enhancer of activated B-cells (NFκB) to upregulate iNOS/NO production in microglia (Le et al., 2001; Sánchez-Mejorada & Rosales, 1998). In this study, the use of IgG-FITC-beads to stimulate FcγRs in WT and iNOS$^{-/-}$ microglia allowed us to examine the influence of endogenous NO production on FcγR-mediated phagocytosis. Our analyses showed that iNOS$^{-/-}$ microglia displayed a significant decrease in phagocytic capacity, while expressing similar FcγRI and FcγRIII mRNA levels to that of WT microglia *in vitro* and *in vivo*. These results indicated that the phagocytic deficit in iNOS$^{-/-}$ microglia is not due to alterations in FcγR expression, but likely a result of reduced calcium influx through TRPV2 channels. It is interesting to note that iNOS$^{-/-}$ microglia are capable of phagocytosis, albeit with a reduced capacity. We speculate that the presence of FcγRs and the low level of PM TRPV2 expression on iNOS$^{-/-}$ microglia are sufficient for the cells to induce low-level phagocytosis. In addition, impaired phagocytosis in iNOS$^{-/-}$ microglia is unlikely a result of distorted ROS signaling, as a previous paper noted ROS production in iNOS$^{-/-}$ mice is not impaired (Lindgren et al., 2004). On the other hand, our assays showed that WT microglia produce significant amounts of NO in response to IgG-FITC-bead stimulation, suggesting an association of NO production with the enhanced phagocytic activity. This notion was supported by the result that supplement of iNOS$^{-/-}$ microglia with a slow-release NO-donor restored their phagocytic capacity.

2.5.2 NO enhances TRPV2 channel-mediated calcium entry in microglia via a PKG-dependent pathway

TRPV2 channel-mediated calcium influx has been proved to be crucial for phagocytosis in macrophages, and more recently, in microglia (Hassan et al., 2014; Lévêque et al., 2018; Link et al., 2010; Santoni & Amantini, 2013). In this regard, previous studies reported the expression of functional TRPV2 but not TRPV1/3 channels in murine microglia (Cao & Ramsey, 2016; Miyake et al., 2015). Consistent with these early reports, our assays revealed high levels of TRPV2 mRNA and protein in WT and iNOS$^{-/-}$ microglia. Although a lower level of TRPV1 mRNA was found in these cells, no TRPV3 mRNA was detected. Indeed, WT and BV2 microglia displayed a large calcium influx when stimulated with the TRPV1-3 agonist 2APB. Notably, the 2APB-mediated calcium influx in these mouse microglia were completely abolished by the selective TRPV2 antagonist tranilast. In contrast, the selective TRPV1 agonist capsaicin failed to induce a calcium response in WT and iNOS$^{-/-}$ microglia in the absence or presence of NO. The TRPV1 sensitivity to capsaicin is influenced by phosphorylation (Bhave et al., 2002), N-glycosylation (Veldhuis et al., 2012), pH (Samways et al., 2008), binding of phosphatidylinositol 4,5-biphosphate (PIP2) (Klein et al., 2008; Liu et al., 2005) and binding of calmodulin (Lishko et al., 2007; Rosenbaum et al., 2004). However, the insensitivity of mouse microglia to capsaicin was unlikely due to alterations in TRPV1 protein sensitivity because TRPV1 protein was not detected in mouse microglia, while being highly expressed in mouse cortical tissues. On the basis of these results, we reasoned that the 2APB-induced calcium influx in mouse microglia is mediated mainly by TRPV2 channels.

Naïve iNOS$^{-/-}$ microglia, however, did not respond to 2APB. It was impressive that minutes after application of the NO-donor SNAP, 2APB induced a rapid calcium rise in iNOS$^{-/-}$ microglia to a level comparable to that in WT cells. These results indicated that the existence of NO signaling is a decisive criterion for normal TRPV2 function in mouse microglia. To authenticate this notion, we performed whole-cell voltage-clamp recordings in primary microglia. Intriguingly, recordings revealed a basal transmembrane conductance in both WT and iNOS$^{-/-}$ microglia with a similar amplitude. We reasoned that the similar amplitude of basal conductance in WT and iNOS$^{-/-}$ microglia was a result of

dilution of endogenous iNOS and NO within WT cells by the intracellular solution after whole-cell configuration. Notably, a prominent nonselective cation conductance in WT microglia appeared 1–2 min after SNAP application, whereas such a conductance in $iNOS^{-/-}$ microglia was enlarged 3–4 min after SNAP treatment. Furthermore, the SNAP-evoked transmembrane conductance in both WT and $iNOS^{-/-}$ microglia was significantly blocked by RR, a broad TRPV channel blocker, confirming that NO indeed enhances a TRPV channel-mediated nonselective conductance in mouse microglia.

NO modulates cellular functions via the classical NO-sGC-cGMP-PKG pathway (Denninger & Marletta, 1999) or by direct *S*-nitrosylation (Okamoto & Lipton, 2015). No study has yet suggested *S*-nitrosylation of TRPV2 influences channel activity; therefore, we examined the classical pathway to observe if NO induced TRPV2 calcium influx through a PKG-dependent mechanism. To this end, naïve BV2 microglia were treated with PKG_i or $PI3K_i$. Here, $PI3K_i$ was used as a control considering its importance in TRPV2 PM trafficking (Nagasawa et al., 2007; Nagasawa & Kojima, 2012; Perálvarez-Marín et al., 2013). Notably, TRPV2-mediated calcium influx in BV2 microglia was significantly abolished by PKG_i and $PI3K_i$ under naïve conditions, or in the presence of SNAP. Importantly, in the presence of a NOS inhibitor, TRPV2-mediated calcium influx in BV2 microglia was also abolished. All of these data indicate that NO regulates TRPV2 channel function via the classical PKG pathway in mouse microglia.

It was intriguing that in the presence of SNAP, the TRPV2 channel-mediated calcium influx in BV2 microglia was prolonged and with a higher amplitude when compared to that in naïve conditions. In relation to this issue, early studies showed that NO-cGMP-PKG signaling inhibits the hydrolysis of phosphatidylinositol 4,5-bisphosphate (PIP2) (Clementi et al., 1995), a membrane lipid that is required for TRPV2 channel activation (Mercado et al., 2010), possibly by preventing TRPV2 desensitization (Mercado et al., 2010). These early studies may explain the sustained calcium influx seen within BV2 cells treated with SNAP.

2.5.3 NO increases TRPV2 expression on the surface of mouse microglia

TRPV2 channels can traffic from ER and/or Golgi stores to the PM (Nagasawa et al., 2007; Nagasawa & Kojima, 2012; Perelvarez-Marin et al., 2013). In this present study, we found that minutes after pretreating iNOS$^{-/-}$ microglia with SNAP, application of 2APB could generate calcium influx. The short interval between the SNAP treatment and the 2APB-induced response suggests that NO-cGMP-PKG signaling may cause TRPV2 trafficking from the intracellular organelles to the PM. To test this idea, we pretreated BV2 microglia with NOS inhibitors or NO-donors with or without PKG_i, and examined subcellular localization of TRPV2 in the cells by means of immunocytochemistry and immunoblot of biotinylated cell surface proteins. Our assays showed that SNAP intensified the immunofluorescence of TRPV2 on the PM and increased the amount of biotinylated TRPV2 protein on the cell surface. The SNAP-induced increase in the PM localization of TRPV2 was abolished by PKG_i. In contrast, treating BV2 microglia with L-NAME to inhibit endogenous NO-production significantly attenuated the immunofluorescence of TRPV2 on the PM.

Consistent with the observations in BV2 microglia, treating primary WT microglia with the selective iNOS inhibitor 1400W significantly decreased the immunofluorescence of TRPV2 on the PM. Notably, treating naive WT microglia or the SNAP-pretreated WT microglia with PKG_i or with $PI3K_i$ also significantly decreased the immunofluorescence of TRPV2 on the PM. However, in the presence of 1400W, PKG_i or $PI3K_i$ had no further effect, signifying the importance of basal NO-cGMP-PKG signaling for TRPV2 to localize in the PM. On the other hand, treating primary iNOS$^{-/-}$ microglia with SNAP significantly increased the PM fluorescence of TRPV2. The effect of SNAP on TRPV2 fluorescence in the PM of iNOS$^{-/-}$ microglia was abolished with PKG_i or $PI3K_i$ treatment. Altogether, these results indicate that NO increases the translocation of TRPV2 from the cytosol to the PM of mouse microglia via the classical PKG signaling cascade.

Curiously, application of PKG_i or $PI3K_i$ to iNOS$^{-/-}$ microglia further decreased the PM localization of TRPV2. These results indicate that basal PKG activity in iNOS$^{-/-}$ microglia is also regulated by an NO-independent mechanism. In this regard, Moriyama et

al. reported that rat microglia express natriuretic peptide receptors (NPRs) and may produce natriuretic peptides (Moriyama et al., 2006). Moreover, stimulation of NPRs produces cGMP (Moriyama et al., 2006). Whether NPR-mediated cGMP production within iNOS$^{-/-}$ microglia contributes to the basal PKG activity as a compensation mechanism for the lack of NO production remains to be investigated in future studies. Our results also signify an important role of PI3K in the NO regulation of the surface expression of TRPV2 channels in microglia. However, it remains unclear whether PI3K activation occurs downstream of PKG activity. Kawasaki et al. reported that PI3K-Akt activity in endothelial cells is regulated by NO signaling via an unknown mechanism independent of *S*-nitrosylation (Kawasaki et al., 2003). Additionally, Lee et al. showed that endothelial NOS/NO signaling can activate PI3K-Akt in astrocytes (Lee et al., 2010). Future studies should explore whether PKG activity directly or indirectly induces PI3K activation in microglia. In summary, the present study for the first time demonstrated that iNOS/NO signaling in mouse microglia upregulates the phagocytic capacity of the cells by increasing TRPV2 trafficking to the PM via PKG/PI3K dependent pathway(s). These novel findings add new insights of how microglia execute phagocytosis in response to changes in their surrounding environment.

As illustrated in **Figure 2.9**, we propose that in response to a signal that triggers FcγR phagocytosis, microglia increase the expression or activity of iNOS and produces higher levels of NO. The NO/sGC/cGMP/PKG-PI3K signaling induces TRPV2 trafficking to the PM and sequential calcium entry thus consequently initiating phagocytosis through further FcγR-clustering (Link et al., 2010) and actin cytoskeleton reorganization. The NO-TRPV2 regulation of microglia phagocytosis may possess therapeutic benefits for treating neurological disorders in which microglia become deficient in phagocytosis (Iadecola et al., 1997; Nagayama et al., 1999; Pérez-Asensio et al., 2005; Sierra et al., 2013).

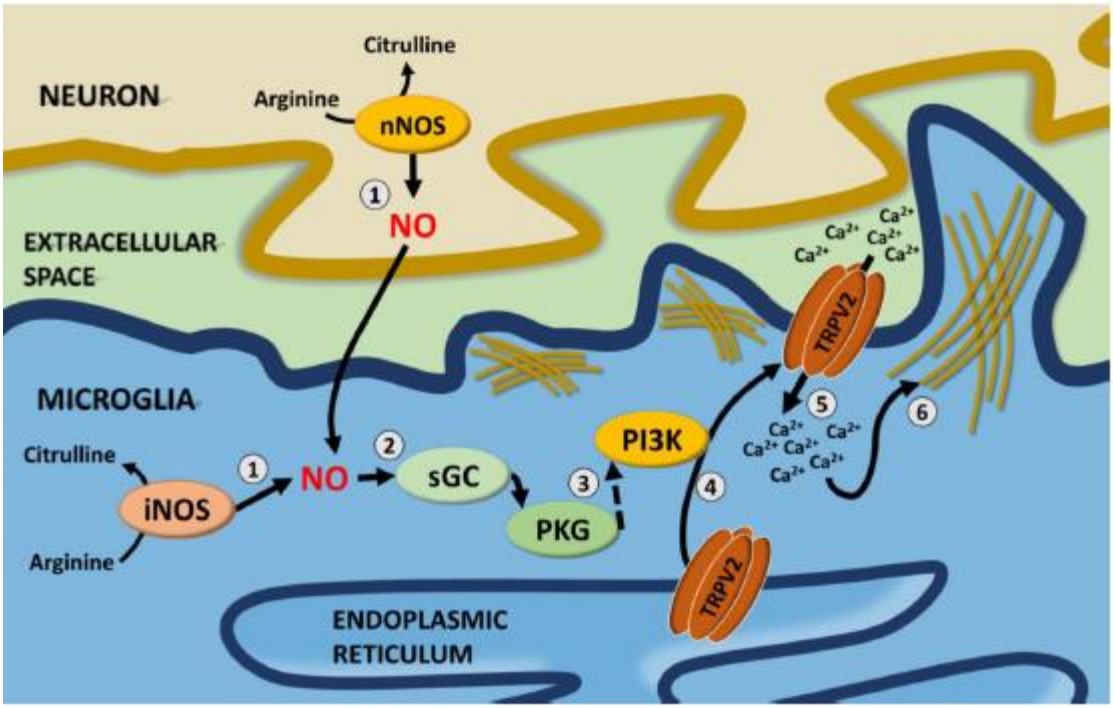

Figure 2.9 Schematic illustration of a proposed mechanism by which iNOS/NO signals to regulate TRPV2 channel trafficking.

The interaction of FcγRs with their ligands increases NO production within microglia through endogenous iNOS activity. In addition, exogenous NO diffused from neighboring cells such as neurons can increase NO levels within microglia. The elevated NO molecules in microglia activate sGC, hence, sequentially increasing cGMP and PKG activity. Through an unknown mechanism, the activated PKG may stimulate PI3K activity, which in turn induces translocation of tetrameric TRPV2 protein complex from the ER to the PM where it acts as a nonselective cation channel. As Link et al. proposed in 2010, the entry of cations, including Na^+ and Ca^{2+} through TRPV2 channels, depolarize the local PM while the elevated intracellular calcium ions initiates the recruitment of more FcγR clusters and the reorganization of cellular cytoskeleton hence enabling the local PM to engulf the FcγR ligand-containing targets.

2.6 Acknowledgements

The authors thank Ms. Michelle Everest for her considerate assistance in the course of RT-qPCR analyses. MJEM and VT are recipients of 2018/2019 Ontario Graduate Scholarship. This work was supported by the Canadian Institutes of Health Research (MOP-133504) awarded to W-Y L.

2.7 References

Aarum, J., Sandberg, K., Haeberlein, S. L. B., & Persson, M. A. A. (2003). Migration and differentiation of neural precursor cells can be directed by microglia. Proceedings of the National Academy of Sciences, 100(26), 15983–15988. https://doi.org/10.1073/pnas.2237050100

Aoyagi, K., Ohara-Imaizumi, M., Nishiwaki, C., Nakamichi, Y., & Nagamatsu, S. (2010). Insulin/phosphoinositide 3-kinase pathway accelerates the glucose-induced first-phase insulin secretion through TrpV2 recruitment in pancreatic β-cells. Biochemical Journal, 432(2), 375–386. https://doi.org/10.1042/bj20100864

Bhave, G., Zhu, W., Wang, H., Brasier, D. J., Oxfordm, G. S., & Gereau, R. W. I. (2002). cAMP-Dependent Protein Kinase Regulates Desensitization of the Capsaicin Receptor (VR1) by Direct Phosphorylation. Neuron, 35, 721–731. https://doi.org/10.1016/S0896-6273(02)00802-4

Bogdan, C. (2001). Nitric oxide and the immune response. Nature Immunology, 2(10), 907–916. https://doi.org/10.1038/ni1001-907

Bogdan, Christian. (2015). Nitric oxide synthase in innate and adaptive immunity: An update. Trends in Immunology, 36(3), 161–178. https://doi.org/10.1016/j.it.2015.01.003

Brown, G. C., & Neher, J. J. (2014). Microglial phagocytosis of live neurons. Nature Publishing Group, 15(4), 209–216. https://doi.org/10.1038/nrn3710

Cao, T., & Ramsey, I. S. (2016). Toll-Like Receptor 4 Activation by LPS Stimulates TRPV2 Channel Activity in Microglia. Biophysical Journal, 110(3), 286a. https://doi.org/10.1016/j.bpj.2015.11.1548

Casano, A. M., & Peri, F. (2015). Review Microglia : Multitasking Specialists of the Brain. Developmental Cell, 32(4), 469–477. https://doi.org/10.1016/j.devcel.2015.01.018

Chung, H., Brazil, M. I., Soe, T. T., & Maxfield, F. R. (1999). Uptake, degradation, and release of fibrillar and soluble forms of Alzheimer's amyloid β-peptide by microglial cells. Journal of Biological Chemistry, 274(45), 32301–32308. https://doi.org/10.1074/jbc.274.45.32301

Ciesielski-Treska, J., Grant, N. J., Ulrich, G., Corrotte, M., Bailly, Y., Haeberle, A. M., … Bader, M. F. (2004). Fibrillar Prion Peptide (106-126) and Scrapie Prion Protein Hamper Phagocytosis in Microglia. Glia, 46(2), 101–115. https://doi.org/10.1002/glia.10363

Clementi, E., Sciorati, C., Riccio, M., Miloso, M., Meldolesi, J., & Nisticò, G. (1995). Nitric Oxide Action on Growth Factor-elicited Signals. Journal of Biological Chemistry, 270(38), 22277–22282. https://doi.org/10.1074/jbc.270.38.22277

Denninger, J. W., & Marletta, M. A. (1999). Guanylate cyclase and the.NO/cGMP signaling pathway. Biochimica et Biophysica Acta - Bioenergetics, 1411(2–3), 334–350. https://doi.org/10.1016/S0005-2728(99)00024-9

Derecki, N. C., Cronk, J. C., Lu, Z., Xu, E., Abbott, S. B. G., Guyenet, P. G., & Kipnis, J. (2012). Wild-type microglia arrest pathology in a mouse model of Rett syndrome. Nature, 484(7392), 105–109. https://doi.org/10.1038/nature10907

Förstermann, U., & Sessa, W. C. (2012). Nitric oxide synthases: Regulation and function. European Heart Journal, 33(7), 829–837. https://doi.org/10.1093/eurheartj/ehr304

Fu, R., Shen, Q., Xu, P., Luo, J. J., & Tang, Y. (2014). Phagocytosis of microglia in the central nervous system diseases. Molecular Neurobiology, 49(3), 1422–1434. https://doi.org/10.1007/s12035-013-8620-6

Garvey, E. P., Oplinger, J. A., Furfine, E. S., Kiff, R. J., Laszlo, F., Whittle, B. J. R., & Knowles, R. G. (1997). 1400W Is a Slow, Tight Binding, and Highly Selective Inhibitor of Inducible Nitric-oxide Synthase in Vitro and in Vivo. Journal of Biological Chemistry, 272(8), 4959–4963. https://doi.org/10.1074/jbc.272.8.4959

Gu, M., Lynch, J., & Brecher, P. (2000). Nitric Oxide Increases p21 Waf1 / Cip1 Expression by a cGMP-dependent Pathway That Includes Activation of Extracellular Signal-regulated Kinase and p70 S6k *, 275(15), 11389–11396.

Harry, G. J., & Kraft, A. D. (2012). Microglia in the developing brain : A potential target with lifetime effects. Neurotoxicology, 33(2), 191–206. https://doi.org/10.1016/j.neuro.2012.01.012

Haslund-Vinding, J., McBean, G., Jaquet, V., & Vilhardt, F. (2017). NADPH oxidases in oxidant production by microglia: activating receptors, pharmacology and association with disease. British Journal of Pharmacology, 174(12), 1733–1749. https://doi.org/10.1111/bph.13425

Hassan, S., Eldeeb, K., Millns, P. J., Bennett, A. J., Alexander, S. P. H., & Kendall, D. A. (2014). Cannabidiol enhances microglial phagocytosis via transient receptor potential (TRP) channel activation. British Journal of Pharmacology, 171(9), 2426–2439. https://doi.org/10.1111/bph.12615

Hisanaga, E., Nagasawa, M., Ueki, K., Kulkarni, R. N., Mori, M., & Kojima, I. (2009). Regulation of Calcium-Permeable TRPV2 Channel by Insulin in Pancreatic -Cells. Diabetes, 58(1), 174–184. https://doi.org/10.2337/db08-0862

Hu, H. Z., Gu, Q., Wang, C., Colton, C. K., Tang, J., Kinoshita-Kawada, M., … Zhu, M. X. (2004). 2-Aminoethoxydiphenyl borate is a common activator of TRPV1, TRPV2, and TRPV3. Journal of Biological Chemistry, 279(34), 35741–35748. https://doi.org/10.1074/jbc.M404164200

Iadecola, C., Zhang, F., Casey, R., Nagayama, M., & Ross, M. E. (1997). Delayed Reduction of Ischemic Brain Injury and Neurological Deficits in Mice Lacking the Inducible Nitric Oxide Synthase Gene. The Journal of Neuroscience, 17(23), 9157–9164. https://doi.org/10.1523/JNEUROSCI.17-23-09157.1997

Juvin, V., Penna, A., Chemin, J., Lin, Y.-L., & Rassendren, F.-A. (2007). Pharmacological Characterization and Molecular Determinants of the Activation of Transient Receptor Potential V2 Channel Orthologs by 2-Aminoethoxydiphenyl Borate. Molecular Pharmacology, 72(5), 1258–1268. https://doi.org/10.1124/mol.107.037044

Kakita, H., Aoyama, M., Nagaya, Y., Asai, H., Hussein, M. H., Suzuki, M., … Asai, K. (2013). Diclofenac enhances proinflammatory cytokine-induced phagocytosis of cultured microglia via nitric oxide production. Toxicology and Applied Pharmacology, 268(2), 99–105. https://doi.org/10.1016/j.taap.2013.01.024

Kanzaki, M., Zhang*, Y.-Q., Mashima*, H., Li*, L., Shibata*, H., & Kojima, I. (1999). Translocation of a calcium-permeable cation channel induced by insulin-like growth factor-I. Nature Cell Biology, 1(3), 165–170. https://doi.org/10.1038/11086

Kawasaki, K., Smith, R. S., Hsieh, C., Sun, J., Chao, J., & Liao, J. K. (2003). Activation of the Phosphatidylinositol 3-Kinase / Protein Kinase Akt Pathway Mediates Nitric Oxide-Induced Endothelial Cell Migration and Angiogenesis, 23(16), 5726–5737. https://doi.org/10.1128/MCB.23.16.5726

Klein, R. M., Ufret-Vincenty, C. A., Hua, L., & Gordon, S. E. (2008). Determinants of molecular specificity in phosphoinositide: Regulation phosphatidylinositol (4,5)-bisphosphate (PI(4,5)P2) is the endogenous lipid regulating TRPV1. Journal of Biological Chemistry, 283(38), 26208–26216. https://doi.org/10.1074/jbc.M801912200

Kopec, K. K., & Carroll, R. T. (2000). Phagocytosis is Regulated by Nitric Oxide in Murine Microglia, 4(2), 103–111. https://doi.org/10.1006/niox.2000.0280

Kraus, B., Wolff, H., Elstner, E. F., & Heilmann, J. (2010). Hyperforin is a modulator of inducible nitric oxide synthase and phagocytosis in microglia and macrophages. Naunyn-Schmiedeberg's Archives of Pharmacology, 381(6), 541–553. https://doi.org/10.1007/s00210-010-0512-y

Lanone, S., Bloc, S., Foresti, R., Almolki, A., Taillé, C., Callebert, J., … Boczkowski, J. (2005). Bilirubin decreases nos2 expression via inhibition of NAD(P)H oxidase: implications for protection against endotoxic shock in rats. The FASEB Journal, 19(13), 1890–1892. https://doi.org/10.1096/fj.04-2368fje

Le, W., Rowe, D., Xie, W., Ortiz, I., He, Y., & Appel, S. H. (2001). Microglial Activation and Dopaminergic Cell Injury: An In Vitro Model Relevant to Parkinson's Disease. J. Neurosci., 21(21), 8447–8455. https://doi.org/21/21/8447 [pii]

Lee, S. H., Byun, J. S., Kong, P. J., Lee, H. J., Kim, D. K., Kim, H. S., … Kim, S. S. (2010). Inhibition of eNOS / sGC / PKG Pathway Decreases Akt Phosphory- lation Induced by Kainic Acid in Mouse Hippocampus, 14, 37–43. https://doi.org/10.4196/kjpp.2010.14.1.37

Lévêque, M., Penna, A., Le Trionnaire, S., Belleguic, C., Desrues, B., Brinchault, G., … Martin-Chouly, C. (2018). Phagocytosis depends on TRPV2-mediated calcium

influx and requires TRPV2 in lipids rafts: Alteration in macrophages from patients with cystic fibrosis. Scientific Reports, 8(1), 1–13. https://doi.org/10.1038/s41598-018-22558-5

Lindgren, H., Stenmark, S., Chen, W., Tarnvik, A., & Sjostedt, A. (2004). Distinct Roles of Reactive Nitrogen and Oxygen Species To Control Infection with the Facultative Intracellular Bacterium Francisella tularensis. Infection and Immunity, 72(12), 7172–7182. https://doi.org/10.1128/IAI.72.12.7172-7182.2004

Link, T. M., Park, U., Vonakis, B. M., Raben, D. M., Soloski, M. J., & Caterina, M. J. (2010). TRPV2 has a pivotal role in macrophage particle binding and phagocytosis. Nature Immunology, 11(3), 232–239. https://doi.org/10.1038/ni.1842

Lishko, P. V., Procko, E., Jin, X., Phelps, C. B., & Gaudet, R. (2007). The Ankyrin Repeats of TRPV1 Bind Multiple Ligands and Modulate Channel Sensitivity. Neuron, 54(6), 905–918. https://doi.org/10.1016/j.neuron.2007.05.027

Liu, B., Zhang, C., & Qin, F. (2005). Functional Recovery from Desensitization of Vanilloid Receptor TRPV1 Requires Resynthesis of Phosphatidylinositol 4,5-Bisphosphate. Journal of Neuroscience, 25(19), 4835–4843. https://doi.org/10.1523/JNEUROSCI.1296-05.2005

Marín-Teva, J. L., Dusart, I., Colin, C., Gervais, A., van Rooijen, N., & Mallat, M. (2004). Microglia Promote the Death of Developing Purkinje Cells. Neuron, 41(4), 535–547. https://doi.org/10.1016/S0896-6273(04)00069-8

Mercado, J., Gordon-shaag, A., Zagotta, W. N., & Gordon, S. E. (2010). Ca 2 𝜍 -Dependent Desensitization of TRPV2 Channels Is Mediated by Hydrolysis of Phosphatidylinositol 4 , 5-Bisphosphate, 30(40), 13338–13347. https://doi.org/10.1523/JNEUROSCI.2108-10.2010

Mihara, H., Boudaka, A., Shibasaki, K., Yamanaka, A., Sugiyama, T., & Tominaga, M. (2010). Involvement of TRPV2 Activation in Intestinal Movement through Nitric Oxide Production in Mice, 30(49), 16536–16544. https://doi.org/10.1523/JNEUROSCI.4426-10.2010

Miyake, T., Shirakawa, H., Nakagawa, T., & Kaneko, S. (2015). Activation of mitochondrial transient receptor potential vanilloid 1 channel contributes to microglial migration. Glia, 63(10), 1870–1882. https://doi.org/10.1002/glia.22854

Moriyama, N., Taniguchi, M., Miyano, K., Miyoshi, M., & Watanabe, T. (2006). ANP inhibits LPS-induced stimulation of rat microglial cells by suppressing NF-κB and AP-1 activations. Biochemical and Biophysical Research Communications, 350(2), 322–328. https://doi.org/10.1016/j.bbrc.2006.09.034

Nagasawa, M., & Kojima, I. (2012). Translocation of calcium-permeable TRPV2 channel to the podosome: Its role in the regulation of podosome assembly. Cell Calcium, 51(2), 186–193. https://doi.org/10.1016/j.ceca.2011.12.012

Nagasawa, M., Nakagawa, Y., Tanaka, S., & Kojima, I. (2007). Chemotactic peptide fMetLeuPhe induces translocation of the TRPV2 channel in macrophages. Journal of Cellular Physiology, 210(3), 692–702. https://doi.org/10.1002/jcp.20883

Nagayama, M., Aber, T., Nagayama, T., Ross, M. E., & Iadecola, C. (1999). Age-Dependent Increase in Ischemic Brain Injury in Wild-Type Mice and in Mice Lacking the Inducible Nitric Oxide Synthase Gene. Journal of Cerebral Blood Flow & Metabolism, 19(6), 661–666. https://doi.org/10.1097/00004647-199906000-00009

Okamoto, S. I., & Lipton, S. A. (2015). S-Nitrosylation in neurogenesis and neuronal development. Biochimica et Biophysica Acta - General Subjects, 1850(8), 1588–1593. https://doi.org/10.1016/j.bbagen.2014.12.013

Park, J. Y., Paik, S. R., Jou, I., & Park, S. M. (2008). Microglial phagocytosis is enhanced by monomeric α-synuclein, not aggregated α-synuclein: Implications for Parkinson's disease. Glia, 56(11), 1215–1223. https://doi.org/10.1002/glia.20691

Pautz, A., Art, J., Hahn, S., Nowag, S., Voss, C., & Kleinert, H. (2010). Regulation of the expression of inducible nitric oxide synthase. Nitric Oxide - Biology and Chemistry, 23(2), 75–93. https://doi.org/10.1016/j.niox.2010.04.007

Perálvarez-Marín, A., Doñate-Macian, P., & Gaudet, R. (2013). What do we know about the transient receptor potential vanilloid 2 (TRPV2) ion channel? FEBS Journal, 280(21), 5471–5487. https://doi.org/10.1111/febs.12302

Pérez-Asensio, F. J., Hurtado, O., Burguete, M. C., Moro, M. A., Salom, J. B., Lizasoain, I., … Lorenzo, P. (2005). Inhibition of iNOS activity by 1400W decreases glutamate release and ameliorates stroke outcome after experimental ischemia. Neurobiology of Disease, 18(2), 375–384. https://doi.org/10.1016/j.nbd.2004.10.018

Rosenbaum, T., Gordon-Shaag, A., Munari, M., & Gordon, S. E. (2004). Calcium/Calmodulin Modulates TRPV1 Activation by Capsaicin. The Journal of General Physiology, 123(1), 53–62. https://doi.org/10.1085/jgp.200308906

Samways, D. S. K., Khakh, B. S., & Egan, T. M. (2008). Tunable calcium current through TRPV1 receptor channels. Journal of Biological Chemistry, 283(46), 31274–31278. https://doi.org/10.1074/jbc.C800131200

Sánchez-Mejorada, G., & Rosales, C. (1998). Fcγ receptor-mediated mitogen-activated protein kinase activation in monocytes is independent of Ras. Journal of Biological Chemistry, 273(42), 27610–27619. https://doi.org/10.1074/jbc.273.42.27610

Santoni, M., & Amantini, C. (2013). The role of transient receptor potential vanilloid type-2 ion channels in innate and adaptive immune responses, 4(February), 1–9. https://doi.org/10.3389/fimmu.2013.00034

Schafer, D. P., Lehrman, E. K., & Stevens, B. (2013). The ‘“ Quad-Partite ”’ Synapse : Microglia-Synapse Interactions in the Developing and Mature CNS, 36(June 2012), 24–36. https://doi.org/10.1002/glia.22389

Scheiblich, H., & Bicker, G. (2016). Nitric oxide regulates antagonistically phagocytic and neurite outgrowth inhibiting capacities of microglia. Developmental Neurobiology, 76(5), 566–584. https://doi.org/10.1002/dneu.22333

Schindelin, J., Arganda-Carreras, I., Frise, E., Kaynig, V., Longair, M., Pietzsch, T., … Cardona, A. (2012). Fiji: An open-source platform for biological-image analysis. Nature Methods, 9(7), 676–682. https://doi.org/10.1038/nmeth.2019

Shemer, A., Erny, D., Jung, S., & Prinz, M. (2015). Microglia Plasticity During Health and Disease : An Immunological Perspective. Trends in Immunology, 36(10), 614–624. https://doi.org/10.1016/j.it.2015.08.003

Sheng, W., Zong, Y., Mohammad, A., Ajit, D., Cui, J., Han, D., … Sun, G. Y. (2011). Pro-inflammatory cytokines and lipopolysaccharide induce changes in cell morphology, and upregulation of ERK1/2, iNOS and sPLA2-IIA expression in astrocytes and microglia. Journal of Neuroinflammation, 8(1), 121. https://doi.org/10.1186/1742-2094-8-121

Sierra, A., Abiega, O., Shahraz, A., & Neumann, H. (2013). Janus-faced microglia: beneficial and detrimental consequences of microglial phagocytosis. Frontiers in Cellular Neuroscience, 7(January), 1–22. https://doi.org/10.3389/fncel.2013.00006

Sierra, A., Encinas, J. M., Deudero, J. J. P., Chancey, J. H., Enikolopov, G., Overstreet-wadiche, L. S., … Maletic-savatic, M. (2010). Article Microglia Shape Adult Hippocampal Neurogenesis through Apoptosis-Coupled Phagocytosis. Stem Cell, 7(4), 483–495. https://doi.org/10.1016/j.stem.2010.08.014

Veldhuis, N. A., Lew, M. J., Abogadie, F. C., Poole, D. P., Jennings, E. A., Ivanusic, J. J., … McIntyre, P. (2012). N-glycosylation determines ionic permeability and desensitization of the TRPV1 capsaicin receptor. Journal of Biological Chemistry, 287(26), 21765–21772. https://doi.org/10.1074/jbc.M112.342022

Chapter 3

3 Nitric oxide displays a biphasic effect on microglia calcium dynamics.

3.1 Abstract

Calcium is a critical secondary messenger in microglia. In response to inflammation, microglia mobilize intracellular calcium and increase the expression of inducible nitric oxide synthase (iNOS), which produces copious amounts of nitric oxide (NO). This study set to explore whether NO regulates intracellular calcium dynamics through transient receptor potential (TRP) channels in primary wildtype (WT) and iNOS knockout ($iNOS^{-/-}$) microglia, and the BV2 microglial cell line using calcium imaging and voltage-clamp recordings. Our results demonstrated that application of the NO-donor SNAP induced a biphasic calcium response in naïve murine microglia. Specifically, phase I was characterized by a decline in calcium influx that was attenuated by the store operated calcium channel (SOCC) inhibitor SKF96365, while phase II presented with a calcium influx that was abolished by the TRP vanilloid type 2 (TRPV2) channel inhibitor tranilast. Importantly, in the presence of a protein kinase G (PKG) inhibitor, the SNAP-mediated calcium decline in phase I persisted while the calcium influx in phase II was abolished. Application of thapsigargin to activate SOCCs caused a calcium influx through a nonselective cation conductance in BV2 microglia, which SNAP abruptly attenuated. Importantly, $iNOS^{-/-}$ microglia cultures displayed a significantly larger calcium influx though SOCCs than WT microglia, while simultaneously expressing less stromal interaction molecule 1 and TRP canonical type 1 and 3 mRNA when compared to WT cultures. Together, these results demonstrate that NO signaling restricts calcium influx through SOCCs independent of PKG signaling and increases calcium influx through TRPV2 channels in a PKG-dependent mechanism in murine microglia.

3.2 Introduction

Calcium is a crucial secondary messenger that facilitates many physiological responses within microglia. In response to extracellular stimuli, microglia mobilize calcium using a variety of ion channels present on their cell-surface to carry out functions such as migration, proliferation, phagocytosis, and cytokine secretion (Kettenmann et al., 2011; Sharma & Ping, 2014). Microglia express a wide array of calcium-permeable transient receptor potential (TRP) channels on their plasma membrane, including but not limited to canonical (TRPC) and vanilloid (TRPV) subfamilies (Kettenmann et al., 2011; Sharma & Ping, 2014).

Calcium influx through TRPC1 and TRPC3 channels occurs in response to calcium depletion from the endoplasmic reticulum (ER), and sequential stromal interaction molecule-1 (STIM1) multimerization (Worley et al., 2007; Yuan et al., 2007). Specifically, neurons and astrocytes respond to cell stress and/or tissue damage by secreting extracellular nucleotides that activate purinergic G_q protein coupled receptors (P_2Y_xR) on microglia (Ferreira & Schlichter, 2013). Specifically, P_2Y_xR activation primes phospholipase-C production of inositol-trisphosphate (IP3), which binds to IP3 receptors on the ER membrane to trigger calcium release from the ER lumen (Färber & Kettenmann, 2006; McLarnon, 2005). The calcium depleted environment within the ER lumen causes the calcium sensor STIM1 to oligomerize and gate the opening of store operated calcium channels (SOCCs) on the plasma membrane surface (Kraft, 2015; Michaelis et al., 2015; Ohana et al., 2009; Roos et al., 2005). Activity of the sarco/endoplasmic reticulum Ca^{2+}-ATPase (SERCA) pumps cytosolic calcium into the ER lumen to replenish the intracellular calcium reservoir, while activity of the plasma membrane Ca^{2+}-ATPase (PMCA) and the Na^{+}/Ca^{2+} exchanger transports cytosolic calcium out of the cell in order to maintain intracellular calcium homeostasis (Kettenmann et al., 2011; Möller, 2002).

Microglia express a variety of STIM1-gated ion channels on their plasma membrane that mobilize calcium influx and replenish intracellular calcium stores. For example, the calcium specific ion channel made up of Orai proteins is characterized by an inwardly rectifying small conductance and is expressed in microglia (Michaelis et al.,

2015; Ohana et al., 2009; Prakriya, 2009). Additionally, microglia express a variety of TRPC channels such as TRPC1 and TRPC3, which are nonselective cation channels that are permeable to calcium, sodium, and potassium (Echeverry et al., 2016; Ohana et al., 2009; Worley et al., 2007). It was reported that STIM1 physically interacts with TRPC1 to gate channel opening (Lee et al., 2014; Yuan et al., 2007). Importantly, knockout of any one SOCC does not dramatically affect store operated calcium entry (SOCE) however, knockout of STIM significantly attenuates SOCE (Roos et al., 2005; Yuan et al., 2007), emphasizing the important role of STIM in gating multiple SOCCs that are present on the plasma membrane.

In response to pathological events such as bacterial infection, microglia mobilize calcium to become active. It is previously reported that exposing microglia to lipopolysaccharide (LPS), an endotoxin found on the outer membrane of Gram-negative bacteria, suppressed P2YR-mediated calcium influx (Hoffmann et al., 2003) and SOCC conductance (Michaelis et al., 2015). Exposing microglia to LPS also upregulates the expression of inducible nitric oxide synthase (iNOS) and the production of nitric oxide (NO) in microglia (Bogdan, 2015; Svensson et al., 2010; Zhang et al., 2012). It is reported that NO can activate TRPC and TRPV channels in endothelial cells (Yoshida et al., 2006). However, NO has also been reported to inhibit STIM1 clustering and gating of SOCCs in cardiomyocytes (Gui et al., 2018). Despite these reports, it is still unknown if acute NO exposure effects calcium dynamics through STIM-mediated channels in microglia.

Therefore, this present study set forth to examine if iNOS/NO signaling regulates calcium influx through SOCCs in microglia. Using calcium imaging and whole-cell electrophysiology, our primary aim was to examine the effect of NO on basal calcium levels in microglia isolated from wildtype (WT), iNOS-knockout ($iNOS^{-/-}$) mice, as well as the BV2 cell-line. We also characterized the effect of acute NO exposure on TG-induced SOCC activity in these murine microglia. Our results demonstrated that acute treatment of the fast-release NO-donor on murine microglia induced a biphasic calcium response. The biphasic calcium response was characterized by a decline in calcium influx during phase I, which was mediated by SOCCs and occurred independent of PKG signaling, while a calcium influx occurred through TRPV2 channels in a PKG dependent manner during

phase II as previously reported (Maksoud et al., 2019). Uncovering NO signaling mechanisms that influence calcium signaling in microglia may lead to a better understanding of microglial responses to pathology.

3.3 Materials and methods

3.3.1 Pharmacological Drug Treatments

Compounds were purchased from the following sources: fast release NO-donor: S-Nitroso-N-acetyl-DL-penicillamine (SNAP, 250μM) (Maksoud et al., 2019; Wong et al., 2010), store operated calcium channel inhibitors: SKF96365 hydrochloride (SKF96365, 20μM) (Ohana et al., 2009; Yang et al., 2009) and 2-aminoethoxybiphenyl borate (2APB, 50μM) (Ohana et al., 2009; Trebak et al., 2002), (Santa Cruz Biotechnology, Dallas, TX); TRPV inhibitor: ruthenium red (RR, 3μM)(Hu et al., 2004) (Enzo Life Sciences, Farmingdale, NY); PKG inhibitory peptide: arginyl-lysyl-arginyl-alanyl-arginyl-lysyl-glutamic acid (PKG_i, 10μM) (Maksoud et al., 2019) (Cayman Chemical, Ann Arbor, MI); TRPV2 inhibitor: tranilast (75μM, Tocris Bioscience, Oakville, ON) (Maksoud et al., 2019); sarco/endoplasmic reticulum calcium ATPase inhibitor: thapsigargin, (TG, 1μM) (Ohana et al., 2009; Sun et al., 2014) (Alomone Labs, Jerusalem, Isreal).

3.3.2 Primary microglia cultures

WT (C57BL/6) and $iNOS^{-/-}$ (B6.129P2-$Nos2^{tm1Lau}$) mice were purchased from The Jackson Laboratory. All experiments were conducted in accordance with the regulations of the Animal Care and Veterinary Services at The University of Western Ontario, Canada.

Primary microglia cultures, were carried out as previously described (Joseph & Venero, 2013). Briefly, mouse cortices were isolated from entire litters containing male and female postnatal day-1 WT or $iNOS^{-/-}$ mice and placed in ice cold Leibowitz L-15 media (ThermoFischer Scientific, Waltham, MA). Cortices were homogenized, filtered through a 70μm nylon filter, and centrifuged for 4 min at 900g. The pelleted cells were resuspended in Dulbecco's modified eagle's medium (DMEM) containing 1x penicillin/streptomycin (P/S) and 10% fetal bovine serum (FBS) (Thermo Fischer Scientific, Waltham MA). Next, cells were plated in T-75 flasks with approximately 3 cortices per flask and cultured at normal conditions of 5% CO_2 at 37^oC. Two weeks after culturing, flasks were shaken for 2hrs at 37^oC to facilitate microglia detachment from the astrocyte monolayer. Culture media containing detached microglia was collected, spun

down at 900g for 4 min, and the cell pellet containing microglia was resuspended in fresh culture media and plated at $5x10^4$ cells/ml for experiments. Plated microglia were allowed to rest overnight before conducting experiments.

3.3.3 BV2 microglia cultures

The BV2 microglia cell-line was generously gifted to us from Dr. Michael J. Strong at The University of Western Ontario. BV2 cells were cultured in DMEM containing 1x P/S and 10% FBS at normal conditions of 5% CO_2 at 37ºC. Once BV2 cell confluency reached 70%, cells were washed with PBS and incubated for 2 min in 0.25% trypsin (ThermoFischer Scientific, Waltham, MA) in PBS to facilitate detachment. Trypsin was neutralized using equal parts of culture media containing FBS and BV2 cells were passaged 1:40 into a new 100mm culture dish with DMEM containing 1x P/S, and 10% FBS 3x a week. For experiments, BV2 cells were plated at $5x10^4$ cells/ml and allowed to rest overnight before conducting experiments.

3.3.4 Calcium Imaging

For calcium-imaging in cultured murine microglia, culture media was removed and replaced with bath solution containing (in mM): 130 NaCl, 5 KCl, 3 $MgCl_2$, 2 $CaCl_2$, 5 glucose, and 10 4-(2-hydroxyethyl)-1-piperazineethanesulfonic acid (HEPES). Microglia cultures were incubated with 3 μM rhod-4AM (AAT Bioquest, Sunnyvale, CA) for 1hr under normal conditions, then excess rhod-4AM was washed out using bath solution. Changes of intracellular calcium levels in microglia were assayed by imaging rhod-4 fluorescence using the Olympus FV1000 microscope or the EVOS FL-Auto microscope under 20X magnification. In some experiments microglia were pretreated with the store operated calcium channel inhibitors; SKF96365 (20μM)(Choi et al., 2003) or 2APB (50μM) (Papanikolaou et al., 2017) for 10min before imaging. Two and a half minutes after recording the baseline fluorescent intensity of rhod-4, a test drug was applied to the dish. The changes in rhod-4 fluorescence to the test drug were continuously recorded until the end of the trial. The rhod-4 fluorescent changes were normalized to the average baseline level in every cell within the imaging field using FIJI open source software (Schindelin et

al., 2012). The average value for the normalized rhod-4 fluorescent intensity in all test cells were plotted along with the time of imaging using Excel.

In response to SNAP treatment, a biphasic response was seen in test cells. The following criteria was used to designate phase I and phase II in control microglia: phase I encompassed the period of time between the initial drug application and when the rhod-4 fluorescent response crossed baseline (y-axis at 1); while phase II encompassed the period of time starting at the end of phase I and continuing until the end of the recording. Importantly, the duration of phase I and phase II remained consistent between controls and pre-treatments to allow for accurate comparisons between control microglia and pre-treated microglia.

3.3.5 Whole-cell voltage-clamp electrophysiology

The effect of NO signaling on SOCCs in BV2 microglia was examined by whole-cell voltage-clamp electrophysiology. BV2 microglia plated on 35mm dishes were kept in bath solution containing (in mM): 130 NaCl, 5 KCl, 3 $MgCl_2$, 2 $CaCl_2$, 5 glucose, and 10 HEPES. However, a potassium free extracellular solution containing (in mM): 135 NaCl, 3 $MgCl_2$, 2 $CaCl_2$, 10 HEPES, and 5 glucose was used during patch-clamp recordings to eliminate the inwardly rectifying potassium current in BV2 cells. The pH and osmolarity of all solutions were adjusted to 7.4 and 300 mOsm, respectively. The intracellular solution contained (in mM): 140 K-gluconate, 8 NaCl, 1 $MgCl_2$, 10 Cesium-BAPTA, and 10 HEPES. The pH of the intracellular pipette solution was adjusted to 7.4 using cesium hydroxide to block delayed rectified potassium channels, which can mask smaller channel conductance when recording. Patch pipettes were pulled with final input resistance between 3 and 5 megaohms. Whole cell recordings were performed at room temperature using MultiClamp 700B Amplifier and Digidata 1440A low-noise data acquisition system (Molecular Devices, Sunnyvale, CA). After a stable whole-cell configuration was achieved, cellular capacitance of each test cell was measured and then voltage-ramps from -100mV to +70mV over 150ms were repeatedly applied in 10 second intervals from a holding potential of 0mV.

Test drugs were perfused toward the test cell using a gravity perfusion system delivering solution at 2ml/min. Once a stable baseline recording was obtained, test drugs were applied to the bath solution in the following order; 1μM TG to deplete intracellular stores and evoke SOCE (Chen et al., 2016); 250μM SNAP, a fast release NO-donor (Maksoud et al., 2019); followed by 3μM RR, the nonelective TRP channel inhibitor (Hu et al., 2004). The average of 4 voltage-ramp recordings were taken for each cell at baseline and after each drug response stabilized. The average currents were divided by the cell capacitance to calculate the current density (pA/pF) before and after drug treatments. The current density was plotted against the clamping voltage to display the current density-voltage relationship. Experimental n-values represent number of cells recorded over different days.

3.3.6 Reverse transcription quantitative polymerase chain reaction (RT-qPCR)

Total RNA from cultured primary WT or iNOS$^{-/-}$ microglia was extracted in accordance with the RNeasy Mini Kit (Qiagen, Toronto, ON). Reverse transcription of 1 μg total extracted RNA to cDNA was carried out using qScript XLT cDNA Supermix (Quantabio, Beverly, MA) following the manufacturer's instructions. Quantitative PCR was conducted using Perfecta SYBR Green FastMix for iQ (Quantabio, Beverly, MA), 25 ng of cDNA template, and 500 nM of both forward and reverse primers specific to the specific gene of interest. Forward and reverse primers for the following murine genes of interest were used: STIM1 forward 5'CTCCTCTCTTGACTCGGCAT3', reverse 5'AGCCACCCACACCAATAACG3'; TRPC1 forward 5'ACGGTTGTCAGAAACTTATGGA3', reverse 5'GCAGCTAAAATAACAGGTGCGA3'; TRPC3 forward 5'AGAAGGATCTGGAACTGGGC3', reverse 5'ACTCTCGAGTTAGACTGTGTGAA3'. Using a 40-cycle protocol, RT-qPCR reactions were run in triplicate 25 μL reaction volumes with a no-template control on a BioRad MyiQ Single-colour Real-Time PCR detection system (BioRad, Mississauga, ON). The difference in cycle threshold (ΔCt) between the reference gene β-actin forward

5’CTGTCCCTGTATGCCTCTG3’, reverse 5’ATGTCACGCACGATTTCC3’, and the genes of interest were graphed using Excel.

3.3.7 Statistics

Statistical analyses were conducted using GraphPad Prism 6. All results are presented as mean ± standard error of the mean (SEM). One-way ANOVA was conducted using Tukey’s post hoc comparison when comparing between multiple treatment groups. Two-way ANOVA was conducted using Bonferroni’s post hoc comparison when comparing between multiple treatment groups and primary microglia genetic background. Unpaired Two-tailed t-test was used when only comparing between two groups. All stats were determined from at least N = 3 and a *p*-value of less than 0.05 was considered significant (*$p<0.05$, **$p<0.01$, ***$p<0.001$, ****$p<0.0001$).

3.4 Results

3.4.1 Application of the NO-donor SNAP induces a biphasic calcium response in murine microglia.

To examine the effect of NO on basal calcium dynamics in murine microglia, we applied the fast release NO-donor SNAP to WT or iNOS$^{-/-}$ microglia cultures. Application of SNAP (250μM) induced a biphasic change in intracellular calcium for both WT and iNOS$^{-/-}$ microglia. Specifically, phase I exhibited a rapid decline in calcium influx while phase II displayed calcium influx in both WT and iNOS$^{-/-}$ microglia **(Figure 3.1A** and **3.1B** respectively**).** Importantly, the duration of the calcium decline that occurred in phase I in WT microglia cultures lasted 6.9 ± 0.4 min whereas the duration of the phase I calcium decline in iNOS$^{-/-}$ microglia lasted 8.2 ± 0.6 min. In addition, the area under the rhod-4 fluorescent curve during phase I in WT microglia **(Figure 3.1C)** appeared smaller than that of iNOS$^{-/-}$ microglia **(Figure 3.1D)**. These results suggest that an acute increase in exogenous NO rapidly inhibits basal calcium influx while slowly increasing calcium influx in murine microglia.

It is known that NO rapidly inhibits SOCC activity by *S*-nitrosylation of STIM1 in primary cardiomyocytes (Gui et al., 2018). Therefore, to examine whether this biphasic SNAP response was occurring from SOCC activity, we pre-treated murine microglia with 50μM of 2APB, which is commonly used as a SOCC inhibitor at this concentration (Ohana et al., 2009; Papanikolaou et al., 2017; Trebak et al., 2002) and examined the calcium dynamics in response to SNAP treatment. Importantly, in the presence of 2APB, SNAP application on WT microglia cultures induced a predominant calcium influx in phase I **(Figure 3.1A).** On the other hand, SNAP application to the 2APB-pretreated iNOS$^{-/-}$ microglia induced a shorter-lasting phase I with a smaller amplitude than control cells **(Figure 3.1C).** Importantly, in the presence of 2APB the area under the calcium curves displayed significantly more calcium influx in phase I when compared to controls for both WT and iNOS$^{-/-}$ microglia **(Figure 3.1B** and **3.1D)**. In the presence of 2APB, SNAP treatment on both WT and iNOS$^{-/-}$ microglia maintained a similar calcium influx during phase II as under control conditions **(Figure 3.1A** and **3.1C)**, which was not significantly

different **(Figure 3.1B** and **3.1D).** Together this data suggests that SNAP restricts calcium influx during phase I through SOCCs and induces calcium influx in phase II, independently of SOCCs in primary murine microglia.

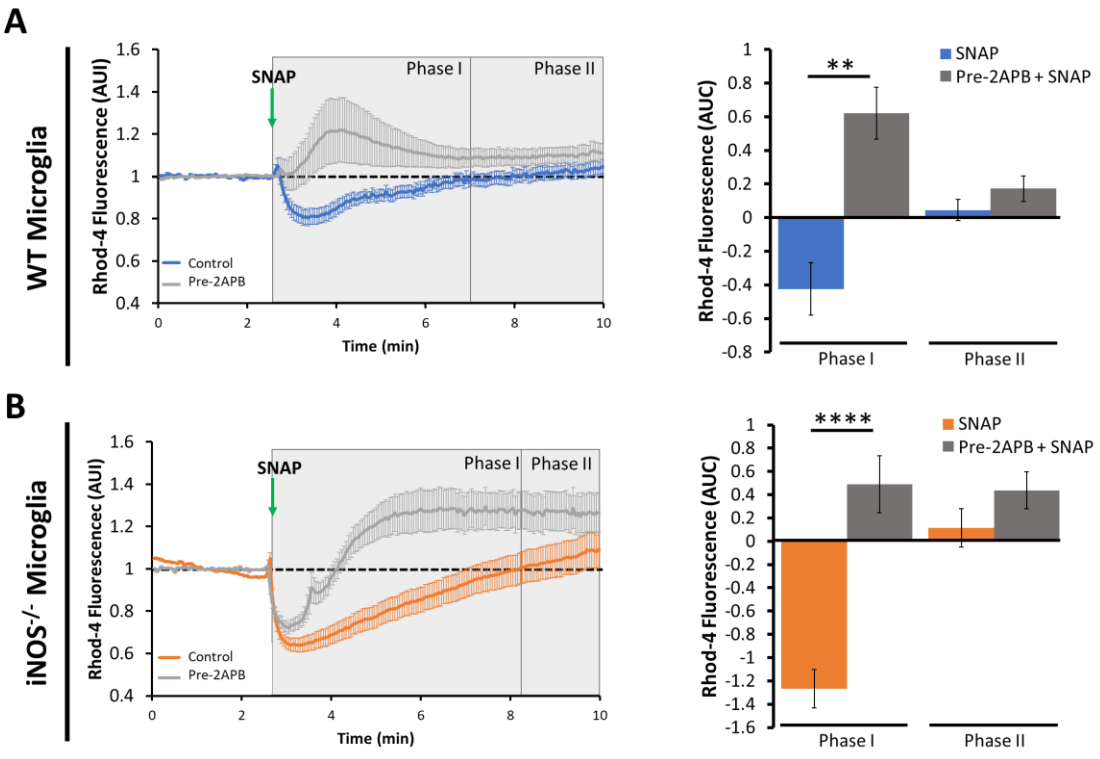

Figure 3.1 Application of the NO-donor SNAP induces a biphasic change in intracellular calcium levels in primary murine microglia.

Changes in rhod-4 fluorescence in response to the fast release NO-donor SNAP (250µM) application on control or 2APB (50µM, grey) pretreated **A)** WT (blue) and **B)** iNOS$^{-/-}$ (orange) microglia. The biphasic intracellular calcium response in WT and iNOS$^{-/-}$ control cells was divided into two phases for data analysis as previously described. The duration of the two phases were applied to the SNAP-induced calcium changes in WT and iNOS$^{-/-}$ microglia pretreated with 2APB. Bar graphs represent the mean normalized area under the calcium curve (AUC) for phase I and phase II from (A) and (B). Significance was determined from n = 60 WT control cells; n = 48 2APB pretreated WT cells; n = 40 iNOS$^{-/-}$ control cells; n = 54 2APB pretreated iNOS$^{-/-}$ cells from N = 3 replicates and $p<0.05$ using individual two-tailed t-tests for phase I and phase II separately. **$p<0.01$, ****$p<0.0001$.

3.4.2 The NO-donor SNAP decreases calcium influx independent of PKG signaling.

We next examined the effect of the NO-donor SNAP on the intracellular calcium dynamics in BV2 microglia. Results from our assays demonstrated that application of SNAP to naïve BV2 microglia induced a biphasic calcium response similar to primary WT and iNOS$^{-/-}$ microglia **(Figure 3.2)**. Additionally, pretreating BV2 cells with 2APB significantly attenuated the SNAP-induced decline in calcium influx observed in phase I, but did not significantly affect the SNAP-evoked calcium influx observed in phase II **(Figure 3.2A** and **3.2D).** Importantly, SNAP application on BV2 microglia displayed a more defined phase I and II when compared to primary microglia. Therefore, using BV2 microglia allowed us to clearly examine the calcium dynamics in both phase I and phase II in response to further pharmacological manipulations to elucidate the mechanisms by which NO regulates intracellular calcium dynamics in microglia.

We first examined if NO decreases intracellular calcium by signaling through the classical PKG pathway. Specifically, we examined the intracellular calcium dynamics in response to SNAP in BV2 microglia pretreated with the 10μM of a PKG_i. Results from our assays demonstrated that in the presence of the PKG_i, SNAP induced a prolonged decline in calcium influx (**Figure 3.2B;** purple trace**).** Specifically, in the presence of the PKG_i, SNAP treatment abolished the calcium influx occurring in phase II that was observed under control conditions (**Figure 3.2B;** purple trace**)**. Moreover, in the presence of the PKG_i, both phase I and phase II displayed a significantly larger decline in calcium influx the control trace (**Figure 3.2D**; purple bars**).** This result indicates that the biphasic action of SNAP is partially dependent on PKG signaling. Specifically, the rapid decrease in intracellular calcium during phase I occurs independent of PKG signaling while calcium influx during phase II requires PKG signaling.

3.4.3 The NO-donor SNAP induces calcium influx through a RR-sensitive TRP channel.

The inhibitory effects of RR act on a variety of calcium permeable TRP channels within the melastatin (TRPM) and vanilloid (TRPV) families (Hu et al., 2004), without effecting TRPC channels that contribute to SOCE (Castro et al., 2009). We therefore examined the effect of SNAP on the calcium dynamics within BV2 microglia pretreated with 3μM RR. Results from our assays showed that in the presence of RR, application of SNAP induced a prolonged decrease in calcium influx during phase I and a small delayed calcium influx during phase II when compared to control cells **(Figure 3.2C** and **3.2D**; red trace and bars respectively**)**. These results demonstrate that RR-sensitive TRP channels are not related to the NO-induced decrease of intracellular calcium, while possibly contributing to the NO-induced calcium increase in murine microglia.

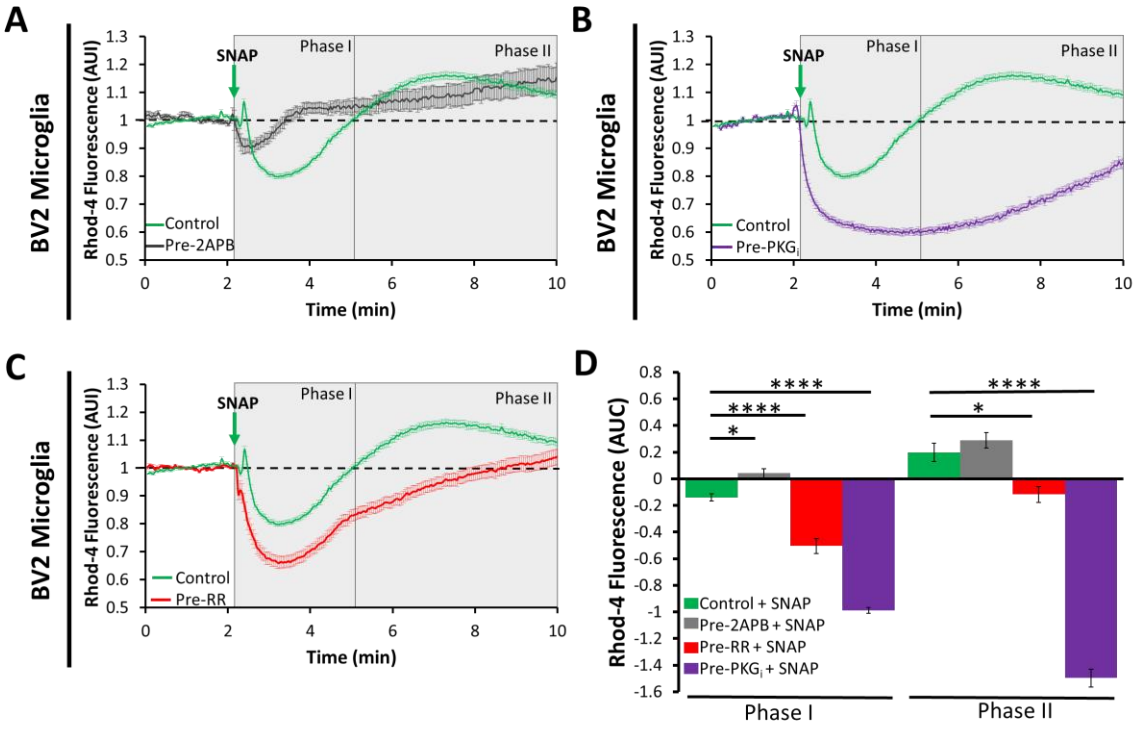

Figure 3.2 NO restricts calcium influx through SOCCs and induces a calcium influx through a PKG-mediated RR-sensitive TRP channel in BV2 microglia.

Rhod-4 fluorescent changes in response to SNAP application on BV2 microglia relative to a signle control condition (green trace) or in the presence of **A)** 2APB (50µM, grey trace), **B)** PKG_i (10µM, purple trace), or **C)** RR (3µM, red trace). The biphasic intracellular calcium response in BV2 control cells was divided into two phases for data analysis as previously described. The duration of the two phases were then applied to the SNAP-induced calcium changes in BV2 microglia pretreated with 2APB, RR, or PKG_i. All control and experimental conditions were conducted at the same time. **D)** Bar graph reports the mean ± SEM for the normalized area under the rhod-4 fluorescent curve (AUC) within phase I and phase II under all test conditions. Significance was determined from n = 150 control cells; n = 129 2APB pretreated cells; n = 100 PKG_i pretreated cells; and n = 143 RR pretreated cells from N = 3 replicates and $p<0.05$ using a one-way ANOVA and Tukey's post hoc comparison within phase I and phase II separately. *$p<0.05$, ****$p<0.0001$.

3.4.4 NO-donor SNAP abruptly inhibits TG-mediated SOC entry in BV2 microglia.

Next, we explored whether the NO-donor SNAP decreases intracellular calcium influx by inhibiting SOCCs. To that end, we used the SERCA inhibitor: TG (1μM) to induce SOCE (Michelangeli & East, 2011) in BV2 microglia. Application of TG induced a transient calcium influx that returned to baseline levels in BV2 microglia **(Figure 3.3A)**. Importantly, the TG-mediated calcium influx that was observed under control conditions was completely abolished in the presence of either SOCC inhibitor SKF96365 or 2APB **(Figure 3.3A)**. Importantly, in the presence of SKF96365 or 2APB, the intracellular calcium influx dropped below baseline levels (**Figure 3.3A)**. Quantification of the area under the calcium dynamic curve in response to TG was significantly smaller in the presence of the SOCC inhibitors **(Figure 3.3B).** These results demonstrate that TG mediates SOCE and that SOCCs contribute to basal intracellular calcium influx within BV2 microglia.

We also examined the direct effect of the NO-donor SNAP on the TG-mediated SOCE in BV2 microglia. To do this we measured the change in rhod-4 fluorescence after sequentially treating BV2 microglia with TG followed by SNAP. Results from our assays demonstrated that 250μM SNAP treatment during the TG-induced calcium influx caused a rapid decline in intracellular calcium to levels below baseline in BV2 microglia **(Figure 3.3C)**. Importantly, SNAP treatment displayed a biphasic response and the rapid decline in calcium influx from SNAP treatment was followed by a prolonged increase in calcium influx **(Figure 3.3C)**. Quantification of the AUC demonstrated that SNAP treatment significantly attenuated the TG-mediated calcium influx in phase I, while significantly increasing calcium influx within phase II **(Figure 3.3D)**. Together this data demonstrates that NO abruptly inhibits TG-mediated SOCCs while inducing calcium influx through an alternative mechanism.

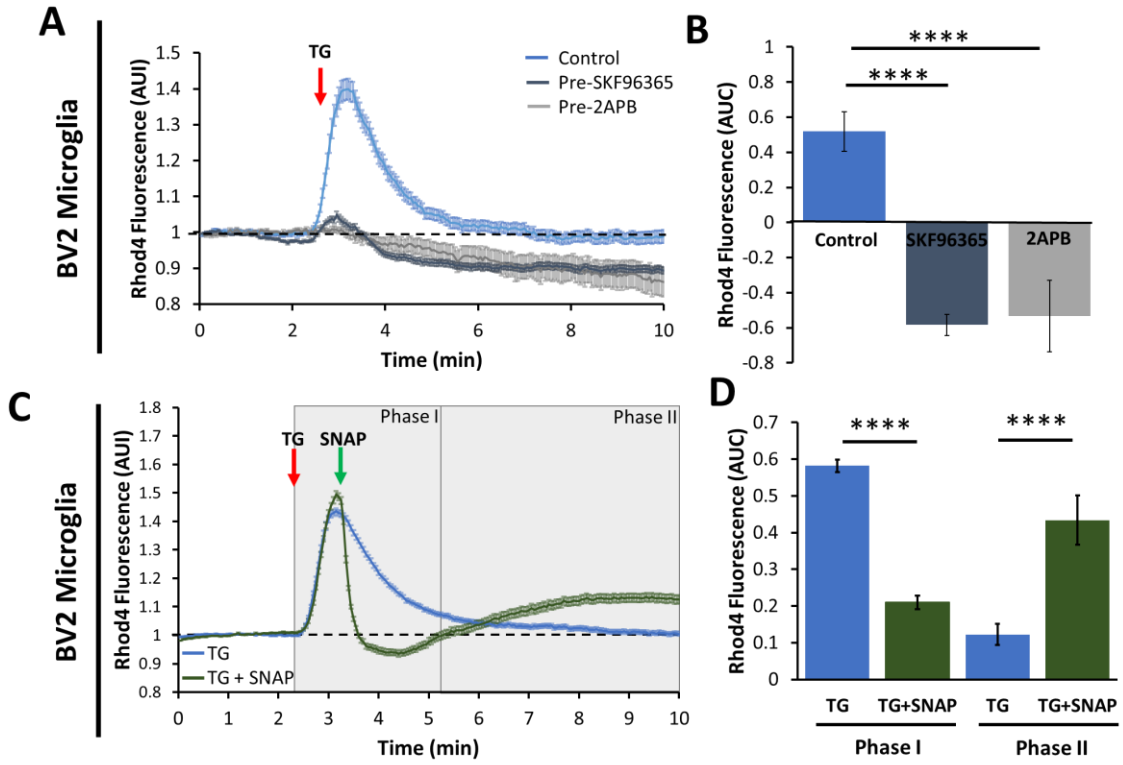

***** Figure legend on next page*****

Figure 3.3 NO-donor SNAP abruptly inhibits TG-mediated SOC entry in BV2 microglia.

A) Rhod-4 fluorescent changes with time in response to TG (1μM) treatment on BV2 microglia under conditions of control (blue trace), or pretreated with SKF96365 (10μM, dark blue trace), or 2APB (50μM, grey trace). **B)** Bar graph reports the normalized AUC from (A) as mean ± SEM. **C)** Rhod-4 fluorescent changes with time in BV2 microglia in response to TG (1μM) alone (blue trace) or TG with SNAP (250μM) application (green trace). The biphasic intracellular calcium response to SNAP was divided into two phases for data analysis. Phase I encompassed the duration from initial TG treatment to when SNAP application induced calcium influx above baseline. Phase II encompassed the duration from the end of phase I to the end of the recording. **D)** Bar graph reports the normalized AUC from (C) as mean ± SEM for phase I and phase II. Significance between treatment groups from (B) was determined from n = 208 control cells; n = 159 SKF96365 pretreated cells; n = 125 2APB pretreated cells from N = 3 replicates and $p<0.05$ using a one-way ANOVA and Tukey's post hoc comparison. Significance between treatment groups from (D) was determined from n = 211 TG treated cells and n = 201 TG + SNAP treated cells from N = 4 replicates and $p<0.05$ using an unpaired two-tailed student's t-test for phase I and phase II separately. ****$p<0.0001$.

3.4.5 The NO-donor SNAP quickly inhibits a TG-mediated nonselective cation conductance and slowly activates a RR-sensitive TRP channel in BV2 microglia.

It has been reported that microglia express a variety of STIM-gated SOCCs including those made up of either Orai (Michaelis et al., 2015) or TRPC1/3 proteins (Mizoguchi et al., 2014; Mizoguchi & Monji, 2017). Orai-formed channels selectively mediate calcium entry and display a small conductance with an inwardly rectifying current-voltage (I-V) relationship (Michaelis et al., 2015; Ohana et al., 2009; Prakriya, 2009). On the other hand, TRPC1/3 proteins form a non-selective cation conductance that displays a relatively linear I-V relationship. Therefore, we examined the specific type of SOCC that contributes to the TG-mediated calcium influx in BV2 microglia using whole-cell voltage-ramp electrophysiology **(Figure 3.4)**. Our results showed that under control conditions, BV2 microglia exhibited a low amplitude transmembrane current with a linear I-V relationship that reversed around 0mV, indicating the presence of a non-selective cation current. Application of TG on BV2 microglia enlarged the nonselective cation current (**Figure 3.4A** and **3.4D)**. Importantly, in the presence of TG, application of SNAP caused an abrupt and short-lasting decrease of the nonselective cation conductance that lasted roughly 4 min **(Figure 3.4B** and **3.4D)**. This decrease in current conductance was followed by a gradual increase in another nonselective cation conductance (**Figure 3.4C** and **3.4D)**. This result implies that SNAP quickly inhibits TRPC1/3 SOCCs while slowly amplifying another nonselective TRP channel. Indeed, RR treatment greatly attenuated the SNAP-induced nonselective cation conductance to a level comparable to the TG-mediated conductance (**Figure 3.4E).** Together, this data suggests that SNAP induces a biphasic response on nonselective cation channels in microglia, whereby inhibition of a TG-mediated nonselective cation channel occurs in phase I, while amplification of a RR-sensitive nonselective cation channel occurs in phase II.

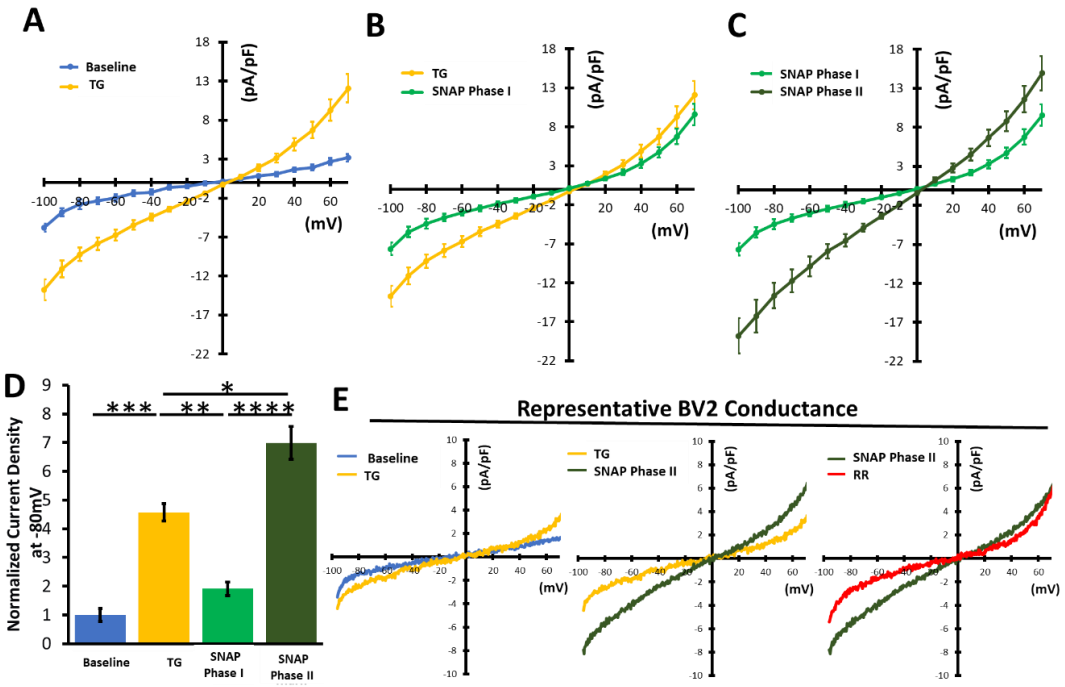

Figure 3.4 The NO-donor SNAP quickly inhibits a TG-mediated nonselective cation conductance and slowly activates a RR-sensitive TRP channel in BV2 microglia.

I-V relationship graphs reporting the current density revealed by voltage-ramps from -100mV to +70mV in BV2 microglia during control (baseline, blue trace) and after sequential application of **A)** TG (1μM, yellow trace), **B)** SNAP (250μM, phase I, green trace), **C)** 4 min after SNAP (phase II, dark green trace). **D)** Bar-graph reports the normalized current density of BV2 microglia at -80mV under sequential treatments from (A-C). **E)** Representative BV2 microglia current-voltage relationship graphs depicting *Left panel:* baseline (blue trace) and TG treatment (yellow trace), *middle panel:* TG (yellow trace) and 4 min after SNAP treatment (dark green trace), and *right panel:* 4 min after SNAP treatment (dark green trace) and after 3μM RR treatment (red trace). Significance was determined from n = 9 cells and $p<0.05$ using a one-way ANOVA and Tukey's post hoc comparison. *$p<0.05$, **$p<0.01$, ***$p<0.001$, ****$p<0.0001$

3.4.6 iNOS$^{-/-}$ microglia display a larger TG-mediated calcium influx, and express less STM1, TRPC1, and TRPC3 mRNA transcripts than WT microglia.

To examine how the absence of basal iNOS/NO signaling influences the activity of SOCCs, we examined the calcium signaling dynamics in response to TG treatment in both WT and iNOS$^{-/-}$ primary murine microglia cultures **(Figure 3.5).** TG treatment induced a sustained calcium influx in both WT and iNOS$^{-/-}$ microglia cultures **(Figure 3.5A** and **C)**. Importantly, iNOS$^{-/-}$ microglia displayed a significantly larger calcium influx in response to TG when compared to WT microglia**.** Furthermore, the TG-mediated calcium influx was significantly inhibited with the pretreatment of either SOCC inhibitor; SKF96365 or 2APB **(Figure 3.5A-D)**. Together, this data demonstrates that TG-mediated SOCE is larger in murine microglia lacking iNOS than in WT microglia.

Considering that iNOS$^{-/-}$ microglia cultures displayed a significantly larger calcium influx through SOCCs than WT microglia, we wanted to examine the relative expression of certain SOCE transcripts within primary murine microglia cultures. Bearing in mind that previous electrophysiology experiments demonstrated the presence of nonselective TRP-like current in microglia, we therefore conducted RT-qPCR for the ER calcium sensor STIM1, and the SOCCs TRPC1 and TRPC3 in WT and iNOS$^{-/-}$ microglia cultures. Our assays showed that WT microglia displayed a significantly larger mRNA expression of STIM1, TRPC1 and TRPC3 relative to β-actin when compared to iNOS$^{-/-}$ microglia **(Figure 3.5E** and **3.5F).** Together, this data demonstrates that iNOS$^{-/-}$ microglia in culture display less mRNA transcripts for SOCE proteins while simultaneously producing a larger calcium influx through SOCCs.

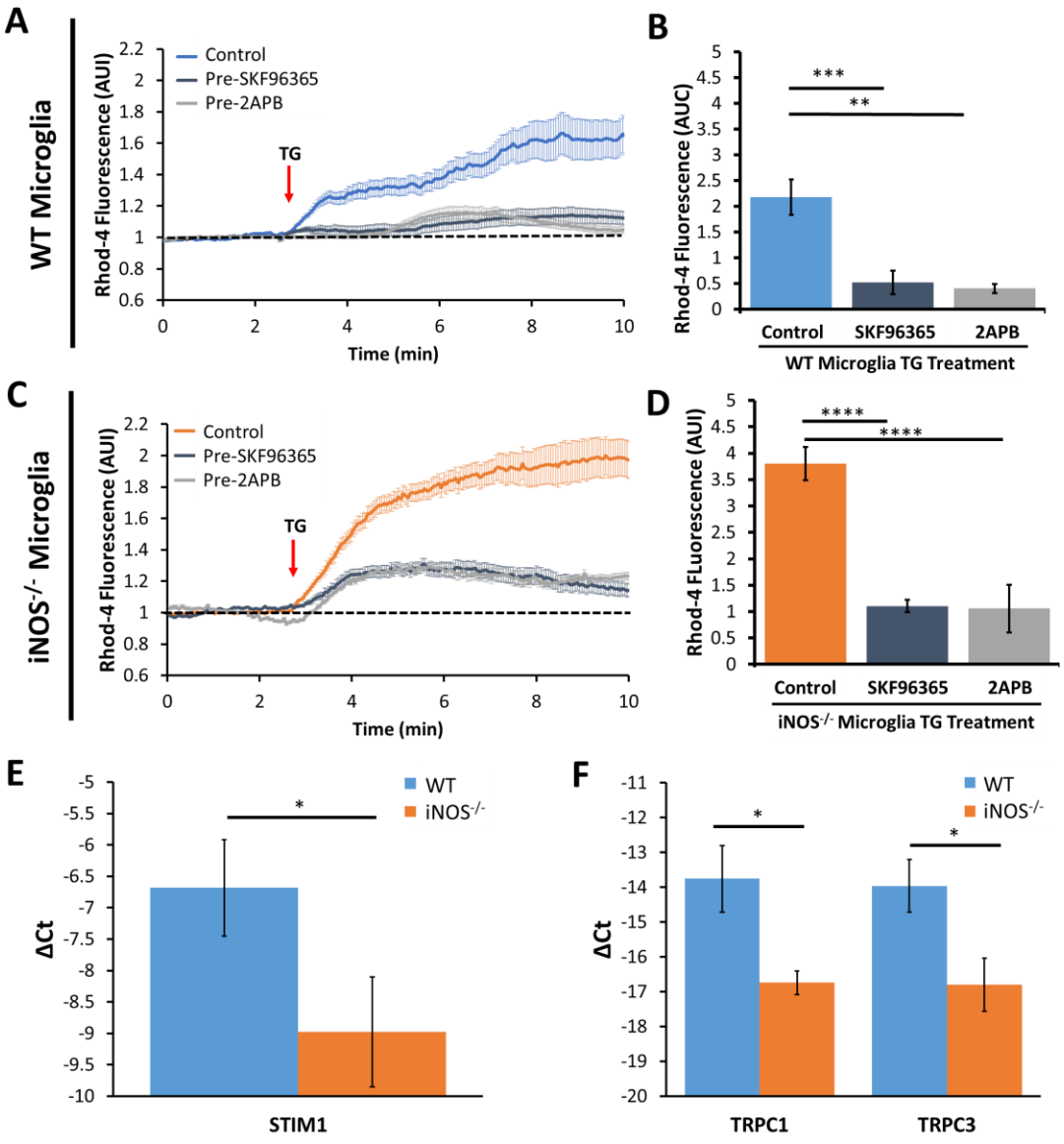

Figure legend on next page

Figure 3.5 iNOS$^{-/-}$ microglia display a larger TG-mediated calcium influx, and express less STM1, TRPC1, and TRPC3 mRNA transcripts than WT microglia.

A) Changes in rhod-4 fluorescence with time to application of TG (1μM) on WT microglia under conditions of control (light blue trace), pretreatment with SKF96365 (10μM, dark blue trace), or pretreatment with 2APB (50μM, grey trace). **B)** Bar graph reports the AUC in WT microglia under treatment conditions from (A) **C)** Changes in rhod-4 fluorescence with time to application of TG (1μM) on iNOS$^{-/-}$ microglia under conditions of control (orange trace), pretreatment with SKF96365 (10μM, dark blue trace), or pretreatment with 2APB (50μM, grey trace). **D)** Bar graph reports the AUC in iNOS$^{-/-}$ microglia under treatment conditions from (C). The mRNA levels of **E)** STIM1 and **F)** TRPC1 and TRPC3 in primary WT and iNOS$^{-/-}$ microglia cultures presented as ΔCt using β-actin mRNA as the reference gene. For AUC analyses, significance was determined from n = 44 control WT cells; n = 48 SKF96365 pretreated WT cells; n = 30 2APB pretreated WT cells; n = 48 control iNOS$^{-/-}$ cells; n = 39 SKF96365 pretreated iNOS$^{-/-}$ cells; n = 32 2APB pretreated iNOS$^{-/-}$ cells from N = 4 and $p<0.05$ using individual one-way ANOVAs and Tukeys post hoc comparison. For ΔCt analysis, significance was determined from N = 5 wells and $p<0.05$ using individual unpaired two-tailed t-tests for mRNA genes of interest. *$p<0.05$, **$p<0.01$, ***$p<0.001$, ****$p<0.0001$.

3.4.7 NO-donor SNAP induces a slow onset calcium influx through TRPV2 channels in primary murine microglia.

We previously demonstrated that NO enhances the plasma membrane expression of TRPV2 channels in primary microglia through a PKG dependent mechanism (Maksoud et al., 2019). Considering that the SNAP-mediated calcium influx observed in phase II is a RR-sensitive TRP channel that also requires PKG-activity, we wanted to specifically examine TRPV2 activity. Therefore, we pretreated microglia cultures with the TRPV2 inhibitor tranilast (75μM) and examined the effect of SNAP application on the calcium dynamics in these microglia **(Figure 3.6)**. Results from our assay showed that in the presence of tranilast, application of SNAP induced a prolonged decrease in intracellular calcium in both WT and $iNOS^{-/-}$ microglia, when compared to the biphasic effect observed in control cells **(Figure 3.A** and **3.6C)**. Specifically, quantifications of the SNAP-induced changes in the area under the rhod-4 fluorescent curve in the presence of tranilast revealed a significantly larger decline in intracellular calcium in phase I and phase II in both WT and $iNOS^{-/-}$ microglia cultures when compared to controls **(Figure 3.6B** and **3.6D)**. This data demonstrates that the SNAP-mediated calcium influx observed in phase II occurs through TRPV2 channels in primary murine microglia cultures.

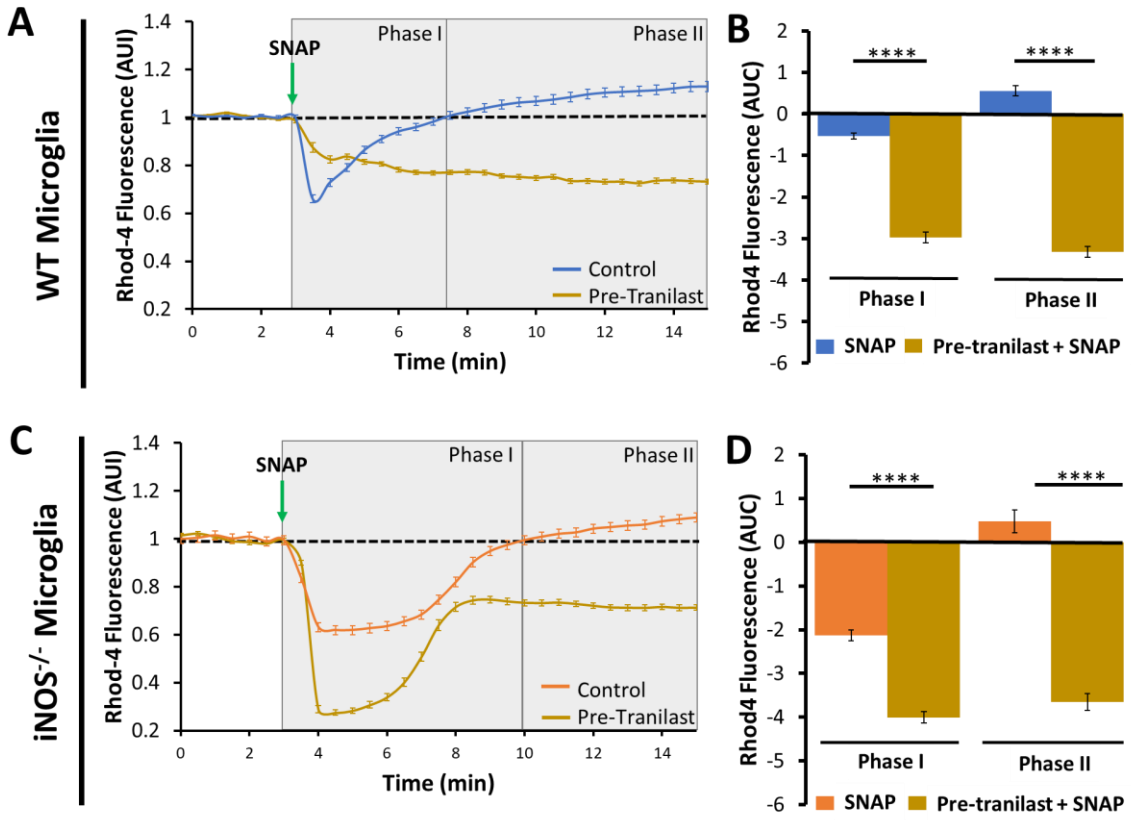

***** Figure legend on next page*****

Figure 3.6 NO-donor SNAP induces a slow onset calcium influx through TRPV2 channels in primary murine microglia.

A) Fluorescent changes in rhod-4 with time in response to SNAP (250μM) application in WT microglia under conditions of control (light blue trace) or in the presence of tranilast (75μM, gold trace). **B)** Bar graph reports the AUC values as mean ± SEM in WT microglia under conditions from (A). **C)** Fluorescent changes in rhod-4 with time in response to SNAP (250μM) application in $iNOS^{-/-}$ microglia under conditions of control (orange trace) or in the presence of tranilast (gold trace). **D)** Bar graph reports the AUC values as mean ± SEM in $iNOS^{-/-}$ microglia under conditions from (C). The biphasic intracellular calcium response in primary microglia cultures was divided into two phases for data analysis as previously described. The duration of the two phases were applied to the SNAP-induced calcium changes in primary microglia pretreated with tranilast. Significance was determined from n = 319 control WT cells; n = 210 tranilast pretreated WT cells; n = 211 control $iNOS^{-\backslash-}$ cells; n = 93 tranilast pretreated $iNOS^{-/-}$ cells from N = 4 wells and $p<0.05$ using individual two-tailed t-tests between treatment groups of phase I and phase II separately. ****$p<0.0001$.

3.5 Discussion

Calcium is an important secondary messenger that critically regulates microglial functions. In response to environmental signals, calcium ions flow down their concentration gradients from the extracellular fluid and/or ER lumen into the cytosol of microglia through calcium permeable channels (Kettenmann et al., 2011). On the other hand, activity of the PMCA and SERCA drives calcium ions against the concentration gradient back into the extracellular space or ER lumen, respectively (Srikanth & Gwack, 2012). Therefore, calcium homeostasis coincides with active calcium mobilization across the cell membrane. Following increased intracellular calcium mobilization, microglia become active and produce NO via iNOS activity (Gebicke-Haerter, 2001). This present study is the first to examine how NO influences intracellular calcium dynamics within microglia. We found that acute exposure of the fast release NO-donor SNAP on murine microglia abruptly inhibited SOCE independent of PKG signaling, while simultaneously inducing a slow-onset calcium influx through TRPV2 channels in a PKG-dependent mechanism.

3.5.1 The SNAP-mediated decrease in calcium influx during phase I occurs through SOCCs.

This is the first study to uncover that an acute increase of NO mobilizes intracellular calcium within microglia by affecting two different molecular targets. Previous studies reported that SOCCs are important for microglia activity (Beck et al., 2008; Ferreira & Schlichter, 2013; Michaelis et al., 2015). Therefore, we performed a series of experiments to examine SOCCs as one of the molecular mechanisms that underly the dual actions of NO on endogenous calcium signaling.

Ferreira and colleagues previously demonstrated that 50μM of 2APB inhibited calcium influx through SOCCs in rat microglia cultures (Ferreira & Schlichter, 2013). Therefore, we pretreated murine microglia with 50μM of 2APB and then examined the effect of SNAP on intracellular calcium dynamics. Importantly, application of SNAP on murine microglia pretreated with 2APB caused a shorter-lasting inhibition of calcium

influx during phase I and a dominant increase in intracellular calcium when compared to control traces. The activity of PMCA or the sodium-calcium exchanger moves calcium ions against its concentration gradient back into the extracellular space (Srikanth & Gwack, 2012). Such calcium efflux may also contribute to the decreased calcium observed during phase I. Importantly, application of SNAP on BV2 microglia pretreated with the TRPV/M inhibitor RR maintained the inhibition of calcium influx observed during phase I. Therefore, these results suggest that phase I is characterized by 2APB sensitive SOCCs (Mandal et al., 2008; Papanikolaou et al., 2017) and not other RR-sensitive TRPV/M channels (Castro et al., 2009).

To further examine the impact of NO on SOCCs we utilized TG. Application of TG blocks the activity of SERCA, which results in ER calcium depletion and SOCE (Vazquez-Martinez, 2003). We demonstrated that the SOCC inhibitors 2APB or SKF96365 (Bakowski & Parekh, 2002; Choi et al., 2003; Ferreira & Schlichter, 2013; Mandal et al., 2008; Roos et al., 2005; Yang et al., 2009) could significantly abolish the TG-mediated SOCE in murine microglia. Therefore, we further utilized TG to directly examine the effects of NO on SOCE in BV2 microglia. Results from our assays showed that SNAP caused a rapid drop in calcium influx to levels below baseline when applied at the peak of TG-mediated SOCE in BV2 microglia. Moreover, TG treatment on $iNOS^{-/-}$ microglia displayed a significantly larger calcium influx than WT microglia. These results demonstrate that iNOS/NO signaling rapidly inhibits SOCE in murine microglia.

We next wanted to examine the specific SOCC that was activated in response to TG in murine microglia. Previous reports describe current-voltage relationship of Orai channels as small-amplitude inwardly rectifying currents with a very positive reversal potential (Hahn et al., 2000; Nörenberg et al., 1997; Ohana et al., 2009), whereas TRPC channels display a linear current-voltage relationship with a reversal potential around 0mV (Nilius & Flockerzi, 2014; Xu et al., 2008). Our voltage-clamp recordings in BV2 microglia demonstrated that perfusion of TG to test cells evoked a linear non-selective cation conductance with a large amplitude, which implicates TRPC channels that are mediated by STIM1 gating, such as TRPC1/3 (Clapham et al., 2001). Whether an Orai-channel mediated current conductance is also present but masked within the large linear

TRPC conductance remains a possibility to be examined in future studies. Importantly, perfusing SNAP to test cells caused a rapid inhibition of the nonselective cation conductance induced by TG, confirming that NO restricts SOCC activity in murine microglia. Interestingly, minutes after SNAP application, microglia gradually developed a RR-sensitive nonselective cation conductance, further confirming the biphasic actions of NO on TRP channels in murine microglia.

3.5.2 NO attenuates SOCC activity in murine microglia independent of PKG.

The signaling of NO occurs through soluble guanylyl cyclase (sGC) signaling of PKG, or direct *S*-nitrosylation of cysteine residues on proteins (Denninger & Marletta, 1999; Stamler et al., 2001; Villalobo, 2006). Therefore, to examine whether the SNAP-induced decrease in calcium during phase I was occurring through the PKG signaling pathway, we pretreated BV2 microglia with a PKG_i and then examined the effect of SNAP on intracellular calcium levels. We demonstrated that the effects of NO were restricting SOCC activity independent of PKG signaling. To that end, it is known that STIM1 is required for SOCE (Michaelis et al., 2015) and that *S*-nitrosylation of two different cysteine residues – Cys^{49} and Cys^{56} – within STIM1 inhibits SOCE in cardiomyocytes (Gui et al., 2018). On the other hand, there are conserved cysteine residues within TRPC channels that are proposed *S*-nitrosylation sites that may also influence SOCE (Wong et al., 2010; Xu et al., 2008; Yoshida et al., 2006).

Importantly, we observed that $iNOS^{-/-}$ microglia display significantly more SOCE under basal culture conditions, while also expressing decreased mRNA expression of STIM1, TRPC1, and TRPC3 when compared to WT microglia. Therefore, $iNOS^{-/-}$ microglia may decrease transcription of SOCE proteins as a mode to compensate for the lost iNOS/NO posttranslational regulation of these SOCE proteins. Examining whether NO mediates inhibitory effects on SOCCs by S-nitrosylation of cysteine residues on STIM1 or TRPC channels in microglia should be studied in future investigations.

3.5.3 NO-donor induced slow-onset calcium influx occurs through TRPV2 channels.

Microglia express a variety of TRP channels that can regulate calcium dynamics in addition to SOCCs (Ohana et al., 2009; Sharma & Ping, 2014). We have previously demonstrated that NO induces a slow-onset calcium entry in murine microglia by facilitating the translocation of TRPV2 channels to the plasma membrane via PKG-signaling (Maksoud et al., 2019). Considering that the NO-donor SNAP induced a slow-onset calcium influx that was decreased by the TRPV/M channel inhibitor RR and abolished by the PKG_i, we therefore examined the calcium dynamics in primary murine microglia pretreated with the specific TRPV2 inhibitor tranilast. Results showed that in the presence of tranilast, the SNAP-induced calcium influx observed in phase II was completely abolished in both WT and $iNOS^{-/-}$ microglia. Therefore, this NO-sGC-PKG-TRPV2 signaling mechanism accounts for the slow-onset calcium influx observed in phase II.

3.5.4 Conclusion

Results from this study demonstrates a crucial role of NO in regulating the mobilization of calcium within murine microglia. Based on these findings, we propose that environmental factors such as purinergic signals and growth factors influence the activity of various ion channels expressed on murine microglia, which contributes to the mobilization of cytosolic calcium in these cells. For instance, purinergic receptor signaling induces ER calcium release, STIM1 oligomerization, and SOCE through TRPC1/3 and/or Orai channels. At the same time, NO produced by low-level of iNOS activity signals to limit SOCE, possibly by *S*-nitrosylation of STIM1 or TRPC proteins to maintain a stable level of intracellular calcium within microglia **(Figure 3.7A)**. This basal SOCE may be critical for maintaining a low-level of microglial proliferation (Chen et al., 2016; Guo et al., 2009; Takahashi et al., 2007).

However, under pathological conditions such as central nervous system injuries or infection, increased iNOS expression produces substantial amounts of NO in microglia.

The increase in NO can influence calcium dynamics within microglia by significantly reducing SOCE (Michaelis et al., 2015) and enhancing translocation of TRPV2 channels to the plasma membrane (Maksoud et al., 2019) **(Figure 3.7B)**. Therefore, we propose that the endogenous production of NO within microglia balances a negative feedback on SOCCs and a positive feedforward on TRPV2 channels to control intracellular calcium dynamics and control microglial functions such as proliferation and phagocytosis.

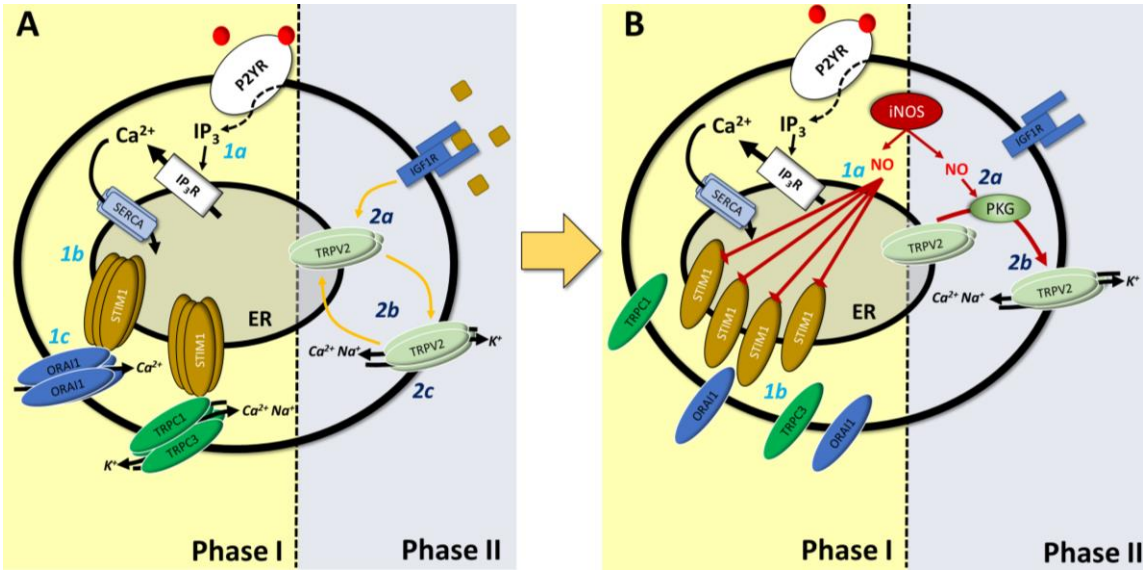

Figure 3.7 Schematic illustrating how NO signaling differentially regulates calcium dynamics in murine microglia.

A) Purinergic signaling on G_q-metabotropic receptors induce IP3 production which will bind its endogenous IP3R on the ER membrane (*1a*). IP_3R stimulation mediates calcium release from the ER into the cytosol. TG blockade of SERCA inhibits calcium refilling of the ER (*1b*). The low calcium concentration in the ER induces STIM1 oligomerization and gating of SOCCs such as orai1 or TRPC1/3 heteromeric channels on the plasma membrane. 2APB and SKF96365 are known inhibitors of SOCCs (*1c*). Insulin-like growth factor 1 stimulation induces TRPV2 trafficking to the plasma membrane (Perálvarez-Marín et al., 2013) (*2a*). TRPV2 expression on the plasma membrane induces calcium influx into the cytosol of the cell (*2b*). Tranilast and RR both act as inhibitors for the TRPV2 ion channel (*2c*). **B)** In the presence of iNOS/NO signaling, *S*-nitrosylation of STIM1 occurs quickly, such that under the low calcium condition within the ER, STIM1 does not oligomerize (Gui et al., 2018) (*1a*). As a result, STIM1 fails to gate the opening of SOCCs present on the plasma membrane (*1b*). NO signals through the sGC-cGMP-PKG cascade to induce TRPV2 trafficking to the plasma membrane (Maksoud et al., 2019) (*2a*). Once on the plasma membrane, TRPV2 channels allow for calcium influx into the cytosol of the microglia (*2b*).

3.6 References

Bakowski, D., & Parekh, A. B. (2002). Permeation through store-operated CRAC channels in divalent-free solution : potential problems and implications for putative CRAC channel genes. Cell Calcium, 32, 379–391. https://doi.org/10.1016/S0143-4160(02)00191-4

Beck, A., Penner, R., & Fleig, A. (2008). Lipopolysaccharide-induced down-regulation of Ca2+ release-activated Ca2+ currents (I CRAC) but not Ca2+-activated TRPM4-like currents (I CAN) in cultured mouse microglial cells. The Journal of Physiology, 586(2), 427–439. https://doi.org/10.1113/jphysiol.2007.145151

Bogdan, C. (2015). Nitric oxide synthase in innate and adaptive immunity: an update. Trends in Immunology, 36(3), 161–178. https://doi.org/10.1016/j.it.2015.01.003

Castro, J., Aromataris, E. C., Rychkov, G. Y., & Barritt, G. J. (2009). A small component of the endoplasmic reticulum is required for store-operated Ca2+ channel activation in liver cells: evidence from studies using TRPV1 and taurodeoxycholic acid. Biochemical Journal, 418(3), 553–566. https://doi.org/10.1042/BJ20081052

Chen, Y.-W., Chen, Y.-F., Chen, Y.-T., Chiu, W.-T., & Shen, M.-R. (2016). The STIM1-Orai1 pathway of store-operated Ca(2+) entry controls the checkpoint in cell cycle G1/S transition. Scientific Reports, 6(October 2015), 22142. https://doi.org/10.1038/srep22142

Choi, H. B., Hong, S. H., Ryu, J. K., Kim, S. U., & McLarnon, J. G. (2003). Differential activation of subtype purinergic receptors modulates Ca2+ mobilization and COX-2 in human microglia. Glia, 43(2), 95–103. https://doi.org/10.1002/glia.10239

Clapham, D. E., Runnels, L. W., & Strübing, C. (2001). The trp ion channel family. Nature Reviews Neuroscience, 2(6), 387–396. https://doi.org/10.1038/35077544

Denninger, J. W., & Marletta, M. A. (1999). Guanylate cyclase and the c NO / cGMP signaling pathway. Biochemica et Biophysica Acta Research Communications, 1411(3), 334–350.

Echeverry, S., Rodriguez, M. J., & Torres, Y. P. (2016). Transient Receptor Potential Channels in Microglia: Roles in Physiology and Disease. Neurotoxicity Research, 30(3), 467–478. https://doi.org/10.1007/s12640-016-9632-6

Färber, K., & Kettenmann, H. (2006). Functional role of calcium signals for microglial function. Glia, 54(7), 656–665. https://doi.org/10.1002/glia.20412

Ferreira, R., & Schlichter, L. C. (2013a). Selective Activation of KCa3.1 and CRAC Channels by P2Y2 Receptors Promotes Ca2+ Signaling, Store Refilling and Migration of Rat Microglial Cells. PLoS ONE, 8(4), e62345. https://doi.org/10.1371/journal.pone.0062345

Ferreira, R., & Schlichter, L. C. (2013b). Selective Activation of KCa3.1 and CRAC Channels by P2Y2 Receptors Promotes Ca2+ Signaling, Store Refilling and Migration of Rat Microglial Cells. PLoS ONE, 8(4). https://doi.org/10.1371/journal.pone.0062345

Gebicke-Haerter, P. J. (2001). Microglia in neurodegeneration: Molecular aspects. Microscopy Research and Technique, 54(1), 47–58. https://doi.org/10.1002/jemt.1120

Gui, L., Zhu, J., Lu, X., Sims, S. M., Lu, W.-Y., Stathopulos, P. B., & Feng, Q. (2018). S -Nitrosylation of STIM1 by Neuronal Nitric Oxide Synthase Inhibits Store-Operated Ca 2+ Entry. Journal of Molecular Biology, 430(12), 1773–1785. https://doi.org/10.1016/j.jmb.2018.04.028

Guo, R.-W., Wang, H., Gao, P., Li, M.-Q., Zeng, C.-Y., Yu, Y., … Huang, L. (2009). An essential role for stromal interaction molecule 1 in neointima formation following arterial injury. Cardiovascular Research, 81(4), 660–668. https://doi.org/10.1093/cvr/cvn338

Hahn, J., Jung, W., Kim, N., Uhm, D.-Y., & Chung, S. (2000). Characterization and regulation of rat microglial Ca2+ release-activated Ca2+ (CRAC) channel by protein kinases. Glia, 31(2), 118–124. https://doi.org/10.1002/1098-1136(200008)31:2<118::AID-GLIA30>3.0.CO;2-0

Hoffmann, A., Kann, O., Ohlemeyer, C., Hanisch, U.-K., & Kettenmann, H. (2003). Elevation of Basal Intracellular Calcium as a Central Element in the Activation of Brain Macrophages (Microglia): Suppression of Receptor-Evoked Calcium Signaling and Control of Release Function. The Journal of Neuroscience, 23(11), 4410–4419. https://doi.org/10.1523/JNEUROSCI.23-11-04410.2003

Hu, H. Z., Gu, Q., Wang, C., Colton, C. K., Tang, J., Kinoshita-Kawada, M., … Zhu, M. X. (2004). 2-Aminoethoxydiphenyl borate is a common activator of TRPV1, TRPV2, and TRPV3. Journal of Biological Chemistry, 279(34), 35741–35748. https://doi.org/10.1074/jbc.M404164200

Joseph, B., & Venero, J. L. (2013). Microglia Methods. Methods in Molecular Biology. https://doi.org/10.1007/978-1-62703-520-0_1

Kettenmann, H., Hanisch, U.-K., Noda, M., & Verkhratsky, A. (2011). Physiology of microglia. Physiological Reviews, 91(2), 461–553. https://doi.org/10.1152/physrev.00011.2010

Kraft, R. (2015). STIM and ORAI proteins in the nervous system. Channels (Austin, Tex.), (September), 235–243. https://doi.org/10.1080/19336950.2015.1071747

Lee, K. P., Choi, S., Hong, J. H., Ahuja, M., Graham, S., Ma, R., … Yuan, J. P. (2014). Molecular Determinants Mediating Gating of Transient Receptor Potential Canonical (TRPC) Channels by Stromal Interaction Molecule 1 (STIM1). Journal of Biological Chemistry, 289(10), 6372–6382. https://doi.org/10.1074/jbc.M113.546556

Maksoud, M. J. E., Tellios, V., An, D., Xiang, Y., & Lu, W. (2019). Nitric oxide upregulates microglia phagocytosis and increases transient receptor potential vanilloid type 2 channel expression on the plasma membrane. Glia, 67(12), 2294–2311. https://doi.org/10.1002/glia.23685

Mandal, A., Delamere, N. A., & Shahidullah, M. (2008). Ouabain-induced stimulation of sodium-hydrogen exchange in rat optic nerve astrocytes. American Journal of Physiology-Cell Physiology, 295(1), C100–C110. https://doi.org/10.1152/ajpcell.90636.2007

McLarnon, J. G. (2005). Purinergic mediated changes in Ca2+ mobilization and functional responses in microglia: Effects of low levels of ATP. Journal of Neuroscience Research, 81(3), 349–356. https://doi.org/10.1002/jnr.20475

Michaelis, M., Nieswandt, B., Stegner, D., Eilers, J., & Kraft, R. (2015). STIM1, STIM2, and orai1 regulate store-operated calcium entry and purinergic activation of microglia. Glia, 63(4), 652–663. https://doi.org/10.1002/glia.22775

Michelangeli, F., & East, J. M. (2011). A diversity of SERCA Ca2+ pump inhibitors. Biochemical Society Transactions, 39(3), 789–797. https://doi.org/10.1042/BST0390789

Mizoguchi, Y., Kato, T. A., Seki, Y., Ohgidani, M., Sagata, N., Horikawa, H., … Monji, A. (2014). Brain-derived neurotrophic factor (BDNF) induces sustained intracellular Ca2+ elevation through the up-regulation of surface transient receptor potential 3 (TRPC3) channels in rodent microglia. Journal of Biological Chemistry, 289(26), 18549–18555. https://doi.org/10.1074/jbc.M114.555334

Mizoguchi, Y., & Monji, A. (2017). Microglial Intracellular Ca2+ Signaling in Synaptic Development and its Alterations in Neurodevelopmental Disorders. Frontiers in Cellular Neuroscience, 11, 69. https://doi.org/10.3389/fncel.2017.00069

Mizuma, A., Kim, J. Y., Kacimi, R., Stauderman, K., Dunn, M., Hebbar, S., & Yenari, M. A. (2019). Microglial Calcium Release-Activated Calcium Channel Inhibition Improves Outcome from Experimental Traumatic Brain Injury and Microglia-Induced Neuronal Death. Journal of Neurotrauma, 36(7), 996–1007. https://doi.org/10.1089/neu.2018.5856

Möller, T. (2002). Calcium signaling in microglial cells. Glia, 40(2), 184–194. https://doi.org/10.1002/glia.10152

Möller, T., Hanisch, U.-K., & Ransom, B. R. (2002). Thrombin-Induced Activation of Cultured Rodent Microglia. Journal of Neurochemistry, 75(4), 1539–1547. https://doi.org/10.1046/j.1471-4159.2000.0751539.x

Nilius, B., & Flockerzi, V. (2014). Mammalian Transient Receptor Potential (TRP) Cation Channels. Handbook of Experimental Pharmacology 223, 223(April), 795–826. https://doi.org/10.1007/978-3-319-05161-1

Nörenberg, W., Cordes, A., Blöhbaum, G., Fröhlich, R., & Illes, P. (1997). Coexistence of purino- and pyrimidinoceptors on activated rat microglial cells. British Journal of Pharmacology, 121(6), 1087–1098. https://doi.org/10.1038/sj.bjp.0701241

Ohana, L., Newell, E. W., Stanley, E. F., & Schlichter, L. C. (2009). The Ca 2+ release-activated Ca 2+ current (I CRAC) mediates store-operated Ca 2+ entry in rat microglia. Channels, 3(2), 129–139. https://doi.org/10.4161/chan.3.2.8609

Papanikolaou, M., Lewis, A., & Butt, A. M. (2017). Store-operated calcium entry is essential for glial calcium signalling in CNS white matter. Brain Structure and Function, 222(7), 2993–3005. https://doi.org/10.1007/s00429-017-1380-8

Prakriya, M. (2009). The molecular physiology of CRAC channels. Immunological Reviews, 231(1), 88–98. https://doi.org/10.1111/j.1600-065X.2009.00820.x

Roos, J., DiGregorio, P. J., Yeromin, A. V., Ohlsen, K., Lioudyno, M., Zhang, S., … Stauderman, K. A. (2005). STIM1, an essential and conserved component of store-operated Ca 2 + channel function. The Journal of Cell Biology, 169(3), 435–445. https://doi.org/10.1083/jcb.200502019

Schindelin, J., Arganda-Carreras, I., Frise, E., Kaynig, V., Longair, M., Pietzsch, T., … Cardona, A. (2012). Fiji: An open-source platform for biological-image analysis. Nature Methods, 9(7), 676–682. https://doi.org/10.1038/nmeth.2019

Sharma, P., & Ping, L. (2014). Calcium ion influx in microglial cells: Physiological and therapeutic significance. Journal of Neuroscience Research, 92(4), 409–423. https://doi.org/10.1002/jnr.23344

Srikanth, S., & Gwack, Y. (2012). Orai1, STIM1, and their associating partners. The Journal of Physiology, 590(Pt 17), 4169–4177. https://doi.org/10.1113/jphysiol.2012.231522

Stamler, J. S., Lamas, S., & Fang, F. C. (2001). Nitrosylation: The Prototypic Redox-Based Signaling Mechanism. Cell, 106(6), 675–683. https://doi.org/10.1016/S0092-8674(01)00495-0

Sun, Y., Chauhan, A., Sukumaran, P., Sharma, J., Singh, B. B., & Mishra, B. B. (2014). Inhibition of store-operated calcium entry in microglia by helminth factors: implications for immune suppression in neurocysticercosis. Journal of Neuroinflammation, 11(1), 210. https://doi.org/10.1186/s12974-014-0210-7

Svensson, C., Fernaeus, S. Z., Part, K., Reis, K., & Land, T. (2010). LPS-induced iNOS expression in Bv-2 cells is suppressed by an oxidative mechanism acting on the JNK pathway—A potential role for neuroprotection. Brain Research, 1322, 1–7. https://doi.org/10.1016/j.brainres.2010.01.082

Takahashi, Y., Watanabe, H., Murakami, M., Ono, K., Munehisa, Y., Koyama, T., … Ito, H. (2007). Functional role of stromal interaction molecule 1 (STIM1) in vascular

smooth muscle cells. Biochemical and Biophysical Research Communications, 361(4), 934–940. https://doi.org/10.1016/j.bbrc.2007.07.096

Trebak, M., St. J. Bird, G., McKay, R. R., & Putney, J. W. (2002). Comparison of Human TRPC3 Channels in Receptor-activated and Store-operated Modes. Journal of Biological Chemistry, 277(24), 21617–21623. https://doi.org/10.1074/jbc.M202549200

Vazquez-Martinez, O. (2003). Biochemical characterization, distribution and phylogenetic analysis of Drosophila melanogaster ryanodine and IP3 receptors, and thapsigargin-sensitive Ca2+ ATPase. Journal of Cell Science, 116(12), 2483–2494. https://doi.org/10.1242/jcs.00455

Villalobo, A. (2006). REVIEW ARTICLE: Nitric oxide and cell proliferation. FEBS Journal, 273(11), 2329–2344. https://doi.org/10.1111/j.1742-4658.2006.05250.x

Wong, C.-O., Sukumar, P., Beech, D. J., & Yao, X. (2010). Nitric oxide lacks direct effect on TRPC5 channels but suppresses endogenous TRPC5-containing channels in endothelial cells. Pflügers Archiv - European Journal of Physiology, 460(1), 121–130. https://doi.org/10.1007/s00424-010-0823-3

Worley, P. F., Zeng, W., Huang, G. N., Yuan, J. P., Kim, J. Y., Lee, M. G., & Muallem, S. (2007). TRPC channels as STIM1-regulated store-operated channels. Cell Calcium, 42(2), 205–211. https://doi.org/10.1016/j.ceca.2007.03.004

Xu, S.-Z., Sukumar, P., Zeng, F., Li, J., Jairaman, A., English, A., … Beech, D. J. (2008). TRPC channel activation by extracellular thioredoxin. Nature, 451(7174), 69–72. https://doi.org/10.1038/nature06414

Yang, S., Zhang, J. J., & Huang, X.-Y. (2009). Orai1 and STIM1 Are Critical for Breast Tumor Cell Migration and Metastasis. Cancer Cell, 15(2), 124–134. https://doi.org/10.1016/j.ccr.2008.12.019

Yoshida, T., Inoue, R., Morii, T., Takahashi, N., Yamamoto, S., Hara, Y., … Mori, Y. (2006). Nitric oxide activates TRP channels by cysteine S-nitrosylation. Nature Chemical Biology, 2(11), 596–607. https://doi.org/10.1038/nchembio821

Yuan, J. P., Zeng, W., Huang, G. N., Worley, P. F., & Muallem, S. (2007). STIM1 heteromultimerizes TRPC channels to determine their function as store-operated channels. Nature Cell Biology, 9(6), 636–645. https://doi.org/10.1038/ncb1590

Zhang, G., He, J.-L., Xie, X.-Y., & Yu, C. (2012). LPS-induced iNOS expression in N9 microglial cells is suppressed by geniposide via ERK, p38 and nuclear factor-κB signaling pathways. International Journal of Molecular Medicine, 30(3), 561–568. https://doi.org/10.3892/ijmm.2012.1030

Chapter 4

This chapter was published in the journal *Nitric Oxide*, volume 94, pages 125 – 134. It has been reproduced with permission from Elsevier.

4 Nitric oxide signaling inhibits microglia proliferation by activation of protein kinase-G.

4.1 Abstract

Microglia population is primarily determined by a finely regulated proliferation process during early development of the central nervous system (CNS). Nitric oxide (NO) is known to inhibit proliferation in numerous cell types. However, how NO signaling regulates microglia proliferation remains elusive. Using wildtype (WT) and inducible nitric oxide synthase knockout ($iNOS^{-/-}$) mice, this study investigated the role and underlying mechanisms of iNOS/NO signaling in microglia proliferation. Here we reported that $iNOS^{-/-}$ mice displayed significantly more BrdU-labeled proliferating microglia in the cortex than WT mice at postnatal day 10. Compared to microglia isolated from WT mouse cortex, significantly more $iNOS^{-/-}$ microglia displayed the specific cell-cycle markers Ki67 and phospho-histone H3 (pH3) in their nuclei. In addition, treating WT microglia with the NOS inhibitor L-NAME drastically increased the percentage of cells expressing Ki67 and pH3, whereas treating $iNOS^{-/-}$ microglia with NOC18, a slow-release NO-donor, significantly decreased the percentage of microglia expressing the two cell-cycle markers. Moreover, inhibition of protein kinase-G (PKG) in WT microglia increased the proportion of microglia expressing Ki67 and pH3, whereas activation of PKG signaling using 8Br-cGMP in $iNOS^{-/-}$ microglia significantly decreased the fraction of microglia displaying Ki67 and pH3. Interestingly, in the presence of a PKG inhibitor, NOC18 increased the quantity of $iNOS^{-/-}$ microglia expressing Ki67 and pH3. Together, these results indicate that basal activity of iNOS/NO signaling impedes microglial cell-cycle progression and attenuates proliferation through activation of the cGMP-PKG pathway. However, NO increases microglia cell-cycle progression in the absence of cGMP-PKG signaling.

4.2 Introduction

Microglial progenitors emerge from the yolk sac and infiltrate the brain parenchyma during embryogenesis (Francoise Alliot et al., 1999). Once the blood brain barrier is formed, microglia rapidly proliferate to become a self-sustaining population within the entire central nervous system (CNS) (Nikodemova et al., 2015). As the primary immune cells in the CNS, microglia play an essential role in the maintenance of proper CNS function through neuronal axon guidance, pruning redundant synapses, and removing unnecessary neuronal precursor cells (Cunningham et al., 2013; Marín-Teva et al., 2004; Stevens et al., 2007; Wakselman et al., 2008). Previous studies demonstrated that the population of microglia in a healthy adult brain remains stable, and that the microglia exhibit long life spans while remaining within a non-proliferative state (Matcovitch-Natan et al., 2016; Nikodemova et al., 2015). In rodent models of microglia depletion, behavioural analyses revealed alterations in spatial and motor learning (Parkhurst et al., 2013; Torres et al., 2016), anxiety-like behaviours (Rosin et al., 2018; Vanryzin et al., 2016), and hyperactivity (Rosin et al., 2018). These data indicate that regulation of microglia proliferation, and microglia number into adulthood, is important for CNS homeostasis. However, the factors and mechanisms related to microglia proliferation during development remain largely elusive.

It has long been known that nitric oxide (NO) critically regulates the proliferation of various types of cells in the CNS (Adachi et al., 2010; Pinnock et al., 2007), and that microglia produce large amounts of NO through the catalytic activity of inducible nitric oxide synthase (iNOS). During embryonic development, undifferentiated amoeboid microglia that infiltrate the CNS express inducible nitric oxide synthase (iNOS) (Brenneman et al., 1992; Crain et al., 2013; Giulian et al., 1988; Sierra et al., 2014). Additionally, behavioural studies carried out in mice lacking iNOS ($iNOS^{-/-}$) report increased motor activity (Montezuma et al., 2012) and trichotillomania (Casarotto et al., 2018), suggesting iNOS expression and NO production are both critical for proper CNS and behavioural development. Therefore, a delicate balance between iNOS/NO expression and microglia proliferation should be present within the CNS during development. One of the primary molecular mechanisms in which NO regulates cellular functions is through the

activation of soluble guanylyl cyclase (sGC) to produce cyclic guanosine monophosphate (cGMP), which is required for protein kinase-G (PKG) activity (Bogdan, 2001; Bogdan, 2015; Forstermann & Sessa, 2012). In this regard, both NO and PKG have been shown to inhibit cell proliferation by arresting cell cycle progression in the G_1/S phase (Gu et al., 2000; Gu & Brecher, 2000; Sarkar et al., 1997). The present study used wildtype (WT) and iNOS-knockout ($iNOS^{-/-}$) mice to determine whether endogenous iNOS/NO influences postnatal microglia proliferation; and whether this NO signaling occurs through the classical sGC/cGMP/PKG pathway. Results from this study demonstrate that iNOS/NO signaling attenuates microglia proliferation primarily through activation of PKG.

4.3 Materials and Methods

4.3.1 Materials

Compounds were purchased from the following sources – slow release NO-donor: diethylenetriamine NONOate (NOC18), NOS inhibitor: G-nitro-L-arginine-methyl ester (L-NAME), arginyl-lysyl-arginyl-alanyl-arginyl-lysyl-glutamic acid (PKG inhibitory peptide; PKG_i), 8-bromo-cyclic GMP (8Br-cGMP) (Cayman Chemical, Ann Arbor, MI); bromodeoxyuridine (BrdU), phosphate buffered saline (PBS), paraformaldehyde (PFA), 4',6-diamidino-2-phenylindole (DAPI), Triton X-100, glycine, poly-D-lysine (PDL), sucrose, glycerol, ethylene glycol (Sigma-Aldrich, Oakville, On); Dulbecco's modified eagle medium (DMEM), fetal bovine serum (FBS), trypsin, sodium-pyruvate, penicillin/streptomycin, (ThermoFischer Scientific, Waltham, Ma); Fluoromount-G, (Electron Microscopy Sciences, Hatfield, PA); Isoflurane, (Baxter Corporation, Mississauga, Ontario); normal donkey serum (NDS), (Jackson ImmunoResearch Laboratories, Inc., West Grove, PA).

4.3.2 BrdU Injections

WT (C57BL/6, Stock No: 000664) and $iNOS^{-/-}$ (B6.129P2-$Nos2^{tm1Lau}$, Stock No: 002609) mice were purchased from The Jackson Laboratory. All experiments were conducted in accordance with the Animal Care and Veterinary Services at The University of Western Ontario, Canada (AUP#2018-106). Given that microglia highly proliferate within the first 2 postnatal weeks (Eyo et al., 2017; Harry & Kraft, 2012; Nikodemova et al., 2015), male WT (N=4) and $iNOS^{-/-}$ (N=4) mice at postnatal day-10 (p10) were administered a single intraperitoneal injection of BrdU at 100mg/kg in PBS (Fukushima et al., 2015). Six hours after BrdU injection, mice were anaesthetised using isoflurane, perfused with saline followed by 4% PFA, and brain tissue was collected and placed in 4% PFA for three days before being used for immunohistochemistry.

4.3.3 Immunohistochemistry

Three days after placement within PBS containing 30% sucrose, fixed mouse brains were sliced in coronal sections of 40μm thickness using a Pelco Vibratome Sectioning System (Redding CA, 96003), placed in cryoprotectant buffer containing 25% glycerol and 30% ethylene glycol in PBS, and stored at -20^{o}C until stained. After 3 washes using PBS, brain slices were blocked using 5% NDS and 0.3% triton for 1hr at room temperature (RT). Then tissues were incubated with Iba-1 (Wako Chemical Inc., CAT#019-19741, 1:5000) and BrdU (AbCam, CAT#1893, 1:300) primary antibodies diluted in a 1% NDS and 0.3% triton solution for 24hrs at RT. Following 3 washes with PBS, tissue samples were incubated with secondary Alexa Fluor-488 (Jackson immunooresearch, CAT#711-546-152, 1:500) and Cy3 antibodies (Jackson Immunoresearch Labs, CAT#713-165-003, 1:500) diluted in 1% NDS and 0.3% triton solution for 2h at RT. Tissue slices were set to dry in the dark on cover glass before mounting using Fluromount-G (Electron Microscopy Sciences). Four images were taken within the parietal cortex (Bregma -2.5 mm) from each biological replicate using the Olympus FV-1000 confocal laser scanning microscope at 20× using a water immersion objective. Images were segmented in non-overlapping 300μm × 300μm regions and cells expressing BrdU and/or Iba1 were counted in each region using FIJI open source software and graphed using Microsoft Excel.

4.3.4 Primary Microglia Cultures

Microglia were cultured as previously described (Joseph & Venero, 2013). Briefly, entire litters of postnatal day 1 pups – containing male and female pups – from either WT (n = 64) or iNOS$^{-/-}$ (n = 72) mice were decapitated and cortices were isolated in ice cold Leibowitz L-15 media (Thermo Fischer Scientific, Waltham MA). Cortices were then homogenized and cell suspension was filtered through a 70μm nylon filter, and then centrifuged at 900g for 4min at RT. The pellet, containing cortical cells, was resuspended in DMEM containing 1x Penicillin/streptomycin and 10% FBS (Thermo Fischer Scientific, Waltham MA). Cells were cultured in T-75 flasks, and media was changed every 3 days for 2 weeks. After 2 weeks of culture, T-75 flasks were placed on a shaker at 36^{o}C and 200rpm for 2hrs. The media containing detached microglia cells was spun down at 900g

for 4 min, and the supernatant removed. The cell pellet containing microglia was resuspended in fresh culture media and plated at $5x10^4$ cells/ml before conducting experiments

4.3.5 Cell Viability Assay

Primary microglia were cultured in 24 well plates using DMEM supplemented with 2.5% FBS, 5% sodium pyruvate, and 1% penicillin/streptomycin antibiotics. Twenty-four hours after plating, microglia were treated at 37ºC and 5% CO_2, with pharmacological compounds at concentrations recommended by the manufacture data sheets and reported in literature. These compounds included NOC18 (100μM) (Carreira et al., 2014; Tegenge & Bicker, 2009), L-NAME (100μM) (Maksoud et al., 2019; Quintas et al., 2014), PKG_i (10μM) (Maksoud et al., 2019; Wexler et al., 1998), 8Br-cGMP (10μM) (Gu et al., 2000) for 48hrs (Carreira et al., 2014; Tian et al., 2010). Cell viability was measured using trypan blue (Sigma-Aldrich, Oakville, On) staining. Briefly, culture medium containing floating microglia was collected. Then microglia within plates were detached using 50μL of 2.5% trypsin in PBS with gentle pipetting, followed by 50μL of media to neutralize the trypsin. Media containing detached and floating microglia were combined and spun down at 900g for 4min, the supernatant was removed, and the pellet was replaced with 100μL of fresh media. One hundred μL of trypan blue (0.4%) was added to each tube consisting of microglia and 10μL was loaded into a hemocytometer. Within each well (N=4), the total number of trypan blue stained microglia were divided by the total number of counted microglia to obtain a percent of viable cells in accordance with the following equation: % viable cells = [1-(number of trypan stained cells / total number of cells)]×100.

4.3.6 Immunocytochemistry and cell cycle classification

Primary microglia were plated on cover glass coated with PDL and cultured using DMEM supplemented with 2.5% FBS, 5% sodium pyruvate, and 1% penicillin/streptomycin antibiotics for 24hrs to allow microglia to rest before pharmacology treatments. The concentration of each drug was determined by the effective dose-ranges reported on data sheets as well as from previous literature. Specifically,

microglia cultures were treated with the following compounds: NOC18 (100μM), L-NAME (100μM), PKG_i (10μM), 8Br-cGMP (10μM), or a combination of NOC18 + PKG_i or L-NAME + 8Br-cGMP for 48hrs under normal culture conditions of 37ºC and 5% CO_2 before cell fixation using 4% PFA for 5min at RT. Notably, at the test concentration, these compound did not change cell viability. Fixed microglia cells were washed with 0.1M glycine in PBS followed by two washes of PBS for 5 min each. Cell membranes were permeabilized using 0.1% triton in PBS for 5min followed by blocking solution containing 5% NDS in PBS for 1hr at RT. Primary CD11b (BioRAD, CAT#MCA74G, 1:150) and Ki67 (AbCam, CAT#ab15580, 1:300) antibodies were incubated on coverslips in 1% NDS for 2hrs at RT. The secondary antibodies – Cy3 (Jackson Immunoresearch Labs, CAT#711-166-152) and Alexa Fluor-647 (Invitrogen, CAT#A21246) – were incubated in 1% NDS in PBS for 1h at RT, followed by 3 washes in PBS. Finally, microglia cells were incubated with the primary antibody phosphorylated histone 3 (S10+T11) conjugated to Alexa Fluor 488 (AbCam, CAT#ab200614, 1:5000) in 1% NDS for 2hrs at RT, followed by 3 washes in PBS for 10min. Cells were washed with PBS 3x for 10min each, followed by DAPI staining (1μg/ml) for 10min at RT. Microglia on glass cover slips were mounted onto slides using Fluormount-G. Multiple images were taken from 3 individual wells (N = 3) for each control and experimental group using the Olympus FV-1000 confocal laser scanning microscope at 60× using an oil immersion objective.

4.3.7 Cell-Cycle Classification

Images displayed 96.4±1.8% of WT cultures and 94.5±1.6% of $iNOS^{-/-}$ cultures were CD11b positive microglia, and only CD11b positive cells were included in the analysis. Microglia were classified into 3 different cell cycle stages. Specifically, microglia with nuclear staining of DAPI and Ki67 were classified as being in interphase; DAPI, Ki67, and pH3 were classified as being in mitosis; and only DAPI stained microglia were classified as in G0. Individual channels containing DAPI, Ki67, and pH3 staining were thresholded using the Otsu method (Otsu, 1979), which remained consistent between images and treatments, to removed background fluorescence staining. Only cells with marker expression above the thresholded range were included in the analysis. Cell-cycle

classification of $CD11b^+$ cells were reported as a percent of total $CD11b^+$ cells per image using FIJI open source software and graphed using Microsoft Excel.

4.3.8 Statistics

Statistical analyses were done using Graphpad Prisim 6. All results are shown as mean ± SEM. A two-tailed, unpaired t-test, one-way ANOVA with Tukey's post hoc comparison, or two-way ANOVA with Bonferroni's post hoc comparison was used where appropriate, with P-values of less than 0.05 taken as showing significant differences between means.

4.4 Results

4.4.1 iNOS$^{-/-}$ microglia proliferate more than WT microglia in the cortex of p10 mice.

Images from mouse p10 cortical slices displayed significantly more BrdU^{+} cells in the cortex of iNOS$^{-/-}$ mice in comparison to WT mice (**Figures 4.1A** and **4.1B**). BrdU fluorescence was associated with both Iba1 positive (BrdU^{+}Iba1^{+}) microglia and Iba1 negative (BrdU^{+}Iba1^{-}) cells. Notably, significantly more BrdU^{+}Iba1^{+} and BrdU^{+}Iba1^{-} cells in the cortices of iNOS$^{-/-}$ mice compared to that of WT mice (**Figure 4.1C** and **4.1D**). Interestingly, the total number of Iba1^{+} microglia in the cortex of p10 iNOS$^{-/-}$ mice was not significantly different from that of age-matched WT mice (**Figure 4.1E)**. These results indicated that cells lacking iNOS/NO signaling in the mouse cortex proliferate more during early postnatal development.

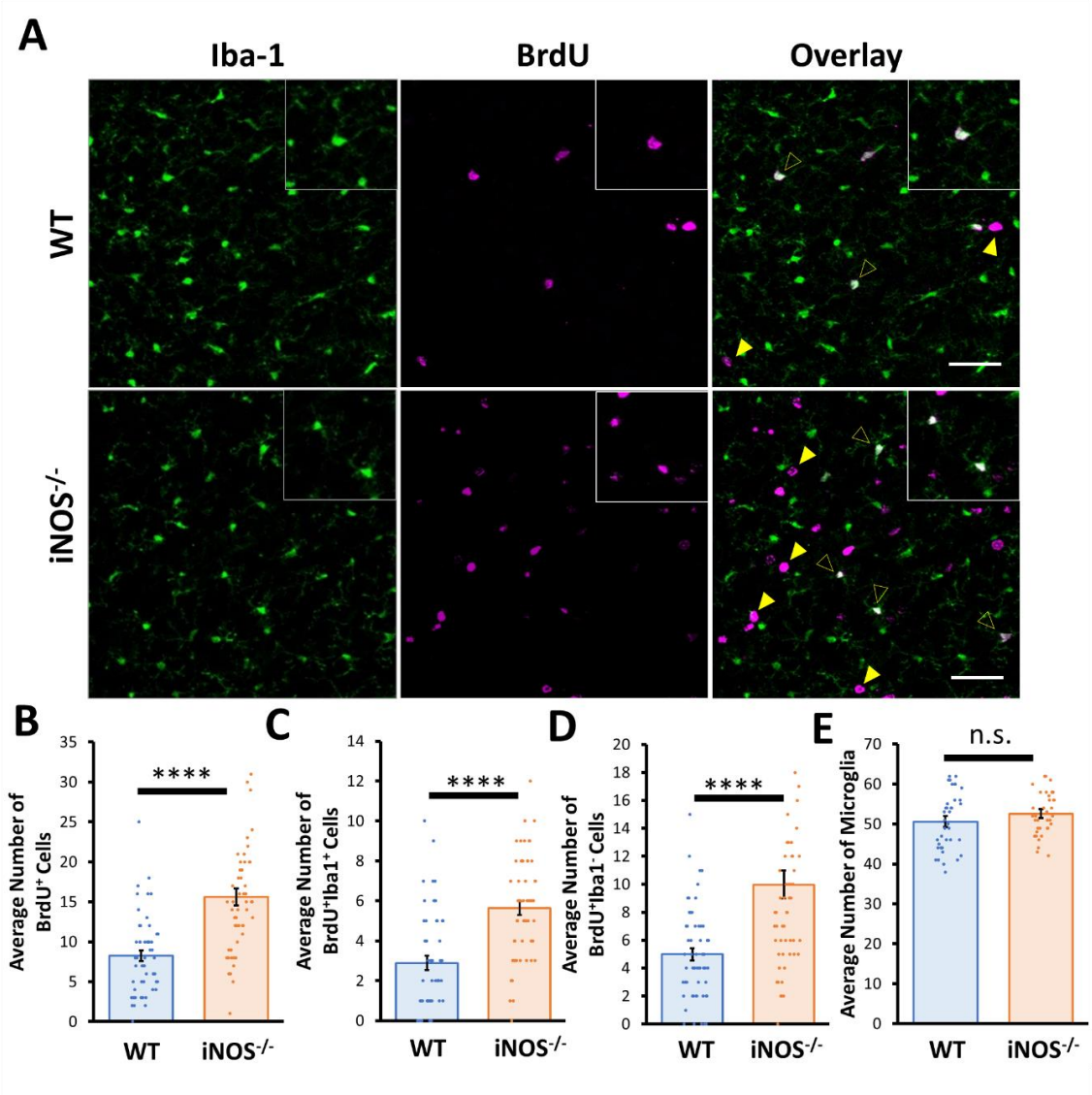

Figure legend on next page

Figure 4.1 More iNOS$^{-/-}$ microglia proliferate than WT microglia in the cortex of male p10 mice.

A) Representative immunostained images of Iba-1 (green) and BrdU (purple) in the cortices of WT and iNOS$^{-/-}$ mice. Inset boxes show zoomed in Iba-1 and/or BrdU staining. Open arrows point to BrdU^{+}Iba1^{+} cells, closed arrows point to BrdU^{+}Iba1^{-} cells. Scale bars represent 50μm. Bar graphs depict the average number of **B)** BrdU^{+} cells, **C)** BrdU^{+}Iba1^{+} cells, **D)** BrdU^{+}Iba1^{-} cells, or **E)** microglia cell bodies, per 300μm x 300μm region in WT and iNOS$^{-/-}$ parietal cortices. Significance was determined from an N=4 and $p<0.05$ using a two-tailed, unpaired t-test. ****$p<0.0001$.

4.4.2 iNOS$^{-/-}$ microglia express more Ki67 and pH3 than WT microglia *in vitro*

To examine if endogenous iNOS expression influences microglia proliferation, we cultured primary microglia isolated from WT and iNOS$^{-/-}$ mice and examined differences in the expression of the cell-cycle markers Ki67 and pH3 **(Figure 4.2A)**. Immunofluorescent analyses displayed significantly less iNOS$^{-/-}$ microglia stained with DAPI when compared to WT control **(Figure 4.2B)**, while significantly more iNOS$^{-/-}$ microglia displayed nuclear presence of either Ki67 or pH3 when compared to WT microglia **(Figure 4.2C** and **4.2D)**. These results indicated that the lack of iNOS expression within microglia increases proliferation, evidenced by the amount of cells expressing Ki67 and pH3.

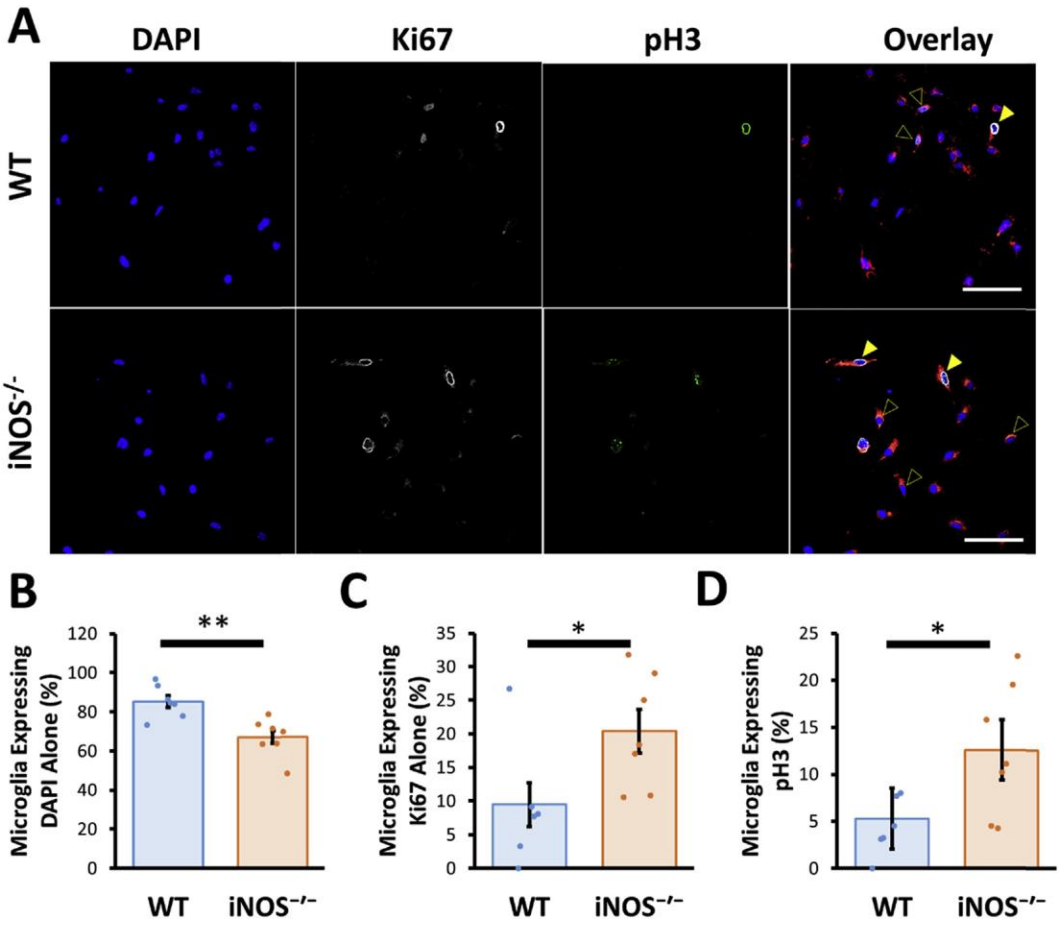

Figure 4.2 Under culture conditions more iNOS$^{-/-}$ microglia express Ki67 and pH3 than WT microglia.

A) representative images of cultured WT and iNOS$^{-/-}$ microglia stained with DAPI (Blue), Ki67 (grey), pH3 (green), and the microglial marker CD11b (red). Closed arrows point to mitotic microglia expressing pH3. Open arrows point to microglia expressing Ki67. Scale bars represent 50µm. Bar graphs report the percentages of WT and iNOS$^{-/-}$ microglia having nuclei stained with **B)** DAPI only, **C)** DAPI and Ki67, and **D)** DAPI, Ki67, and pH3. Significance was determined from an N = 3 and $p<0.05$ using a two-tailed, unpaired t-test. *$p<0.05$, **$p<0.01$.

4.4.3 Pharmacological manipulation of the NO/PKG signaling pathway does not change the viability of primary WT or iNOS$^{-/-}$ microglia *in vitro*.

To understand the downstream mechanism by which iNOS/NO regulates microglial proliferation, we studied whether pharmacological manipulation of the NO/PKG signaling pathway regulates the nuclear expression of cell-cycle markers. Firstly, we used trypan blue exclusion assay to examine the viability of cultured WT and iNOS$^{-/-}$ microglia in response to the pharmacological compounds: NOC18, 8Br-CGMP, PKG$_i$ and L-NAME, which were used for modulating iNOS/PKG signaling respectively. Results showed that there were no significant differences in cell viability between WT and iNOS$^{-/-}$ microglia, as well as between control and test drug concentrations (**Figure 4.3)**.

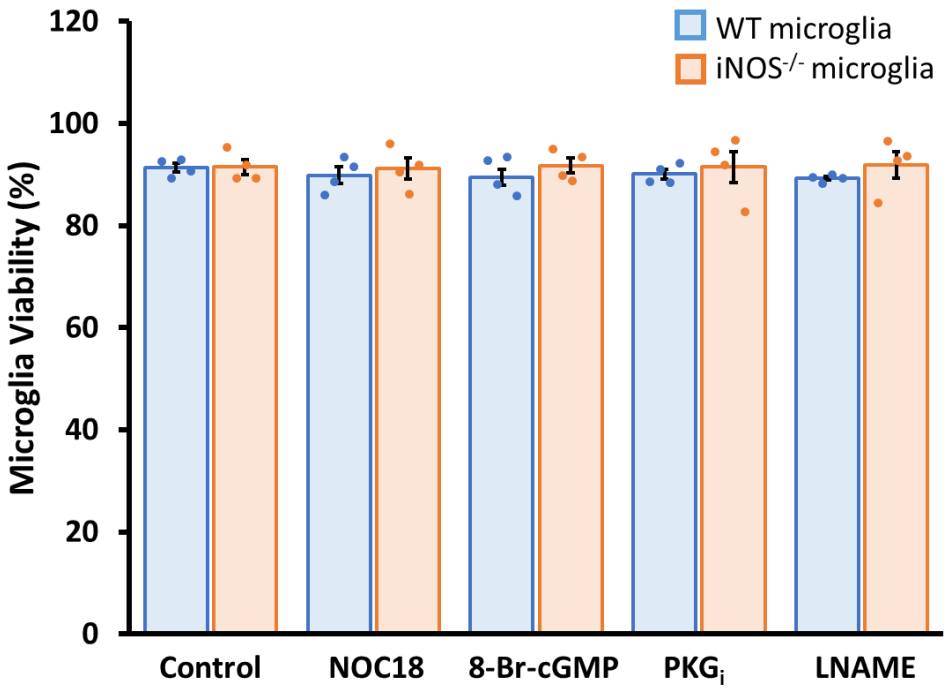

Figure 4.3 Pharmacological manipulation of the NO/PKG pathway does not affect the viability of primary WT and iNOS$^{-/-}$ microglia.

The bar graph reports the percentage of viable WT (blue) and iNOS$^{-/-}$ (orange) microglia under different pharmacological treatments NOC18 (100µM), 8Br-cGMP (10µM), PKG$_i$ (10µM), L-NAME (100µM). Significance was assessed from WT (N = 4) and iNOS$^{-/-}$ (N = 4) microglia by two-way ANOVA and Bonferroni's post hoc comparisons.

4.4.4 Inhibition of iNOS increases the percentage of Ki67- and pH3-expressing WT microglia *in vitro*.

To confirm that basal iNOS activity influences the proliferation of microglia, we treated WT microglia with either the NOS inhibitor L-NAME (100μM) or a vehicle control for 48hrs and examined the nuclear presence of only DAPI, Ki67, and pH3 **(Figure 4.4A)**. Our assays showed that in response to L-NAME treatment, there were significantly less microglia stained with DAPI alone **(Figures 4.4B**) and significantly more nuclear Ki67 **(Figures 4.4C)** and/or pH3 (**Figures 4.4D)** expression in comparison to the vehicle controls. Together these results suggest iNOS expression restricts proliferation, evidenced by the Ki67 and pH3 nuclear expression within WT microglia.

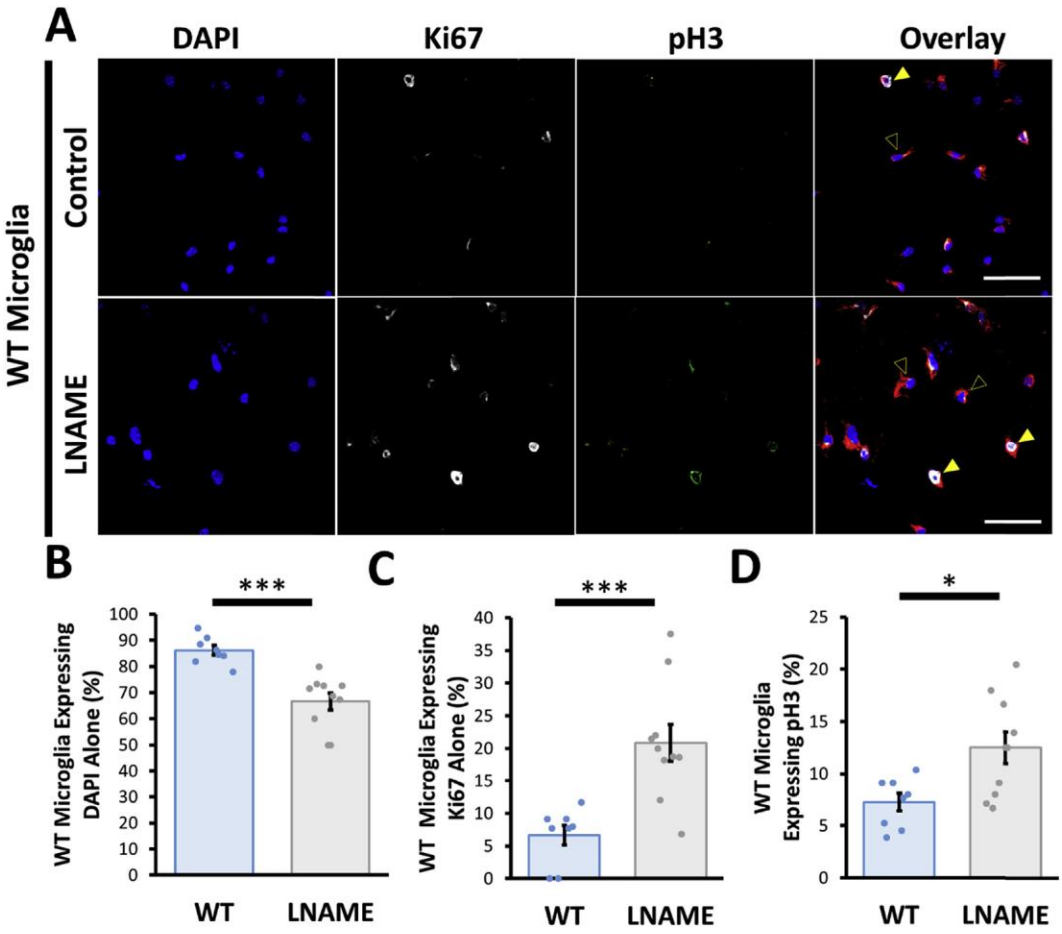

Figure 4.4 Inhibition of iNOS using L-NAME increases the percentage of Ki67 and pH3 expressing WT microglia *in vitro*.

A) Representative images of control and L-NAME (100μM)-treated WT microglia stained with DAPI (Blue), Ki67 (grey), pH3 (green), and the microglial marker CD11b (red). Closed arrows point to WT microglia expressing pH3, and open arrows point to WT microglia expressing Ki67. Scale bars represent 50μm. Bar graphs report the percentages of WT microglia having nuclei stained with **B)** DAPI only, **C)** DAPI and Ki67, and **D)** DAPI, Ki67, and pH3. Significance was determined from an N = 3 and $p<0.05$ using a two-tailed, unpaired t-test. *$p<0.05$, ***$p<0.001$.

4.4.5 Exogenous NO decreases the percentage of Ki67- and pH3-expressing iNOS$^{-/-}$ microglia *in vitro*.

To examine if exogenous NO attenuates proliferation within iNOS$^{-/-}$ microglia, we treated iNOS$^{-/-}$ microglia with the slow-release NO-donor NOC18 (100μM) for 48hrs and examined the nuclear staining of only DAPI, Ki67, and pH3 (**Figure 4.5A**). In response to NOC18 treatment, there were significantly more iNOS$^{-/-}$ microglia displaying DAPI only **(Figure 4.5B)** while significantly less iNOS$^{-/-}$ microglia displayed the nuclear presence of Ki67 **(Figures 4.5C**) and pH3 **(Figures 4.5D**) when compared to the vehicle controls. Importantly, treatment with L-NAME (100μM) had no significant effect on the amount of microglia stained with only DAPI, Ki67, or pH3 within iNOS$^{-/-}$ microglia when compared to vehicle controls (data not shown). Together these results demonstrate that iNOS/NO signaling is a crucial factor in regulating proliferation within microglia.

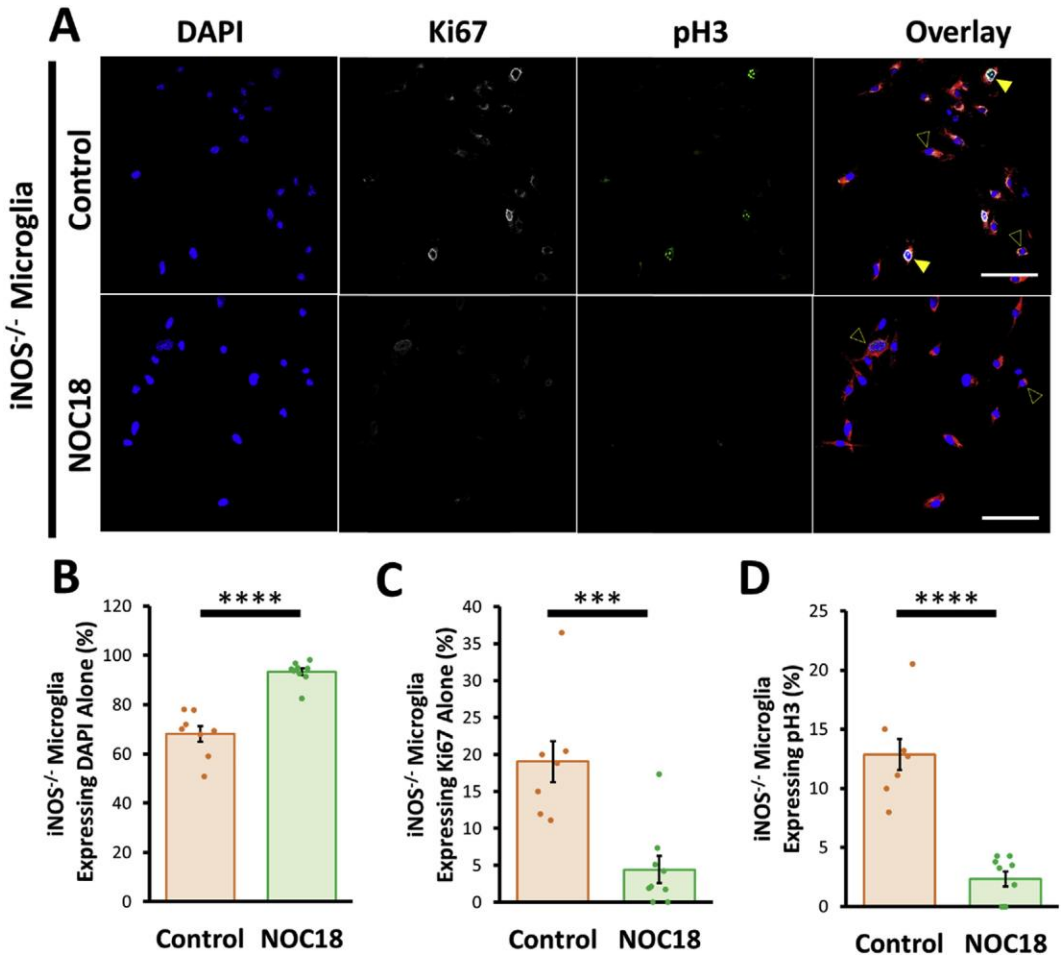

Figure 4.5 Exogenous NO decreases the percentage of Ki67 and pH3 expressing iNOS$^{-/-}$ microglia *in vitro*.

A) Representative images of control and NOC18 (100μM)-treated iNOS$^{-/-}$ microglia that were stained with DAPI (Blue), Ki67 (grey), pH3 (green), and the microglial marker CD11b (red). Closed arrows point to iNOS$^{-/-}$ microglia stained with pH3, and open arrows point to iNOS$^{-/-}$ microglia stained with Ki67. Scale bars represent 50μm. Bar graphs report the percentages of iNOS$^{-/-}$ having nuclei stained with **B)** DAPI only, **C)** DAPI and Ki67, and **D)** DAPI, Ki67, and pH3. Significance was determined from an N = 3 and $p<0.05$ using a two-tailed, unpaired t-test. ***$p<0.001$, ****$p<0.0001$.

4.4.6 Inhibiting PKG signaling increases the percentage of WT microglia expressing Ki67 and pH3 *in vitro*.

To examine if the PKG pathway within microglia regulates cell-cycle progression, we treated WT microglia with either the PKG agonist 8Br-cGMP (10μM), PKG_i (10μM) alone, or L-NAME (100μM) with 8Br-cGMP and examined the nuclear staining of only DAPI, Ki67, and pH3 **(Figure 4.6A)**. Results demonstrated that in comparison to the vehicle control, 8Br-cGMP had no significant effect on nuclear presence of DAPI alone, Ki67, or pH3 in WT microglia **(Figures 4.6B-4.6D)**. Notably, WT microglia treated with PKG_i displayed significantly less DAPI only and significantly more Ki67 and/or pH3 nuclear expression when compared to control **(Figure 4.6B-4.6D).** However, in the presence of both 8Br-cGMP and L-NAME, the nuclear presence of Ki67 or pH3 was comparable to that in WT control microglia **(Figures 4.6A-4.6D).** Together these results demonstrate that NO signaling through the classical PKG-pathway attenuates proliferation, evidenced by the amount of microglia expressing Ki67 and pH3.

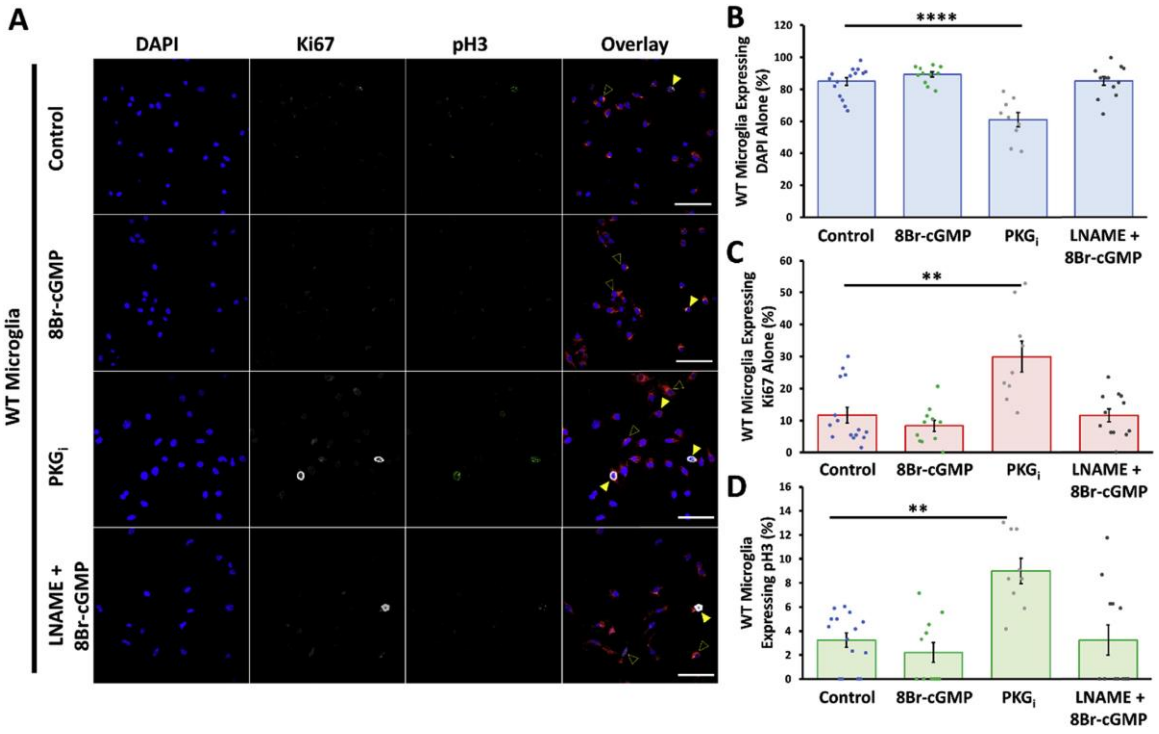

Figure 4.6 Inhibiting PKG signaling increases the percentage of WT microglia expressing Ki67 and pH3 *in vitro*.

A) Representative images of control and WT microglia treated with 8Br-cGMP (10μM), PKG_i (10μM), or L-NAME (100μM) + 8Br-cGMP, and stained with DAPI (Blue), Ki67 (grey), pH3 (green), and the microglial marker CD11b (red)**.** Closed arrows point to WT microglia expressing pH3, and open arrows point to WT microglia expressing Ki67. Scale bars represent 50μm. Bar graphs report the percentages of WT microglia having nuclei stained with **B)** DAPI alone, **C)** DAPI and Ki67, and **D)** DAPI, Ki67, and pH3. Significance was determined from an N = 3 and $p<0.05$ using a one-way ANOVA and Tukey's post hoc comparison. **$p<0.01$, ****$p<0.0001$.

4.4.7 Exogenous NO signaling in iNOS$^{-/-}$ microglia decreases the percentage of Ki67- and pH3-expressing microglia through a PKG dependent mechanism.

We examined if exogenous NO signaling through the PKG pathway regulates the expression of the proliferation markers Ki67 and/or pH3 within iNOS$^{-/-}$ microglia. Therefore, we treated iNOS$^{-/-}$ microglia with either 8Br-cGMP (10μM), PKG$_i$ (10μM), or NOC18 (100μM) in combination with PKG$_i$ and examined the expression of Ki67 and/or pH3 **(Figure 4.7A**). Analyses showed that 8Br-cGMP increased the percentage of iNOS$^{-/-}$ microglia stained with only DAPI, and significantly decreased the percentage of iNOS$^{-/-}$ microglia expressing Ki67 and/or pH3 when compared to the control cells (**Figures 4.7B-D).** In the presence of PKG$_i$, there was no difference in the percentage of iNOS$^{-/-}$ microglia stained with only DAPI, Ki67 or pH3 (**Figure 4.7B-D**)**.** Interestingly, in the presence of PKG$_i$, NOC18 treatment significantly lowered the percentage of iNOS$^{-/-}$ microglia displaying only DAPI, and significantly increased the percentage of iNOS$^{-/-}$ microglia expressing Ki67 and/or pH3 in comparison to vehicle controls **(Figures 4.7B-D).** Together this data suggests that exogenous NO signaling attenuates proliferation through the classical PKG-pathway and may potentiate proliferation in the absence of PKG-signaling.

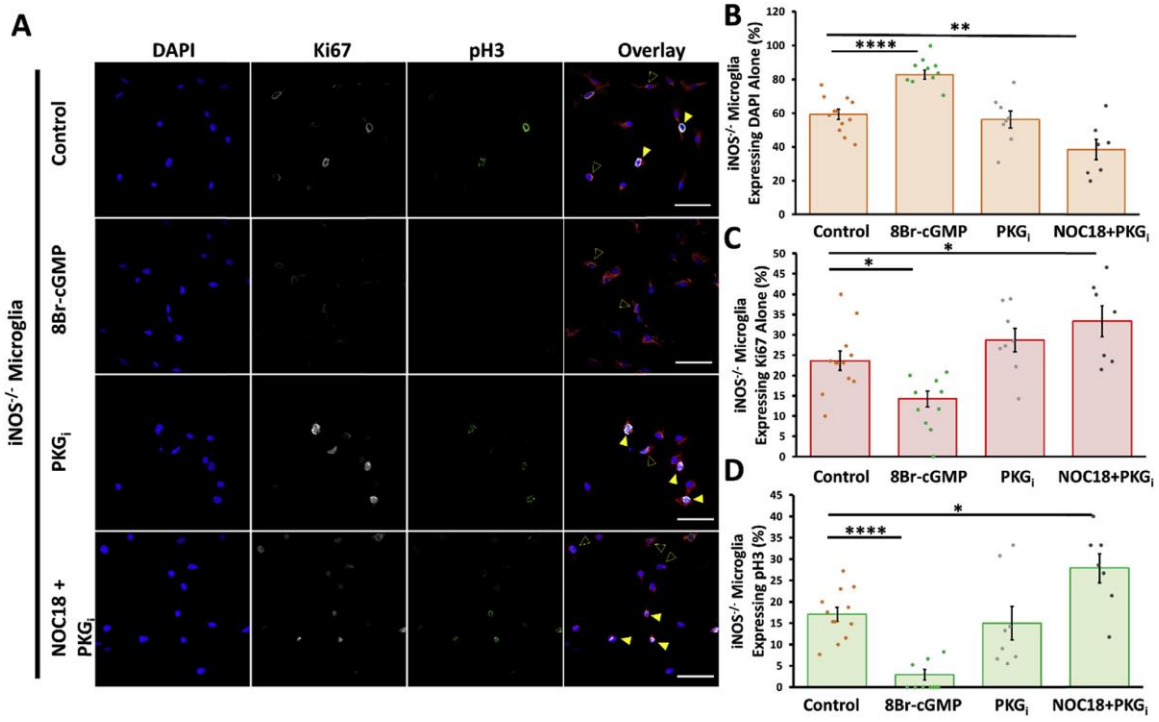

Figure 4.7 Exogenous NO decreases or increases the percentage of Ki67 and pH3 expressing iNOS$^{-/-}$ microglia through a PKG dependent or PKG-independent mechanism, respectively.

A) Representative images of control iNOS$^{-/-}$ microglia and iNOS$^{-/-}$ microglia treated with 8Br-cGMP (10μM), PKG$_i$ (10μM), or NOC18 (100μM) + PKG$_i$, and stained with DAPI (Blue), Ki67 (grey), pH3 (green), and the microglial marker CD11b (red)**.** Closed arrows point to iNOS$^{-/-}$ microglia expressing pH3. Open arrows point to iNOS$^{-/-}$ microglia expressing Ki67. Scale bars represent 50μm. Bar graphs report the percentages of iNOS$^{-/-}$ microglia having nuclei stained with **B)** DAPI alone, **C)** DAPI and Ki67, and **D)** DAPI, Ki67, and pH3. Significance was determined from an N = 3 and $p<0.05$ using a one-way ANOVA and Tukey's post hoc comparison. *$p<0.05$, **$p<0.01$, ****$p<0.0001$.

4.5 Discussion

Previous studies have demonstrated an inhibitory role of NO in regulating proliferation of different cell types (Carreira et al., 2014; Chong et al., 2018; Gu & Brecher, 2000), however, few studies have shown this inhibitory effect within microglia. The present study is the first to demonstrate that iNOS/NO signaling through the classical PKG pathway is critical for regulating microglia proliferation.

Our results showed that at p10, a critical time in murine development (Eyo et al., 2017; Harry & Kraft, 2012; Nikodemova et al., 2015), the absence of iNOS expression increases the proliferation of microglia in the cortex. The $iNOS^{-/-}$ model used within this study is characterized by iNOS deletion in all cell types. The increased numbers of proliferating microglial and non-microglial cells in the cortex indicates that during early postnatal developmental, iNOS-derived NO plays critical roles in the regulation of multiple brain cell types. During normal postnatal development iNOS mRNA is upregulated within ameboid microglia (Crain et al., 2013; Cunningham et al., 2013; Sierra et al., 2014), while iNOS expression within neural progenitor cells is reported in abnormal development such as in Niemann-Pick disease type C (Kim et al., 2008). Interestingly, a study by Carreira et al reported that stimulation of WT microglia – to induce NO production – inhibited neural stem cell proliferation while activation of $iNOS^{-/-}$ microglia using the same stimulant did not, suggesting that the NO production in microglia may regulate neuronal cell proliferation (Carreira et al., 2014). In the present study, we set to explore how iNOS/NO regulates the proliferation of microglia. Therefore, the cellular and molecular mechanisms by which iNOS/NO regulates non-microglial cell proliferation remains to be studied in the future.

Here, our results indicated that iNOS-related signaling attenuates but does not fully obstruct microglia proliferation during early postnatal stages, because many $BrdU^{+}/Iba1^{+}$ microglia were also seen in the cortex of p10 WT mice. It is evident that microglia proliferation is also strongly regulated by NO-independent factors such as transcription and growth factors (Fransen et al., 2013; Koguchi et al., 2003). For example, cyclin-dependent kinase inhibitor-1B ($p27^{Kip1}$) inhibits cell-cycle progression at G_1 (Polyak et al., 1994;

Toyoshima & Hunter, 1994), and its expression increases as microglia morphology shifts from amoeboid to ramified during development (Koguchi et al., 2003). This correlation between microglia morphology and proliferation strongly suggests $p27^{kip1}$ is involved in microglia contact inhibition, therefore restricting microglia proliferation at later timepoints, independent of NO signaling.

It is intriguing that the total number of microglia in the cortex of p10 WT and $iNOS^{-/-}$ mice were not significantly different, suggesting that the increased proliferating microglia within $iNOS^{-/-}$ cortices may be accompanied by increased apoptosis (Nikodemova et al., 2015). Additionally, the increased number of $BrdU^{+}/Iba1^{-}$ cortical cells within the $iNOS^{-/-}$ mice is of interest. It is known that neuroprogenitors exist in the cortex (Ritchie et al., 2014) and that iNOS activity critically regulates neurogenesis (Carreira et al., 2014; Luo et al., 2007; Zhu et al., 2003). Therefore, these $BrdU^{+}/Iba1^{-}$ cells may be neuroprogenitors that arise due to insufficient iNOS/NO signaling (Carreira et al., 2014). In relation to this notion, studies including our own, have shown that iNOS expression is critical for microglia phagocytosis (Kakita et al., 2013; Kraus et al., 2010; Maksoud et al., 2019), hence removing excessive neuroprogenitors during development (Brown & Vilalta, 2015; Cunningham et al., 2013; Wakselman et al., 2008). Therefore, the absence of iNOS/NO signaling may jeopardize microglia phagocytic activity leaving redundant neuroprogenitors and immature microglia within the cortex, which is reflected in the increased number of $BrdU^{+}/Iba1^{-}$ and $BrdU^{+}/Iba1^{+}$ cells observed. Additionally, during early development ameboid microglia transiently express endothelins (ETs) that decline by postnatal day 14 (Wu et al., 2006). ETs influence proliferation of neurons and glia, which could also account for the increase in $BrdU^{+}$ cells *in vivo* (Berti-Mattera et al., 2001; Wu et al., 1999). Whether the lack of iNOS influences the expression and activity of ETs and therefore proliferation rates of cortical cells remains to be explored. Moreover, the $iNOS^{-/-}$ model used in this study is characterized by a deletion of iNOS in all cell types; therefore, further research may benefit from a more in-depth examination of how iNOS/NO signaling influences neural progenitor cells as well as other glial subtypes during development.

To determine whether iNOS/NO signaling directly restricts microglial proliferation, we examined differences in the cell-cycle stages of isolated cortical microglia

between WT and iNOS$^{-/-}$ mice. Examining cell-cycle phases instead of BrdU incorporation allows for a more informative representation of proliferation and hence, a more accurate interpretation of the NO effects on microglia cell-cycle progression. Our analyses demonstrated that in comparison to cultured WT microglia, more iNOS$^{-/-}$ microglia were in the active phases of the cell-cycle as evidenced by their nuclear expression of Ki67 and pH3. Although some microglia cells expressed perinuclear staining of Ki67, which is also reported in carcinomas (Faratian et al., 2009; Grzanka et al., 2000), no significant difference in viability was measured between genetic background or between drug treatments, suggesting the intense perinuclear staining may be associated with Ki67 biosynthesis. Furthermore, inhibiting endogenous iNOS activity in WT microglia significantly increased the percentage of WT microglia within the active phase of the cell-cycle to similar levels seen within the iNOS$^{-/-}$ microglia cultures. Moreover, supplementing exogenous NO to iNOS$^{-/-}$ microglia significantly reduced the percentage of cells within the active phase of the cell-cycle, to similar levels as seen within the WT microglia cultures. These results indicate that endogenous iNOS activity and exogenous NO signaling both restrict microglia proliferation. These results are in line with previous reports demonstrating that iNOS/NO signaling in a variety of cell types leads to cell-cycle arrest at G0 or G_1/S, and G_2/M (Huguenin et al., 2004; Takagi et al., 1994).

We also explored whether microglia proliferation is attenuated through the classical NO-sGC/cGMP/PKG pathway. NO generates actions in cells by either utilizing the classical pathway or by *S*-nitrosylation of proteins (Denninger & Marletta, 1999b). Considering the inhibitory effects of NO (Chen et al., 2006; Gu et al., 2000) and PKG on cell-cycle progression (Gu & Brecher, 2000) in other cell types, we first examined the involvement of PKG in microglia proliferation by treating WT and iNOS$^{-/-}$ microglia with a PKG inhibitor or the PKG activator 8Br-cGMP. Interestingly, stimulating PKG activity did not further decrease the percentage of WT microglia within the active phase of the cell-cycle, while inhibiting PKG significantly increased the percentage of WT microglia in the active phase of the cell-cycle. This suggests the presence of endogenous iNOS/NO-sGC-PKG activity under basal culture conditions in WT microglia. In the presence of L-NAME, activating PKG significantly attenuated the percentage of WT microglia within the active phase of the cell-cycle, further suggesting NO acts through the PKG pathway. In contrast,

due to the inability to produce NO, iNOS$^{-/-}$ microglia should have a significantly lower level of basal PKG activity. Therefore, a PKG inhibitor had no effect, while a PKG activator significantly decreased the percentage of iNOS$^{-/-}$ microglia that were in the active phase of cell-cycle. All these results support the notion that endogenous iNOS/NO signaling inhibits microglial cell-cycle progression through the PKG pathway, and further studies may benefit from investigating signaling factors downstream of PKG that may influence cell-cycle progression.

It is interesting to note that in the presence of a PKG_i, not only did NOC18 fail to inhibit proliferation, but instead enhanced the percentage of iNOS$^{-/-}$ microglia within the active phase of the cell-cycle. This result indicated that in the absence of both PKG activity and endogenous iNOS/NO signaling, exogenous NO may enhance microglia proliferation through a PKG-independent mechanism. In this regard, it has been reported that exogenous NO increases proliferation in neural stem cells and human breast cancer cells through *S*-nitrosylation of Cys^{118} on p21RAS (Heo et al., 2005; Pervin et al., 2007). Further research should examine whether exogenous NO enhances microglia proliferation through *S*-nitrosylation of p21RAS within microglia.

During early postnatal CNS development, ameboid microglia express basal levels of iNOS (Brenneman et al., 1992; Crain et al., 2013; Giulian et al., 1988; Sierra et al., 2014). The presented data indicates that basal iNOS/NO signaling through the classical PKG pathway decreases microglia cell-cycle progression and proliferation. As outlined in **Figure 4.8**, microglia proliferation during development is strongly associated with a basal iNOS/NO signaling. On the other hand, decreased iNOS activity and NO production has been shown to synergistically increase arginase activity, which is associated with cell proliferation (Lisi et al., 2016; Morris, 2007; Orihuela et al., 2016; Wei et al., 2001). Given that increased NOS activity and NO production occurs in the brain under various neurological disease conditions such as ischemic stroke (Chen et al., 2017; Niwa et al., 2001; Patel et al., 2013; Terpolilli et al., 2012), further studies on NO regulation of microglia proliferation may deepen the understanding of the pathogenesis associated with these neurological disorders.

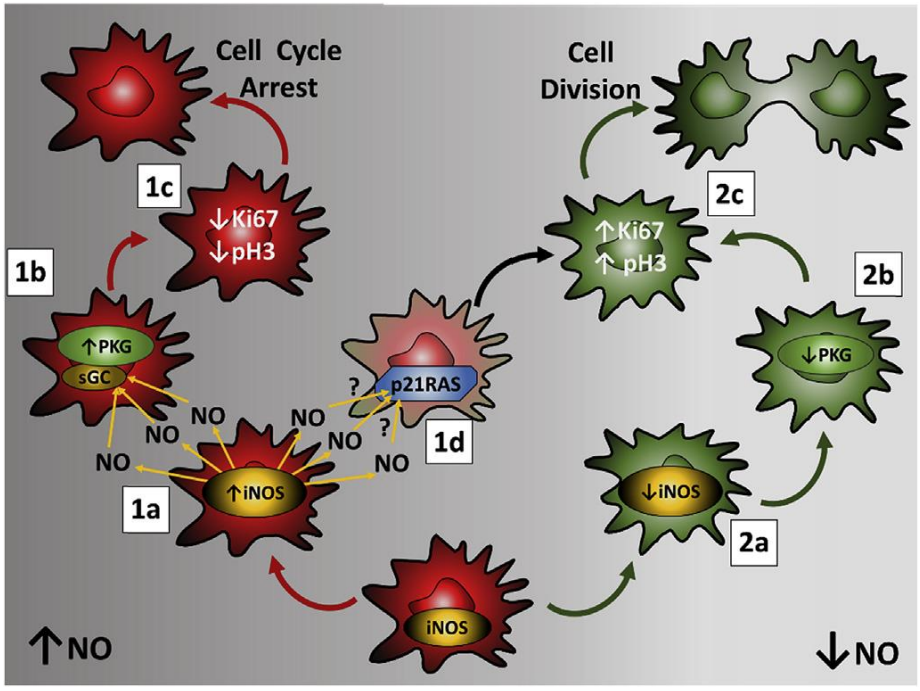

Figure 4.8 Illustration of the signaling pathway by which NO inhibits microglial cell proliferation.

During CNS development, a basal level of iNOS/NO signaling exists in postnatal ameboid microglia. **Left side: 1a)** Postnatal amoeboid microglia may upregulate iNOS expression in response to specific microenvironmental stimulants. **1b)** Increased iNOS catalyzes production of copious amounts of NO, which activates sGC/cGMP/PKG signaling. **1c)** Increased PKG activity attenuates microglial cell cycle progression, leading to cell-cycle arrest depicted by decreased nuclear expression of Ki67 and pH3. **1d)** NO may S-nitrosylate p21RAS (Heo et al., 2005; Pervin et al., 2007) and increase proliferation independent of PKG signaling within microglia. Conversely **Right side: 2a)** when the microenvironment favours proliferation, postnatal amoeboid microglia decrease iNOS expression. **2b)** The lack of NO signaling results in decreased sGC/cGMP/PKG signaling. **2c)** Decreased PKG signaling increases microglial cell-cycle progression, leading to microglial cell division depicted by increased nuclei expression of Ki67 and pH3.

4.6 Acknowledgements

This study was supported from a CIHR grant (MOP-133504) to W-Y L. MJEM and VT have been awarded Ontario Graduate Scholarships.

4.7 References

Adachi, M., Abe, M., Sasaki, T., Kato, H., Kasahara, J., & Araki, T. (2010). Role of inducible or neuronal nitric oxide synthase in neurogenesis of the dentate gyrus in aged mice. Metabolic Brain Disease, 25(4), 419–424. https://doi.org/10.1007/s11011-010-9224-8

Alliot, F., Godin, I., & Pessac, B. (1999). Microglia derive from progenitors , originating from the yolk sac , and which proliferate in the brain. Developmental Brain Research, (117), 145–152.

Berti-Mattera, L. N., Harwalkar, S., Hughes, B., Wilkins, P. L., & Almhanna, K. (2001). Proliferative and morphological effects of endothelins in Schwann cells: Roles of p38 mitogen-activated protein kinase and Ca2+-independent phospholipase A2. Journal of Neurochemistry, 79(6), 1136–1148. https://doi.org/10.1046/j.1471-4159.2001.00642.x

Bogdan, C. (2001). Nitric oxide and the immune response. Nature Immunology, 2(10), 907–916. https://doi.org/10.1038/ni1001-907

Bogdan, Christian. (2015). Nitric oxide synthase in innate and adaptive immunity: an update. Trends in Immunology, 36(3), 161–178. https://doi.org/10.1016/j.it.2015.01.003

Brenneman, D. E., Schultzberg, M., Bartfai, T., & Gozes, I. (1992). Cytokine Regulation of Neuronal Survival. Journal of Neurochemistry, 58(2), 454–460. https://doi.org/10.1111/j.1471-4159.1992.tb09743.x

Brown, G. C., & Vilalta, A. (2015). How microglia kill neurons. Brain Research, 1628, 288–297. https://doi.org/10.1016/j.brainres.2015.08.031

Carreira, B. P., Morte, M. I., Santos, A. I., LourenÃ§o, A. S., AmbrÃ3sio, A. F., Carvalho, C. M., & AraÃojo, I. M. (2014). Nitric oxide from inflammatory origin impairs neural stem cell proliferation by inhibiting epidermal growth factor receptor

signaling. Frontiers in Cellular Neuroscience, 8(October), 1–14. https://doi.org/10.3389/fncel.2014.00343

Casarotto, P. C., Biojone, C., Montezuma, K., Cunha, F. Q., Joca, S. R. L., Castren, E., & Guimaraes, F. S. (2018). Inducible nitric oxide synthase (NOS2) knockout mice as a model of trichotillomania. PeerJ, 6, e4635. https://doi.org/10.7717/peerj.4635

Chen, L., Daum, G., Chitaley, K., Coats, S. A., Bowen-pope, D. F., Thumati, N. R., … Clowes, A. W. (2006). Vasodilator-Stimulated Phosphoprotein Regulates Proliferation and Growth Inhibition by Nitric Oxide in Vascular Smooth Muscle cells, 24(8), 1403–1408.

Chen, Z., Mou, R., Feng, D., Wang, Z., & Chen, G. (2017). The role of nitric oxide in stroke. Medical Gas Research, 7(3), 194. https://doi.org/10.4103/2045-9912.215750

Chong, C., Ai, N., Ke, M., Tan, Y., Huang, Z., Li, Y., … Su, H. (2018). Roles of Nitric Oxide Synthase Isoforms in Neurogenesis. Molecular Neurobiology, 55(3), 2645–2652. https://doi.org/10.1007/s12035-017-0513-7

Crain, J. M., Nikodemova, M., & Watters, J. J. (2013). Microglia express distinct M1 and M2 phenotypic markers in the postnatal and adult central nervous system in male and female mice. Journal of Neuroscience Research, 91(9), 1143–1151. https://doi.org/10.1002/jnr.23242

Cunningham, C. L., Martinez-Cerdeno, V., & Noctor, S. C. (2013). Microglia Regulate the Number of Neural Precursor Cells in the Developing Cerebral Cortex. Journal of Neuroscience, 33(10), 4216–4233. https://doi.org/10.1523/JNEUROSCI.3441-12.2013

Denninger, J. W., & Marletta, M. A. (1999). Guanylate cyclase and the NO/cGMP signaling PAthway. Biochemica et Biophysica Acta Research Communications, 1411(3), 334–350.

Eyo, U. B., Miner, S. A., Weiner, J. A., Dailey, M. E., & City, I. (2017). Developmental Changes in Microglial Mobilization are Independent of Apoptosis in the Neonatal Mouse Hippocampus. Brain Behavior and Immunity, 55(319), 49–59. https://doi.org/10.1016/j.bbi.2015.11.009.Developmental

Faratian, D., Munro, A., Twelves, C., & Bartlett, J. M. (2009). Membranous and cytoplasmic staining of Ki67 is associated with HER2 and ER status in invasive

breast carcinoma. Histopathology, 54(2), 254–257. https://doi.org/10.1111/j.1365-2559.2008.03191.x

Forstermann, U., & Sessa, W. C. (2012). Nitric oxide synthases: regulation and function. European Heart Journal, 33(7), 829–837. https://doi.org/10.1093/eurheartj/ehr304

Fransen, N. L., Suzzi, S., & Perry, V. H. (2013). Regulation of Microglial Proliferation during Chronic Neurodegeneration. J. Neuroscience, 33(6), 2481–2493. https://doi.org/10.1523/JNEUROSCI.4440-12.2013

Fukushima, S., Furube, E., Itoh, M., Nakashima, T., & Miyata, S. (2015). Robust increase of microglia proliferation in the fornix of hippocampal axonal pathway after a single LPS stimulation. Journal of Neuroimmunology, 285, 31–40. https://doi.org/10.1016/j.jneuroim.2015.05.014

Giulian, D., Young, D., Woodward, J., Brown, D., & Lachman, L. (1988). Interleukin-1 is an astroglial growth factor in the developing brain. The Journal of Neuroscience, 8(2), 709–714. https://doi.org/10.1523/jneurosci.08-02-00709.1988

Grzanka, A., Sujkowska, R., Janiak, A., & Adamska, M. (2000). Immunogold labelling of PCNA and Ki-67 antigen at the ultrastructural level in laryngeal squamous cell carcinoma and its correlation with lymph node metastasis and histological grade, 149, 85–94.

Gu, M., & Brecher, P. (2000). Nitric Oxide-Induced Increase in p21 Expression During the Cell Cycle in Aortic Adventitial Fibroblasts. Arterioscler Thromb Vasc Biol., (20), 27–34.

Gu, M., Lynch, J., & Brecher, P. (2000). Nitric Oxide Increases p21 Waf1 / Cip1 Expression by a cGMP-dependent Pathway That Includes Activation of Extracellular Signal-regulated Kinase and p70 S6k *, 275(15), 11389–11396.

Harry, G. J., & Kraft, A. D. (2012). Microglia in the developing brain : A potential target with lifetime effects. Neurotoxicology, 33(2), 191–206. https://doi.org/10.1016/j.neuro.2012.01.012

Heo, J., Prutzman, K. C., Mocanu, V., Campbell, S. L., Carolina, N., & Carolina, N. (2005). Mechanism of Free Radical Nitric Oxide-mediated Ras Guanine Nucleotide Dissociation. Journal Molecular Biology, 346(2), 1423–1440. https://doi.org/10.1016/j.jmb.2004.12.050

Huguenin, S., Fleury-feith, J., Kheuang, L., Jaurand, M., Bolla, M., Riffaud, J., … Vacherot, F. (2004). Nitrosulindac (NCX1102): ANew Nitric Drug (NO-NSAID), Inhibits Proliferation and Induces Apoptosis in Human Prostatic Epithelial Cell Lines. The Prostate, 61, 132–141. https://doi.org/10.1002/pros.20081

Joseph, B., & Venero, J. L. (2013). Microglia Methods. Methods in Molecular Biology. https://doi.org/10.1007/978-1-62703-520-0_1

Kakita, H., Aoyama, M., Nagaya, Y., Asai, H., Hussein, M. H., Suzuki, M., … Asai, K. (2013). Diclofenac enhances proinflammatory cytokine-induced phagocytosis of cultured microglia via nitric oxide production. Toxicology and Applied Pharmacology, 268(2), 99–105. https://doi.org/10.1016/j.taap.2013.01.024

Kim, S.-J., Lim, M.-S., Kang, S.-K., Lee, Y.-S., & Kang, K.-S. (2008). Impaired functions of neural stem cells by abnormal nitric oxide-mediated signaling in an in vitro model of Niemann-Pick type C disease. Cell Research, 18(6), 686–694. https://doi.org/10.1038/cr.2008.48

Koguchi, K., Nakatsuji, Y., Okuno, T., Sawada, M., & Sakoda, S. (2003). Microglial Cell Cycle-Associated Proteins Control Microglial Proliferation In Vivo and In Vitro and Are Regulated by GM-CSF and Density-Dependent Inhibition. Journal of Neuroscience Research, 905(June), 898–905.

Kraus, B., Wolff, H., Elstner, E. F., & Heilmann, J. (2010). Hyperforin is a modulator of inducible nitric oxide synthase and phagocytosis in microglia and macrophages. Naunyn-Schmiedeberg's Archives of Pharmacology, 381(6), 541–553. https://doi.org/10.1007/s00210-010-0512-y

Lisi, L., Laudati, E., Miscioscia, T. F., Dello Russo, C., Topai, A., & Navarra, P. (2016). Antiretrovirals inhibit arginase in human microglia. Journal of Neurochemistry, 136(2), 363–372. https://doi.org/10.1111/jnc.13393

Luo, C. X., Zhu, X. J., Zhou, Q. G., Wang, B., Wang, W., Cai, H. H., … Zhu, D. Y. (2007). Reduced neuronal nitric oxide synthase is involved in ischemia-induced hippocampal neurogenesis by up-regulating inducible nitric oxide synthase expression. Journal of Neurochemistry, 103(5), 1872–1882. https://doi.org/10.1111/j.1471-4159.2007.04915.x

Maksoud, M. J. E., Tellios, V., An, D., Xiang, Y., & Lu, W. (2019). Nitric oxide upregulates microglia phagocytosis and increases transient receptor potential vanilloid type 2 channel expression on the plasma membrane. Glia, 67(12), 2294–2311. https://doi.org/10.1002/glia.23685

Marín-Teva, J. L., Dusart, I., Colin, C., Gervais, A., van Rooijen, N., & Mallat, M. (2004). Microglia Promote the Death of Developing Purkinje Cells. Neuron, 41(4), 535–547. https://doi.org/10.1016/S0896-6273(04)00069-8

Matcovitch-Natan, O., Winter, D. R., Giladi, A., Aguilar, S. V., Spinrad, A., Sarrazin, S., … Amit, I. (2016). Microglia development follows a stepwise program to regulate brain homeostasis. Science, in Press, 353(6301). https://doi.org/10.1126/science.aad8670

Montezuma, K., Biojone, C., Lisboa, S. F., Cunha, F. Q., Guimarães, F. S., & Joca, S. R. L. (2012). Neuropharmacology Inhibition of iNOS induces antidepressant-like effects in mice : Pharmacological and genetic evidence. Neuropharmacology, 62(1), 485–491. https://doi.org/10.1016/j.neuropharm.2011.09.004

Morris, S. M. (2007). Arginine metabolism: boundaries of our knowledge. The Journal of Nutrition, 137(6 Suppl 2), 1602S-1609S. https://doi.org/10.1093/jn/137.6.1602S

Nikodemova, M., Kimyon, R. S., De, I., Small, A. L., Collier, L. S., & Watters, J. J. (2015). Microglial numbers attain adult levels after undergoing a rapid decrease in cell number in the third postnatal week ☆. Journal of Neuroimmunology, 278, 280–288. https://doi.org/10.1016/j.jneuroim.2014.11.018

Niwa, M., Inao, S., Takayasu, M., Kawai, T., Kajita, Y., Nihashi, T., … Yoshida, J. (2001). Time course of expression of three nitric oxide synthase isoforms after transient middle cerebral artery occlusion in rats. Neurologia Medico-Chirurgica, 41, 63–72; discussion 72-73. https://doi.org/10.2176/nmc.41.63

Orihuela, R., McPherson, C. A., & Harry, G. J. (2016). Microglial M1/M2 polarization and metabolic states. British Journal of Pharmacology, 173(4), 649–665. https://doi.org/10.1111/bph.13139

Otsu, N. (1979). A Threshold Selection Method from Grey-Level Histograms. IEEE Transactions on Systems, Man, and Cybernetics, 9(1), 62–66. https://doi.org/10.1109/TSMC.1979.4310076

Parkhurst, C. N., Yang, G., Ninan, I., Savas, J. N., Iii, J. R. Y., Lafaille, J. J., … Gan, W. (2013). Microglia Promote Learning-Dependent Synapse Formation through Brain-Derived Neurotrophic Factor. Cell, 155(7), 1596–1609. https://doi.org/10.1016/j.cell.2013.11.030

Patel, A. R., Ritzel, R., McCullough, L. D., & Liu, F. (2013). Microglia and ischemic stroke: A double-edged sword. International Journal of Physiology, Pathophysiology and Pharmacology, 5(2), 73–90.

Pervin, S., Singh, R., Hernandez, E., Wu, G., & Chaudhuri, G. (2007). Nitric Oxide in Physiologic Concentrations Targets the Translational Machinery to Increase the Proliferation of Human Breast Cancer Cells : Involvement of Mammalian Target of Rapamycin / eIF4E Pathway. Cancer Res, (1), 289–300. https://doi.org/10.1158/0008-5472.CAN-05-4623

Pinnock, S. B., Balendra, R., Chan, M., Hunt, L. T., Turner-Stokes, T., & Herbert, J. (2007). Interactions between Nitric Oxide and Corticosterone in the Regulation of Progenitor Cell Proliferation in the Dentate Gyrus of the Adult Rat. Neuropsychopharmacology, 32(2), 493–504. https://doi.org/10.1038/sj.npp.1301245

Polyak, K., Lee, M. H., Erdjument-Bromage, H., Koff, A., Roberts, J. M., Tempst, P., & Massagué, J. (1994). Cloning of p27Kip1, a cyclin-dependent kinase inhibitor and a potential mediator of extracellular antimitogenic signals. Cell, 78(1), 59–66. https://doi.org/10.1016/0092-8674(94)90572-X

Quintas, C., Pinho, D., Pereira, C., Saraiva, L., Gonçalves, J., & Queiroz, G. (2014). Microglia P2Y6 receptors mediate nitric oxide release and astrocyte apoptosis. Journal of Neuroinflammation, 11(1), 141. https://doi.org/10.1186/s12974-014-0141-3

Ritchie, K., Watson, L. A., Davidson, B., Jiang, Y., & Berube, N. G. (2014). ATRX is required for maintenance of the neuroprogenitor cell pool in the embryonic mouse brain. Biology Open, 3(12), 1158–1163. https://doi.org/10.1242/bio.20148730

Rosin, J. M., Vora, S. R., & Kurrasch, D. M. (2018). Brain , Behavior , and Immunity Depletion of embryonic microglia using the CSF1R inhibitor PLX5622 has adverse sex-speci fi c e ff ects on mice , including accelerated weight gain , hyperactivity and

anxiolytic-like behaviour. Brain Behavior and Immunity, 73(April), 682–697. https://doi.org/10.1016/j.bbi.2018.07.023

Sarkar, R., Gordon, D., Stanley, J. C., & Webb, R. C. (1997). Dual cell cycle-specific mechanisms mediate the antimitogenic effects of nitric oxide in vascular smooth muscle cells. Journal of Hypertension, 15, 275–283.

Sierra, A., Navascués, J., Cuadros, M. A., Calvente, R., Martín-Oliva, D., Ferrer-Martín, R. M., … Marín-Teva, J. L. (2014). Expression of inducible nitric oxide synthase (iNOS) in microglia of the developing quail retina. PloS One, 9(8), e106048. https://doi.org/10.1371/journal.pone.0106048

Stevens, B., Allen, N. J., Vazquez, L. E., Howell, G. R., Christopherson, K. S., Nouri, N., … Barres, B. A. (2007). The Classical Complement Cascade Mediates CNS Synapse Elimination. Cell, 131(6), 1164–1178. https://doi.org/10.1016/j.cell.2007.10.036

Takagi, K., Isobe, Y., Yasukawa, K., Okouchi, E., & Suketac, Y. (1994). Nitric oxide blocks the cell cycle of mouse macrophage-like the early G 2+M phase. FEBS Letters, 340, 159–162.

Tegenge, M. A., & Bicker, G. (2009). Nitric oxide and cGMP signal transduction positively regulates the motility of human neuronal precursor (NT2) cells. Journal of Neurochemistry, 110(6), 1828–1841. https://doi.org/10.1111/j.1471-4159.2009.06279.x

Terpolilli, N. A., Moskowitz, M. A., & Plesnila, N. (2012). Nitric oxide: Considerations for the treatment of ischemic stroke. Journal of Cerebral Blood Flow and Metabolism, 32(7), 1332–1346. https://doi.org/10.1038/jcbfm.2012.12

Tian, C., Ye, F., Wang, L., Deng, Y., Dong, Y., Wang, X., … Wang, X. (2010). Nitric oxide inhibits ghrelin-induced cell proliferation and ERK1/2 activation in GH3 cells. Endocrine, 38(3), 412–416. https://doi.org/10.1007/s12020-010-9402-9

Torres, L., Danver, J., Ji, K., Miyauchi, J. T., Chen, D., Anderson, M. E., … Tsirka, S. E. (2016). Brain , Behavior , and Immunity Dynamic microglial modulation of spatial learning and social behavior. Brain Behavior and Immunity, 55, 6–16. https://doi.org/10.1016/j.bbi.2015.09.001

Toyoshima, H., & Hunter, T. (1994). p27, a novel inhibitor of G1 cyclin-Cdk protein kinase activity, is related to p21. Cell, 78(1), 67–74. https://doi.org/10.1016/0092-8674(94)90573-8

Vanryzin, J. W., Yu, S. J., Perez-pouchoulen, M., & Mccarthy, M. M. (2016). Temporary Depletion of Microglia during the Early Postnatal Period Induces Lasting Sex-Dependent and Sex-Independent Effects on Behavior in Rats, 3(December), 1–19.

Wakselman, S., Bechade, C., Roumier, A., Bernard, D., Triller, A., & Bessis, A. (2008). Developmental Neuronal Death in Hippocampus Requires the Microglial CD11b Integrin and DAP12 Immunoreceptor. Journal of Neuroscience, 28(32), 8138–8143. https://doi.org/10.1523/JNEUROSCI.1006-08.2008

Wei, L. H., Wu, G., Morris, S. M., & Ignarro, L. J. (2001). Elevated arginase I expression in rat aortic smooth muscle cells increases cell proliferation. Proceedings of the National Academy of Sciences, 98(16), 9260–9264. https://doi.org/10.1073/pnas.161294898

Wexler, E. M., Stanton, P. K., & Nawy, S. (1998). Nitric Oxide Depresses GABAA Receptor Function via Coactivation of cGMP-Dependent Kinase and Phosphodiesterase. Journal of Neuroscience, 18(7), 2342–2349.

Wu, C.-Y., Kaur, C., Lu, J., Cao, Q., Guo, C.-H., Zhou, Y., … Ling, E.-A. (2006). Transient expression of endothelins in the amoeboid microglial cells in the developing rat brain. Glia, 54(6), 513–525. https://doi.org/10.1002/glia.20402

Wu, J. J., Chen, J. X., Rothman, T. P., & Gershon, M. D. (1999). Inhibition of in vitro enteric neuronal development by endothelin-3: Mediation by endothelin B receptors. Development, 126(6), 1161–1173.

Zhu, D. Y., Liu, S. H., Sun, H. S., & Lu, Y. M. (2003). Expression of inducible nitric oxide synthase after focal cerebral ischemia stimulates neurogenesis in the adult rodent dentate gyrus. The Journal of Neuroscience : The Official Journal of the Society for Neuroscience, 23(1), 223–229. Retrieved from http://www.ncbi.nlm.nih.gov/pubmed/12514219

Chapter 5

5 Nitric oxide attenuates murine microglia proliferation by sequential activation of TRPV2-mediated calcium influx, NFATC2 nuclear translocation, and p21 expression.

5.1 Abstract

Microglia proliferation is critical for proper development and function of the central nervous system (CNS), while dysregulation of proliferation contributes to pathology. We recently determined that inducible nitric oxide synthase knockout (iNOS$^{-/-}$) mice displayed significantly more proliferating microglia in the postnatal cortex than age-matched wildtype (WT) mice. Moreover, nitric oxide (NO) signaling in mouse microglia critically upregulates calcium entry through transient receptor potential vanilloid type 2 (TRPV2) channels. Considering that TRPV2 activity restricts astrocytic proliferation within glioma tissues, we investigated the combined roles of iNOS/NO signaling and TRPV2 expression in the regulation of microglial proliferation using calcium imaging, immunocytochemistry, western blot, and polymerase chain reaction. Results showed that non-dividing microglia exhibited significantly higher expression of TRPV2 on the plasma membrane and significantly more TRPV2 mediated calcium influx in comparison to dividing microglia. Furthermore, non-dividing WT microglia exhibited significantly more NO production when compared to dividing WT microglia. Additionally, the NO-donor NOC18 increased the nuclear translocation of nuclear factor of activated T-cells cytoplasmic 2 (NFATC2), increased the mRNA expression of the cyclin-dependent kinase inhibitor p21, and decreased the percentage of dividing WT and iNOS$^{-/-}$ microglia in culture. Importantly, the presence of the TRPV2 inhibitor tranilast abolished these effects of NOC18. Together, results from this study indicated that iNOS/NO signaling inhibits microglial proliferation through TRPV2-mediated calcium influx, nuclear translocation of the transcription factor NFATC2, and increased p21 expression.

5.2 Introduction

Microglia are essential immune cells of the central nervous system (CNS) that produce copious amounts of nitric oxide (NO) via inducible nitric oxide synthase (iNOS) to regulate cellular responses such as proliferation (Biber et al., 2014; Maksoud et al., 2019; Saha & Pahan, 2006; Traister et al., 2002). Aberrant microglia proliferation and iNOS expression contribute to neurological disease progression. It has been shown that microglia are the most prominent immune cells that infiltrate and proliferate within gliomas (Simmons et al., 2011), while also exhibiting reduced iNOS expression (He et al., 2006; Kim et al., 2006) and secreting anti-inflammatory cytokines such as IL-10 and TGFβ1 (Komohara et al., 2008; Qiu et al., 2011; Zhang et al., 2007). A positive correlation between glioma malignancy and the number of alternatively activated microglia present within the glioma suggests that microglia contribute to glioma pathology (Badie & Schartner, 2000; Morimura et al., 1990; Roggendorf et al., 1996).

Previous studies also implicated iNOS expression in Alzheimer's like pathology progression (Kamphuis et al., 2012; Togo et al., 2004; Wilcock et al., 2008). For example, using a double transgenic mouse model for Alzheimer's disease that expressed Swedish mutation of the amyloid precursor protein together with presenilin-1 deletion in exon 9 demonstrated cognitive deficits, decreased iNOS mRNA expression, as well as increased microglia proliferation at 6 months of age when compared to age-matched WT mice (Kamphuis et al., 2012). Evidently, iNOS-NO signaling critically regulates microglia proliferation; however, the underlying molecular mechanism that regulates microglia proliferation remains unclear (Engler et al., 2012). We recently demonstrated that mice lacking iNOS expression ($iNOS^{-/-}$) displayed significantly more proliferating microglia in the cortex during early postnatal development than that of age-matched WT mice (Maksoud et al., 2020). Moreover, we further demonstrated that iNOS-NO signaling impedes cell-cycle progression of microglia through cyclic guanosine-monophosphate (cGMP) activation of protein kinase G (PKG) signaling (Maksoud et al., 2020). These novel findings indicate that the iNOS-NO-cGMP-PKG signaling cascade critically restricts microglia proliferation.

The transient receptor potential vanilloid type 2 (TRPV2) ion channel is highly calcium permeable and largely implicated in cellular proliferation, differentiation, and cancer progression (Liberati et al., 2014), while also highly expressed in microglia and other glia cells (Morelli et al., 2012; Nabissi et al., 2010; Zhang et al., 2016). Previous studies demonstrated that TRPV2 expression attenuates astrocytic glioblastoma cell proliferation (Morelli et al., 2012; Nabissi et al., 2010) and clearly established a crucial role of TRPV2 channel activity in restricting cell proliferation. Importantly, we have recently shown that activation of iNOS-NO-cGMP-PKG cascade traffics TRPV2 channel proteins from the cytosol to the plasma membrane to intensify calcium influx in murine microglia (Maksoud et al., 2019).

Therefore, this present study set out to examine if NO-mediated TRPV2-trafficking and subsequent calcium entry attenuates microglia proliferation. Using multiple imaging techniques on primary WT and $iNOS^{-/-}$ murine microglia cultures we examined the TRPV2 surface expression and calcium influx in different cell-cycle stages while exploring subsequent gene expression. Our results showed that NO-TRPV2 signaling critically regulates microglia proliferation whereby actively dividing microglia exhibited less TRPV2 plasma membrane expression and calcium influx, less nuclear expression of nuclear factor of activated T-cells cytoplasmic-2 (NFATC2), and decreased p21 mRNA expression, compared to nondividing microglia. Future studies examining NO-TRPV2-NFATC2-p21 signaling in microglia may uncover the impact that microglia proliferation contributes to the progression of pathology within the CNS.

5.3 Materials and Methods

5.3.1 Materials, compounds, and treatments

Materials and compounds were purchased from the following sources – phosphate buffered saline (PBS), paraformaldehyde (PFA), 4',6-diamidino-2-phenylindole (DAPI), triton, glycine, poly-D-lysine (PDL), sucrose, glycerol, ethylene glycol, 4-(2-hydroxyethyl)-1-piperazineethanesulfonic acid (HEPES) (Millipore-Sigma, Oakville, ON); Dulbecco's modified eagle medium (DMEM), fetal bovine serum (FBS), trypsin, sodium-pyruvate, penicillin/streptomyocin (P/S), Leibowitz L-15 media, bovine serum albumen (BSA) (ThermoFischer Scientific, Waltham, MA); normal donkey serum (NDS), Jackson Immunoresearch Laboratories, inc., West Grove, PA); Fluormount-G (Electron Microscopy Solutions, Hatfield, PA), calcium fluorescent dye: Rhod-4AM, NO-sensitive fluorescent dye: DAX-J2 (AAT Bioquest, Sunnyvale, CA);

Treatment concentrations were adapted from previous literature and purchased from the following sources – slow release NO-donor: diethylenetriamine NONOate (NOC18, 100μM), NOS inhibitor: G-nitro-L-arginin-methyl ester (L-NAME, 100μM), arginyl-lysyl-arginyl-alanyl-arginyl-lysyl-glutamic acid (PKG inhibitory peptide; PKG_i, 10μM), 8-bromo-cyclic guanosine monophosphate (8Br-cGMP, 10μM) (Cayman Chemical, Ann Arbor, MI); TRPV2 agonist: 2-aminoethoxydiphenyl borate (2APB, 250μM) (Santa Cruz Biotechnology, Dallas, TX); TRPV2 agonist: probenecid (100μM), TRPV2 inhibitor: tranilast (75μM) (Tocris Bioscience, Oakville, ON); iNOS substrate: L-arginine (100μM) (Millipore-Sigma, Oakville, ON).

5.3.2 Primary microglia cultures

WT (C57BL/6, Stock No: 000664) and $iNOS^{-/-}$ (B6.129P2-$Nos2^{tm1Lau}$, Stock No: 002609) mice purchased from The Jackson Laboratory. All experiments were conducted in accordance with the Animal Care and Veterinary Services at The University of Western Ontario, Canada. Microglia cultures were performed as we previously described (Maksoud et al., 2019). Briefly, cortices isolated from postnatal day 0-4 WT or $iNOS^{-/-}$ mice and placed in ice cold Leibowitz L-15 media. Next, cortices were homogenized, filtered

through a 70μm nylon filter, and centrifuged for 4 minutes at 900g. The cell pellet was resuspended in DMEM containing 1× P/S and 10% FBS. The collected cortical cells were cultured in T-75 flasks for 2 weeks, with media changes occurring every 3 days. After 2 weeks, T-75 flasks were shaken for 2hrs at 36ºC and 200rpm. The media containing detached microglia was centrifuged at 900g for 4 min, and the supernatant was removed. The microglia cell pellet was resuspended in fresh culture media and plated at 5×10^4 cells/ml for experiments. Microglia were allowed to rest overnight in DMEM supplemented with 2.5% FBS, 5% sodium-pyruvate, and 1% P/S, under culture conditions of 37ºC and 5% CO_2 before conducting experiments.

5.3.3 BV2 cell-line cultures

BV2 microglia were generously gifted to us from Dr. Michael J. Strong at The University of Western Ontario. BV2 cells were cultured in DMEM containing 1× P/S and 10% FBS at normal conditions of 5% CO_2 at 37ºC. Once BV2 cell confluency reached 70%, cells were washed with PBS and incubated for 2 min in 0.25% trypsin in PBS to facilitate detachment. Trypsin was neutralized using equal parts of culture media containing FBS, and BV2 cells were passaged 1:40 into a new culture vessel with DMEM containing 1× P/S and 10% FBS 3× a week. For experiments, BV2 cells were plated at 5×10^4 cells/ml in DMEM supplemented with 2.5% FBS, 5% sodium-pyruvate, and 1% P/S, and allowed to rest overnight before conducting experiments.

5.3.4 Immunocytochemistry

Primary microglia cultured on glass coverslips underwent experimental treatments at previously mentioned concentrations, for 48 hrs under normal culture conditions of 37ºC and 5% CO_2. After 48 hrs, culture media was removed and cells were fixed using 4% PFA for 5 min. Fixed microglia were washed with 0.1M glycine in PBS, followed by two PBS washes of 5 min each. Cell membrane permeabilization occurred using 0.1% triton in PBS for 5min, followed by a 1h incubation with blocking solution containing 5% NDS in PBS to decrease nonspecific antibody binding.

To determine the cell-cycle stages of microglia, primary CD11b (rat, BioRAD, 1:150) and Ki67 (rabbit, AbCam, 1:300) antibodies in 1% NDS in PBS were incubated on coverslips for 2 hrs. The secondary antibodies - Cy3 and Alexa Fluor-647 (Jackson Immunoresearch, West Grove, PA) - were incubated in 1% NDS in PBS for 1h. Following three washes in PBS, microglia were incubated with the primary antibody phosphorylated histone 3 (S10+T11) conjugated to Alexa Fluor 488 (rabbit, AbCam, 1:5000) in 1% NDS in PBS for 2hrs.

To examine subcellular localization of NFATC2, microglia were incubated with primary antibodies for CD11b (rat, BioRAD, 1:150) and NFATC2 (mouse, Thermo Fisher Scientific, 1:200) in 1% NDS in PBS for 2hrs. Next, microglia were incubated with the secondary antibodies Cy3 and Alexa-Fluor-488 in 1% NDS in PBS for 1h. Secondary antibodies were removed and microglia were washed 3× with PBS for 10min each before DAPI staining (1μg/ml) for 10min. Microglia were mounted onto slides using Fluormount-G. Images were taken using the Olympus FV-1000 confocal laser scanning microscope through a 60× oil immersion objective.

5.3.5 Calcium imaging and cell-cycle classification

For calcium-imaging, microglial cultures were grown in 24-well plates and DMEM culture media was washed out with bath solution containing (in mM): 130 NaCl, 5 KCl, 3 $MgCl_2$, 2 $CaCl_2$, 5 glucose, and 10 HEPES. Rhod-4AM was equilibrated to room temperature for 1hr before incubating microglia cultures with 3μM rhod-4AM under normal conditions for 1 hr. Rhod-4AM was washed out of cells using bath solution. The intracellular fluorescent intensity of rhod-4 within microglia were imaged in 10 second intervals using the EVOS FL Auto system under 20× magnification. Baseline levels of rhod-4 fluorescence were recorded before 2APB (250μM) application. Intracellular rhod-4 fluorescent changes in each cell were normalized to the average baseline level within the imaging field using FIJI open source software (Schindelin et al., 2012).

As previously described (Maksoud et al., 2020), microglial cell-cycle stages were classified based on the immuno-detection of cell-cycle markers. Briefly, after calcium imaging, microglia were subjected to immunocytochemistry of cell cycle markers.

Microglial cells were identified by the expression of CD11b, and only CD11b positive cells were included in the image analyses. Using FIJI open source software (Schindelin et al., 2012), microglia were classified into three different cell-cycle phases: G0 microglia display nuclear DAPI fluorescence; interphase microglia exhibited nuclear fluorescence of DAPI and Ki67; or microglia in mitosis displayed nuclear fluorescence of DAPI and pH3. As outlined in **Figure 5.S1**, the calcium response in each microglia was grouped and then averaged based on the cell-cycle phase it presented in. The normalized rhod-4 fluorescence intensity for microglia in each cell-cycle stage were plotted versus time of imaging using Excel.

5.3.6 NO-imaging and cell-cycle classification

Intracellular DAX-J2 fluorescence was used to measure free NO production in primary microglial cultures. Primary microglia were cultured in 24-well plates and culture media was washed out with the same bath solution used in calcium imaging. DAX-J2 was equilibrated to room temperature for 1hr before incubating microglia cultures in 4μM DAX-J2 for 45 min under normal conditions. After washing out extracellular DAX-J2, NO-imaging was performed using the EVOS-FL Auto system under 20× magnification for 20 min. Baseline fluorescent levels of DAX-J2 were recorded before application of the iNOS substrate L-arginine (100μM), and intracellular DAX-J2 fluorescent changes in each cell within the imaging field were normalized to the average baseline level using FIJI open source software (Schindelin et al., 2012).

After NO-imaging, cells were washed 3× with PBS and immunocytochemistry was carried out to probe for the cell-cycle markers pH3, Ki67, and nuclear staining of DAPI as previously described. The microglia within the DAX-J2-imaging field were relocated and grouped based on their expressed cell-cycle markers. Any microglia that were washed away during the immunostaining process were removed from the analysis. The averaged normalized intensity of DAX-J2 fluorescence for each microglia was plotted versus time according to the cell-cycle phases using Excel.

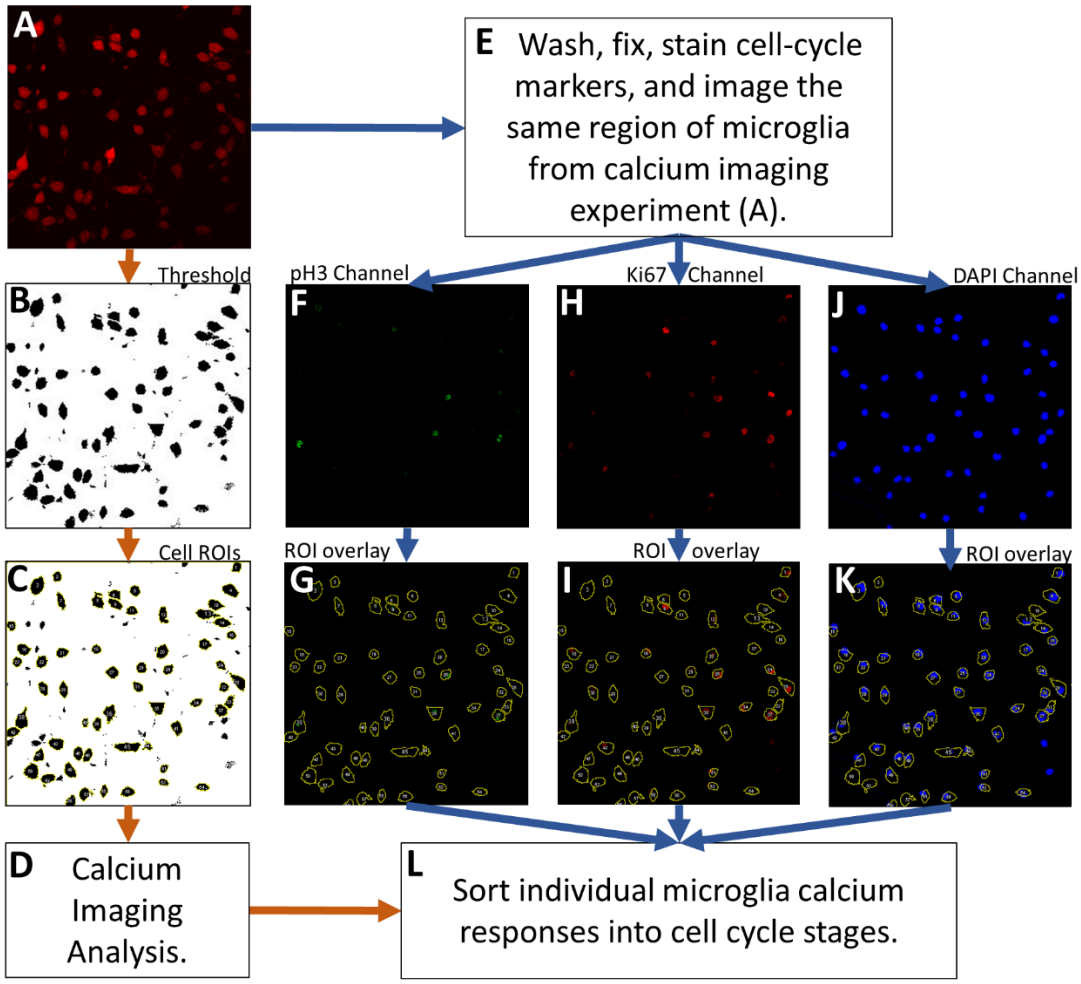

Figure legend on next page

Figure 5.S1 Image processing procedures for examining intracellular calcium and NO levels in specific cell-cycle stages of microglia.

A) The levels of intracellular calcium or NO were imaged using rhod-4 or DAX-J2 fluorescent imaging compounds, respectively. **B)** Fluorescent images from (A) were thresholded using FIJI open source software. **C)** Entire cell regions of interest (ROIs) were obtained using the analyze particle function in FIJI. **D)** ROIs obtained from (C) were overlaid onto original images from (A) and fluorescent intensity within each microglia cell was analyzed. **E)** Immediately after live cell imaging, cell cultures were probed for the cell-cycle markers previously described (Maksoud et al., 2020). Upon completion of the immunocytochemistry staining protocol, the same region examined during live cell imaging was relocated and the fluorescent expression of the cell-cycle markers **F)** pH3, **H)** Ki67, and nuclear staining of **J)** DAPI were imaged. The ROIs obtained from the live cell imaging analysis (C) were accurately overlaid onto the fluorescent images of the cell-cycle markers **G)** pH3, **I)** Ki67, and **K)** DAPI. **L)** The intracellular calcium or NO levels from individual microglia were sorted and grouped based on their expressed cell-cycle markers, and then graphed using Excel.

5.3.7 NFATC2 Localization Analysis

Localization analysis for NFATC2 expression within microglia is outlined in **Figure 5.S2.** Briefly, microglia stained with CD11b, NFATC2, and DAPI were imaged using the Olympus FV-1000 microscope. The DAPI and CD11b fluorescent channels were individually thresholded using constant settings. The particle analyzer function within FIJI (Schindelin et al., 2012) was used to determine the region of interest (ROI) for the nuclear and entire cell regions for individual microglia using the DAPI and CD11b fluorescent channels, respectively. The nuclear ROIs were subtracted from the entire cell ROIs to produce the cytosolic ROIs for each microglia. The nuclear and cytosolic ROIs were overlaid onto the NFATC2 channel for quantifying fluorescent intensity of NFATC2 within the nucleus and cytoplasm of each microglia. A ratio of nuclear/cytoplasmic NFATC2 fluorescence for each microglia was determined to control for variability in fluorescent intensity and cell size between images and individual microglia. Normalized nuclear/cytoplasmic NFATC2 fluorescent intensity was graphed using Excel.

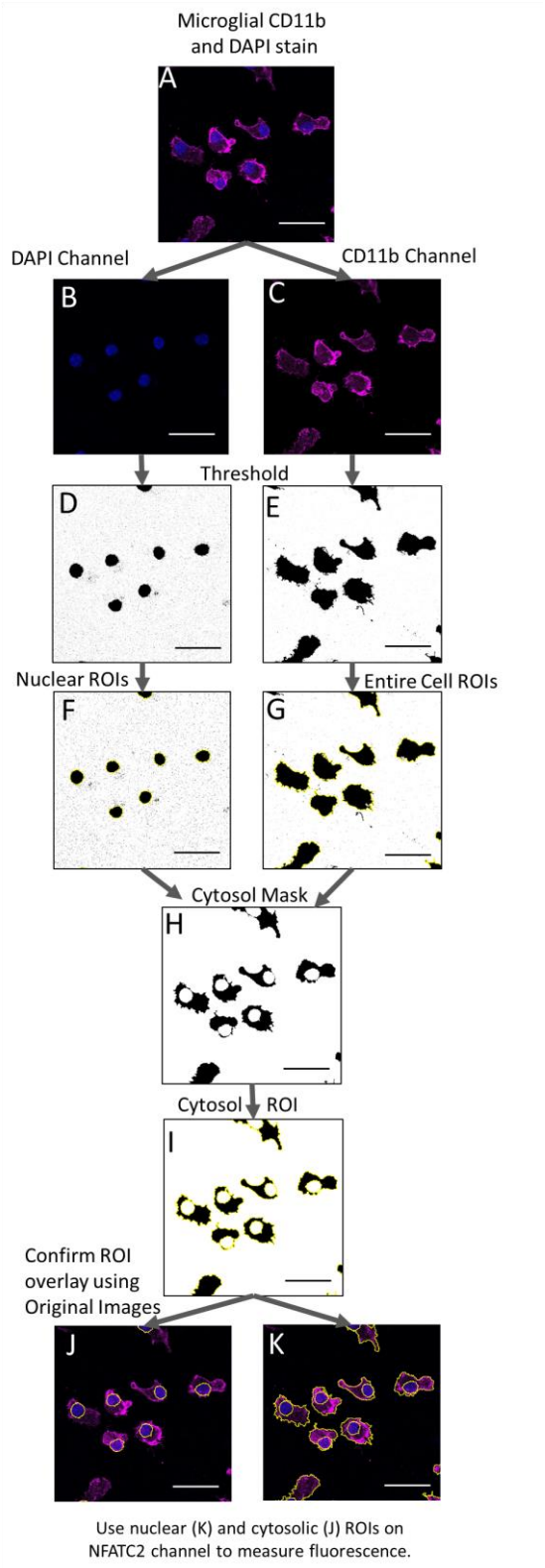

Figure legend on next page

Figure 5.S2 Image processing strategy to examine NFATC2 nuclear translocation.

A) Overlaid immunocytochemistry image of primary microglia stained with DAPI (blue) and CD11b (purple). The image channel containing DAPI fluorescence (B) and CD11b fluorescence (C) were separated. The separated images were thresholded using FIJI Open Source Software for both DAPI (D) and CD11b (E) channels. The particle analyze function in FIJI open source software was used to create ROIs for DAPI and CD11b that correspond to the nuclear regions (F) and entire cell regions (G), respectively. **H)** The nuclear and entire cell ROIs were subtracted to produce a cytosol mask. **I)** The analyze particle function was conducted on the cytosol mask to produce a cytosolic ROI. Overlay of the nuclear (F) and cytosolic (I) ROIs onto the original image from (A) demonstrates accurate representation of nuclear and cytosolic regions within microglia. The nuclear (F) and cytosolic (I) ROIs were overlaid onto the NFATC2 image channel and the fluorescent intensity of NFATC2 was measured in arbitrary units within the nuclear and cytoplasmic regions. Nuclear NFATC2 fluorescence was divided by cytosolic NFATC2 fluorescence within each cell to control for variations in cell size and fluorescent intensity between cells.

5.3.8 Western Blot

To quantify the NFATC2 expression in microglia, the BV2 cell line was used for western blot assays. Cultured BV2 microglia were washed 3× with PBS before being scraped into Eppendorf tubes and lysed using 150μL of radioimmunoprecipitation assay buffer. BV2 lysates were centrifuged at 13000g for 5min, and the supernatant containing proteins was quantified using Bradford assay (Bio-Rad, Hercules, CA). Proteins from different treatment groups were run through SDS-PAGE using an 8% polyacrylamide gel at 100V before being transferred to a polyvinylidene difluoride membrane. Membranes were blocked for 1hr using 5% BSA before being incubated with NFATC2 (ThermoFisher Scientific, Waltham, MA) antibody at 1:1000 dilution. Secondary anti-mouse IgG horseradish peroxidase (HRP) conjugate (1:5000) (Jackson Immunoresearch, Burlington, ON) was then incubated with the membrane for 1.5hrs. NFATC2 protein was normalized to the housekeeping protein glyceraldehyde 3-phosphate dehydrogenase (GAPDH) (1:10000) (Abcam Inc., Cambridge, MA). Protein bands were visualized using enhanced chemiluminescent substrate (Bio-Rad, Hercules, CA) and imaged using the Biod-Rad VersaDoc imaging system. Experimental N-values represent the number of individual wells in which cell-lysates were collected from each treatment group.

5.3.9 Reverse Transcription quantitative Polymerase Chain Reaction (RT-qPCR)

Total RNA was isolated using RNeasy Mini Kit (Qiagen, Toronto, ON) from primary WT or iNOS$^{-/-}$ microglia cultured on 60mm dishes as per manufacturer's instructions. Reverse transcription using qScript^{TM} XLT cDNA SuperMix (Quantabio, Beverly, MA) was carried out on 1μg of extracted microglial RNA. Quantitative PCR was conducted using PerfeCTa® SYBR® Green FastMix® for iQ (Quantabio, Beverly, MA), 25ng of cDNA template, and 500nM of forward and reverse primers specific to the gene of interest, as per manufacturer's instructions. Forward and reverse primers for murine p21 were as follows: forward 5'CATCTCAGGGCCGAAAACGG3', reverse 5'CAGGCCTCTTGCAGGATCTTT3'. The qPCR reactions were run in triplicate 25μL reactions with a no template control on a BioRad MyiQ Single-colour Real-Time PCR

detection system (Biorad, Mississauga, ON), with a 40-cycle protocol. The differences in cycle thresholds between the genes of interest and the reference gene β-actin forward 5'CTGTCCCTGTATGCCTCTG3', reverse 5'ATGTCACGCACGATTTCC3', were normalized to the vehicle control treatment levels using the ΔCt method and graphed using excel.

5.3.10 Statistics

Statistical analyses were done using Graphpad Prisim 6. All results are shown as mean ± SEM. A one-way ANOVA with Tukey's post hoc comparison was used with P-values of less than 0.05 taken as showing significant differences between means.

5.4 Results

5.4.1 Actively dividing WT and BV2 microglia display decreased NO production in response to L-arginine.

We examined whether the enzymatic activity of iNOS within WT and BV2 microglia is correlated to the cell-cycle stages. Specifically, we performed DAX-J2 fluorescent imaging in microglia to assess NO levels in response to treatment with the iNOS substrate L-arginine (100μM), followed by immunocytochemistry to probe for the cell-cycle markers Ki67 and pH3. Results demonstrated that L-arginine treatment on WT and BV2 microglia that were present within the G0 cell-cycle stage displayed gradual and sustained NO production, while actively dividing microglia in interphase and mitosis displayed a decline in NO production **(Figure 5.1A** and **5.1B)**. Together, this data suggests that NO-production occurs mainly in G0 within BV2 and WT microglia.

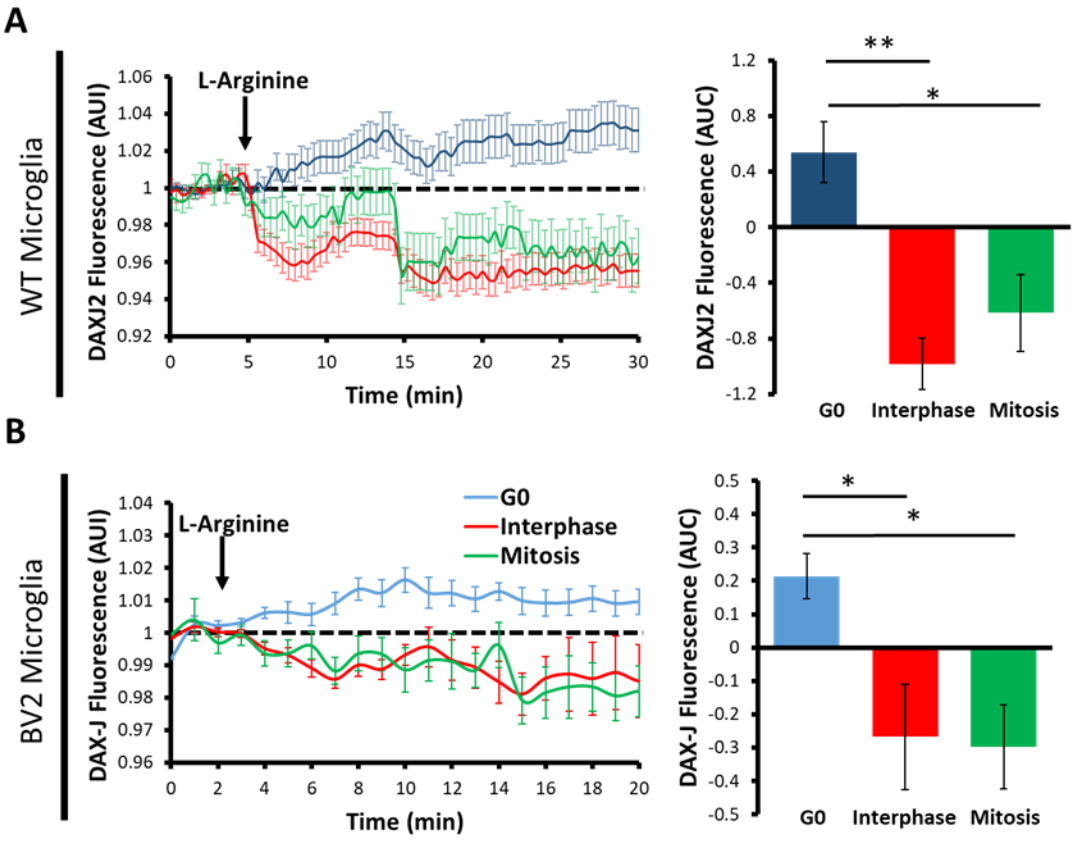

Figure 5.1 Actively dividing WT and BV2 microglia display decreased NO production in response to L-arginine.

Left panels: Changes in DAX-J2 fluorescent intensity with time in response to L-arginine (100μM) treatment in **A)** WT and **B)** BV2 microglia present in G0 (blue), interphase (red), and mitotic (green) cell-cycle stages. *Right panels:* Bar graphs depict the mean area under the NO-dynamic curve ± SEM in response to L-arginine treatment for **A)** WT and **B)** BV2 microglia. Statistical comparisons were determined from n = 193 G0 WT cells; n = 63 interphase WT cells; n = 27 mitotic WT cells; and n = 312 G0 BV2 cells; n = 193 interphase BV2 cells; n = 42 mitotic BV2 cells from multiple imaged fields from N = 4 and N = 5 wells respectively, and $p<0.05$ using a one-way ANOVA and Tukeys post-hoc comparison between cell-cycle stages. *$p<0.05$, **$p<0.01$.

5.4.2 Plasma membrane expression of TRPV2 is decreased in actively dividing microglia.

Considering that NO production is decreased in actively dividing microglia and NO is critical for the plasma membrane expression of TRPV2 (Maksoud et al., 2019), we examined whether the subcellular localization of TRPV2 is also altered in murine microglia cell-cycle stages.

To this end, we conducted immunocytochemistry to probe for TRPV2, Ki67, pH3, and DAPI in WT, iNOS$^{-/-}$, and BV2 microglia. Our confocal microscopy analyses displayed a significantly larger localization of TRPV2 proteins on the plasma membrane versus cytosol within G0 microglia when compared to actively dividing microglia in interphase or mitosis **(Figure 5.2A-C).** There was no significant difference in the ratio of plasma membrane versus cytosolic localization of TRPV2 between interphase and mitotic murine microglia, which all displayed a high cytosolic localization of TRPV2. Importantly, iNOS$^{-/-}$ microglia in G0 displayed significantly less plasma membrane versus cytosolic localization of TRPV2 when compared to WT and/or BV2 microglia (data not shown). Together, this data demonstrates that the plasma membrane expression of TRPV2 in murine microglia is dependent on the cell-cycle stages and is highest in G0 microglia, while plasma membrane expression of TRPV2 is lowest in actively dividing microglia.

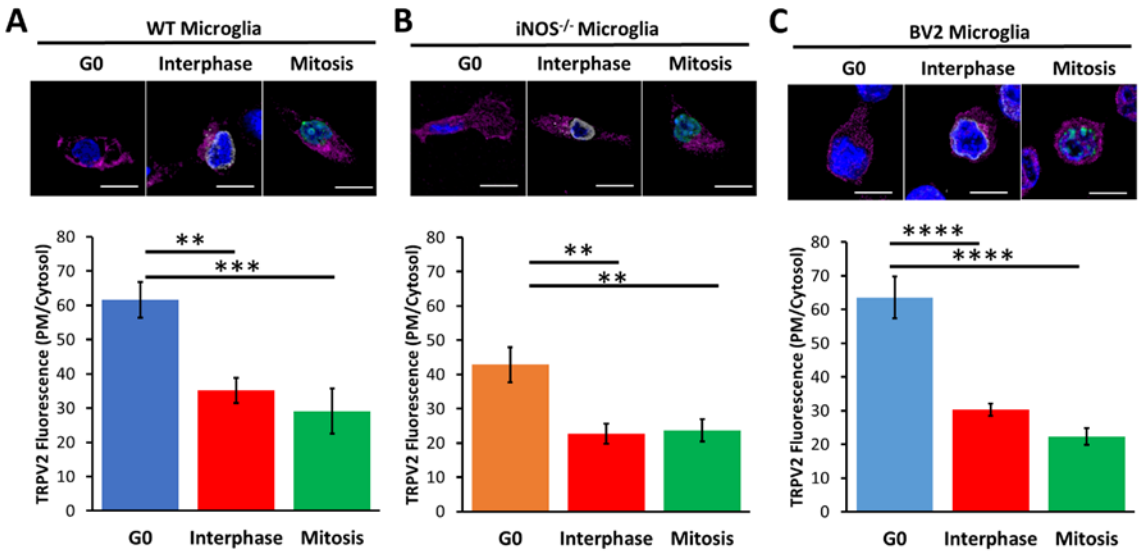

Figure 5.2 Plasma membrane expression of TRPV2 is decreased in actively dividing murine microglia.

Top panels: Representative images of TRPV2 (purple), Ki67 (grey), pH3 (green), and DAPI (blue) immunostaining, in **A)** WT, **B)** iNOS$^{-/-}$, and **C)** BV2 microglia. Scale bars represent 10 μm. *Bottom panels:* Bar graphs depict plasma membrane/cytosolic TRPV2 fluorescent intensity (mean arbitrary units ± SEM) in **A)** WT, **B)** iNOS$^{-/-}$, and **C)** BV2 microglia in G0, interphase, or mitosis. Significance was determined from n = 16 G0, n = 15 interphase, and n = 16 mitotic WT microglia; n = 16 G0, n = 19 interphase, and n = 24 mitotic iNOS$^{-/-}$ microglia; and n = 10 G0, n = 11 interphase, and n = 14 mitotic BV2 microglia, from at least N = 3 wells and a one-way ANOVA with Tukeys post-hoc comparison. $^{**}p<0.01$, $^{***}p<0.001$, $^{****}p<0.0001$.

5.4.3 Activation of TRPV2 channels induces differential levels of calcium influx in microglia at different cell-cycle stages.

We have previously demonstrated that 2APB evokes calcium entry to primary mouse microglia mainly by activation of TRPV2 channels (Cao et al., 2016; Maksoud et al., 2019). To examine the activity level of TRPV2 channels in different microglial cell-cycle stages, we assayed the intracellular calcium levels in WT, iNOS$^{-/-}$, and BV2 microglia before and after the addition of the TRPV2 channel agonist 2APB (250μM) (Cao et al., 2016; Maksoud et al., 2019). Next, we carried out immunocytochemistry to probe for the cell-cycle markers Ki67 and pH3 in the same microglia as previously described. Results from these assays revealed that murine microglia in G0 displayed a large calcium influx upon 2APB administration while microglia in interphase and mitosis displayed significantly less calcium influx **(Figure 5.3A-5.3C)**. This data suggests that microglia in G0 present with increased TRPV2 activity than actively dividing microglia. Importantly, WT and BV2 microglia in G0 displayed a larger calcium influx in comparison to iNOS$^{-/-}$ microglia in G0. Together, this data is consistent with our previous findings that endogenous iNOS/NO signaling regulates TRPV2 function and activity (Maksoud et al., 2019).

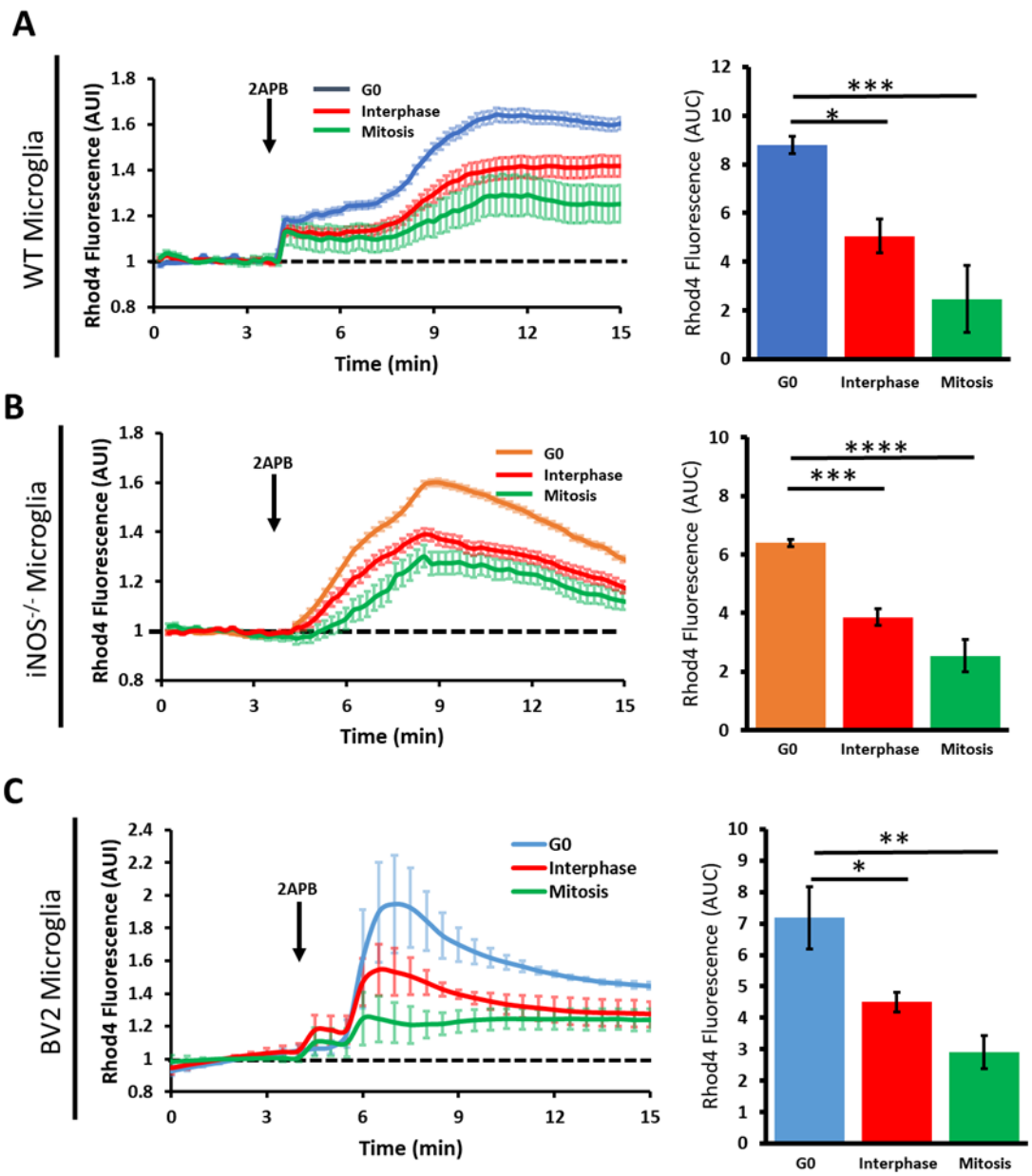

Figure legend on next page

Figure 5.3 Activation of TRPV2 channels induces differential levels of calcium influx in microglia at different cell-cycle stages.

Left Panels: Changes in rhod-4 fluorescent intensity with time in response to 2APB (250μM) treatment on **A)** WT, **B)** iNOS$^{-/-}$, and **C)** BV2 murine microglia in G0, interphase (red trace) and mitosis (green trace). *Right Panels:* Bar graphs depict mean area under the calcium dynamic curve in response to 2APB treatment on **A)** WT, **B)** iNOS$^{-/-}$, and **C)** BV2 microglia in G0, interphase (red bar), and mitosis (green bar) cell-cycle stages. Bars are shown as mean AUC ± SEM. Statistical significance was determined from n = 553 G0; n = 117 interphase; n = 41 mitotic WT cells; n = 194 G0; n = 81 interphase; n = 18 mitotic iNOS$^{-/-}$ cells; and n = 454 G0; n = 226 interphase; n = 53 mitotic BV2 cells from N = 4 wells and $p<0.05$ using a one-way ANOVA and Tukeys post-hoc comparison. *$p<0.05$, **$p<0.01$, ***$p<0.001$, ****$p<0.0001$.

5.4.4 Pharmacological modulation of TRPV2 channel activity influences cell-cycle progression in primary microglia.

Next, we examined if the NO-TRPV2 signaling pathway influences cell-cycle progression of primary WT and iNOS$^{-/-}$ microglia. Specifically, we examined the proportion of WT and iNOS$^{-/-}$ primary microglia expressing the cell-cycle markers Ki67 and pH3 after treatment with either the slow release NO-donor NOC18, the TRPV2 agonist probenecid, the TRPV2 antagonist tranilast, or a combination of both NOC18 + tranilast. Our assays revealed that WT microglia treated with NOC18 or probenecid displayed a significantly larger percentage of cells stained with DAPI only **(Figure 5.4A** and **5.4B)**, and a significantly smaller percentage of cells expressing Ki67 and/or pH3 staining when compared to vehicle control **(Figure 5.4C** and **5.4D)**. In contrast, inhibiting TRPV2 channel activity in WT microglia cultures using tranilast displayed a significantly larger percentage of microglia in the active phase of the cell-cycle – expressing Ki67 and/or pH3 – when compared to control **(Figure 5.4C** and **5.4D)**. Importantly, treating WT microglia with both NOC18 and tranilast displayed a significantly larger percentage of microglia in the active phase of the cell-cycle, expressing Ki67 and/or pH3 **(Figure 5.4C** and **5.4D).**

Furthermore, our assays demonstrated that iNOS$^{-/-}$ microglia treated with NOC18 displayed a significantly larger percentage of cells in G0 **(Figure 5.5A** and **5.5B)**, and significantly smaller percentage of actively dividing microglia when compared to vehicle control **(Figure 5.5C** and **5.5D).** Additionally, activating or inhibiting TRPV2 channels with probenecid or tranilast respectively, displayed no significant effect on the percentage of iNOS$^{-/-}$ microglia actively dividing or in G0 **(Figure 5.5B – 5.5D).** However, application of both NOC18 and tranilast significantly increased the percentage of actively dividing iNOS$^{-/-}$ microglia **(Figure 5.5B** and **5.5C).** Together, this data demonstrates that NO-promoted TRPV2 channel activity at the palsma membrane to restrict cell-cycle progression of microglia.

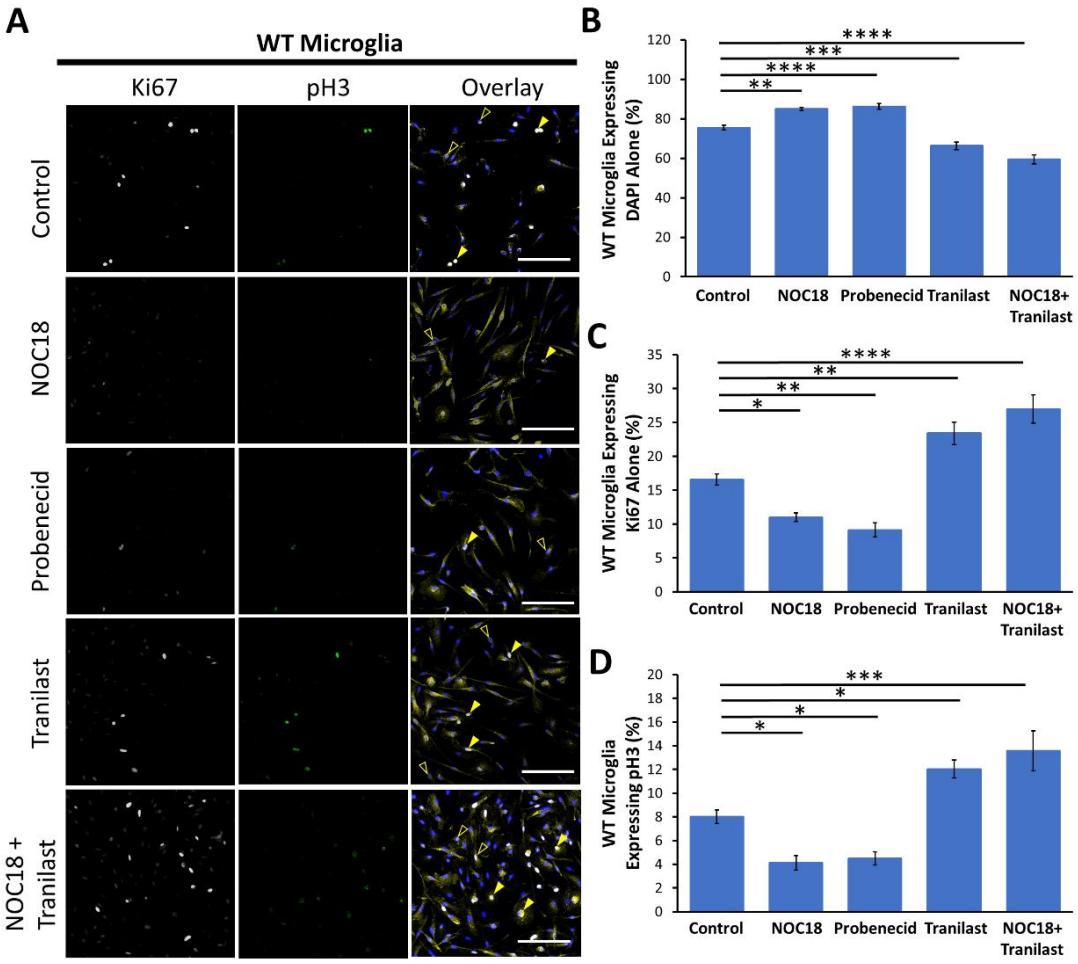

Figure 5.4 Pharmacological activation of TRPV2 channels restrict cell-cycle progression in primary WT microglia.

A) Representative images of Ki67 (grey), pH3 (green), CD11b (yellow), and DAPI fluorescence in WT microglia under vehicle control conditions or treated with NOC18 (100µM), the TRPV2 agonist probenecid (100µM) or the TRPV2 antagonist tranilast (75µM), or a combination of NOC18 + tranilast for 48hrs. Scale bars represent 100 µm. Open arrows point to $Ki67^{+}$ microglia while closed arrows point to $pH3^{+}$ microglia. Bar graphs report the percentages ± SEM of WT microglia having nuclei stained with **B)** DAPI alone, **C)** DAPI and Ki67, or **D)** DAPI, Ki67, and pH3. Statistical significance was determined from multiple imaged fields from N = 3 wells and $p<0.05$ using a one-way ANOVA and Tukeys post-hoc comparison for each cell-cycle stage separately *$p<0.05$, **$p<0.01$, ***$p<0.001$, ****$p<0.0001$.

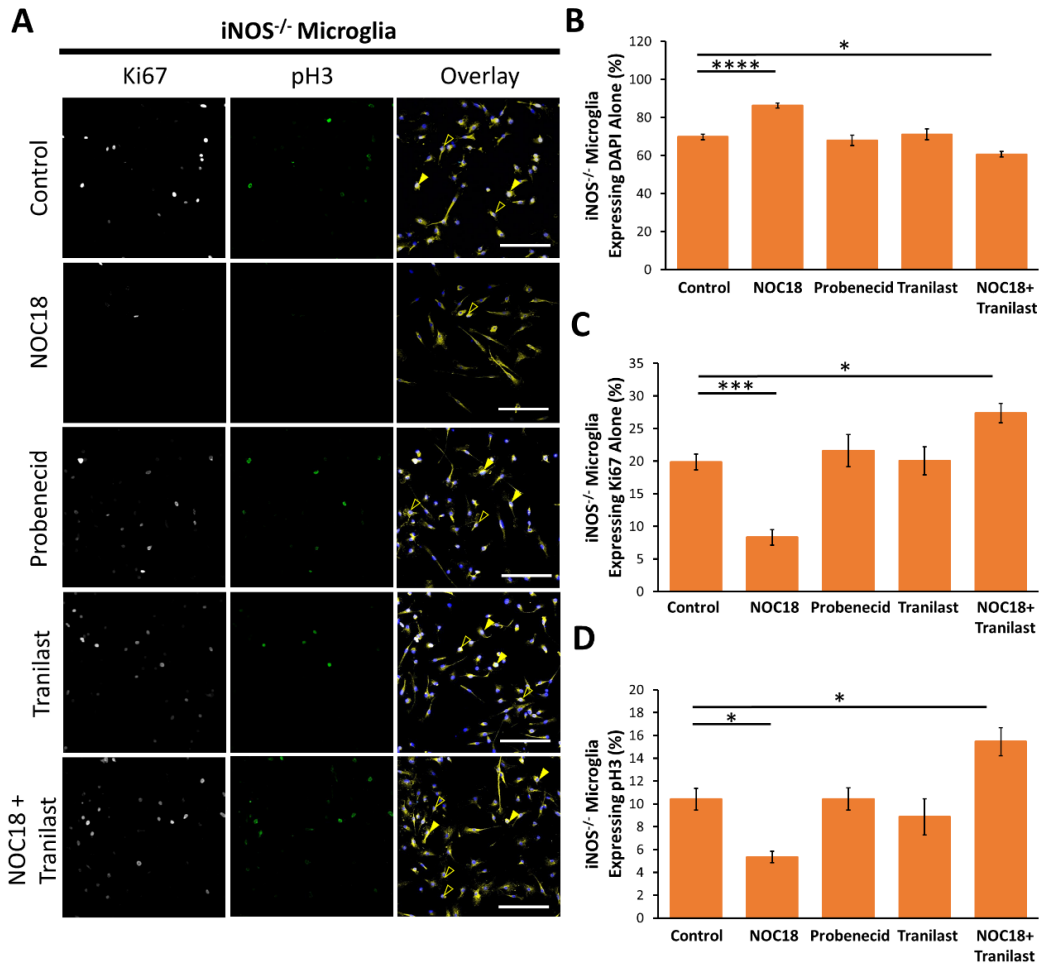

Figure 5.5 NO signaling influences cell-cycle progression in iNOS$^{-/-}$ microglia through TRPV2 channel activity.

A) Representative images of Ki67 (grey), pH3 (green), CD11b (yellow), and DAPI fluorescence in iNOS$^{-/-}$ microglia under control conditions or treated with NOC18 (100µM), the TRPV2 agonist probenecid (100µM), the TRPV2 antagonist tranilast (75µM), or a combination of NOC18 + tranilast for 48hrs. Scale bars represent 100 µm. Open arrows point to Ki67^{+} microglia while closed arrows point to pH3^{+} microglia. Bar graphs report the percentages ± SEM of iNOS$^{-/-}$ microglia having nuclei stained with **B)** DAPI alone, **C)** DAPI and Ki67, or **D)** DAPI, Ki67, and pH3. Statistical significance was determined from multiple imaged fields from N = 3 wells and $p<0.05$ using a one-way ANOVA and Tukeys post-hoc comparison for each cell-cycle stage separately. *$p<0.05$, ***$p<0.001$, ****$p<0.0001$.

5.4.5 NFATC2 nuclear localization and expression in murine microglia is dependent on TRPV2 channel activity.

To examine how calcium influx through TRPV2 channels may influence microglia cell-cycle progression and proliferation, we examined the localization of nuclear-factor of activated T-cells cytoplasmic-2 (NFATC2). NFATC2 is a calcium-dependent transcription factor known to negatively regulate proliferation (Baksh et al., 2000; Carvalho et al., 2007). Specifically, we carried out immunocytochemistry to examine the subcellular localization of NFATC2 in WT and iNOS$^{-/-}$ microglia and immunoblot assays to analyze NFATC2 protein expression in BV2 microglia, in response to treatments with NOC18, probenecid, tranilast, or a combination of NOC18+tranilast **(Figure 5.6)**. Results from our assays demonstrated that NOC-18 treatment significantly increased NFATC2 nuclear localization in WT (**Figure 5.6A** and **5.6B)** and iNOS$^{-/-}$ microglia **(Figure 5.6A** and **5.6C)**, while increasing NFATC2 protein expression within BV2 microglia (**Figure 5.6D)** when compared to vehicle controls. Treating BV2 microglia with the iNOS inhibitor L-NAME did not significantly affect NFATC2 protein expression when compared to vehicle control (**Figure 5.6D).** Notably, the TRPV2 agonist probenecid significantly increased NFATC2 nuclear localization and protein expression in WT **(Figure 5.6A** and **5.6B)** and BV2 (**Figure 5.6D)** microglia, respectively, when compared to vehicle controls. However, probenecid had no effect on NFATC2 nuclear localization in iNOS$^{-/-}$ microglia when compared to vehicle controls **(Figure 5.6A** and **5.6C).** Blocking TRPV2 channel activity with tranilast did not affect NFATC2 nuclear localization in WT and iNOS$^{-/-}$ microglia, or protein expression in BV2 cells when compared to vehicle controls **(Figure 5.6)**. However, tranilast significantly abolished the NOC18-induced increased nuclear localization of NFATC2 in WT and iNOS$^{-/-}$ microglia **(Figure 5.6A-C)**, and increased protein expression in BV2 microglia **(Figure 5.6D).** Together, these data suggest that NO-mediated TRPV2 signaling induces nuclear translocation and activation of NFATC2 in murine microglia.

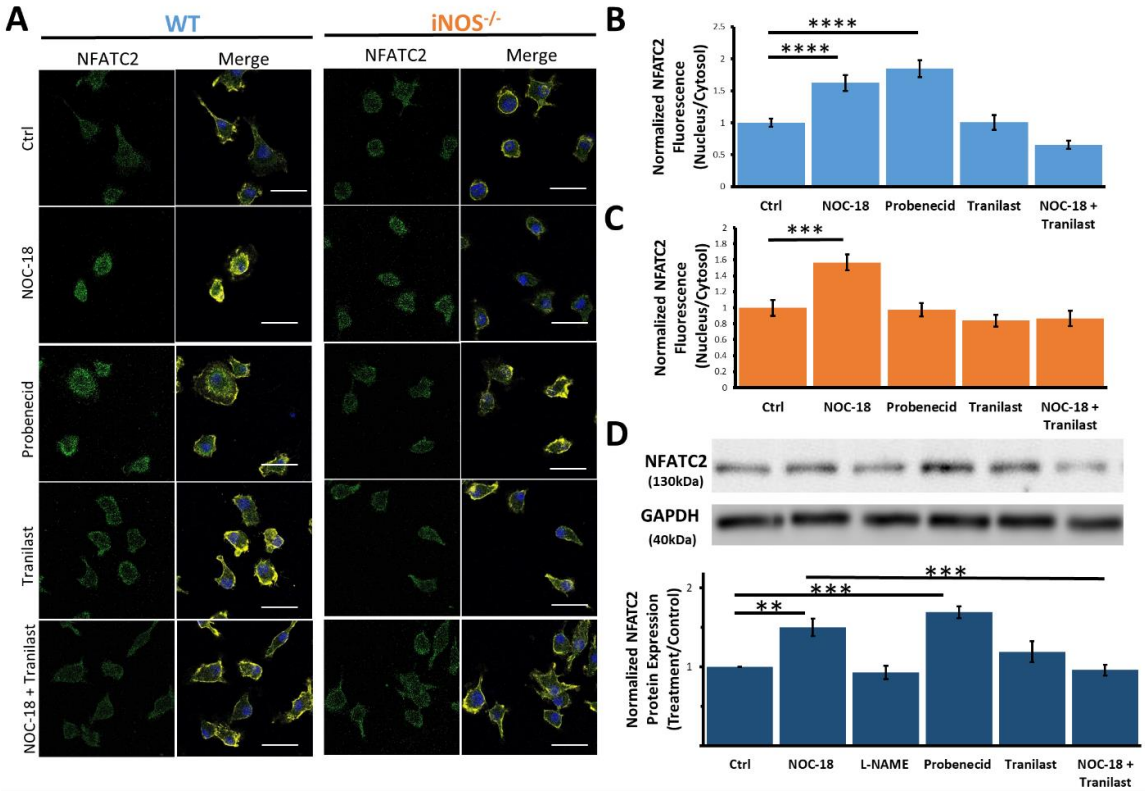

*****Figure legend on next page*****

Figure 5.6 NO-promoted TRPV2 signaling increases NFATC2 nuclear translocation and expression in murine microglia.

A) Representative confocal images of NFATC2 (green), CD11b (yellow), and DAPI (blue) fluorescence in WT (Left two panels) and iNOS$^{-/-}$ (right two panels) microglia under vehicle control conditions or treatments with NOC18 (100μM), probenecid (100μM), tranilast (75μM), or NOC18 + tranilast for 48hrs. Scale bars represent 50 μm. Bar graphs report the ratio of nuclear versus cytoplasmic fluorescence of NFATC2 in arbitrary units normalized to vehicle-treated control levels for **B)** WT and **C)** iNOS$^{-/-}$ microglia under different treatment conditions. **D)** *top panel:* Immunoblot of NFATC2 protein in control BV2 microglia and in response to NOC18 (100 μM), L-NAME (100 μM), probenecid (100 μM), tranilast (75 μM), or NOC18 + tranialst. GAPDH protein levels were used as a loading control. *Bottom panel:* Bar graph depicts the NFATC2 protein expression divided by the GAPDH protein expression and normalized to the control condition (mean ± SEM). Statistical significance for (B) and (C) was determined from n = 175 control WT cells; n = 121 NOC18 treated WT cells; n = 195 probenecid treated WT cells; n = 132 tranilast treated WT cells; n = 97 NOT18 + tranilast treated WT cells; and n = 108 control iNOS$^{-/-}$ cells; n = 148 NOC18 treated iNOS$^{-/-}$ cells; n = 147 probenecid treated iNOS$^{-/-}$ cells; n = 77 tranilast treated iNOS$^{-/-}$ cells; n = 84 NOC18 + Tranilast treated iNOS$^{-/-}$ cells from N = 4 wells while statistical significance for (D) was determined from N = 6 wells using a one-way ANOVA and Tukeys post-hoc comparison. $^{**}p<0.01$, $^{***}p<0.001$, $^{****}p<0.0001$.

5.4.6 NO-TRPV2 signaling regulates p21 transcription in WT and iNOS$^{-/-}$ murine microglia.

We next examined whether the NO-TRPV2 dependent activation of NFATC2 regulates the mRNA expression of the cyclin-dependent kinase inhibitor p21 within WT and iNOS$^{-/-}$ microglia. Given that the gene expression of p21 is under control by NFATC2, we used RT-qPCR to assay the mRNA expression of p21 in response to NOC18, the TRPV2 agonist probenecid, TRPV2 antagonist tranilast, or a combination of NOC18+tranilast **(Figure 5.7)**. Results from our RT-qPCR assays demonstrated that NOC18 treatment increased p21 mRNA expression in both WT and iNOS$^{-/-}$ microglia when compared to their respective vehicle-treated control (**Figure 5.7A** and **5.7B)**. Importantly, probenecid treatment increased the p21 expression in WT microglia (**Figure 5.7A)**, but not in iNOS$^{-/-}$ microglia **(Figure 5.7B)**. Finally, tranilast treatment in WT and iNOS$^{-/-}$ microglia displayed no significant effect on p21 mRNA when compared to controls, however, tranilast in combination with NOC-18 abolished the increased p21 mRNA observed from NOC18 treatment alone **(Figure 5.7A** and **5.7B).** Together, these data suggest that NO-TRPV2 signaling induces transcription of p21 mRNA within primary murine microglia.

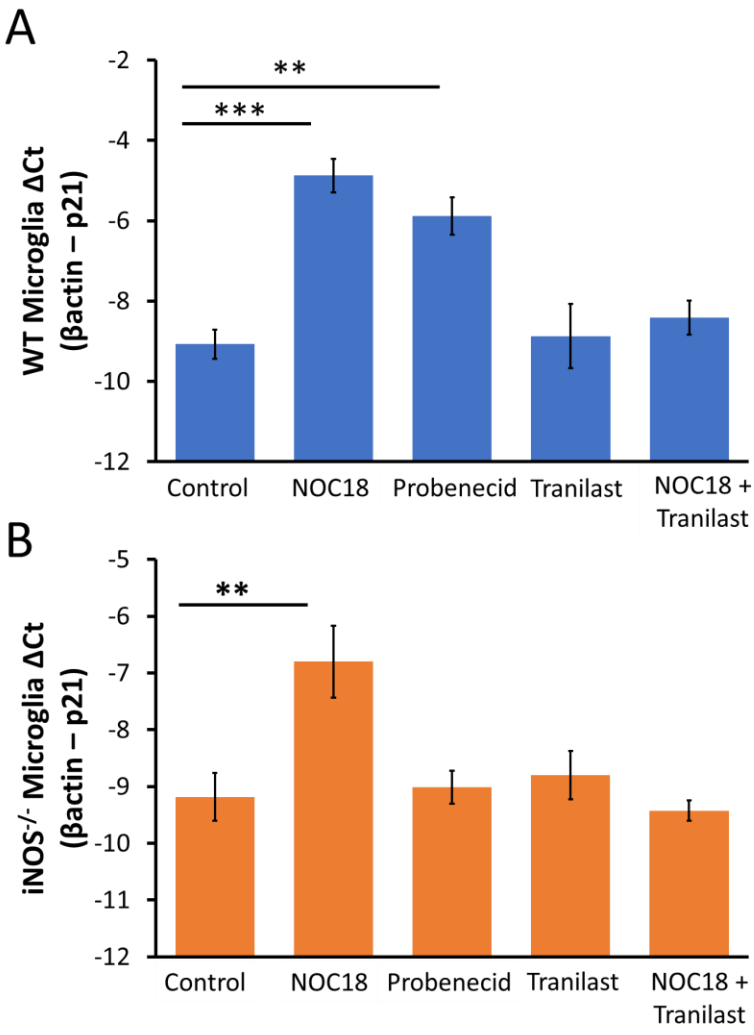

Figure 5.7 NO-mediated TRPV2 signaling regulates p21 transcription in primary WT and iNOS$^{-/-}$ murine microglia..

Graphs report ΔCt values (mean ± SEM) of p21 mRNA in relation to β-actin mRNA within primary **A)** WT or **B)** iNOS$^{-/-}$ microglia cultures under vehicle-treated control conditions or treated with NOC18 (100μM), probenecid (100μM), tranilast (75 μM), or NOC18 + tranialst for 48 hrs. Statistical significance was determined from N = 4 wells using a one-way ANOVA and Tukeys post-hoc comparison for WT and iNOS$^{-/-}$ microglia separately *p<0.05, **p<0.01, ***p<0.001, ****p<0.0001.

5.5 Discussion

Our study is the first to demonstrate a mechanism where microglia in the G0 stage of the cell-cycle produce higher levels of NO, express more TRPV2 channels on the plasma membrane, and display more calcium influx through TRPV2 channels than actively dividing microglia. This NO-TRPV2 signaling further induces the nuclear translocation of the transcription factor NFATC2 and transcription of the cyclin-dependent kinase inhibitor p21. The presence of NO is well-known to restrict proliferation of many cell types including microglia (Garg & Hassid, 1989; Kawahara et al., 2001; MacMicking et al., 1997; Maksoud et al., 2020; Tate et al., 2012). We previously reported that murine microglia possess an NO-sGC-cGMP-PKG signaling cascade that arrests cell-cycle progression at the G0 stage (Maksoud et al., 2020).

L-arginine uptake by microglia occurs through activation of the cationic amino acid transporter (Czapiga & Colton, 2003; Kawahara et al., 2001). The iNOS enzyme catalyzes cytosolic L-arginine into citrulline and NO (Garg & Hassid, 1989; Kawahara et al., 2001; MacMicking et al., 1997; Maksoud et al., 2020; Tate et al., 2012). In the present study, we performed DAX-J2 fluorescent imaging in response to application of L-arginine to measure the production of NO in murine microglia at different cell-cycle stages. Our assays demonstrated that administration of L-arginine produced higher levels of NO in the G0 cell-cycle stage than in actively dividing murine microglia. The production of endogenous NO depends on both the availability of L-arginine within the cell, as well as the activity of the enzymes that compete to catabolize L-arginine, including iNOS and arginase (Pautz et al., 2010). For example, L-arginine can also be catabolized by arginase into L-ornithine, a non-proteinogenic amino acid that is important for polyamine production, cell growth, and proliferation (Li et al., 2016; Medina-Enríquez et al., 2015; Soda, 2011). Therefore, these distinct and opposing metabolic pathways for L-arginine may regulate microglia proliferation and cell division. At present, little is known about the regulation of iNOS and arginase in different cell-cycle stages. Given the important role of arginase in promoting cell proliferation (Chang et al., 2001; Wei et al., 2001) and the pivotal role of NO in restricting cell proliferation (Maksoud et al., 2020), further studies may greatly benefit

from examining the mechanisms surrounding iNOS and arginase regulation in different cell-cycle stages.

Moreover, we previously demonstrated that the production of NO signals through PKG to enhance the plasma membrane expression of TRPV2 channels in murine microglia (Maksoud et al., 2019). Consistent with our previous report, our present assays demonstrated that microglia in the G0 cell-cycle stage displayed increased TRPV2 fluorescence on the plasma membrane and elevated calcium influx through TRPV2 channels when compared to actively dividing microglia. Certainly, calcium signaling during mitosis must be tightly regulated to properly progress the cell through the different stages of the cell-cycle (Cui et al., 2017; Koledova & Khalil, 2006; Lu & Means, 1993). Our calcium imaging assays demonstrated that activation of TRPV2 channels caused a large calcium influx in microglia present in the G0 stage of the cell-cycle, where enhanced NO production also occurred. On the other hand, actively dividing microglia displayed a significantly smaller calcium influx through TRPV2 channels. Interestingly, a sustained calcium influx in all WT microglia cell-cycle stages was observed when compared to the transient calcium influx in all $iNOS^{-/-}$ microglia cell-cycle stages. To that extent, Mercado and colleagues have reported that TRPV2 channels are gated by phosphatidylinositol 4,5, bisphosphate (PIP_2), a membrane phospholipid (Mercado et al., 2010). Importantly, catabolism of PIP_2 is reduced in the presence of NO (Clementi et al., 1995), and therefore the abundant PIP_2 may gate and contribute to the sustained calcium influx through TRPV2 channels observed in WT microglia and not in $iNOS^{-/-}$ microglia.

Similarly, it should also be noted that the presence of growth factors added to the culture media may contribute to TRPV2 plasma membrane expression in $iNOS^{-/-}$ microglia (Nagasawa et al., 2007; Nagasawa & Kojima, 2012; Perálvarez-Marín et al., 2013). Importantly, NO can regulate mitogenic growth factor receptors and their downstream pathways to influence cell proliferation (Parenti et al., 1998; Villalobo, 2006). Therefore, the different calcium influx kinetics observed through TRPV2 channels between WT and $iNOS^{-/-}$ microglia may stem from NO signaling of mitogenic growth factor receptors or PIP_2 gating of TRPV2 channels.

Previous studies demonstrate a critical role of TRPV2 in regulating cellular proliferation, differentiation, and cancer progression (Cui et al., 2017; Liberati et al., 2014; Morelli et al., 2012; Nabissi et al., 2010; H. Zhang et al., 2016). For example, decreased TRPV2 expression and activity enhances the proliferation of astrocytes while also contributing to glioma growth (Cui et al., 2017; Morelli et al., 2012; Nabissi et al., 2010). Consistent with these results, our assays demonstrated that stimulating TRPV2 channels in WT microglia cultures decreased the percentage of actively dividing microglia, while inhibiting TRPV2 channels in WT microglia increased the percentage of actively dividing microglia when compared to controls. On the other hand, activating or inhibiting TRPV2 channels in $iNOS^{-/-}$ microglia had no significant effect on the percentage of microglia actively dividing when compared to controls. The lack of a response to pharmacological modulators of TRPV2 is substantiated by the decreased plasma membrane expression of TRPV2 observed in $iNOS^{-/-}$ microglia when compared to WT microglia.

Moreover, increasing NO by application of the NO-donor NOC18 in both primary WT and $iNOS^{-/-}$ microglia cultures increased the percentage of microglia in the G0 stage of the cell-cycle. Considering that the plasma membrane expression of TRPV2 is elevated in the presence of NOC18 (Maksoud et al., 2019), as well as in the G0 stage of the cell-cycle, we examined whether the effect of NO could be inhibited by restricting TRPV2 activity. To that extent, we demonstrated that inhibiting TRPV2 activity in the presence of NOC18 abolished the NOC18-induced increase of microglia in the G0 stage of the cell-cycle and instead, significantly increased the percentage of actively dividing WT and $iNOS^{-/-}$ microglia in culture. Therefore, NO may signal through an alternative secondary mechanism other than sGC-cGMP-PKG-TRPV2 to enhance microglia proliferation. For example, nitrosylation of Cys^{118} of p21RAS – a protein that promotes cell-cycle progression, proliferation, and survival – has been shown to enhance the proliferation of human breast cancer cells (Heo et al., 2005; Pervin et al., 2007), which may also be a mechanism that enhances microglia proliferation, independent of PKG signaling that we observed.

It is known that TRPV2 channel activity negatively regulates proliferation and enhances cell differentiation through the activation of NFAT transcription factors (Bai et

al., 2018; Caetano et al., 2002; Mognol et al., 2016; Robbs et al., 2008). Specifically, calcium influx through TRPV2 channels induces calmodulin-dependent activation of calcineurin and dephosphorylation, activation, and nuclear translocation of NFATs in osteoclast differentiation (Bai et al., 2018). Along those lines, TRPV2 activity differentiates brown adipose tissue (Sun et al., 2016), and inhibits proliferation of astrocytes and gliomas (Morelli et al., 2012; Nabissi et al., 2010; Zhang et al., 2016). Importantly, NFATC2 is the most abundant NFAT isoform present within microglia (Manocha et al., 2017) that promotes differentiation (Robbs et al., 2008) and cell-cycle arrest through decreased cyclin-dependent kinase-4 expression (Baksh et al., 2002), decreased cyclin-A2 expression (Caetano et al., 2002; Carvalho et al., 2007), and increased expression of the cyclin-dependent kinase inhibitor p21 (Mognol et al., 2016; Santini et al., 2001). Therefore, we examined NFATC2 subcellular localization and p21 mRNA expression to further uncover the mechanism that NO-TRPV2 signaling restricts microglia cell-cycle progression in G0.

In the present study, we observed that NOC18 treatment on primary microglia and BV2 cells significantly increased NFATC2 nuclear localization and protein expression when compared to controls, respectively. Additionally, agonizing TRPV2 channels on WT and BV2 microglia increased NFATC2 nuclear localization and protein expression when compared to controls, respectively. In contrast, agonizing TRPV2 channels on $iNOS^{-/-}$ microglia did not significantly influence NFATC2 nuclear translocation, likely due to the decreased TRPV2 plasma membrane expression observed in $iNOS^{-/-}$ microglia. Furthermore, antagonizing TRPV2 channels in the presence of NOC18 had no effect on NFATC2 nuclear localization, or protein expression in BV2 microglia. Furthermore, our assays demonstrated that NFATC2 nuclear translocation in murine microglia was associated with increased transcriptional levels of p21, a potent cyclin dependent kinase inhibitor that arrests cell-cycle progression in the G0 cell-cycle stage (Santini et al., 2001).

In summary, we have demonstrated for the first time that microglia in the G0 cell-cycle stage produce higher levels of NO, display enhanced expression of TRPV2 on their plasma membrane, and exhibit enhanced calcium influx through TRPV2 channels that constitutively activates NFATC2 causing its nuclear localization and the transcription of

p21. As illustrated in **Figure 5.8** we proposed a molecular mechanism in which NO regulates the cell-cycle progression of murine microglia. Briefly, microglia in G0 express iNOS and produce elevated levels of NO, which signals through the classical PKG signaling cascade to promote TRPV2 translocation to the plasma membrane (Maksoud et al., 2019). The increased calcium influx through TRPV2 channels can activate calmodulin, and the calcium-calmodulin dependent the phosphatase calcineurin dephosphorylates and activates NFATC2 (Mognol et al., 2016). Activated NFATC2 translocates into the nucleus and transcribes the cyclin dependent kinase inhibitor p21 (Santini et al., 2001) that results in cell-cycle arrest (Santini et al., 2001). In contrast, reduced iNOS/NO signaling may enhance microglia proliferation and this excessive microglia proliferation may contribute to the pathological progressions of certain neurological diseases such as glioma (Badie & Schartner, 2000; Morimura et al., 1990; Roggendorf et al., 1996; Simmons et al., 2011).

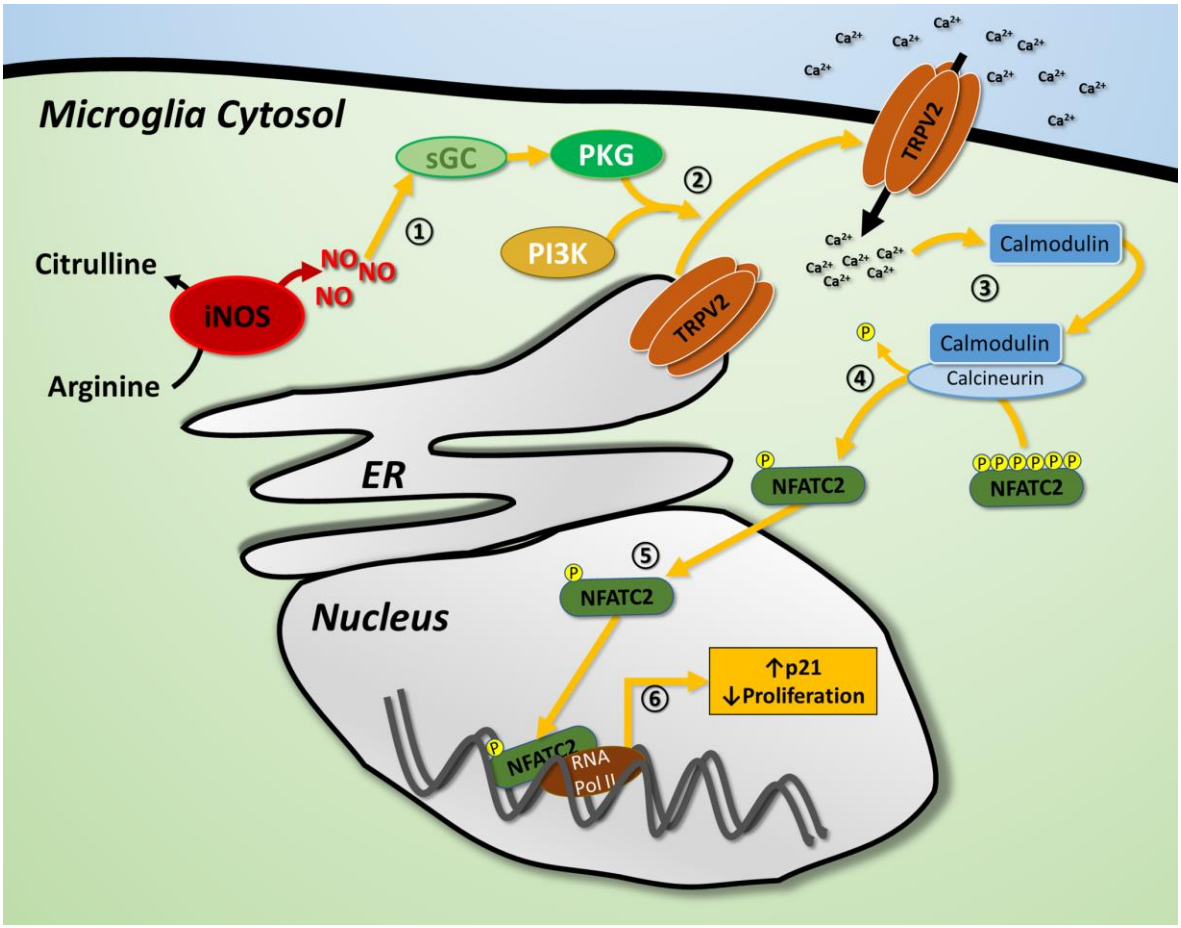

Figure 5.8 P**roposed molecular mechanism by which NO-signaling restricts microglial cell-cycle progression.**

1) iNOS activity in microglia catabolizes the substrate L-arginine into citrulline and NO. **2)** NO binds and activates sGC to produce cGMP, which binds and activates PKG. **3)** PKG activity in combination with PI3K induce the trafficking of TRPV2 ion channels from the ER/Golgi to the plasma membrane as previously described (Maksoud et al., 2019). **4)** Calcium influx through TRPV2 channels promote calcium-calmodulin binding to the phosphatase calcineurin. **5)** Activated calcineurin dephosphorylates NFATC2. **6)** Activated NFATC2 translocates from the cytoplasm to the nucleus. **7)** NFATC2 in the nucleus actively transcribes the cyclin dependent kinase inhibitor p21 and inhibits microglial proliferation.

5.6 References

Badie, B., & Schartner, J. M. (2000). Flow Cytometric Characterization of Tumor-associated Macrophages in Experimental Gliomas. Neurosurgery, 46(4), 957–962. https://doi.org/10.1227/00006123-200004000-00035

Bai, H., Zhu, H., Yan, Q., Shen, X., Lu, X., Wang, J., … Chen, L. (2018). TRPV2-induced Ca2+-calcineurin-NFAT signaling regulates differentiation of osteoclast in multiple myeloma. Cell Communication and Signaling, 16(68), 1–11.

Baksh, S., DeCaprio, J. A., & Burakoff, S. J. (2000). Calcineurin regulation of the mammalian G0/G1 checkpoint element, cyclin dependent kinase 4. Oncogene, 19(24), 2820–2827. https://doi.org/10.1038/sj.onc.1203585

Baksh, S., Widlund, H. R., Frazer-Abel, A. A., Du, J., Fosmire, S., Fisher, D. E., … Burakoff, S. J. (2002). NFATc2-Mediated Repression of Cyclin-Dependent Kinase 4 Expression. Molecular Cell, 10(5), 1071–1081. https://doi.org/10.1016/S1097-2765(02)00701-3

Biber, K., Owens, T., & Boddeke, E. (2014). What is microglia neurotoxicity (Not)? Glia, 62(6), 841–854. https://doi.org/10.1002/glia.22654

Caetano, M. S., Vieira-de-abreu, A., Teixeira, L. K., Miriam, B. F., Barcinski, M. A., & Viola, J. P. B. (2002). Control lymphocyte proliferation and cyclin A2 gene transcription by a mechanism involving the transcription factor NFAT1.

Cao, T., & Ramsey, I. S. (2016). Toll-Like Receptor 4 Activation by LPS Stimulates TRPV2 Channel Activity in Microglia. Biophysical Journal, 110(3), 286a. https://doi.org/10.1016/j.bpj.2015.11.1548

Carvalho, L. D. S., Teixeira, L. K., Carrossini, N., Caldeira, A. T. N., Ansel, K. M., Rao, A., & Viola, J. P. B. (2007). The NFAT1 Transcription Factor is a Repressor of Cyclin A2 Gene Expression. Cell Cycle, 6(14), 1789–1795. https://doi.org/10.4161/cc.6.14.4473

Chang, C. I., Liao, J. C., & Kuo, L. (2001). Macrophage arginase promotes tumor cell growth and suppresses nitric oxide-mediated tumor cytotoxicity. Cancer Research, 61(3), 1100–1106.

Clementi, E., Sciorati, C., Riccio, M., Miloso, M., Meldolesi, J., & Nisticò, G. (1995). Nitric Oxide Action on Growth Factor-elicited Signals. Journal of Biological Chemistry, 270(38), 22277–22282. https://doi.org/10.1074/jbc.270.38.22277

Cui, C., Merritt, R., Fu, L., & Pan, Z. (2017). Targeting calcium signaling in cancer therapy. Acta Pharmaceutica Sinica B, 7(1), 3–17. https://doi.org/10.1016/j.apsb.2016.11.001

Engler, J. R., Robinson, A. E., Smirnov, I., Hodgson, J. G., Berger, M. S., Gupta, N., … Phillips, J. J. (2012). Increased Microglia/Macrophage Gene Expression in a Subset of Adult and Pediatric Astrocytomas. PLoS ONE, 7(8), e43339. https://doi.org/10.1371/journal.pone.0043339

Fischer, J. E. (1971). Rapid publication. Physics Today, 24(5), 13. https://doi.org/10.1063/1.3022720

He, B. P., Wang, J. J., Zhang, X., Wu, Y., Wang, M., Bay, B.-H., & Chang, A. Y.-C. (2006). Differential Reactions of Microglia to Brain Metastasis of Lung Cancer. Molecular Medicine, 12(7–8), 161–170. https://doi.org/10.2119/2006-00033.He

Heo, J., Prutzman, K. C., Mocanu, V., Campbell, S. L., Carolina, N., & Carolina, N. (2005). Mechanism of Free Radical Nitric Oxide-mediated Ras Guanine Nucleotide Dissociation. Journal Molecular Biology, 346(2), 1423–1440. https://doi.org/10.1016/j.jmb.2004.12.050

Kamphuis, W., Orre, M., Kooijman, L., Dahmen, M., & Hol, E. M. (2012). Differential cell proliferation in the cortex of the appsweps1de9 alzheimer's disease mouse model. Glia, 60(4), 615–629. https://doi.org/10.1002/glia.22295

Kawahara, K., Gotoh, T., Oyadomari, S., Kuniyasu, A., Kohsaka, S., Mori, M., & Nakayama, H. (2001). Nitric oxide inhibits the proliferation of murine microglial MG5 cells by a mechanism involving p21 but independent of p53 and cyclic guanosine monophosphate. Neuroscience Letters, 310(2–3), 89–92. https://doi.org/10.1016/S0304-3940(01)02079-1

Kim, Y. J., Hwang, S. Y., & Han, I. O. (2006). Insoluble matrix components of glioma cells suppress LPS-mediated iNOS/NO induction in microglia. Biochemical and Biophysical Research Communications, 347(3), 731–738. https://doi.org/10.1016/j.bbrc.2006.06.149

Koledova, V. V., & Khalil, R. A. (2006). Ca2+, calmodulin, and cyclins in vascular smooth muscle cell cycle. Circulation Research, 98(10), 1240–1243. https://doi.org/10.1161/01.RES.0000225860.41648.63

Komohara, Y., Ohnishi, K., Kuratsu, J., & Takeya, M. (2008). Possible involvement of the M2 anti-inflammatory macrophage phenotype in growth of human gliomas. The Journal of Pathology, 216(1), 15–24. https://doi.org/10.1002/path.2370

Li, H., Meininger, C. J., Bazer, F. W., & Wu, G. (2016). Intracellular sources of ornithine for polyamine synthesis in endothelial cells. Amino Acids, 48(10), 2401–2410. https://doi.org/10.1007/s00726-016-2256-6

Liberati, S., Morelli, M., Amantini, C., Farfariello, V., Santoni, M., Conti, A., … Santoni, G. (2014). Loss of TRPV2 Homeostatic Control of Cell Proliferation Drives Tumor Progression. Cells, 3(1), 112–128. https://doi.org/10.3390/cells3010112

LU, K. P., & MEANS, A. R. (1993). Regulation of the Cell Cycle by Calcium and Calmodulin. Endocrine Reviews, 14(1), 40–58. https://doi.org/10.1210/edrv-14-1-40

MacMicking, J., Xie, Q. W., & Nathan, C. (1997). Nitric oxide and macrophage function. Annual Review of Immunology, 15(1), 323–350. https://doi.org/10.1146/annurev.immunol.15.1.323

Maksoud, M. J. E., Tellios, V., An, D., Xiang, Y., & Lu, W. (2019). Nitric oxide upregulates microglia phagocytosis and increases transient receptor potential vanilloid type 2 channel expression on the plasma membrane. Glia, 67(12), 2294–2311. https://doi.org/10.1002/glia.23685

Maksoud, M. J. E., Tellios, V., Xiang, Y.-Y., & Lu, W.-Y. (2020). Nitric oxide signaling inhibits microglia proliferation by activation of protein kinase-G. Nitric Oxide, 94, 125–134. https://doi.org/10.1016/j.niox.2019.11.005

Manocha, G. D., Ghatak, A., Puig, K. L., Kraner, S. D., Norris, C. M., & Combs, C. K. (2017). NFATc2 Modulates Microglial Activation in the AβPP/PS1 Mouse Model of Alzheimer's Disease. Journal of Alzheimer's Disease, 58(3), 775–787. https://doi.org/10.3233/JAD-151203

Medina-Enríquez, M. M., Alcántara-Farfán, V., Aguilar-Faisal, L., Trujillo-Ferrara, J. G., Rodríguez-Páez, L., & Vargas-Ramírez, A. L. (2015). N-ω-chloroacetyl-l-ornithine, a new competitive inhibitor of ornithine decarboxylase, induces selective growth

inhibition and cytotoxicity on human cancer cells versus normal cells. Journal of Enzyme Inhibition and Medicinal Chemistry, 30(3), 345–353. https://doi.org/10.3109/14756366.2014.926342

Mercado, J., Gordon-Shaag, A., Zagotta, W. N., & Gordon, S. E. (2010). Ca2+-Dependent Desensitization of TRPV2 Channels Is Mediated by Hydrolysis of Phosphatidylinositol 4,5-Bisphosphate. Journal of Neuroscience, 30(40), 13338–13347. https://doi.org/10.1523/JNEUROSCI.2108-10.2010

Mognol, G. P., Carneiro, F. R. G., Robbs, B. K., Faget, D. V, & Viola, J. P. B. (2016). Cell cycle and apoptosis regulation by NFAT transcription factors: new roles for an old player. Cell Death & Disease, 7(4), e2199–e2199. https://doi.org/10.1038/cddis.2016.97

Morelli, M. B., Nabissi, M., Amantini, C., Farfariello, V., Ricci-Vitiani, L., di Martino, S., … Santoni, G. (2012). The transient receptor potential vanilloid-2 cation channel impairs glioblastoma stem-like cell proliferation and promotes differentiation. International Journal of Cancer, 131(7), E1067–E1077. https://doi.org/10.1002/ijc.27588

Morimura, T., Neuchrist, C., Kitz, K., Budka, H., Scheiner, O., Kraft, D., & Lassmann, H. (1990). Monocyte subpopulations in human gliomas: expression of Fc and complement receptors and correlation with tumor proliferation. Acta Neuropathologica, 80(3), 287–294. https://doi.org/10.1007/BF00294647

Nabissi, M., Morelli, M. B., Amantini, C., Farfariello, V., Ricci-Vitiani, L., Caprodossi, S., … Santoni, G. (2010). TRPV2 channel negatively controls glioma cell proliferation and resistance to Fas-induced apoptosis in ERK-dependent manner. Carcinogenesis, 31(5), 794–803. https://doi.org/10.1093/carcin/bgq019

Nagasawa, M., & Kojima, I. (2012). Translocation of calcium-permeable TRPV2 channel to the podosome: Its role in the regulation of podosome assembly. Cell Calcium, 51(2), 186–193. https://doi.org/10.1016/j.ceca.2011.12.012

Nagasawa, M., Nakagawa, Y., Tanaka, S., & Kojima, I. (2007). Chemotactic peptide fMetLeuPhe induces translocation of the TRPV2 channel in macrophages. Journal of Cellular Physiology, 210(3), 692–702. https://doi.org/10.1002/jcp.20883

Parenti, A., Morbidelli, L., Cui, X.-L., Douglas, J. G., Hood, J. D., Granger, H. J., … Ziche, M. (1998). Nitric Oxide Is an Upstream Signal of Vascular Endothelial Growth Factor-induced Extracellular Signal-regulated Kinase½ Activation in Postcapillary Endothelium. Journal of Biological Chemistry, 273(7), 4220–4226. https://doi.org/10.1074/jbc.273.7.4220

Pautz, A., Art, J., Hahn, S., Nowag, S., Voss, C., & Kleinert, H. (2010). Regulation of the expression of inducible nitric oxide synthase. Nitric Oxide - Biology and Chemistry, 23(2), 75–93. https://doi.org/10.1016/j.niox.2010.04.007

Perálvarez-Marín, A., Doñate-Macian, P., & Gaudet, R. (2013). What do we know about the transient receptor potential vanilloid 2 (TRPV2) ion channel? FEBS Journal, 280(21), 5471–5487. https://doi.org/10.1111/febs.12302

Pervin, S., Singh, R., Hernandez, E., Wu, G., & Chaudhuri, G. (2007). Nitric Oxide in Physiologic Concentrations Targets the Translational Machinery to Increase the Proliferation of Human Breast Cancer Cells : Involvement of Mammalian Target of Rapamycin / eIF4E Pathway. Cancer Res, (1), 289–300. https://doi.org/10.1158/0008-5472.CAN-05-4623

Qiu, B., Zhang, D., Wang, C., Tao, J., Tie, X., Qiao, Y., … Wu, A. (2011). IL-10 and TGF-β2 are overexpressed in tumor spheres cultured from human gliomas. Molecular Biology Reports, 38(5), 3585–3591. https://doi.org/10.1007/s11033-010-0469-4

Robbs, B. K., Cruz, A. L. S., Werneck, M. B. F., Mognol, G. P., & Viola, J. P. B. (2008). Dual Roles for NFAT Transcription Factor Genes as Oncogenes and Tumor Suppressors. Molecular and Cellular Biology, 28(23), 7168–7181. https://doi.org/10.1128/MCB.00256-08

Roggendorf, W., Strupp, S., & Paulus, W. (1996). Distribution and characterization of microglia/macrophages in human brain tumors. Acta Neuropathologica, 92(3), 288–293. https://doi.org/10.1007/s004010050520

Saha, R. N., & Pahan, K. (2006). Regulation of Inducible Nitric Oxide Synthase Gene in Glial Cells. Antioxid Redox Signal., 8(5–6), 929–947.

Santini, M. P., Talora, C., Seki, T., Bolgan, L., & Dotto, G. P. (2001). Cross talk among calcineurin, Sp1/Sp3, and NFAT in control of p21WAF1/CIP1 expression in

keratinocyte differentiation. Proceedings of the National Academy of Sciences, 98(17), 9575–9580. https://doi.org/10.1073/pnas.161299698

Schindelin, J., Arganda-Carreras, I., Frise, E., Kaynig, V., Longair, M., Pietzsch, T., … Cardona, A. (2012). Fiji: An open-source platform for biological-image analysis. Nature Methods, 9(7), 676–682. https://doi.org/10.1038/nmeth.2019

Simmons, G. W., Pong, W. W., Emnett, R. J., White, C. R., Gianino, S. M., Rodriguez, F. J., & Gutmann, D. H. (2011). Neurofibromatosis-1 Heterozygosity Increases Microglia in a Spatially and Temporally Restricted Pattern Relevant to Mouse Optic Glioma Formation and Growth. Journal of Neuropathology & Experimental Neurology, 70(1), 51–62. https://doi.org/10.1097/NEN.0b013e3182032d37

Soda, K. (2011). The mechanisms by which polyamines accelerate tumor spread. Journal of Experimental & Clinical Cancer Research, 30(1), 95. https://doi.org/10.1186/1756-9966-30-95

Sun, W., Uchida, K., Takahashi, N., & Iwata, Y. (2016). Activation of TRPV2 negatively regulates the differentiation of mouse brown adipocytes. Pflügers Archiv - European Journal of Physiology, 468(9), 1527–1540. https://doi.org/10.1007/s00424-016-1846-1

Tate Jr., D. J., Patterson, J. R., Velasco-Gonzalez, C., Carroll, E. N., Trinh, J., Edwards, D., … Zea, A. H. (2012). Interferon-Gamma-Induced Nitric Oxide Inhibits the Proliferation of Murine Renal Cell Carcinoma Cells. International Journal of Biological Sciences, 8(8), 1109–1120. https://doi.org/10.7150/ijbs.4694

Togo, T., Katsuse, O., & Iseki, E. (2004). Nitric oxide pathways in Alzheimer's disease and other neurodegenerative dementias. Neurological Research, 26(5), 563–566. https://doi.org/10.1179/016164104225016236

Traister, A., Abashidze, S., Gold, V., Plachta, N., Karchovsky, E., Patel, K., & Weil, M. (2002). Evidence that nitric oxide regulates cell-cycle progression in the developing chick neuroepithelium. Developmental Dynamics, 225(3), 271–276. https://doi.org/10.1002/dvdy.10164

Villalobo, A. (2006). REVIEW ARTICLE: Nitric oxide and cell proliferation. FEBS Journal, 273(11), 2329–2344. https://doi.org/10.1111/j.1742-4658.2006.05250.x

Wei, L. H., Wu, G., Morris, S. M., & Ignarro, L. J. (2001). Elevated arginase I expression in rat aortic smooth muscle cells increases cell proliferation. Proceedings of the National Academy of Sciences, 98(16), 9260–9264. https://doi.org/10.1073/pnas.161294898

Wilcock, D. M., Lewis, M. R., Van Nostrand, W. E., Davis, J., Previti, M. Lou, Gharkholonarehe, N., … Colton, C. A. (2008). Progression of Amyloid Pathology to Alzheimer's Disease Pathology in an Amyloid Precursor Protein Transgenic Mouse Model by Removal of Nitric Oxide Synthase 2. Journal of Neuroscience, 28(7), 1537–1545. https://doi.org/10.1523/JNEUROSCI.5066-07.2008

Zhang, H., Xiao, J., Hu, Z., Xie, M., Wang, W., & He, D. (2016). Blocking transient receptor potential vanilloid 2 channel in astrocytes enhances astrocyte-mediated neuroprotection after oxygen–glucose deprivation and reoxygenation. European Journal of Neuroscience, 44(7), 2493–2503. https://doi.org/10.1111/ejn.13352

Zhang, L., Handel, M., Schartner, J., Hagar, A., Allen, G., Curet, M., & Badie, B. (2007). Regulation of IL-10 expression by upstream stimulating factor (USF-1) in glioma-associated microglia. Journal of Neuroimmunology, 184(1–2), 188–197. https://doi.org/10.1016/j.jneuroim.2006.12.006

Chapter 6 Discussion:

6 NO regulates transient receptor potential channels to promote phagocytosis and inhibit proliferation in murine microglia.

Microglia proliferation and phagocytosis is critical for proper CNS development and maintenance, while dysfunction of microglia proliferation and phagocytosis contributes to a variety of neurological disorders. Specifically, in response to pathology or injury, microglia transform to an activated state that is characterized by elevated iNOS expression, increased NO production, active phagocytosis, and decreased proliferation. Previous studies have demonstrated that microglia phagocytosis and proliferation is tightly regulated by intracellular calcium levels. As non-excitable cells, microglia rely on calcium entry through TRP channels to carry out phagocytosis and proliferation. Indeed, the expression of iNOS and production of NO in microglia are also correlated to phagocytosis and proliferative activities, however, the relationship between iNOS/NO signaling and TRP-mediated calcium dynamics in microglia is not entirely known. For example, SOCCs, such as TRPC1/3, are implicated in cellular proliferation while TRPV2 is implicated in cellular proliferation and phagocytosis. My thesis studies focused on how iNOS/NO signaling regulates TRPV2 and TRPC1/3 channels in murine microglia to coordinate phagocytic and proliferative activities of microglia within the CNS. Here, I will discuss my work surrounding NO regulation of TRPV2 and TRPC1/3 channels in murine microglia, while examining the potential impacts of these regulations on various CNS pathologies such as Alzheimer's disease, stroke, and glioma progression.

6.1 NO induces phagocytosis and upregulates TRPV2 channel expression in microglia

Both the presence of NO and the activity of TRPV2 channels are independently known to induce phagocytosis in macrophages and microglia. For example, recent studies have correlated NO production to the initial increase in microglial phagocytosis (Kakita et

al., 2013; Kraus et al., 2010; Scheiblich & Bicker, 2016). On the other hand, activity of the TRPV2 ion channel is critical for phagocytosis in macrophages (Lévêque et al., 2018; Link et al., 2010; Santoni et al., 2013), and more recently this has also been shown in microglia (Hassan et al., 2014). We are the first to demonstrate that these two pathways – once believed to be separate – are part of the same signaling cascade (Maksoud et al., 2019).

6.1.1 NO signaling upregulates FcγR-mediated phagocytic activity of mouse microglia

Many studies showed that an initial increase in NO production leads to enhanced microglial phagocytosis (Kakita et al., 2013; Scheiblich & Bicker, 2016). Microglia possess a wide range of phagocytic receptors allowing them to recognize various substrates under different microenvironments. Particularly, microglia express a variety of FcγRs that recognize and bind IgG-opsonized targets. Stimulation of FcγRs activates the NFκB transcription factor to upregulate iNOS/NO production in microglia (Le et al., 2001; Sánchez-Mejorada & Rosales, 1998). Therefore, using IgG-FITC-beads to stimulate FcγRs allows for the examination of how endogenous NO production influences FcγR-mediated phagocytosis in microglia. My analyses showed that microglia lacking iNOS expression displayed a significant decrease in NO production and phagocytic capacity *in vitro*, while expressing similar FcγRI and FcγRIII mRNA levels to that of WT microglia *in vitro* **(Figure 2.1)**. Importantly, an NO-donor restored the phagocytic capacity of iNOS$^{-/-}$ microglia to similar levels as WT **(Figure 2.1)**. These results indicated that the FcγR-mediated phagocytic deficit in iNOS$^{-/-}$ microglia is due to reduced production of NO.

6.1.2 TRPV2 is the dominant vanilloid channel member expressed in murine microglia.

Another factor crucial for macrophage and microglial phagocytosis is the TRPV2 ion channel (Hassan et al., 2014; Lévêque et al., 2018; Link et al., 2010; Santoni et al., 2013). Previous studies reported the expression of functional TRPV2 but not TRPV1/3 channels in murine microglia (Cao et al., 2016; Miyake et al., 2015). Consistent with these early reports, my assays demonstrated a higher level of TRPV2 mRNA than TRPV1 mRNA in

both WT and iNOS$^{-/-}$ microglia, while TRPV3 mRNA was not detected **(Figure 2.4)**. Importantly, the selective TRPV1 agonist, capsaicin, failed to induce a calcium response in WT and iNOS$^{-/-}$ microglia, while the calcium response to the nonselective TRPV1-3 agonist, 2APB, was abolished in the presence of the specific TRPV2 antagonist tranilast **(Figure 2.4)**. These combined results demonstrated that the expression and activity of TRPV2 in murine microglia is more dominant than the other vanilloid channel members.

6.1.3 NO enhances PM expression of TRPV2 channels in microglia via a PKG/PI3K-dependent pathway

Activity of PI3K is important for TRPV2 translocation from the ER and/or Golgi stores to the PM (Kanzaki et al., 1999; Nagasawa et al., 2007; Nagasawa & Kojima, 2012; Perálvarez-Marín et al., 2013). My studies also showed that the presence of NO is crucial for the PM expression of TRPV2 in murine microglia (Maksoud et al., 2019). NO modulates cellular functions via the classical NO-sGC-cGMP-PKG pathway (Denninger & Marletta, 1999; Ha et al., 2003) or by direct *S*-nitrosylation of proteins (Okamoto & Lipton, 2015). Importantly, no study has suggested *S*-nitrosylation of TRPV2 influences channel activity; however, my analyses demonstrated that NO signals through the classical PKG pathway to induce TRPV2 PM expression and calcium influx. Specifically, elevated calcium influx and TRPV2 PM expression was observed in naïve WT **(Figure 2.4** and **2.7,** respectively**)** and BV2 **(Figure 2.5** and **2.6** respectively**)** microglia culture conditions, while iNOS$^{-/-}$ microglia displayed negligible calcium influx and decreased TRPV2 PM expression **(Figure 2.4** and **2.7,** respectively**).** Importantly, the PM expression and calcium influx in WT **(Figure 2.7)** or BV2 **(Figure 2.5** and **2.6** respectively) microglia could be abolished in the presence of a NOS inhibitor, suggesting endogenous NO signaling regulates TRPV2 PM expression. On the other hand, introducing the NO-donor SNAP into the culture conditions significantly increased the PM expression of TRPV2 in murine microglia which was abolished in the presence of a PKG_i, or a $PI3K_i$ **(Figure 2.7** and **2.8)**. This data indicates that NO regulates TRPV2 channel PM expression by activating PKG/PI3K signaling in mouse microglia.

Collectively, these novel findings add new insights into how microglia execute phagocytosis in response to changes in their surrounding environment. I propose that in

response to a signal that triggers FcγR phagocytosis, microglia increase the expression or activity of iNOS and produce higher levels of NO that activates the sGC/cGMP/PKG-PI3K signaling cascade to induce TRPV2 trafficking to the PM (Maksoud et al., 2019). The increased plasma membrane expression of TRPV2 channels leads to a large amount of calcium entry that consequently initiates phagocytosis. Fully understanding the NO-TRPV2 regulation of microglia phagocytosis may lead to novel therapeutic strategies for the treatment of neurological disorders in which microglia phagocytosis is suppressed (Iadecola, 1997; Nagayama et al., 1999; Pérez-Asensio et al., 2005; Sierra et al., 2013).

6.2 Targeting NO-mediated TRPV2 signaling in pathological diseases with altered microglial phagocytosis

Studies have revealed altered FcγR expression and activity in microglia during pathology and disease (Lunnon et al., 2011; Peress et al., 1993). In fact, the progression of many neurological diseases such as Alzheimer's, stroke, or Parkinson's, are correlated to altered NO signaling and increased FcyR expression in the CNS (Cao et al., 2010; Cribbs et al., 2012; Lira et al., 2011; Lunnon et al., 2011). To that extent, considering NO-TRPV2 signaling crucially regulates microglial phagocytosis, modulating the NO-TRPV2 signaling cascade may pose potential mechanisms to treat neurological pathologies that display altered microglial phagocytosis.

6.2.1 Alzheimer's pathology and the potential benefits of increased microglial phagocytosis

Alzheimer's is a progressive neurological disease characterized by neuronal dysfunction, memory impairments, changes to personality, and a decline in rational thinking and social skills (Selkoe, 2001). Attempting to understand the cause and progression of Alzheimer's disease is a prominent aspect in the neuroscience research field. At the molecular level, Alzheimer's pathology presents with misfolded protein aggregates that accumulate in neurons or extracellular locations (Gowing et al., 1994; Grundke-Iqbal et al., 1987; Iwatsubo et al., 1994). Specifically, the microtubule associated tau proteins produce neurofibrillary tangles within neurons when hyperphosphorylated (Grundke-Iqbal

et al., 1987). On the other hand, improper cleavage of the amyloid precursor protein in neurons forms extracellular Aβ-plaques (Gowing et al., 1994; Iwatsubo et al., 1994). These protein aggregates are toxic and cause a loss of functional synapses, neuronal apoptosis, and neuronal death.

Importantly, abnormalities in Fcγ-mediated phagocytosis contributes to the progression of Alzheimer's pathology (Nathan et al., 2005; Peress et al., 1993; Ulvestad et al., 1994). Specifically, FcγRI-III was observed in microglia surrounding plaques throughout the white matter and cortex of humans with Alzheimer's disease (Peress et al., 1993; Ulvestad et al., 1994). Interestingly, intraperitoneal injection of blood-brain-barrier-permeable antibodies against Aβ plaques were able to reduce the presence of Aβ plaques in the frontal cortex of a mouse model of AD by triggering FcγRs on microglia (Bard et al., 2000). Additionally, tau-directed immunotherapies have also demonstrated improved cognitive performance without significantly influencing microglia activity in a murine model of tau deposition (Schroeder et al., 2016). The authors suggest multiple pathways in which tau-directed immunotherapies may exert its beneficial effects including, neuronal uptake of tau antibodies and accumulation of tau aggregates within lysosomes for degradation and removal (Ding & Yin, 2008; Schroeder et al., 2016), as well as microglial recognition and removal of opsonized tau aggregates through phagocytosis (Schroeder et al., 2016; Sigurdsson, 2008). These reports support a favorable notion that increased FcγR expression is correlated with Aβ-plaque and tau removal in Alzheimer's disease.

On the other hand, iNOS/NO signaling is reported to be associated with the progression of Alzheimer's disease. However, the roles of iNOS/NO signaling in microglia during the progression of Alzheimer's disease remains controversial. For example, using a double transgenic mouse model that expresses human β-amyloid precursor protein (hAPP) and human presenilin-1 (hPS1), Nathan and colleagues demonstrated that ablation of iNOS protected the hAPP+hPS1 double transgenic mice from Alzheimer's-like pathology (Nathan et al., 2005). Specifically, removal of iNOS expression within the transgenic mouse model revealed significantly increased survival as well as decreased plaque load within the cortex and hippocampus, when compared to the transgenic mouse model that over-expressed iNOS (Nathan et al., 2005). Additionally, decreased microgliosis was

observed in the cortex and hippocampus in the transgenic mouse model lacking iNOS when compared to when iNOS was present (Nathan et al., 2005). To that extent, widespread expression of iNOS in Alzheimer's disease patients has been reported (Vodovotz et al., 1996). The expression of iNOS and production of NO may induce cytotoxicity from mitochondrial electron transport chain inhibition, release of free radicals, and through the production of secondary inflammation, which may propagate disease progression. Therefore, the high catalytic activity of iNOS is capable of quickly inflicting both nitrosative and oxidative injury to neurons and supporting tissue.

Alternatively, the ideology that iNOS/NO signaling protects against Alzheimer's pathology is supported by some literature. It is suggested that microglia associated with amyloid plaques are unresponsive and incapable of becoming activated and producing NO (Gentleman, 2013; Streit, 2006). This suggests that iNOS/NO signaling is crucial for microglia phagocytosis to restrict progression of neurological diseases such as Alzheimer's. For example, Colton and colleagues utilized two different double transgenic mouse models that displayed differing mutations in the human amyloid precursor protein and the same knockout of the iNOS gene (Colton et al., 2008). Specifically, one mouse displayed human Swedish mutation without the iNOS gene (APPSw/iNOS$^{-/-}$), while the other transgenic mouse displayed Swedish, Dutch, and Iowa mutations in the human amyloid precursor protein without the iNOS gene (APPSwDI/iNOS$^{-/-}$) (Colton et al., 2008). Both double transgenic mice displayed significantly more pathological amyloid deposition, more hyperphosphorylated tau, more aggregated tau, increased neuron loss, and increased memory loss than their respective single transgenic littermates expressing only human amyloid precursor protein mutations or iNOS gene knockout (Colton et al., 2008). These unique findings imply that basal iNOS/NO signaling may be beneficial to prevent Aβ aggregation in Alzheimer's pathology, possibly through increasing microglia phagocytosis of Aβ plaques. Given that the role of NO in Alzheimer's disease is unclear and that TRPV2 channel activity is critical for microglial phagocytosis, developing NO-independent methods to stimulate TRPV2 mediated microglial phagocytosis may lead to new treatments for Alzheimer's disease.

6.2.2 Attenuating microglial phagocytosis to treat stroke recovery

Stroke is a cerebrovascular disease characterized by a sudden decrease in blood supply to part(s) of the brain resulting in a loss of brain function. During an ischemic stroke, occlusion of a brain blood vessel results in neuronal damage that presents as an infarct and consists of mainly dead cells with no recovery potential, while the peri-infarct region, or penumbra, surrounds the infarct and consists of metabolically stressed tissue that is still viable (McCabe et al., 2017).

Within minutes of ischemia, endogenous NO production within the brain increases from nanomolar to micromolar concentrations, mainly due to nNOS and eNOS activity (Chen et al., 2017) and can remain chronically elevated for days (Zhang et al., 2016). On the other hand, expression of iNOS within astrocytes and microglia increases 12 hrs after stroke, and further contributes to chronic NO production during chronic stroke recovery, lasting up to 7 days (Niwa et al., 2001). Previous studies have demonstrated that $iNOS^{-/-}$ mice display decreased infarct volumes and improved behavioural and motor outcomes after middle cerebral artery occlusion when compared to WT controls (Iadecola et al., 1997; Nagayama et al., 1999; Pérez-Asensio et al., 2005)

The pathological production of NO within the ischemic tissue pose negative effects on neuronal cells including stress, DNA damage, and the production of ROS and RNS. Specifically, elevated NO concentrations within the penumbra can cause neuronal cells to express stress signals also known as "eat me" signals (Neher et al., 2012). Phosphatidylserine (PS), a phospholipid normally expressed on the inner leaflet of cells, gets flipped to the outer leaflet in response to RNS from elevated NO levels (Neher et al., 2012). Importantly, Neher and colleagues have shown that PS exposure in response to inflammation is fully reversible (Neher et al., 2011; Neniskyte et al., 2011) Specifically, Neurons *in vitro* can express PS in response to oxygen glucose deprivation or inflammatory stress (Meloni et al., 2011), and can recover and internalize the PS in the absence of microglia (Neher et al., 2011). However, when microglia are present with neurons expressing PS, the neurons are phagocytosed and lost (Neher et al., 2011; Neniskyte et al., 2011). Therefore, microglial phagocytosis may propagate the removal of stressed but viable neurons during ischemic stroke and allow the infarct to grow at the expense of the penumbra.

On another note, I have shown that NO contributes to TRPV2 expression and microglial FcγR-mediated phagocytosis. Therefore, future research examining if TRPV2 also contributes to PS-mediated phagocytosis could unveil TRPV2 as a potential therapeutic target for stroke recovery. To that extent, Komine-Kobayashi and colleagues demonstrated that mice lacking Fcγ receptors displayed reduced microglial activation, iNOS expression, as well as smaller infarct sizes 72hrs after transient cerebral ischemia when compared to WT mice (Komine-Kobayashi et al., 2004). Therefore, restricting TRPV2 activity may be a modifiable factor in restraining microglia phagocytosis and supporting post-stroke recovery. Future research examining TRPV2 as a potential therapeutic target to treat post-stroke recovery in a model of ischemic stroke by attenuating phagocytosis may prove beneficial.

6.3 NO regulation of store operated calcium channels

Calcium is a critical secondary messenger allowing microglia to carry out functions such as proliferation, migration, and phagocytosis. Microglia contain endogenous calcium stores in the ER, and SOCCs on their PM to help regulate calcium homeostasis (Ohana et al., 2009). Specifically, stimulation of purinergic P_2Y_x receptors on the surface of microglia endogenously signals for calcium release from the ER and subsequent activation of SOCE by ion channels throughout the PM. Two well-studied store operated calcium channels are Orai (Feske et al., 2006; Vig et al., 2006) and TRPC channels (Birnbaumer, 2009; Worley et al., 2007). Both Orai and TRPC channels are gated by the ER calcium sensor STIM1, a transmembrane protein that spans the ER membrane (Parekh, Nature Reviews 2010) and has several binding domains to gate the opening of Orai and TRPC channels (Lee et al., 2014). Specifically, STIM1 oligomerizes under low ER calcium conditions to gate the opening of Orai and/or TRPC channels on the PM (Kettenmann et al., 2011; Michaelis et al., 2015; Moccia et al., 2015; Parekh, 2010; Srikanth & Gwack, 2012; Worley et al., 2007). Importantly, both Orai- and TRPC-channel mediated SOCE occurs in microglia (Michaelis et al., 2015; Mizoguchi et al., 2014; Sun et al., 2014). My thesis work focused on the NO regulation of TRPC-mediated store operated calcium entry in murine microglia.

A variety of TRPC channels including TRPC1/3 are present on microglia (Ohana et al., 2009) and form nonselective cation channels that are permeable to calcium (Echeverry et al., 2016; Worley et al., 2007). Although many TRPC channels are present and active in microglia, the function and regulation of these channels are not entirely known. For example, an environment high in NO concentration can cause the *S*-nitrosylation of TRPC channels at cysteine residues Cys^{553} and Cys^{558} that are conserved within TRPC1, TRPC4, and TRPC5 (Wong et al., 2010; Xu et al., 2008; Yoshida et al., 2006). Although this *S*-nitrosylation event on TRPC channels remains controversial in endothelial cells, with some studies suggesting it mediates calcium influx (Yoshida et al., 2006) while other studies suggesting it attenuates calcium influx (Wong et al., 2010). My thesis work is the first to demonstrate that NO rapidly diminishes calcium signaling through TRPC1/3-mediated SOCCs in murine microglia, independent of PKG signaling.

6.3.1 NO attenuates calcium influx through store operated calcium channels in microglia

Within chapter 3, I have shown that store operated calcium channels contribute to basal calcium homeostasis in murine microglial cultures. Specifically, my assays demonstrated that application of the NO donor SNAP on murine microglia restricted basal calcium influx through SOCCs **(Figure 3.1** and **3.2)**. Importantly, the presence of a PKG_i did not block the inhibitory effect of NO on TRPC channels **(Figure 3.2)**. Additionally, application of the SERCA inhibitor TG – used to induce SOCE – on murine microglia induced a calcium influx with a nonselective cation conductance typical of TRPC channels, which was abruptly inhibited by SNAP application **(Figure 3.4)**. Considering that the inhibitory effect of NO on store operated TRPC channels was instantaneous in murine microglia, the notion that NO inhibits SOCE by *S*-nitrosylation of proteins rather than activation of the sGC-PKG signaling cascade is supported. Indeed, a previous study has demonstrated that NO inhibits SOCE in cardiomyocytes by direct *S*-nitrosylation of Cys^{49} and Cys^{56} in the STIM1 protein, which restricts STIM1 oligomerization under low calcium conditions (Gui et al., 2018). Therefore, this available data suggests that NO production decreases tonic TRPC1/3 channel mediated store operated calcium entry in murine microglia.

Moreover, I further showed that microglia lacking endogenous iNOS/NO expression displayed increased calcium influx through store operated TRPC channels while simultaneously expressing significantly less TRPC1, TRPC3, and STIM1 mRNA levels when compared to WT microglia cultures **(Figure 3.5)**. The observed decrease in mRNA expression of SOCE genes that was observed in $iNOS^{-/-}$ microglia may be a negative-feedback mechanism that compensates for the loss of iNOS/NO post-translational regulation of these proteins.

Importantly, in response to NO, the decreased calcium influx through SOCCs was followed by a sustained calcium influx through TRPV2 channels **(Figure 3.6)**. We are the first to demonsotrate that NO induces a biphasic calcium response in murine microglia by inhibiting SOCE and potentiating calcium influx through TRPV2 channels. The abrupt decrease of SOCE in response to a surge of NO into the microenvironment of microglia halts cell-cycle progression and proliferation (Chen et al., 2016; Guo et al., 2009; Takahashi et al., 2007). Subsequently, the sustained calcium influx through TRPV2 channels maintains prolongued cell-cycle arrest by increasing the expression of the cyclin dependent kinase inhibitor p21 **(Figure 5.7)**. Importantly, proliferating microglia in a highly oxidadive environment, such as in the presence of NO, may cause DNA mutations, DNA damage, and could further propogate an inflammatory response. Therefore, this biphasic calcium response may be a protective mechanism for regulating microglia proliferation in a highly oxidative environment.

6.4 NO signaling in microglial proliferation

The presence of NO is widely associated with inhibiting cell-cycle progression in the G_1/S or G_2/M stage. For example, macrophage-like cells treated with IL6 displayed increased iNOS expression and cell-cycle arrest in G_1/S and G_2/M (Takagi et al., 1994). NO inhibits cell proliferation by mainly upregulating p21 expression (Gansauge et al., 1998; Gu et al., 2000; Huang et al., 2005; Oliveira et al., 2003). In the case of MG5 microglia, NO increases the expression of p21 and inhibits cell-cycle progression (Kawahara et al., 2001).

Chapter 4 of my thesis work was the first to demonstrate that NO inhibits microglial proliferation through a PKG-dependent mechanism. Specifically, I discovered that endogenous iNOS/NO signaling restrained WT microglia into the G0 stage of the cell-cycle, while microglia lacking endogenous iNOS/NO signaling were actively dividing to a larger extent **(Figure 4.2)**. Importantly, restricting iNOS activity in WT microglia increased the percentage of actively dividing microglia **(Figure 4.4)**. Furthermore, in the absence of iNOS/NO signaling, the PKG agonist 8Br-cGMP further restricted WT microglia cell-cycle progression **(Figure 4.6)**. Further, the presence of an exogenous NO-donor or 8Br-cGMP restricted cell-cycle progression of $iNOS^{-/-}$ microglia **(Figure 4.5** and **4.7)**. These results from my assays confirmed that the iNOS/NO signaling restricts microglia proliferation through the classical cGMP-PKG pathway.

6.4.1 NO production and plasma membrane expression of TRPV2 is corelated to cell-cycle stage in microglia

As presented in Chapter 2, my work has shown that NO signaling in murine microglia facilitates PM expression of TRPV2 channels (Maksoud et al., 2019). Importantly, both NO and TRPV2 are independently known to restrict proliferation (Morelli et al., 2012; Nabissi et al., 2010; Zhang et al., 2016). The expression and activity of TRPV2 has been associated with progressing cell differentiation (Morelli et al., 2012) and restricting proliferation (Nabissi et al., 2010). For example, inhibition of TRPV2 expression in astrocytes enhanced the proliferation of astrocytes (Zhang et al., 2016). Accordingly, my in-depth assays demonstrated that NO signaling inhibits murine microglia proliferation through PM expression of TRPV2 channels. Specifically, actively dividing murine microglia displayed reduced NO production **(Figure 5.1)**, reduced TRPV2 PM expression **(Figure 5.2)**, and reduced calcium influx through TRPV2 channels **(Figure 5.3)** when compared to microglia in the G0 stage of the cell-cycle. Furthermore, pharmacological manipulation of TRPV2 activity influenced microglia cell-cycle progression. Specifically, inhibiting TRPV2 activity in WT microglia increased the percentage of actively dividing WT microglia, even in the presence of an NO-donor, when compared to control WT microglia **(Figure 5.4)**. These novel findings demonstrate that

NO-regulated PKG signaling restricts microglia proliferation and cell-cycle progression through TRPV2 plasma membrane expression.

6.4.2 NO-TRPV2 signaling induces NFATC2 nuclear localization and p21 expression

My thesis further lead me to study how the TRPV2 mediated calcium influx restricts cell-cycle progression in microglia. To this end, I demonstrated that application of an NO-donor or TRPV2 agonist on cultured murine microglia increased the nuclear localization of the NFATC2 transcription factor and the mRNA expression of the p21 gene **(Figure 5.6** and **5.7,** respectively**)**.

NFATC2 is abundantly expressed within microglia and influences microglia chronic inflammatory activation (Manocha et al., 2017; Nagamoto-Combs & Combs, 2010). For example, increased expression and activity of NFAT within microglia is accompanied by increases in proinflammatory cytokine secretions (Nagamoto-Combs & Combs, 2010). Importantly, NFATC2 stimulates the expression of p21 (Santini et al., 2001), which is a potent cyclin dependent kinase inhibitor that acts strongly on CDK2 to inhibit cell-cycle progression from G_1 to S and G_2 to mitosis (Besson et al., 2008). In fact, cells with high levels of p21 eventually enter G0, a phase where DNA replication stops and the cell exists in a quiescent state outside of the cell-cycle (Hawkes et al., 2009; Hawkes & Alkan, 2011; Karimian et al., 2016). Although proliferation stops in G0, other functions such as phagocytosis are reported to occur in G_1/G0 stage of the cell-cycle of macrophage-like cells (Blair et al., 1986).

6.4.3 Uncovering the microglia contribution to glioma pathology

Gliomas are a type of tumor that aggressively proliferate within the central nervous system and consist of glia cells such as astrocytes (Bender et al., 2010), oligodendrocytes (Watanabe et al., 2009), and ependymal cells (Romero-Rojas et al., 2012; Sato et al., 2003). Glioma diagnoses constitute one of the most aggressive and rarely curable prognoses, whereby the life expectancy is rarely more than 3 years (Brown et al., 2005; Taphoorn et al., 2005). As resident macrophages of the CNS, microglia are the most prominent immune

cells that infiltrate and proliferate within gliomas (Simmons et al., 2011). However, the proliferative role microglia play within gliomas remains disputed (Platten et al., 2003; Roesch et al., 2018). A positive correlation between the malignancy and the number of microglia present within the glioma suggests that microglia contribute to glioma pathology (Badie & Schartner, 2000; Morimura et al., 1990; Roggendorf et al., 1996). However, the underlying mechanism that regulates microglia proliferation within the glioma mass remains unclear (Engler et al., 2012).

As previously introduced in Chapter 1, microglia respond to microenvironmental stimuli to polarize towards a classical, pro-inflammatory state termed M1 phenotype, or towards an alternatively activated, anti-inflammatory state termed M2 phenotype. Importantly, the expression and activity levels of iNOS and arginase – two enzymes important for L-arginine metabolism – are tightly associated with microglial M1 and M2 phenotypes. Generally, an increased ratio of iNOS/arginase activity is characteristic of the M1 phenotype, while a decreased ratio of iNOS/arginase activity is characteristic of the M2 phenotype. Although this traditional M1/M2 classification of monocytes was once thought to be mutually exclusive, *in vitro* and *in vivo* studies have demonstrated that microglia and can simultaneously express both M1 and M2 markers (Crain et al., 2013). Therefore, this dichotomy of M1/M2 is largely disputed and instead replaced with a spectrum of possible activation states between the two extremes of M1 and M2 phenotypes. However, microglia present within the glioma mass express increased anti-inflammatory cytokines such as IL-10 and TGFβ1 (Komohara et al., 2008; Qiu et al., 2011; Zhang et al., 2007) that promote tumor progression, while also expressing reduced iNOS/NO expression (He et al., 2006; Kim et al., 2006). Considering we have shown that microglia proliferate in the absence of iNOS/NO signaling (Maksoud et al., 2020), the reduced iNOS/NO signaling in the glioma microenvironment may potentiate microglia proliferation to further contribute to glioma pathology.

Another crucial factor implicated in glioma proliferation is the decreased expression of TRPV2 (Morelli et al., 2012; Nabissi et al., 2010; Zhang et al., 2016). Specifically, TRPV2 expression negatively regulates glioma cell proliferation (Nabissi et al., 2010) while overexpressing TRPV2 increases differentiation and decreases

proliferation (Morelli et al., 2012). Therefore, examining TRPV2 activity as a potential approach to regulate the aggressive proliferation seen within glioma cells is beneficial to explore. To that extent, my studies have shown that NO signaling increases TRPV2-trafficking and subsequent calcium entry, which attenuates microglia proliferation. Understanding how NO-TRPV2 influences microglia proliferation revealed in the present thesis has provided important clues on the potential TRPV2 contribution to glioma progression and pathology.

6.5 Concluding remarks and outstanding questions for future directions

Excessive inflammation from increased cellular debris, pathogens, or molecular irritants must be tightly regulated by microglia to prevent the progression and/or development of CNS pathologies. Specifically, results from my studies showed that deletion of the iNOS gene results in an increased population of microglia in the cortex of mice, indicating that iNOS/NO is critical for regulating microglia proliferation *in vivo.* In the absence of iNOS/NO signaling, increased microglial proliferation was associated with increased calcium influx through store operated calcium channels and reduced calcium influx through TRPV2 channels.

On the other hand, microglia produce NO in response to inflammatory signals to induce phagocytosis. Importantly, the iNOS/NO signaling that is accompanied by a decrease in proliferation and an increase in phagocytosis was associated with decreased calcium influx through SOCCs and increased calcium influx through TRPV2 channels. Vaeth and colleagues demonstrated that conditional knockout of STIM1 and STIM2 did not significantly affect the phagocytic functions of macrophages (Vaeth et al., 2015), further suggesting the importance of NO-TRPV2 signaling in phagocytic functions.

Evidently, we are the first to directly demonstrate that iNOS/NO signaling in murine microglia coordinates calcium dynamics between TRPV2 and TRPC channels, which potentiates microglial phagocytosis and attenuates microglial proliferation. Although this thesis uncovered the fundamental actions by which iNOS/NO signaling regulated TRP

channel mediated calcium dynamics, there remains questions that inspire directions for future microglia studies that will be described in detail next.

6.5.1 Does PKG directly induce PI3K activity to cause TRPV2 translocation?

As described in Chapter 2, NO signaling through the sGC-PKG pathway induces TRPV2 translocation to the plasma membrane in murine microglia. Importantly, my results also signify an important role of PI3K in the regulation of TRPV2 plasma membrane expression in microglia. Specifically, the presence of a PKG inhibitor or a PI3K inhibitor restricted TRPV2 translocation to the plasma membrane in murine microglia. Therefore, this suggests that both PKG as well as PI3K are required for TRPV2 translocation to the plasma membrane in murine microglia. However, it remains unclear whether PI3K activation occurs downstream of or in parallel to PKG activity. For instance, Kawasaki and colleagues reported that PI3K-Akt activity in endothelial cells is regulated by NO signaling via an unknown mechanism independent of *S*-nitrosylation (Kawasaki et al., 2003). Additionally, Lee and colleagues showed that endothelial NOS/NO signaling can activate PI3K-Akt in astrocytes (Lee et al., 2010). Furthermore, Ha and colleagues also demonstrated that NO-sGC-PKG-PI3K-Akt signaling occurs in PC12 cells, however they did not provide evidence of PKG directly activating PI3K (Ha et al., 2003). Future studies should explore whether PKG activity directly or indirectly induces PI3K activation in microglia.

6.5.2 To what extent does naturitic peptide receptors (NPRs) influence PKG activity and TRPV2 expression?

The production of cGMP in microglia occurs when sGC or pGC is activated (Baltrons et al., 2008; Prado et al., 2010). The membrane bound pGC hydrolyzes GTP to produce cGMP in the presence of natriuretic peptides, of which there are 3 main types: ANP, BNP, and CNP. Therefore, the activity of pGC is independent of NO production. Related to this notion, I have demonstrated that application of PKG inhibitor to $iNOS^{-/-}$ microglia decreased the plasma membrane localization of TRPV2. Interestingly, these

results indicate that basal PKG activity in iNOS$^{-/-}$ microglia is regulated by an NO-independent mechanism. In this regard, Moriyama and colleagues reported that rat microglia express NPRs and may produce natriuretic peptides (Moriyama et al., 2006). Whether NPR-mediated cGMP production within iNOS$^{-/-}$ microglia contributes to the basal PKG activity – and TRPV2 translocation – as a compensation mechanism for the lack of NO production remains to be investigated in future studies.

6.5.3 Does NO reduce TRPV2 desensitization by attenuating PLC activity in microglia?

The signaling of TRPV2 is highly dependent on its translocation from the membrane of intracellular organelles to the plasma membrane. Once expressed on the plasma membrane, the regulation of TRPV2 activity is maintained by PIP_2 binding to its C-terminal region (Lishko et al., 2007; Mercado et al., 2010). For example, Mercado and colleagues demonstrated that PLC mediated PIP_2 hydrolysis contributes to TRPV2 desensitization; therefore, TRPV2 activity is directly regulated by PIP_2 abundance (Mercado et al., 2010). From my own experiments in BV2 microglia, it is intriguing that in the presence of the fast release NO-donor SNAP, the calcium influx through TRPV2 was prolonged and displayed a higher amplitude when compared to the transient response in control conditions. In relation to this notion, early studies showed that NO-cGMP-PKG signaling inhibits the hydrolysis of PIP_2 (Clementi et al., 1995), the membrane lipid that is required for TRPV2 channel activation (Mercado et al., 2010). Therefore, examining if NO signaling restricts PLC cleavage of PIP_2 to prolong TRPV2 activity within microglia would be of interest to explore in future studies.

6.5.4 Are STIM1 and/or TRPC proteins sights for *S*-nitrosylation in murine microglia?

It is known that NO signaling regulates a variety of TRP channels in endothelial cells (Yoshida et al., 2006). However, NO also inhibits STIM1 clustering and gating of store operated calcium channels within cardiomyocytes (Gui et al., 2018). Despite these reports, I demonstrated that NO signaling restricts calcium influx through SOCCs within

murine microglia cultures in a PKG independent mechanism. It is known that STIM1 is required for store operated calcium channel activity (Michaelis et al., 2015) and that *S*-nitrosylation of the two different cysteine residues Cys^{49} and Cys^{56} within STIM1 inhibits gating of SOCCs in cardiomyocytes (Gui et al., 2018). Therefore, examining if NO inhibits SOCE through *S*-nitrosylation of STIM1 in murine microglia should be studied.

Additionally, the cysteine residues Cys^{553} and Cys^{558} that are conserved within many TRPC proteins are proposed *S*-nitrosylation sights that display controversial effects on SOCE in endothelial cells (Wong et al., 2010; Xu et al., 2008; Yoshida et al., 2006). For example, Yoshida and colleagues demonstrated that *S*-nitrosylation of TRPC channels mediates calcium influx (Yoshida et al., 2006), while Wong and colleagues demonstrated an attenuation of calcium influx (Wong et al., 2010). Examining if NO inhibits SOCE through *S*-nitrosylation of TRPC channels in microglia should be studied in future investigations.

6.5.5 What is the role of store operated calcium channels in microglia proliferation?

SOCCs are known to facilitate proliferation in many types of cells (Chen et al., 2016). For example, STIM1 positively regulates proliferation in smooth muscle cells (Guo et al., 2009; Takahashi et al., 2007). Specifically, Takahashi and colleagues demonstrated that knockdown of STM1 caused decreased thymidine incorporation into DNA as well as decreased radiolabeled leucine incorporation into proteins (Takahashi et al., 2007). Furthermore, the authors proposed that STIM1 mediated calcium influx may progress cell growth through CREB phosphorylation and activation (Takahashi et al., 2007), which occurs in response to STIM1-mediated calcium entry (Pulver-Kaste et al., 2006; Pulver et al., 2004). Evidently, this data demonstrates a positive influence of SOCE on cell-cycle progression and proliferation. Considering we have demonstrated that NO inhibits both proliferation and SOCE in murine microglia, future studies should examine if SOCCs positively regulates microglial proliferation and the possible cellular signaling mechanisms that underlies this process.

6.5.6 Does *S*-nitrosylation of p21RAS enhance microglia proliferation independent of PKG signaling?

It is evident that NO signaling negatively regulates proliferation in a wide variety of cell types including microglia (Reveneau et al., 1999; Takagi et al., 1994). Importantly, NO is widely associated with inhibiting cell-cycle progression in the G_1/S or G_2/M stage, primarily by enhancing p21 expression (Gansauge et al., 1998; Gu et al., 2000; Huang et al., 2005; Oliveira et al., 2003). From my work, it was demonstrated that NO-sGC-cGMP-PKG signaling inhibits microglia proliferation through NFATC2 expression of p21. However, I consistently showed that in the presence of a PKG inhibitor, NOC18 (an NO donor) failed to inhibit iNOS$^{-/-}$ microglia proliferation and instead enhanced the percentage of actively dividing iNOS$^{-/-}$ microglia. This result suggests that exogenous NO may enhance microglia proliferation through a PKG-independent mechanism. In this regard, it has been reported that exogenous NO increases proliferation in neural stem cells (Carreira et al., 2010) and human breast cancer cells through *S*-nitrosylation of Cys^{118} on p21RAS (Heo et al., 2005; Pervin et al., 2007). Further research should examine whether exogenous NO enhances microglia proliferation through *S*-nitrosylation of p21RAS within microglia.

6.6 References

Badie, B., & Schartner, J. M. (2000). Flow Cytometric Characterization of Tumor-associated Macrophages in Experimental Gliomas. Neurosurgery, 46(4), 957–962. https://doi.org/10.1227/00006123-200004000-00035

Baltrons, M. A., Borán, M. S., Pifarré, P., & García, A. (2008). Regulation and Function of Cyclic GMP-Mediated Pathways in Glial Cells. Neurochemical Research, 33(12), 2427–2435. https://doi.org/10.1007/s11064-008-9681-1

Bard, F., Cannon, C., Barbour, R., Burke, R.-L., Games, D., Grajeda, H., … Yednock, T. (2000). Peripherally administered antibodies against amyloid β-peptide enter the central nervous system and reduce pathology in a mouse model of Alzheimer disease. Nature Medicine, 6(8), 916–919. https://doi.org/10.1038/78682

Bender, A. M., Collier, L. S., Rodriguez, F. J., Tieu, C., Larson, J. D., Halder, C., … Jenkins, R. B. (2010). Sleeping Beauty –Mediated Somatic Mutagenesis Implicates CSF1 in the Formation of High-Grade Astrocytomas. Cancer Research, 70(9), 3557–3565. https://doi.org/10.1158/0008-5472.CAN-09-4674

Besson, A., Dowdy, S. F., & Roberts, J. M. (2008). CDK Inhibitors: Cell Cycle Regulators and Beyond. Developmental Cell, 14(2), 159–169. https://doi.org/10.1016/j.devcel.2008.01.013

Birnbaumer, L. (2009). The TRPC Class of Ion Channels: A Critical Review of Their Roles in Slow, Sustained Increases in Intracellular Ca 2+ Concentrations . Annual Review of Pharmacology and Toxicology, 49(1), 395–426. https://doi.org/10.1146/annurev.pharmtox.48.113006.094928

Blair, O. C., Carbone, R., & Sartorelli, A. C. (1986). Differentiation of HL-60 promyelocytic leukemia cells: Simultaneous determination of phagocytic activity and cell cycle distribution by flow cytometry. Cytometry, 7(2), 171–177. https://doi.org/10.1002/cyto.990070208

Brown, P. D., Maurer, M. J., Rummans, T. A., Pollock, B. E., Ballman, K. V., Sloan, J. A., … Buckner, J. C. (2005). A Prospective Study of Quality of Life in Adults with Newly Diagnosed High-grade Gliomas: The Impact of the Extent of Resection on Quality of Life and Survival. Neurosurgery, 57(3), 495–504. https://doi.org/10.1227/01.NEU.0000170562.25335.C7

Cao, S., Theodore, S., & Standaert, D. G. (2010). Fcγ receptors are required for NF-κB signaling, microglial activation and dopaminergic neurodegeneration in an AAV-synuclein mouse model of Parkinson's disease. Molecular Neurodegeneration, 5(1), 42. https://doi.org/10.1186/1750-1326-5-42

Cao, T., & Ramsey, I. S. (2016). Toll-Like Receptor 4 Activation by LPS Stimulates TRPV2 Channel Activity in Microglia. Biophysical Journal, 110(3), 286a. https://doi.org/10.1016/j.bpj.2015.11.1548

Carreira, B. P., Morte, M. I., Inácio, Â., Costa, G., Rosmaninho-Salgado, J., Agasse, F., … Araújo, I. M. (2010). Nitric Oxide Stimulates the Proliferation of Neural Stem Cells Bypassing the Epidermal Growth Factor Receptor. STEM CELLS, 28(7), N/A-N/A. https://doi.org/10.1002/stem.444

Chen, Y., Chen, Y., Chen, Y., Chiu, W., & Shen, M. (2016). The STIM1-Orai1 pathway of store-operated Ca 2 + entry controls the checkpoint in cell cycle G1 / S transition. Nature Publishing Group, (February), 1–13. https://doi.org/10.1038/srep22142

Chen, Z., Mou, R., Feng, D., Wang, Z., & Chen, G. (2017). The role of nitric oxide in stroke. Medical Gas Research, 7(3), 194. https://doi.org/10.4103/2045-9912.215750

Clementi, E., Sciorati, C., Riccio, M., Miloso, M., Meldolesi, J., & Nisticò, G. (1995). Nitric Oxide Action on Growth Factor-elicited Signals. Journal of Biological Chemistry, 270(38), 22277–22282. https://doi.org/10.1074/jbc.270.38.22277

Colton, C. A., Wilcock, D. M., Wink, D. A., Davis, J., Van Nostrand, W. E., & Vitek, M. P. (2008). The effects of NOS2 gene deletion on mice expressing mutated human AβPP. Journal of Alzheimer's Disease, 15(4), 571–587. https://doi.org/10.3233/JAD-2008-15405

Crain, J. M., Nikodemova, M., & Watters, J. J. (2013). Microglia express distinct M1 and M2 phenotypic markers in the postnatal and adult central nervous system in male and female mice. Journal of Neuroscience Research, 91(9), 1143–1151. https://doi.org/10.1002/jnr.23242

Cribbs, D. H., Berchtold, N. C., Perreau, V., Coleman, P. D., Rogers, J., Tenner, A. J., & Cotman, C. W. (2012). Extensive innate immune gene activation accompanies brain aging, increasing vulnerability to cognitive decline and neurodegeneration: a

microarray study. Journal of Neuroinflammation, 9(1), 643. https://doi.org/10.1186/1742-2094-9-179

Denninger, J. W., & Marletta, M. A. (1999). Guanylate cyclase and the c NO / cGMP signaling pathway. Biochemica et Biophysica Acta Research Communications, 1411(3), 334–350.

Ding, W.-X., & Yin, X.-M. (2008). Sorting, recognition and activation of the misfolded protein degradation pathways through macroautophagy and the proteasome. Autophagy, 4(2), 141–150. https://doi.org/10.4161/auto.5190

Echeverry, S., Rodriguez, M. J., & Torres, Y. P. (2016). Transient Receptor Potential Channels in Microglia: Roles in Physiology and Disease. Neurotoxicity Research, 30(3), 467–478. https://doi.org/10.1007/s12640-016-9632-6

Engler, J. R., Robinson, A. E., Smirnov, I., Hodgson, J. G., Berger, M. S., Gupta, N., … Phillips, J. J. (2012). Increased Microglia/Macrophage Gene Expression in a Subset of Adult and Pediatric Astrocytomas. PLoS ONE, 7(8), e43339. https://doi.org/10.1371/journal.pone.0043339

Feske, S., Gwack, Y., Prakriya, M., Srikanth, S., Puppel, S. H., Tanasa, B., … Rao, A. (2006). A mutation in Orai1 causes immune deficiency by abrogating CRAC channel function. Nature, 441(7090), 179–185. https://doi.org/10.1038/nature04702

Gansauge, S., Nussler, A. K., Beger, H. G., & Gansauge, F. (1998). Nitric oxide-induced apoptosis in human pancreatic carcinoma cell lines is associated with a G1-arrest and an increase of the cyclin-dependent kinase inhibitor p21WAF1/CIP1. Cell Growth & Differentiation : The Molecular Biology Journal of the American Association for Cancer Research, 9(8), 611–617. Retrieved from http://www.ncbi.nlm.nih.gov/pubmed/9716178

Gentleman, S. M. (2013). Review: Microglia in protein aggregation disorders: friend or foe? Neuropathology and Applied Neurobiology, 39(1), 45–50. https://doi.org/10.1111/nan.12017

Gowing, E., Roher, A. E., Woods, A. S., Cotter, R. J., Chaney, M., Little, S. P., & Ball, M. J. (1994). Chemical characterization of A beta 17-42 peptide, a component of diffuse amyloid deposits of Alzheimer disease. The Journal of Biological Chemistry,

269(15), 10987–10990. Retrieved from http://www.ncbi.nlm.nih.gov/pubmed/8157623

Grundke-Iqbal, I., Iqbal, K., Tung, Y.-C., Quinlan, M., Wisniewski, H., & Binder, L. (1987). Abnormal phosphorylation of the microtubule-associated protein? (tau) in Alzheimer cytoskeletal pathology. Alzheimer Disease & Associated Disorders, 1(3), 202. https://doi.org/10.1097/00002093-198701030-00020

Gu, M., Lynch, J., & Brecher, P. (2000). Nitric Oxide Increases p21 Waf1 / Cip1 Expression by a cGMP-dependent Pathway That Includes Activation of Extracellular Signal-regulated Kinase and p70 S6k *, 275(15), 11389–11396.

Gui, L., Zhu, J., Lu, X., Sims, S. M., Lu, W.-Y., Stathopulos, P. B., & Feng, Q. (2018). S -Nitrosylation of STIM1 by Neuronal Nitric Oxide Synthase Inhibits Store-Operated Ca 2+ Entry. Journal of Molecular Biology, 430(12), 1773–1785. https://doi.org/10.1016/j.jmb.2018.04.028

Guo, R.-W., Wang, H., Gao, P., Li, M.-Q., Zeng, C.-Y., Yu, Y., … Huang, L. (2009). An essential role for stromal interaction molecule 1 in neointima formation following arterial injury. Cardiovascular Research, 81(4), 660–668. https://doi.org/10.1093/cvr/cvn338

HA, K.-S., KIM, K.-M., KWON, Y.-G., BAI, S.-K., NAM, W.-D., YOO, Y.-M., … KIM, Y.-M. (2003). Nitric oxide prevents 6-hydroxydopamine-induced apoptosis in PC12 cells through cGMP-dependent PI3 kinase/Akt activation. The FASEB Journal, 17(9), 1036–1047. https://doi.org/10.1096/fj.02-0738com

Hassan, S., Eldeeb, K., Millns, P. J., Bennett, A. J., Alexander, S. P. H., & Kendall, D. A. (2014). Cannabidiol enhances microglial phagocytosis via transient receptor potential (TRP) channel activation. British Journal of Pharmacology, 171(9), 2426–2439. https://doi.org/10.1111/bph.12615

Hawkes, W. C., & Alkan, Z. (2011). Delayed cell cycle progression from SEPW1 depletion is p53- and p21-dependent in MCF-7 breast cancer cells. Biochemical and Biophysical Research Communications, 413(1), 36–40. https://doi.org/10.1016/j.bbrc.2011.08.032

Hawkes, W. C., Wang, T. T. Y., Alkan, Z., Richter, B. D., & Dawson, K. (2009). Selenoprotein W Modulates Control of Cell Cycle Entry. Biological Trace Element Research, 131(3), 229–244. https://doi.org/10.1007/s12011-009-8367-0

He, B. P., Wang, J. J., Zhang, X., Wu, Y., Wang, M., Bay, B.-H., & Chang, A. Y.-C. (2006). Differential Reactions of Microglia to Brain Metastasis of Lung Cancer. Molecular Medicine, 12(7–8), 161–170. https://doi.org/10.2119/2006-00033.He

Heo, J., Prutzman, K. C., Mocanu, V., Campbell, S. L., Carolina, N., & Carolina, N. (2005). Mechanism of Free Radical Nitric Oxide-mediated Ras Guanine Nucleotide Dissociation. Journal Molecular Biology, 346(2), 1423–1440. https://doi.org/10.1016/j.jmb.2004.12.050

Huang, J. S., Chuang, L. Y., Guh, J. Y., Chen, C. J., Yang, Y. L., Chiang, T. A., … Liao, T. N. (2005). Effect of nitric oxide-cGMP-dependent protein kinase activation on advanced glycation end-product-induced proliferation in renal fibroblasts. Journal of the American Society of Nephrology, 16(8), 2318–2329. https://doi.org/10.1681/ASN.2005010030

Iadecola, C. (1997). Bright and dark sides of nitric oxide in ischemic brain injury. Trends in Neurosciences, 20(3), 132–139. https://doi.org/S0166-2236(96)10074-6 [pii]

Iadecola, Costantino, Zhang, F., Casey, R., Nagayama, M., & Ross, M. E. (1997). Delayed Reduction of Ischemic Brain Injury and Neurological Deficits in Mice Lacking the Inducible Nitric Oxide Synthase Gene. The Journal of Neuroscience, 17(23), 9157–9164. https://doi.org/10.1523/JNEUROSCI.17-23-09157.1997

Iwatsubo, T., Odaka, A., Suzuki, N., Mizusawa, H., Nukina, N., & Ihara, Y. (1994). Visualization of Aβ42(43) and Aβ40 in senile plaques with end-specific Aβ monoclonals: Evidence that an initially deposited species is Aβ42(43). Neuron, 13(1), 45–53. https://doi.org/10.1016/0896-6273(94)90458-8

Kakita, H., Aoyama, M., Nagaya, Y., Asai, H., Hussein, M. H., Suzuki, M., … Asai, K. (2013). Diclofenac enhances proinflammatory cytokine-induced phagocytosis of cultured microglia via nitric oxide production. Toxicology and Applied Pharmacology, 268(2), 99–105. https://doi.org/10.1016/j.taap.2013.01.024

Kanzaki, M., Zhang*, Y.-Q., Mashima*, H., Li*, L., Shibata*, H., & Kojima, I. (1999). Translocation of a calcium-permeable cation channel induced by insulin-like growth factor-I. Nature Cell Biology, 1(3), 165–170. https://doi.org/10.1038/11086

Karimian, A., Ahmadi, Y., & Yousefi, B. (2016). Multiple functions of p21 in cell cycle, apoptosis and transcriptional regulation after DNA damage. DNA Repair, 42, 63–71. https://doi.org/10.1016/j.dnarep.2016.04.008

Kawahara, K., Gotoh, T., Oyadomari, S., Kuniyasu, A., Kohsaka, S., Mori, M., & Nakayama, H. (2001). Nitric oxide inhibits the proliferation of murine microglial MG5 cells by a mechanism involving p21 but independent of p53 and cyclic guanosine monophosphate. Neuroscience Letters, 310(2–3), 89–92. https://doi.org/10.1016/S0304-3940(01)02079-1

Kawasaki, K., Smith, R. S., Hsieh, C., Sun, J., Chao, J., & Liao, J. K. (2003). Activation of the Phosphatidylinositol 3-Kinase / Protein Kinase Akt Pathway Mediates Nitric Oxide-Induced Endothelial Cell Migration and Angiogenesis, 23(16), 5726–5737. https://doi.org/10.1128/MCB.23.16.5726–5737

Kettenmann, H., Hanisch, U.-K., Noda, M., & Verkhratsky, A. (2011). Physiology of microglia. Physiological Reviews, 91(2), 461–553. https://doi.org/10.1152/physrev.00011.2010

Kim, Y. J., Hwang, S. Y., & Han, I. O. (2006). Insoluble matrix components of glioma cells suppress LPS-mediated iNOS/NO induction in microglia. Biochemical and Biophysical Research Communications, 347(3), 731–738. https://doi.org/10.1016/j.bbrc.2006.06.149

Komine-Kobayashi, M., Chou, N., Mochizuki, H., Nakao, A., Mizuno, Y., & Urabe, T. (2004). Dual Role of Fcγ Receptor in Transient Focal Cerebral Ischemia in Mice. Stroke, 35(4), 958–963. https://doi.org/10.1161/01.STR.0000120321.30916.8E

Komohara, Y., Ohnishi, K., Kuratsu, J., & Takeya, M. (2008). Possible involvement of the M2 anti-inflammatory macrophage phenotype in growth of human gliomas. The Journal of Pathology, 216(1), 15–24. https://doi.org/10.1002/path.2370

Kraus, B., Wolff, H., Elstner, E. F., & Heilmann, J. (2010). Hyperforin is a modulator of inducible nitric oxide synthase and phagocytosis in microglia and macrophages.

Naunyn-Schmiedeberg's Archives of Pharmacology, 381(6), 541–553. https://doi.org/10.1007/s00210-010-0512-y

Le, W., Rowe, D., Xie, W., Ortiz, I., He, Y., & Appel, S. H. (2001). Microglial Activation and Dopaminergic Cell Injury: An In Vitro Model Relevant to Parkinson's Disease. J. Neurosci., 21(21), 8447–8455. https://doi.org/21/21/8447 [pii]

Lee, K. P., Choi, S., Hong, J. H., Ahuja, M., Graham, S., Ma, R., … Yuan, J. P. (2014). Molecular Determinants Mediating Gating of Transient Receptor Potential Canonical (TRPC) Channels by Stromal Interaction Molecule 1 (STIM1). Journal of Biological Chemistry, 289(10), 6372–6382. https://doi.org/10.1074/jbc.M113.546556

Lee, S. H., Byun, J. S., Kong, P. J., Lee, H. J., Kim, D. K., Kim, H. S., … Kim, S. S. (2010). Inhibition of eNOS/sGC/PKG Pathway Decreases Akt Phosphorylation Induced by Kainic Acid in Mouse Hippocampus. The Korean Journal of Physiology and Pharmacology, 14(1), 37. https://doi.org/10.4196/kjpp.2010.14.1.37

Lévêque, M., Penna, A., Le Trionnaire, S., Belleguic, C., Desrues, B., Brinchault, G., … Martin-Chouly, C. (2018). Phagocytosis depends on TRPV2-mediated calcium influx and requires TRPV2 in lipids rafts: Alteration in macrophages from patients with cystic fibrosis. Scientific Reports, 8(1), 1–13. https://doi.org/10.1038/s41598-018-22558-5

Link, T. M., Park, U., Vonakis, B. M., Raben, D. M., Soloski, M. J., & Caterina, M. J. (2010). TRPV2 has a pivotal role in macrophage particle binding and phagocytosis. Nature Immunology, 11(3), 232–239. https://doi.org/10.1038/ni.1842

Lira, A., Kulczycki, J., Slack, R., Anisman, H., & Park, D. S. (2011). Involvement of the Fcγ receptor in a chronic N-methyl-4-phenyl-1,,2, 3,6-tetrahydropyridine mouse model of dopaminergic loss. Journal of Biological Chemistry, 286(33), 28783–28793. https://doi.org/10.1074/jbc.M111.244830

Lishko, P. V., Procko, E., Jin, X., Phelps, C. B., & Gaudet, R. (2007). The Ankyrin Repeats of TRPV1 Bind Multiple Ligands and Modulate Channel Sensitivity. Neuron, 54(6), 905–918. https://doi.org/10.1016/j.neuron.2007.05.027

Lunnon, K., Teeling, J. L., Tutt, A. L., Cragg, M. S., Glennie, M. J., & Perry, V. H. (2011). Systemic Inflammation Modulates Fc Receptor Expression on Microglia during

Chronic Neurodegeneration. The Journal of Immunology, 186(12), 7215–7224. https://doi.org/10.4049/jimmunol.0903833

Maksoud, M. J. E., Tellios, V., An, D., Xiang, Y., & Lu, W. (2019). Nitric oxide upregulates microglia phagocytosis and increases transient receptor potential vanilloid type 2 channel expression on the plasma membrane. Glia, 67(12), 2294–2311. https://doi.org/10.1002/glia.23685

Maksoud, M. J. E., Tellios, V., Xiang, Y.-Y., & Lu, W.-Y. (2020). Nitric oxide signaling inhibits microglia proliferation by activation of protein kinase-G. Nitric Oxide, 94, 125–134. https://doi.org/10.1016/j.niox.2019.11.005

Manocha, G. D., Ghatak, A., Puig, K. L., Kraner, S. D., Norris, C. M., & Combs, C. K. (2017). NFATc2 Modulates Microglial Activation in the AβPP/PS1 Mouse Model of Alzheimer's Disease. Journal of Alzheimer's Disease, 58(3), 775–787. https://doi.org/10.3233/JAD-151203

McCabe, C., Arroja, M. M., Reid, E., & Macrae, I. M. (2017). Animal models of ischaemic stroke and characterisation of the ischaemic penumbra. Neuropharmacology, 1–9. https://doi.org/10.1016/j.neuropharm.2017.09.022

Meloni, B. P., Meade, A. J., Kitikomolsuk, D., & Knuckey, N. W. (2011). Characterisation of neuronal cell death in acute and delayed in vitro ischemia (oxygen-glucose deprivation) models. Journal of Neuroscience Methods, 195(1), 67–74. https://doi.org/10.1016/j.jneumeth.2010.11.023

Mercado, J., Gordon-Shaag, A., Zagotta, W. N., & Gordon, S. E. (2010). Ca2+-Dependent Desensitization of TRPV2 Channels Is Mediated by Hydrolysis of Phosphatidylinositol 4,5-Bisphosphate. Journal of Neuroscience, 30(40), 13338–13347. https://doi.org/10.1523/JNEUROSCI.2108-10.2010

Michaelis, M., Nieswandt, B., Stegner, D., Eilers, J., & Kraft, R. (2015a). STIM1, STIM2, and orai1 regulate store-operated calcium entry and purinergic activation of microglia. Glia, 63(4), 652–663. https://doi.org/10.1002/glia.22775

Michaelis, M., Nieswandt, B., Stegner, D., Eilers, J., & Kraft, R. (2015b). STIM1, STIM2, and Orai1 regulate store-operated calcium entry and purinergic activation of microglia. Glia, 63(4), 652–663. https://doi.org/10.1002/glia.22775

Miyake, T., Shirakawa, H., Nakagawa, T., & Kaneko, S. (2015). Activation of mitochondrial transient receptor potential vanilloid 1 channel contributes to microglial migration. Glia, 63(10), 1870–1882. https://doi.org/10.1002/glia.22854

Mizoguchi, Y., Kato, T. A., Seki, Y., Ohgidani, M., Sagata, N., Horikawa, H., … Monji, A. (2014). Brain-derived neurotrophic factor (BDNF) induces sustained intracellular Ca2+ elevation through the up-regulation of surface transient receptor potential 3 (TRPC3) channels in rodent microglia. Journal of Biological Chemistry, 289(26), 18549–18555. https://doi.org/10.1074/jbc.M114.555334

Moccia, F., Zuccolo, E., Soda, T., Tanzi, F., Guerra, G., Mapelli, L., … D'Angelo, E. (2015). Stim and Orai proteins in neuronal Ca2+ signaling and excitability. Frontiers in Cellular Neuroscience, 9(April), 1–14. https://doi.org/10.3389/fncel.2015.00153

Morelli, M. B., Nabissi, M., Amantini, C., Farfariello, V., Ricci-Vitiani, L., di Martino, S., … Santoni, G. (2012). The transient receptor potential vanilloid-2 cation channel impairs glioblastoma stem-like cell proliferation and promotes differentiation. International Journal of Cancer, 131(7), E1067–E1077. https://doi.org/10.1002/ijc.27588

Morimura, T., Neuchrist, C., Kitz, K., Budka, H., Scheiner, O., Kraft, D., & Lassmann, H. (1990). Monocyte subpopulations in human gliomas: expression of Fc and complement receptors and correlation with tumor proliferation. Acta Neuropathologica, 80(3), 287–294. https://doi.org/10.1007/BF00294647

Moriyama, N., Taniguchi, M., Miyano, K., Miyoshi, M., & Watanabe, T. (2006). ANP inhibits LPS-induced stimulation of rat microglial cells by suppressing NF-κB and AP-1 activations. Biochemical and Biophysical Research Communications, 350(2), 322–328. https://doi.org/10.1016/j.bbrc.2006.09.034

Nabissi, M., Morelli, M. B., Amantini, C., Farfariello, V., Ricci-Vitiani, L., Caprodossi, S., … Santoni, G. (2010). TRPV2 channel negatively controls glioma cell proliferation and resistance to Fas-induced apoptosis in ERK-dependent manner. Carcinogenesis, 31(5), 794–803. https://doi.org/10.1093/carcin/bgq019

Nagamoto-Combs, K., & Combs, C. K. (2010). Microglial Phenotype Is Regulated by Activity of the Transcription Factor, NFAT (Nuclear Factor of Activated T Cells).

Journal of Neuroscience, 30(28), 9641–9646. https://doi.org/10.1523/JNEUROSCI.0828-10.2010

Nagasawa, M., & Kojima, I. (2012). Translocation of calcium-permeable TRPV2 channel to the podosome: Its role in the regulation of podosome assembly. Cell Calcium, 51(2), 186–193. https://doi.org/10.1016/j.ceca.2011.12.012

Nagasawa, M., Nakagawa, Y., Tanaka, S., & Kojima, I. (2007). Chemotactic peptide fMetLeuPhe induces translocation of the TRPV2 channel in macrophages. Journal of Cellular Physiology, 210(3), 692–702. https://doi.org/10.1002/jcp.20883

Nagayama, M., Aber, T., Nagayama, T., Ross, M. E., & Iadecola, C. (1999). Age-Dependent Increase in Ischemic Brain Injury in Wild-Type Mice and in Mice Lacking the Inducible Nitric Oxide Synthase Gene. Journal of Cerebral Blood Flow & Metabolism, 19(6), 661–666. https://doi.org/10.1097/00004647-199906000-00009

Nathan, C., Calingasan, N., Nezezon, J., Ding, A., Lucia, M. S., La Perle, K., … Beal, M. F. (2005). Protection from Alzheimer's-like disease in the mouse by genetic ablation of inducible nitric oxide synthase. Journal of Experimental Medicine, 202(9), 1163–1169. https://doi.org/10.1084/jem.20051529

Neher, J. J., Neniskyte, U., Zhao, J.-W., Bal-Price, A., Tolkovsky, A. M., & Brown, G. C. (2011). Inhibition of Microglial Phagocytosis Is Sufficient To Prevent Inflammatory Neuronal Death. The Journal of Immunology, 186(8), 4973–4983. https://doi.org/10.4049/jimmunol.1003600

Neher, Jonas J., Neniskyte, U., & Brown, G. C. (2012). Primary phagocytosis of neurons by inflamed microglia: Potential roles in neurodegeneration. Frontiers in Pharmacology, 3 FEB(February), 1–9. https://doi.org/10.3389/fphar.2012.00027

Neniskyte, U., Neher, J. J., & Brown, G. C. (2011). Neuronal death induced by nanomolar amyloid ?? is mediated by primary phagocytosis of neurons by microglia. Journal of Biological Chemistry, 286(46), 39904–39913. https://doi.org/10.1074/jbc.M111.267583

Niwa, M., Inao, S., Takayasu, M., Kawai, T., Kajita, Y., Nihashi, T., … Yoshida, J. (2001). Time course of expression of three nitric oxide synthase isoforms after transient

middle cerebral artery occlusion in rats. Neurologia Medico-Chirurgica, 41, 63–72; discussion 72-73. https://doi.org/10.2176/nmc.41.63

Ohana, L., Newell, E. W., Stanley, E. F., & Schlichter, L. C. (2009). The Ca 2+ release-activated Ca 2+ current (I CRAC) mediates store-operated Ca 2+ entry in rat microglia. Channels, 3(2), 129–139. https://doi.org/10.4161/chan.3.2.8609

Okamoto, S. I., & Lipton, S. A. (2015). S-Nitrosylation in neurogenesis and neuronal development. Biochimica et Biophysica Acta - General Subjects, 1850(8), 1588–1593. https://doi.org/10.1016/j.bbagen.2014.12.013

Oliveira, C. J. ., Schindler, F., Ventura, A. M., Morais, M. S., Arai, R. J., Debbas, V., … Monteiro, H. P. (2003). Nitric oxide and cGMP activate the Ras-MAP kinase pathway-stimulating protein tyrosine phosphorylation in rabbit aortic endothelial cells. Free Radical Biology and Medicine, 35(4), 381–396. https://doi.org/10.1016/S0891-5849(03)00311-3

Parekh, A. B. (2010). Store-operated CRAC channels: function in health and disease. Nature Reviews. Drug Discovery, 9(5), 399–410. https://doi.org/10.1038/nrd3136

Perálvarez-Marín, A., Doñate-Macian, P., & Gaudet, R. (2013). What do we know about the transient receptor potential vanilloid 2 (TRPV2) ion channel? FEBS Journal, 280(21), 5471–5487. https://doi.org/10.1111/febs.12302

Peress, N. S., Fleit, H. B., Perillo, E., Kuljis, R., & Pezzullo, C. (1993). Identification of FcγRI, II and III on normal human brain ramified microglia and on microglia in senile plaques in Alzheimer's disease. Journal of Neuroimmunology, 48(1), 71–79. https://doi.org/10.1016/0165-5728(93)90060-C

Pérez-Asensio, F. J., Hurtado, O., Burguete, M. C., Moro, M. A., Salom, J. B., Lizasoain, I., … Lorenzo, P. (2005). Inhibition of iNOS activity by 1400W decreases glutamate release and ameliorates stroke outcome after experimental ischemia. Neurobiology of Disease, 18(2), 375–384. https://doi.org/10.1016/j.nbd.2004.10.018

Pervin, S., Singh, R., Hernandez, E., Wu, G., & Chaudhuri, G. (2007). Nitric Oxide in Physiologic Concentrations Targets the Translational Machinery to Increase the Proliferation of Human Breast Cancer Cells : Involvement of Mammalian Target of Rapamycin / eIF4E Pathway. Cancer Res, (1), 289–300. https://doi.org/10.1158/0008-5472.CAN-05-4623

Platten, M., Kretz, A., Naumann, U., Aulwurm, S., Egashira, K., Isenmann, S., & Weller, M. (2003). Monocyte chemoattractant protein-1 increases microglial infiltration and aggressiveness of gliomas. Annals of Neurology, 54(3), 388–392. https://doi.org/10.1002/ana.10679

Prado, J., Baltrons, M. A., Pifarré, P., & García, A. (2010). Glial cells as sources and targets of natriuretic peptides. Neurochemistry International, 57(4), 367–374. https://doi.org/10.1016/j.neuint.2010.03.004

Pulver-Kaste, R. A., Barlow, C. A., Bond, J., Watson, A., Penar, P. L., Tranmer, B., & Lounsbury, K. M. (2006). Ca 2+ source-dependent transcription of CRE-containing genes in vascular smooth muscle. American Journal of Physiology-Heart and Circulatory Physiology, 291(1), H97–H105. https://doi.org/10.1152/ajpheart.00753.2005

Pulver, R. A., Rose-Curtis, P., Roe, M. W., Wellman, G. C., & Lounsbury, K. M. (2004). Store-Operated Ca 2+ Entry Activates the CREB Transcription Factor in Vascular Smooth Muscle. Circulation Research, 94(10), 1351–1358. https://doi.org/10.1161/01.RES.0000127618.34500.FD

Qiu, B., Zhang, D., Wang, C., Tao, J., Tie, X., Qiao, Y., … Wu, A. (2011). IL-10 and TGF-β2 are overexpressed in tumor spheres cultured from human gliomas. Molecular Biology Reports, 38(5), 3585–3591. https://doi.org/10.1007/s11033-010-0469-4

Reveneau, S., Arnould, L., Jolimoy, G., Hilpert, S., Lejeune, P., Saint-Giorgio, V., … Jeannin, J. F. (1999). Nitric oxide synthase in human breast cancer is associated with tumor grade, proliferation rate, and expression of progesterone receptors. Laboratory Investigation, 79(10), 1215–1225. https://doi.org/10532585

Roesch, S., Rapp, C., Dettling, S., & Herold-Mende, C. (2018). When Immune Cells Turn Bad—Tumor-Associated Microglia/Macrophages in Glioma. International Journal of Molecular Sciences, 19(2), 436. https://doi.org/10.3390/ijms19020436

Roggendorf, W., Strupp, S., & Paulus, W. (1996). Distribution and characterization of microglia/macrophages in human brain tumors. Acta Neuropathologica, 92(3), 288–293. https://doi.org/10.1007/s004010050520

Romero-Rojas, A. E., Díaz-Pérez, J. A., & Ariza-Serrano, L. M. (2012). CD99 is expressed in chordoid glioma and suggests ependymal origin. Virchows Archiv, 460(1), 119–122. https://doi.org/10.1007/s00428-011-1170-2

Sánchez-Mejorada, G., & Rosales, C. (1998). Fcγ receptor-mediated mitogen-activated protein kinase activation in monocytes is independent of Ras. Journal of Biological Chemistry, 273(42), 27610–27619. https://doi.org/10.1074/jbc.273.42.27610

Santini, M. P., Talora, C., Seki, T., Bolgan, L., & Dotto, G. P. (2001). Cross talk among calcineurin, Sp1/Sp3, and NFAT in control of p21WAF1/CIP1 expression in keratinocyte differentiation. Proceedings of the National Academy of Sciences, 98(17), 9575–9580. https://doi.org/10.1073/pnas.161299698

Santoni, G., Farfariello, V., Liberati, S., Morelli, M. B., Nabissi, M., Santoni, M., & Amantini, C. (2013). The role of transient receptor potential vanilloid type-2 ion channels in innate and adaptive immune responses. Frontiers in Immunology, 4(February), 1–9. https://doi.org/10.3389/fimmu.2013.00034

Sato, K., Kubota, T., Ishida, M., Yoshida, K., Takeuchi, H., & Handa, Y. (2003). Immunohistochemical and ultrastructural study of chordoid glioma of the third ventricle: its tanycytic differentiation. Acta Neuropathologica, 106(2), 176–180. https://doi.org/10.1007/s00401-003-0713-2

Scheiblich, H., & Bicker, G. (2016). Nitric oxide regulates antagonistically phagocytic and neurite outgrowth inhibiting capacities of microglia. Developmental Neurobiology, 76(5), 566–584. https://doi.org/10.1002/dneu.22333

Schroeder, S. K., Joly-Amado, A., Gordon, M. N., & Morgan, D. (2016). Tau-Directed Immunotherapy: A Promising Strategy for Treating Alzheimer's Disease and Other Tauopathies. Journal of Neuroimmune Pharmacology, 11(1), 9–25. https://doi.org/10.1007/s11481-015-9637-6

Selkoe, D. J. (2001). Alzheimer's disease: genes, proteins, and therapy. Physiological Reviews, 81(2), 741–766. https://doi.org/10.1152/physrev.2001.81.2.741

Sierra, A., Abiega, O., Shahraz, A., & Neumann, H. (2013). Janus-faced microglia: beneficial and detrimental consequences of microglial phagocytosis. Frontiers in Cellular Neuroscience, 7(January), 1–22. https://doi.org/10.3389/fncel.2013.00006

Sigurdsson, E. M. (2008). Immunotherapy Targeting Pathological Tau Protein in Alzheimer's Disease and Related Tauopathies. Journal of Alzheimer's Disease, 15(2), 157–168. https://doi.org/10.3233/JAD-2008-15202

Simmons, G. W., Pong, W. W., Emnett, R. J., White, C. R., Gianino, S. M., Rodriguez, F. J., & Gutmann, D. H. (2011). Neurofibromatosis-1 Heterozygosity Increases Microglia in a Spatially and Temporally Restricted Pattern Relevant to Mouse Optic Glioma Formation and Growth. Journal of Neuropathology & Experimental Neurology, 70(1), 51–62. https://doi.org/10.1097/NEN.0b013e3182032d37

Srikanth, S., & Gwack, Y. (2012). Orai1, STIM1, and their associating partners. The Journal of Physiology, 590(Pt 17), 4169–4177. https://doi.org/10.1113/jphysiol.2012.231522

Streit, W. J. (2006). Microglial senescence: does the brain's immune system have an expiration date? Trends in Neurosciences, 29(9), 506–510. https://doi.org/10.1016/j.tins.2006.07.001

Sun, Y., Chauhan, A., Sukumaran, P., Sharma, J., Singh, B. B., & Mishra, B. B. (2014). Inhibition of store-operated calcium entry in microglia by helminth factors: implications for immune suppression in neurocysticercosis. Journal of Neuroinflammation, 11(1), 210. https://doi.org/10.1186/s12974-014-0210-7

Takagi, K., Isobe, Y., Yasukawa, K., Okouchi, E., & Suketac, Y. (1994). Nitric oxide blocks the cell cycle of mouse macrophage-like the early G 2+M phase. FEBS Letters, 340, 159–162.

Takahashi, Y., Watanabe, H., Murakami, M., Ono, K., Munehisa, Y., Koyama, T., … Ito, H. (2007). Functional role of stromal interaction molecule 1 (STIM1) in vascular smooth muscle cells. Biochemical and Biophysical Research Communications, 361(4), 934–940. https://doi.org/10.1016/j.bbrc.2007.07.096

Taphoorn, M. J. B., Stupp, R., Coens, C., Osoba, D., Kortmann, R., van den Bent, M. J., … Bottomley, A. (2005). Health-related quality of life in patients with glioblastoma: a randomised controlled trial. The Lancet Oncology, 6(12), 937–944. https://doi.org/10.1016/S1470-2045(05)70432-0

Ulvestad, E., Williams, K., Matre, R., Nyland, H., Olivier, A., & Antel, J. (1994). Fc Receptors for IgG on Cultured Human Microglia Mediate Cytotoxicity and

Phagocytosis of Antibody-coated Targets. Journal of Neuropathology and Experimental Neurology, 53(1), 27–36. https://doi.org/10.1097/00005072-199401000-00004

Vaeth, M., Zee, I., Concepcion, A. R., Maus, M., Shaw, P., Portal-Celhay, C., … Feske, S. (2015). Ca 2+ Signaling but Not Store-Operated Ca 2+ Entry Is Required for the Function of Macrophages and Dendritic Cells. The Journal of Immunology, 195(3), 1202–1217. https://doi.org/10.4049/jimmunol.1403013

Vig, M., Peinelt, C., A, B., Koomoa, D. L., Rabah, D., Koblan-Huberson, M., … Kinet, J.-P. (2006). CRACM1 Is a Plasma Membrane Protein Essential for Store-Operated Ca2+ Entry. Science, 312(5777), 1220–1223. https://doi.org/10.1126/science.1127883

Vodovotz, Y., Lucia, M. S., Flanders, K. C., Chesler, L., Xie, Q. W., Smith, T. W., … Sporn, M. B. (1996). Inducible nitric oxide synthase in tangle-bearing neurons of patients with Alzheimer's disease. The Journal of Experimental Medicine, 184(4), 1425–1433. https://doi.org/10.1084/jem.184.4.1425

Watanabe, T., Nobusawa, S., Kleihues, P., & Ohgaki, H. (2009). IDH1 Mutations Are Early Events in the Development of Astrocytomas and Oligodendrogliomas. The American Journal of Pathology, 174(4), 1149–1153. https://doi.org/10.2353/ajpath.2009.080958

Wong, C.-O., Sukumar, P., Beech, D. J., & Yao, X. (2010). Nitric oxide lacks direct effect on TRPC5 channels but suppresses endogenous TRPC5-containing channels in endothelial cells. Pflügers Archiv - European Journal of Physiology, 460(1), 121–130. https://doi.org/10.1007/s00424-010-0823-3

Worley, P. F., Zeng, W., Huang, G. N., Yuan, J. P., Kim, J. Y., Lee, M. G., & Muallem, S. (2007). TRPC channels as STIM1-regulated store-operated channels. Cell Calcium, 42(2), 205–211. https://doi.org/10.1016/j.ceca.2007.03.004

Xu, S.-Z., Sukumar, P., Zeng, F., Li, J., Jairaman, A., English, A., … Beech, D. J. (2008). TRPC channel activation by extracellular thioredoxin. Nature, 451(7174), 69–72. https://doi.org/10.1038/nature06414

Yoshida, T., Inoue, R., Morii, T., Takahashi, N., Yamamoto, S., Hara, Y., … Mori, Y. (2006). Nitric oxide activates TRP channels by cysteine S-nitrosylation. Nature Chemical Biology, 2(11), 596–607. https://doi.org/10.1038/nchembio821

Zhang, D., Wang, H., Liu, H., Tao, T., Wang, N., & Shen, A. (2016). nNOS Translocates into the Nucleus and Interacts with Sox2 to Protect Neurons Against Early Excitotoxicity via Promotion of Shh Transcription. Molecular Neurobiology, 53(9), 6444–6458. https://doi.org/10.1007/s12035-015-9545-z

Zhang, H., Xiao, J., Hu, Z., Xie, M., Wang, W., & He, D. (2016). Blocking transient receptor potential vanilloid 2 channel in astrocytes enhances astrocyte-mediated neuroprotection after oxygen–glucose deprivation and reoxygenation. European Journal of Neuroscience, 44(7), 2493–2503. https://doi.org/10.1111/ejn.13352

Zhang, L., Handel, M., Schartner, J., Hagar, A., Allen, G., Curet, M., & Badie, B. (2007). Regulation of IL-10 expression by upstream stimulating factor (USF-1) in glioma-associated microglia. Journal of Neuroimmunology, 184(1–2), 188–197. https://doi.org/10.1016/j.jneuroim.2006.12.006

Curriculum Vitae

MATTHEW JOSEPH-ELIAS MAKSOUD

EDUCATION

The University of Western Ontario, London, ON

Doctor of Philosophy (Ph.D.) Neuroscience **2015 – 2020**

- The effect of nitric oxide on microglia function and activity: Implications on transient receptor potential ion channels
- Supervisor: Dr. Wei-Yang Lu

Honours Bachelor of Science (H.B.Sc.) **2015**

- Double Major: Biology, Medical Sciences

PUBLICATIONS

Matthew J.E. Maksoud[1], Vasiliki Tellios, and Wei-Yang Lu, Nitric oxide attenuates murine microglia proliferation by sequential activation of TRPV2-mediated calcium influx, NFATC2 nuclear translocation, and p21 expression, **In Preparation.**

Matthew J.E. Maksoud[1], Vasiliki Tellios, Yun-Yan Xiang, and Wei-Yang Lu, Nitric oxide displays a biphasic effect on microglia calcium dynamics, **In Preparation.**

William Binning[1], Aja E. Hogan-Cann[1], Diana Yae Sakae[1], **Matthew Maksoud**, Valeriy Ostapchenko, Mohammed Al-Onaizi, Sara Matovic, Wei-Yang Lu, Marco A. M. Prado, Wataru Inoue, Vania F. Prado, Chronic hM3Dq signaling in microglia ameliorates neuroinflammation in male mice. *Brain, Behaviour, and Immunity*. https://doi.org/10.1016/j.bbi.2020.05.041

Vasiliki Tellios[1], **Matthew J.E. Maksoud,** Yun-Yan Xiang, and Wei-Yang Lu, Nitric oxide is a critical regulator of Purkinje neuron dendritic morphology through a metabotropic glutamate receptor type-1 mediated mechanism. *The Cerebellum.* (2020). https://doi.org/10.1007/s12311-020-01125-7.

Matthew J.E. Maksoud[1], Vasiliki Tellios, Yun-Yan Xiang, and Wei-Yang Lu, Nitric oxide signaling inhibits microglia proliferation by activation of protein kinase-G, *Nitric Oxide.* 94 (2019) 125–134. https://doi.org/10.1016/j.niox.2019.11.005

Matthew J.E. Maksoud[1], Vasiliki Tellios, Dong An, Yun-Yan Xiang, and Wei-Yang Lu, Nitric Oxide upregulates microglia phagocytosis and increases transient receptor potential vanilloid type 2 channel expression on the plasma membrane, *Glia.* 67 (2019) 2294–2311. https://doi.org/10.1002/glia.23685

Luan Januzi[1], Jacob W. Poirier[1], **Matthew J.E. Maksoud[1]**, Yun-Yan Xiang, Rudolf A.W. Veldhuizen, Sean E. Gill, Sean P. Cregan, Haibo Zhang, Gregory A. Dekaban[*], Wei-Yang Lu, Autocrine GABA signaling distinctively regulates phenotypic activation of mouse pulmonary macrophages, *Cellular Immunology*. 332 (2018). https://doi.org/10.1016/j.cellimm.2018.07.001

PUBLISHED ABSTRACTS

M. J.-E. Maksoud, V. Tellios, Y.-Y. Xiang, W.-Y. Lu, Nitric oxide production from iNOS inhibits microglia proliferation via TRPV2-mediated calcium influx. Canadian Association for Neuroscience. 2019

Aja Hogan-Cann, Diana Sakae, William Binning, Matthew Maksoud, Valeriy Ostapchenko, Mohammed Al Onaizi, Sara Matovic, Wataru Inoue, Wei-Yang Lu, Vania F. Prado, Marco A.M. Prado, In vivo modulation of microglial activity using chemogenetics. Canadian Association for Neuroscience. 2019.

V. Tellios, M. J.-E. Maksoud, Y.-Y. Xiang, W.-Y. Lu, Bergmann glia morphology and GLAST expression is downregulated in nNOS-/- cerebellum. Canadian Association for Neuroscience. 2019.

M. J.-E. Maksoud, V. Tellios, D. An, Y.-Y. Xiang, W.-Y. Lu, Nitric oxide regulates transient receptor potential vanilloid type 2 channel trafficking in microglia. Society for Neuroscience. 2018.

V. Tellios, M. J.-E. Maksoud, Y.-Y. Xiang, W.-Y. Lu., Neuronal nitric oxide synthase in the cerebellum: Implications on development of the parallel fiber-Purkinje neuron synapse in mice. Society for Neuroscience. 2018.

Matthew Maksoud, Dong An, Yun-Yan Xiang, Wei-Yang Lu, Regulation of calcium entry in microglia by nitric oxide. Canadian Association for Neuroscience. 2017.

ACADEMIC AWARDS, Scholarships & Funding

Physiology & Pharmacology Research Day Poster Award
The University of Western Ontario, London, ON
Awarded to the best poster presentation, $200. **2019**

Neuroscience Research Day Collaborative Award

The University of Western Ontario, London, ON

Awarded to the best proposed collaborative research project, $500. **2019**

Project proposal: Examining the adverse effects of familiar or novel THC exposure in pregnant dams: Implications on microglia activity.

Ontario Graduate Scholarship

The University of Western Ontario, London, ON

In support for graduate study in science and technology, $15000. **2019**

Cayman Chemical Travel Award

Cayman Chemical Company.

In support for CAN 2019 travels (Toronto, ON), $250 USD. **2019**

In support for SFN 2018 travels (Sand Diego, CA), $400 USD. **2018**

Neuroscience Graduate Travel Award

The University of Western Ontario, London, ON

In support for CAN 2017 travels (Montreal, ON), $500. **2017**

TEACHING EXPERIENCE

The University of Western Ontario, London, ON

Western Certificate in University Teaching and Learning. **2020**

Developed active learning techniques to engage students and promote learning.
Learned different methods to plan and facilitate discussions within the classroom.
Developed a syllabus and curriculum for a novel course: *Physiology of Microglia*.
Revised current teaching strategies to develop a more constructive and effective student learning experience.

Teaching Assistant – Medical Sciences Laboratory (MedSci 4900F/G) **2018 – 2020**

Explained theory behind wet lab procedures with safety expectations.
Directed proper laboratory techniques in a hands-on basis in weekly labs.
Guided discussions for planning experimental wet-lab research.

Teaching Assistant – Neuroscience for Rehabilitation Sciences (ACB 9531A/B) **2015 – 2017**

Guided self-directed learning in weekly labs.
Marked written assignments dealing with rehabilitation for neurological disorders.

Project Supervisor Roles **2017 – 2020**

Supervised Students in wet lab research.
Developed & discussed research proposals while emphasizing previous literature.
Explained laboratory procedures & techniques with emphasis on safety protocols.
Managed students' progress and helped with technique troubleshooting.
Guided basic neuroanatomy learning on the weekly basis.

Project Supervisor – Physiology & Pharmacology Thesis (4980E; 5 Students) **2016 – 2020**

Anmol Gill – Project: Autocrine GABA signaling in SH-SY5Y cell differentiation. 2020

Donghyun Lee – Project: Regulation of TRPV channels in PC12 cells by nitric oxide. *Accepted to the Schulich School of Medicine Program at the University of Western Ontario.* 2018

Abdelheady Osman – Project: Nitric oxide critically regulates Bergmann glia morphology *in vivo*. 2017

Dong An – Project: Nitric oxide regulation of TRPV2 plasma membrane expression in BV2 cells. *Accepted to the University of Toronto Medical Program*. 2016

Yimo Wang – Project: Autocrine GABA signaling in SH-SY5Y cells. *Accepted to the Physiotherapy Program at McMaster University*. 2016

Project Supervisor – Neuroscience (4000E; 2 Students) **2019 – 2020**

Vlad Marinescu – Project: Examining changes in cerebellar microglia morphology according to nitric oxide synthase expression. 2020

Ravneet Nagra – Project: Regulation of the endocannabinoid system by nitric oxide in cerebellar Purkinje neurons. 2019

Partners in Experiential Learning Supervisor – (Co-op; 4 Students) **2017 – 2019**

Katie Schornagel – Project: Changes in microglial morphology according to nitric oxide synthase expression. 2019

Sharisse Velasquez – Project: Changes in microglial morphology according to nitric oxide synthase expression 2018

Mridula Debnath – Project: Changes in microglial morphology according to nitric oxide synthase expression 2017

Ching Yuan – Project: Changes in microglial morphology according to nitric oxide synthase expression 2017

Teaching Assistant Training Program Certificate **2015**

Uncovered the basics behind effective lecture styles for science-specific teaching.